University of Florida Health Science Center

2011 Annual Report

Age Related Memory Loss (ARML) Program
& Cognitive Aging and Memory Clinical and
Translational Research Program (CAM-CTRP)

Prepared for the McKnight Brain Research Foundation
by the University of Florida
McKnight Brain Institute and Insitute on Aging

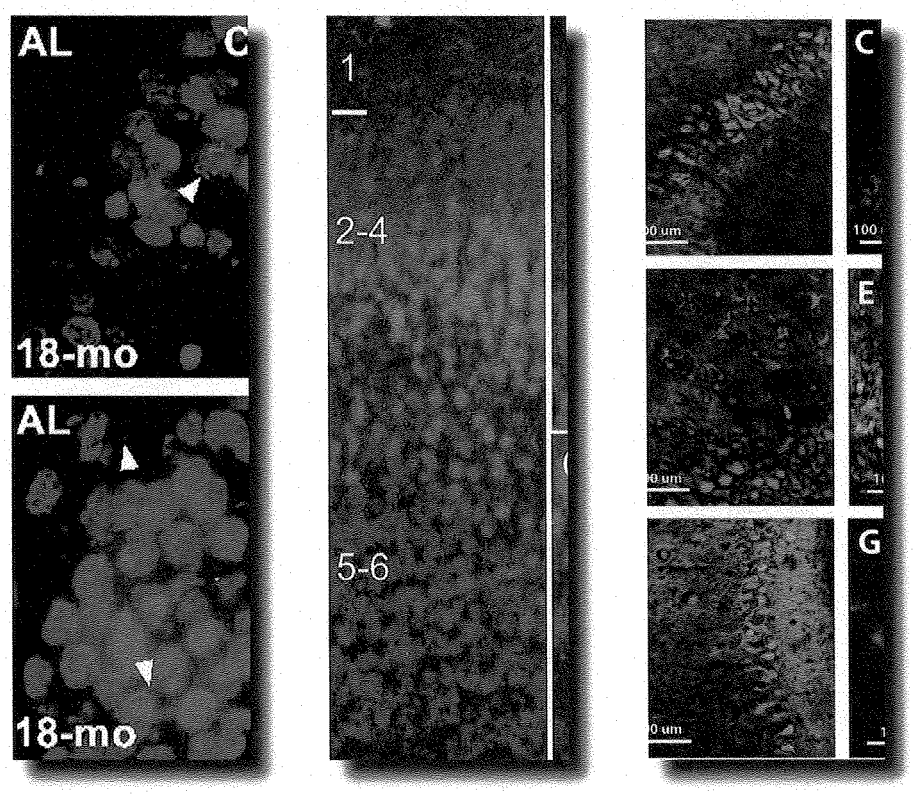

UF | Health Science Center
UNIVERSITY of FLORIDA

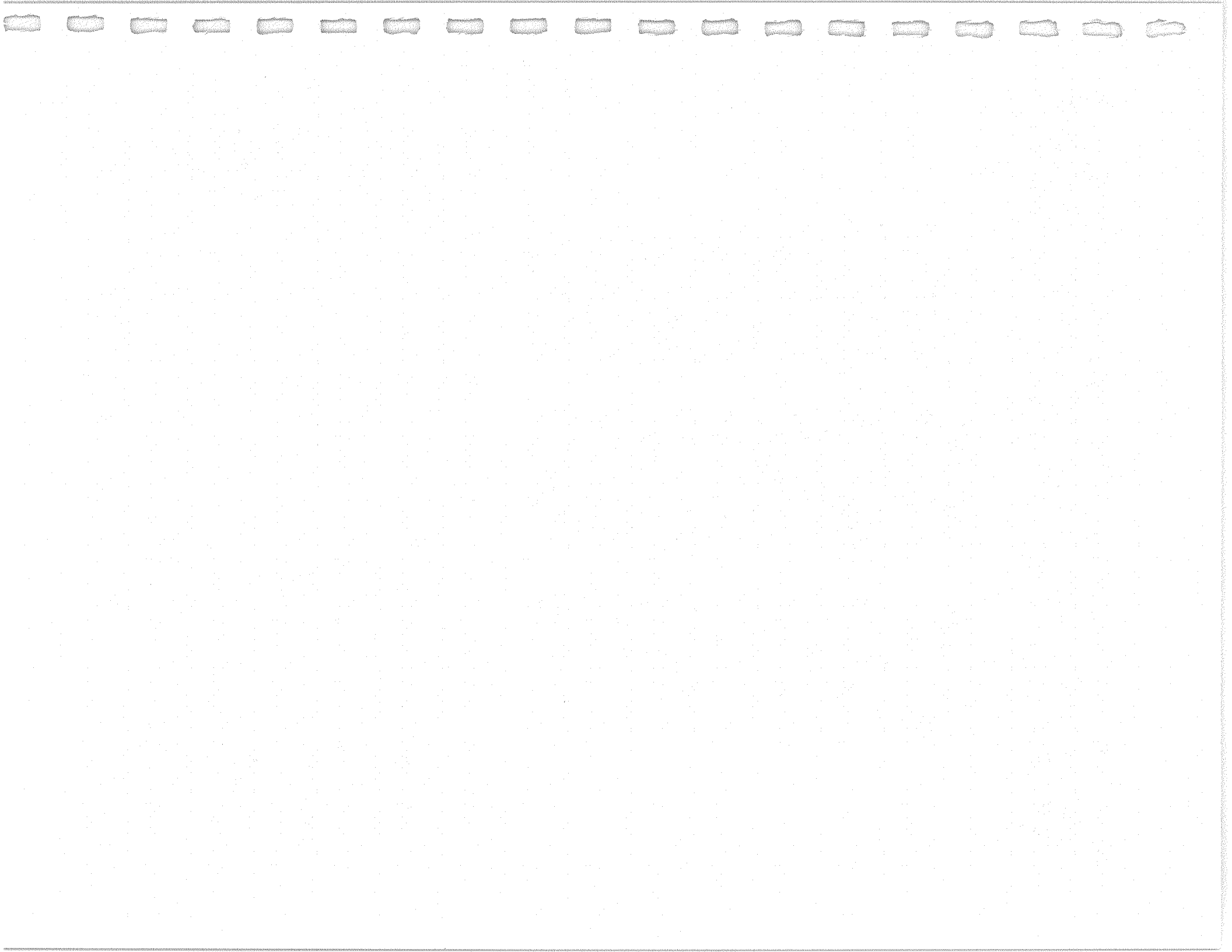

Table of Contents

Contact Information

Mary Ann Kiely
Associate Vice President for Development, UFHSC
Vice President for Development, Shands HealthCare
email: mkiely@ufl.edu

Russell E. Armistead, M.B.A., C.P.A.
Associate Vice President for Finance & Planning
UF Health Science Center
email: rea@ufl.edu

P.O. Box 100014 ▪ Gainesville, FL 32610-0014 ▪ 352-273-9620

UF | UNIVERSITY of FLORIDA

Office of the Senior Vice President, Health Affairs
President, UF & Shands Health System

1600 SW Archer Road
PO Box 100014
Gainesville, FL 32610-0014
352-273-5600 Tel
352-392-9395 Fax

January 9, 2012

The McKnight Brain Research Foundation
The SunTrust Bank
Mail Code FL-ORL-2160
300 South Orange Avenue, Suite 1600
Orlando, FL 32801

Dear Trustees:

It is my pleasure to share with you the latest research developments at the McKnight Brain Institute, and in doing so, express my deep gratitude for the ongoing support of the McKnight Brain Research Foundation. The resources provided by the MBRF have made a vital difference in our pursuit of new understanding of age-related memory loss.

Under the expert guidance of Dr. Tetsuo Ashizawa, Director of UF's McKnight Brain Institute, an impressive interdisciplinary team of nationally recognized scientists and clinicians have made significant progress on two key fronts: the Age-Related Memory Loss Program (ARML) and the Cognitive Aging and Memory Clinical Translational Research Program (CAM-CTRP). Both of these major initiatives received additional external funding from the National Institutes of Health based on the research achievements that were initially made possible through the support of the MBRF.

The enclosed report provides a comprehensive look at these accomplishments and many other research and patient care developments in neuro-medicine. We look forward to another productive year, and thank you again for your partnership and support.

Sincerely,

David S. Guzick, M.D., Ph.D.
Senior Vice President, Health Affairs
President, UF&Shands Health System

UF UNIVERSITY of FLORIDA

College of Medicine
Office of the Dean

PO Box 100215
Gainesville, FL 32610-0215
352-273-7500
352-273-8309 Fax

January 9, 2012

The McKnight Brain Research Foundation
The SunTrust Bank
Mail Code FL-ORL-2160
300 South Orange Avenue, Suite 1600
Orlando, FL 32801

Dear Trustees:

On behalf of the UF College of Medicine, please accept my sincere appreciation for the ongoing support and partnership of the McKnight Brain Research Foundation. The past year has been extremely productive for both the Age-Related Memory Loss Program (ARML) and the Cognitive Aging and Memory Clinical Translational Research Program (CAM-CTRP). Our faculty have made significant progress on several key studies, leading enhanced collaboration across the University and successful submission of several manuscripts to scientific journals.

The support of the MBRF fueled studies by more than a dozen leading researchers in 2011, and we continue to aggressively recruit emerging leaders in neuro-medicine to join this impressive team. The research resources provided by the MBRF are critical to ensuring that the University of Florida continues on its journey to becoming a national leader in brain research.

I hope you enjoy reviewing the enclosed report and learning more about this year's work and results. Thank you again for all that you make possible in neuro-medicine through your support. We look forward to another year of strong collaboration and discovery.

Sincerely,

ML Good, MD

Michael L. Good, M.D.
Dean, College of Medicine
Folke H. Peterson Dean's Distinguished Professor

University of Florida Health Science Center

2011 Annual Report

Age Related Memory Loss (ARML) Program
& Cognitive Aging and Memory Clinical and
Translational Research Program (CAM-CTRP)

Prepared for the McKnight Brain Research Foundation
by the University of Florida
McKnight Brain Institute and Insitute on Aging

Institution Report & Age Related Memory Loss Program

UF | Health Science Center
UNIVERSITY of FLORIDA

UF UNIVERSITY of FLORIDA

Evelyn F. and William L. McKnight Brain Institute

PO Box 100015
Gainesville, FL 32610-0015
352-273-8500 Tel.
352-846-0185 Fax
www.mbi.ufl.edu

January 7, 2012

McKnight Brain Research Foundation
Foundations & Endowments Specialty Practice
SunTrust Banks, Inc.
Mail Code FL-ORL-2160
300 South Orange Ave., Suite 1600
Orlando, FL 32801
Attn: Tiffany Ahlfield

Dear McKnight Brain Research Foundation Trustees:

I am sending the attached annual report of the research activities supported by the McKnight Brain Research Foundation (MBRF) from January 2011 to December 2011. The funds provided by the MBRF have been a precious resource for our researchers who are engaged in research on Age-Related Memory Loss/Cognitive Aging at the Evelyn F. and William L. McKnight Brain Institute (MBI) at the University of Florida. I am pleased to tell you that we made important advances by supporting two major programs, the Age Related Memory Loss (ARML) Program at the MBI and the Cognitive Aging and Memory Clinical Translational Research Program (CAM-CTRP) at the Institute on Aging (IOA) at the University of Florida.

The Age Related Memory Loss (ARML) Program

Dr. Thomas Foster, Director, ARML, was recognized by the National Institute of Aging with an NIH MERIT Award in 2011 for his research on age related memory loss. The MERIT Award provides long-term funding to ensure the continuation of research programs of scientists that demonstrate a history of exceptional research achievements. As you can see in his Chair report, he continues to be productive in his research. Dr. Jennifer Bizon, who was recruited in 2010, successfully launched her behavioral research program on age related memory loss. She is now performing her research at the full speed to accomplish her goals. The VITAL study funded by the ARML Program is an ongoing clinical research project conducted at the AvMed SantaFe Village under the direction of Dr. Dawn Bowers. After a peer review of many competitive applications, Drs. Vonetta Dotson, J. Charles Frazier and Leonid Moroz were selected for ARML awards in 2011. The funding is to facilitate the research on age related memory loss by the promising investigators at UF. Dr. Todd Manini continued his research from funds distributed in 2010. Dr. Brandi Omerod received a six month no-cost extension to continue her project awarded 2010. Previous funding to Dr. Matthew Sarkisian ended in October 2011. Individual achievements of these investigators in 2011 are included in the annual report. Another important goal for the ARML Program is to recruit another strong investigator on cognitive aging. The advertisements for this recruit were posted in November 2011 to major journals. The addition of a strong investigator will enhance the synergy in the ARML Program.

The Cognitive Aging and Memory Clinical and Translational Research Program (CAM-CTRP)

After unsuccessful recruitment of the CAM-CTRP Director in 2010-2011, a new Search Committee was appointed with Dr. David Nelson as Chair. The previous search faced a difficulty in identifying an adequate number of qualifying candidates because of the requirement of an M.D. degree. The new search loosened the requirement to include Ph.D. clinicians in the candidate pool. While the search is still ongoing, the Search Committee has identified two strong candidates - one M.D. psychiatrist and one Ph.D. clinical psychologist. The priority has been set to appoint the CAM-CTRP Director in early 2012.

Improvements of Research Environment for Age Related Memory Loss Research

A shortage of space where investigators can communicate with each other in MBI has been a major problem. The fifth floor of the MBI (MBI Director's office and administrative space) has been renovated into the MBI Faculty Lounge. Conference facilities including the DeWeese Auditorium and LG110A/B have been renovated with updated audiovisual equipment. Renovating the animal facility for behavioral studies of age-related memory loss was completed. Management of the MBI animal facility has been transferred to the University of Florida Animal Care Service (Dr. Gus Battles, Director). This arrangement allows MBI investigators to access the entire UF Health Science Center animal facilities and save the MBI the operational cost. A new telemetry unit will be allocated and the capacity of rodent housing will be doubled at the MBI animal facility. To ensure the optimal utilization of the MBI animal facility the users' group was formed to establish effective communications between the MBI animal users and the management. Integration of the MBI Cell Sorter Core into Interdisciplinary Center for Biotechnology Research (ICBR) has been completed with improved service and cost savings.

Reorganizing the Administration Office

Kelly Sharp was appointed as the new MBI Administrator and the MBI Administrative Office has been moved from the fifth floor to the ground floor. Transparency and accountability of the office have been established. Drs. William Friedman (Neurosurgery Chair, Neuro ICAP Director), Mark Gold (Psychiatry Chair), Lucia Notterpek (Neuroscience Chair), Marco Pahor (Institute on Aging Director, Geriatrics Chair), Tom Foster (ARML Program Director) and Todd Golde (Center for Translational Research in Neurodegenerative Disease) have been appointed to be members of the MBI Steering Committee, which governs the MBI operation under Dr. Tee Ashizawa (MBI Director) as the Committee Chair.

In summary, important progress has been made. However, it remains the priority to recruit a Director of the CAM-CTRP before we can take our clinical and basic science research programs on age related memory loss to the next level. Once it is done, I expect dynamic synergy will be generated in close collaborations between the MBI and the IOA to advance the understanding of the cognitive aging mechanism and the development of solutions. I believe Year 2012 will be a critical year for the successful leap of our programs.

Best regards,

Tetsuo Ashizawa, M.D.
Executive Director, McKnight Brain Institute
Melvin Greer Professor of Neurology
Chair, Department of Neurology

Annual Report
McKnight Brain Research Foundation
Sponsored Institutes and Research Programs
(Include activity of all McKnight supported faculty and trainees)
Report Period: January 2011 – December 2011

Some gift agreements require both Institute reports and Chair reports. If applicable, please clearly state whether a particular response relates to a Chair or Institute.

Any capitalized terms used on the template are intended to have the same meaning as the term is defined in the Gift Agreement.

Institution Report

1. **Summary of scientific achievements since last report**

Dr. Jennifer Bizon

In the past year, Dr. Bizon has been successful in relocating and setting up a laboratory at the McKnight Brain Institute at University of Florida. Two prior grants relevant to age-related memory loss have now been transferred to UF (an R01 and a F31 NRSA for one of the graduate students, both from NIA). A second R01, in collaboration with Dr. Barry Setlow (funded from NIDA), has also been successfully reestablished at UF. In addition, a new graduate fellowship from the National Science Foundation was awarded in this past year to support work investigating age-related changes in prefrontal cortical-supported cognition. While a large portion of this year has been devoted to establishing the laboratory at UF-COM, productivity has been maintained; numerous papers and abstracts with relevance to age-related cognitive loss have been published as well as on topics related to other extramurally funded projects. For 2011, Dr. Bizon has had 9 manuscripts that have either been published or are now *in press*, has made numerous conference presentations, and has submitted four new grant applications. Of particular note is a manuscript (*GABA (B) receptor GTP-binding is decreased in the prefrontal but not the hippocampus of aged rats*) currently *in press* at ***Neurobiology of Aging*** in which Dr. Bizon's lab describes regionally specific changes in GABA (B) receptor expression and function in behaviorally characterized aged rats. This manuscript reports the findings from experiments under one of the aims in her current NIA-funded R01 and, together with data from several other studies, will provide the foundation for her renewal to be submitted later this year. A second notable publication (*Dopaminergic modulation of risky decision-making*) is a manuscript with collaborator Dr. Barry Setlow which was recently published in ***The Journal of Neuroscience***. In this paper, they describe robust individual differences in young rats with respect to risk-taking, and provide evidence linking these individual differences to alterations in forebrain dopaminergic signaling. This paper builds on a productive collaboration with the Setlow laboratory related to decision-making (thus far resulting in 5 manuscripts - 2 focused on aging) and the data therein provide an essential foundation for an R01 application to be submitted this January in response to a joint RFA issued by NIMH and NIA. Indeed, a third notable manuscript from the Bizon laboratory (*Risk, reward and decision-making in a rodent model of cognitive aging*) will be published in a special upcoming issue of ***Frontiers in Neuroscience*** devoted to the topic of aging and decision making. In addition, they have made considerable efforts in the past year to build collaborations with other MBI faculty, which we hope will have long-term programmatic potential. One such project focuses on age-related changes in connectivity and cognitive decline and includes Drs. Steve Blackband, Lucia Notterpek and Tom Foster. This group has been meeting regularly and is currently in the process of collecting preliminary data for a multiple-PI grant which we plan to submit in the near future. This past year, Dr. Bizon also had the opportunity to serve on the Inter-Institute McKnight "Cognitive Test Battery Working Group" which met both in New Orleans, LA and Denver, CO with the goal of developing recommendations for a library of tests which will harmonize cognitive assessment tools across McKnight institutions. As a result of these meetings, she will author or co-author several manuscripts in the next year focused on the opportunities and challenges in characterizing executive function and memory across species to be published in a special issue of Frontiers in Aging.

Dr. Dawn Bowers

The Age-related Memory Loss funding that Dr. Bowers' lab received from the McKnight Brain Institute for the project "*The Vital Study: The Village Interactive Training and Learning Study*" for their work investigating the effects of exercise pre-dosing on the cognitive training gains of older adults have been fundamentally important for launching a new research infrastructure and a new program of research. Innovations of the funded project are (a) examining the effects of exercise pre-dosing on cognitive training outcomes in older adults, and (b) enrollment of a much older cohort of elders (mean age = 82) than is typical of most cognitive aging studies. The pre-dosing question is innovative because many studies have shown benefits of physical and cognitive training on mental outcomes for older adults in isolation, but few human studies have asked whether improved aerobic fitness might actually boost cognitive plasticity. The very old nature of their sample means that they have a higher proportion of adults in the "high decline" phase of lifespan, including a sample much more likely to experience negative cognitive changes within a very narrow time window. Thus, the protective effects of cognitive and physical exercise are more likely to be seen in a shorter time frame. The project will provide essential preliminary study data to establish effect sizes for future NIH trials. The project has also facilitated an extensive set of community and university partnerships that will serve future ARML studies well as infrastructure. Specifically, the funding has enabled them to establish a collaborative relationship with The Village of Gainesville and its owner, Santa Fe Healthcare Corporation. In response to this, they have established an on-site testing and learning laboratory that includes spaces for aerobic exercise training (4 stations), training via a Nintendo Wii platform (4 stations), and computerized training in speeded visual processing (6 stations). The project has also enabled partnerships with neuroscience (BDNF capture from serum samples), Health and Human Performance (dynamic posturography and balance assessments of exercising older adults). The project has received significant student support (from the College of Public Health and Health Professions, and from the Colleges of Liberal Arts and Sciences, as well as Health and Human Performance), for both graduate and undergraduate students. Future plans will include "interim look" data analysis on 50% of the final anticipated sample in February 2012 (with resulting manuscripts and grant proposals if the results are promising). Both the co-investigators of this project have active age-related research programs – in older adults who are 'normal agers' and those with more rapid dopaminergic depletion disorders (i.e., Parkinson disease). Marsiske has been PI of a 10-year NIA-funded cognitive intervention trial as well as a more recent Robert Wood Johnson Foundation pilot trial. Dr. Marsiske's ability to leverage this project is further supported by his status as a ten-year program director of an NIA-funded predoctoral T32 program, and in his role as Recruitment Core leader of the UF NIA-funded Pepper Center on Aging.

Following three investigators received the ARML funding started in 2011.

Dr. Vonetta Dotson

Title: "*Effect of Exercise on Memory in Geriatric Depression: An fMRI Pilot Study*"

The relationship between depression and age-related memory deficits is well established, and there is increasing evidence to suggest that the underlying neurobiological changes in depression may be the basis of this relationship. Consequently, interventions that reverse or minimize depression-related changes in the brain may have the potential to simultaneously treat memory deficits secondary to depression. The overall aims of this proposal are 1) to examine whether aerobic exercise (AE) improves memory functioning and alters memory-related brain functioning in depressed older adults, and 2) gather preliminary data for an R01 application examining potential mechanisms for the antidepressant and cognitive-enhancing effect of AE in older adults.

This funding has been essential to maintaining her laboratory over the past 9 months and has allowed her to begin developing a new avenue of research, in exercise interventions. Because of difficulty in establishing a consistent recruitment base for the study, data collection began later than expected, but the Dotson lab has now begun enrolling subjects and is eager to gather post-treatment data in the spring to begin their initial analyses. While they have not yet been able to publish data or present at meetings based on the data they have gathered thus far, this project has spurred efforts to achieve NIH funding for this line of research in exercise, aging and depression, and she was recently notified that a diversity supplement to the Lifestyle

Interventions and Independence for Elders (LIFE) Study, which focused on this topic, will be awarded early next year. Dr. Dotson anticipates submitting an R01 in June 2012 based on pilot data from her ARML project, in addition to submitting two manuscripts and an abstract to the Society for Neuroscience conference next year.

Dr. Charles Jason Frazier

Title: "*The Role of Calcium Activated Potassium Channels in Geriatric Memory Dysfunction*"

Many decades of research have confirmed that memory formation depends critically on both the activity and the connectivity of excitable cells in an area of the temporal lobe known as the hippocampus. In his view, one of the central challenges in the study of geriatric memory dysfunction is the identification of specific cellular mechanisms that are both altered by aging and ultimately responsible for decreased memory formation. To date, perhaps the best known single cell correlate of both normal memory formation and geriatric memory dysfunction is the activity of calcium activated potassium channels (SK channels) in hippocampal pyramidal cells. SK channels may be primarily activated by calcium influx through nearby NMDA receptors. Specific aims of this project are to test two hypotheses: 1) two distinct populations of SK channels in CA1 pyramidal cells (those on spine heads vs. those expressed elsewhere in the cell) each have distinct and non-equal effects on calcium influx in dendritic spines and on the induction of spike timing dependent synaptic plasticity, and 2) NMDA receptor hypofunction is apparent at the level of individual dendritic spines in aged CA1 pyramidal cells.

The funding period for Dr. Frazier's ARML award began on April, 2011. Two new members of the team are now actively working on the project – an outstanding graduate student and an experienced cellular neurophysiologist from Harvard Medical School. Their primary experimental effort to date has focused on establishing techniques that will allow them to routinely obtain high quality whole cell patch clamp recordings using tissue taken from aged animals. Issues with viability of acute slices form aged animals has long hampered or outright prevented detailed and mechanistic studies of single cell physiology in aged tissue. Thus, addressing this problem effectively is a key early goal of their proposed studies. Further, they believe that success in this initial step will have significant impact not only for the proposed studies, but also more broadly in the field. In that regard, Dr. Frazier is pleased to note that progress in this area has been exceptional. In fact, after some trial an error, they have now refined their techniques to the point that they have been able to successfully record from > 10 visually identified individual CA1 pyramidal cells in aged tissue taken from just two animals. Thus it appears likely that their modified slice making techniques will effectively enable new and more mechanistic single cell physiological studies in aged tissue.

They have also had reasonably good success so far in establishing techniques for quantitative calcium imaging in these cells using 2-photon based laser scanning epifluorescence microscopy. These efforts have been delayed somewhat by a hardware failure involving the photomultiplier tubes used on the 2P microscope, however, these issues are close to being resolved. Other efforts have gone into establishing protocols for measuring and quantifying SK channel currents in CA1 pyramidal cells, and just this week, into establishing protocols for induction of spike timing dependent plasticity that have a clearly definable threshold for successful induction. Overall, while we are still in the early stages, Dr. Frazier considers the project to be on track. Further, he expects the rate of progress to accelerate in the coming months with the addition of the experienced cellular neurophysiologist to their staff. This project would bring a unique and powerful combination of state of the art techniques not previously used into the field and apply them to investigate a hippocampal neuronal mechanism critically important for age related memory loss.

Dr. Leonid Moroz

Title: *"Epigenomic Bases of Age-related Memory Loss: Single-Neuron Approach"*

All kinds of *long-term* associative and non-associative memories require neuron-specific changes in transcription and translation. Yet, how our memories are formed, and more importantly, how they are stored for an entire human lifetime (i.e. far beyond a few days or few weeks – the maximal half-life of proteins in our body) is one of the greatest enigmas in modern science. How are memories lost as a result of disease, or normal aging, is an opposing set of questions to conceptually the

same fundamental problem. Recent evidence indicates that formation and maintenance of *long-term* memories are in fact pigenetic processes. These processes, which do not change the order of DNA sequences, directly modify access of >1500 transcription factors and other regulators to the core regions in the nuclear genome to activate, suppress, or even change the dynamics of transcription. It is recognized that at least several thousand genes dynamically and persistently change their expression in virtually any neuron in memory-forming circuits to maintain long-term plasticity. However, the scope of these processes at the level of any specific neuronal circuit is completely unknown. Dr. Moroz proposes to investigate two specific aims: 1) to obtain integrated single-neuron transcriptome/methylome genome-wide profiling in age-sensitive and age resistant neurons, and 2) to elucidate dynamics of targets of DNA methylation in individual neurons as function of aging.

As prelude to investigating these specific aims, Dr. Moroz has demonstrated (1) Novel Deuterostome Phylogeny using phylogenomics and deep transcriptome profiling across more than 40 animal lineages (Philippe et al., ***Nature***, 2011a), and (2) evolutionary relationships among the phylum Mollusca representing dozens of experimental models used in fundamental neuroscience and neurobiology of aging (***Nature***, 2011b). These two papers, combined with the relevant cladistic analysis, provided strong evidence for independent origins of complex brains. In fact, his data suggests that complex brains may have independently evolved at least 9-11 times in animal evolution. He also characterized the first synaptic transcriptome (***Cell***, 2011 submitted); it reveals key molecules responsible for learning and memory; plus he identified novel targets that directly link neuronal aging to epigenomic cell machinery (such as 5-hmC and TET) responsible for memory formation and decline. Furthermore, he identified elementary components of molecular machinery that couple cellular excitability with localized protein synthesis (*Nature*, in revision). They consist of novel slack-type channels and RNA-Binding proteins. Cutting edge genomic technology was developed and used to characterize the regulation of transcription associated with synaptic plasticity and brain aging. As a result, Moroz's lab initiated the first genomic dissection of a complete memory-forming circuit using semiconductor sequencing (in preparation). Using these tools of phylogenomics and single-neuron genomics their goal is to determine whether there is a subset of epigenomic "master regulators" responsible for ARML. While he uses a range of species including non-vertebrates, the novel concept should be applicable to higher species up to humans. The investigation of the novel molecular mechanism by this exceptional investigator may revolutionalize the understanding of the biology of age related memory loss. This work has evolved into novel collaborations between Drs. Moroz, Frazier, and Foster. An R21 has been submitted to NIH. In addition, the College of Medicine has invited the researchers to submit a full proposal for the 2012 UF Research Opportunity Seed Fund competition.

Following investigators initiated their research project in 2010 or prior.

Dr. Todd Manini

Title: "*Resveratrol for Improved Performance in Elderly: The RIPE TRIAL*"

Loss in cognitive and physical performance is a frequent complaint in older adults and a growing public health issue. Although the etiology of these age-associated losses is complex and multi-factorial, accumulating research suggests that a key mechanism underlying these declines may be the deleterious effects of oxidative stress. The goal of this research is to develop interventions that are effective in improving or preserving both cognitive and physical function in older persons, and to gather insights into the mechanisms underlying such improvement. Resveratrol, a natural polyphenol present in high concentration in the skin of grapes and in other foods and plants (e.g., peanuts, blueberries), has been found to have potent antioxidant, anti-inflammatory, and neuroprotective effects in both in vitro and in vivo models. A growing body of research suggests that resveratrol supplementation also improves mitochondria function, as well as physical and memory performance in rodents. This suggests that resveratrol may attenuate age-related decrements in cognitive and physical performance in humans. No study to date, however, has tested this hypothesis. The proposed double-blind, randomized, placebo-controlled phase I clinical trial will test the effects of two doses of resveratrol (300 and 1000 mg/day) over 12 weeks on physical and mental function, as well as biomarkers of oxidative stress and inflammation. Study participants will be generally healthy, but overweight, older adults (age range = 65 to 100).

It is hypothesized that resveratrol supplementation will (1) improve cognitive and physical performance and increase hippocampal brain activation patterns in older adults, and (2) reduce systemic oxidative stress and inflammation, which will be negatively correlated with changes in cognitive and physical performance. Thus, the proposed study represents cutting edge, translational research that has the potential to lead to novel treatments for preventing or reducing age-related cognitive and physical decline. This work has resulted in two (2) international oral presentations. Please see references below. All data from this study will be collected and analyzed by the end of January 2012, and the findings of this study will be presented in February 2012.

Dr. Brandi Ormerod
Title: "*Neurogenesis and Cognition Across Age*"
The hippocampus and olfactory bulb add significant numbers of neurons though life. Although the function of adult neurogenesis is speculative, evidence suggests that hippocampal neurogenesis is linked to spatial memory. Dr. Ormerod's lab has just submitted a manuscript to Neurobiology of Aging entitled "Environmental enrichment restores neurogenesis and rapid acquisition in senescent rats" by Speisman, Kumar, Pastoriza, Severance, Foster and Ormerod that shows improved cognition on early water maze training trials and elevated levels of hippocampal neurogenesis in rats exposed to daily enrichment. They are currently preparing 2 other manuscripts from data collected collaborative with the Foster Laboratory. The first shows that running (physical activity) modulates inflammatory cytokines, improves cognition on the rapid morris water maze and enhances neurogenesis in aged rats. The second shows the effects of age on central and circulating inflammatory cytokines and their relationship to water maze performance. The body of work generated by the ARML funds suggests that lifestyle may modulate pro-inflammatory cytokines that affect both cognition and neurogenesis across age.

Dr. Matthew Sarkisian
Title: "*Cilia in Hippocampal Neuronal Plasticity*"
One way to view the cells of the brain is through a continuum of growth potential, where the extremes represent exuberant growth (e.g. cancer) and reduced growth associated with advancing age. Thanks to the start-up funding support of the McKnight Brain Research Institute, Dr. Sarkisian's laboratory has been able to make significant progress in understanding how cilia in the brain contribute to cell growth during development, aging and neurologic disease (e.g., brain tumors). Cilia are tiny hair-like organelles found on virtually every neuron in the brain. Emerging work suggests changes in neural cilia function can disrupt learning and memory, food intake, generation of new neurons in the hippocampus, and neuronal plasticity. The results suggest that age-related changes in cilia (anatomical or physiological) could contribute to memory decline and diminishing neural plasticity during aging. In their quest to determine the general contribution of cilia to brain function, and brain aging in particular, they have examined cilia across brain regions and over the lifespan. In the past year, they reported that every normal cortical neuron has a single cilium. They also characterized the first appearance of neuronal cilia in the cerebral cortex, the growth patterns of these cilia over the lifespan of an animal, and identified cilia on different neuronal subtypes (Arellano et al 2011). Ongoing unpublished data is suggesting that if they tweak the function of neuronal cilia, they can disrupt growth of neuronal processes and synapses. In collaboration with the Foster lab, Dr. Sarkisian's lab has found that cilia persist in the aged brain. Interestingly, the normal molecular machinery evident in neuronal cilia in younger brains (including those shown to influence learning and memory) show altered expression in the aged brain. The results provide a new avenue for investigation of markers of brain aging and suggest potential mechanisms for cognitive changes during aging. The data above has been presented at several meetings including local and Annual Society for Neuroscience and they currently have a manuscript in preparation.

2. Publications in peer reviewed journals

Dr. Jennifer Bizon:
McQuail JA, Bañuelos C, LaSarge CL, Nicolle MM, **Bizon JL** GABAB receptor GTP-binding is decreased in the prefrontal cortex but not the hippocampus of aged rats. *Neurobiology of Aging. In Press.*

{M2588587; 1}

6. **Awards (other):**

Dr. Jennifer Bizon:
Source: NSF Graduate Research Fellowship Award -,
Title: Graduate Research Fellowship Award – Student Blanca Sofia Beas - To study Dopaminergic mechanisms underlying age-related changes in working memory and executive function.
Amount: $100,000.00
Funding Period: 2011-2013
Role: Mentor

Dr. Dawn Bowers:
Source: NIH Predoctoral NRSA grant (F31-NS-073331) - (Graduate student Jenna Dietz
Title: Emotion Psychophysiology in Parkinson's disease.
Funding Period: 05/2011 – 06/2013
Role: Mentor

Award: Previous graduate student Lindsey Kirsch-Darrow, now a post-doc at Johns Hopkins, was 2011 recipient of "Young Investigator Award" from the American Neuropsychiatric Association" for her body of research during graduate school including her dissertation.

Award: graduate student Laura Zahodne was recipient of two national awards from the American Psychological Association. These included: a) 2011 Benton Meier Award for Excellence in Neuropsychology given by Division 40 (Neuropsychology); and b) the 2011 Walter McMillen Memorial Award in Parkinson Disease Research jointly awarded by Divisions 20 (Aging) and 40 (Neuropsychology). Ms. Zahodne also received a scholarship from the Bryan Robinson Endowment for Neuroscience Research, Tallahassee, FL

Award: Dr. Michael Marsiske received the 2010 Doctoral Mentorship award and the 2011 Classroom Teaching award from the Department of Clinical and Health Psychology.

Award: Dr. Marsiske received the 2010 Master Mentor award from the Oak Hammock Institute for Learning in Retirement in Gainesville.

Source: NIA – NRSA (Dr. Marsiske's) graduate student, Shannon Sisco, (F31-AG-034002)
Title: "Neighborhood Influences on Cognitive Level and Training Gains in the ACTIVE Study".
Funding Period: 2011-2013
Role: Mentor

Award: Shannon Sisco also won the Robert Levitt Award for Excellence in Neuropsychology from the Department of Clinical and Health Psychology.

Dr. Todd Manini:
Award: Thomas H. Maren Junior Investigator Award Recipient. Awarded each year to one Assistant Professor in the College of Medicine, University of Florida, Gainesville, FL
Role: Principal Investigator (Anton)

Award: National Institute on Aging, Claude D. Pepper Center
Resveratrol for reduced muscle lipid content in older adults
Role: Principal Investigator (Manini)

Dr. Leonid Moroz:
Source: NIH/NIH R21AG042887
Title: "*Genomic Bases of Differential Aging in Hippocampal Circuits: Single Cell Approach*"
Submitted: Oct 15, 2011
Role: PI

Source: NIH; 1S10RR033041
Title: "*Pacific Biosciences Sequencing Platform*". **Priority Score: 21**; Pending Council review. This proposal is designed to establish a NeuroGenomic Center at UF. We will primarily target neural circuits in mammalian CNS and human tissues.
Role: PI

Dr. Brandi Omerod:
Award: Graduate student Rachel Speisman received an NSF Graduate Research Fellowship award. Awarded $30,000/year for 3 years, 2010-2013, "Using biomarkers to predict successful versus unsuccessful aging in rats".

Dr. Matthew Sarkisian:
Source: American Cancer Society Chris DiMarco Institutional Research Grant Junior Investigator Award
Title: Towards Inhibiting Ciliogenesis to Prevent Glioblastoma"
Amount: $30,000
Funding Period: 12/01/10-11/30/11
Role: PI

Source: University of Florida 2011 Research Opportunity Seed Fund Award from
Title: "Mechanisms of Abnormal Brain Development in the VPA Model of Autism"
Award: $84,000
Funding Period: 05/01/11-04/30/13
Role: Co-PI (with Dr. Mark Lewis, Psychiatry)

Source: University of Florida McKnight Brain Institute Agency: Brain & Spinal Cord Injury Research Trust Fund (BSCIRTF
Title: "A Comparison of Pathogenic Processes in Acute Spinal Cord Injury and ALS"
Award: $50,000
Funding Period: 07/01/11-06/30/12
Role: Co-PI (with Dr. David Borchelt, Neuroscience)

7. **Faculty. Please include abbreviated CV with publications for previous 12 months:**
   See Attached

8. **Trainees**

   a) Post doctoral

   Dr. Jennifer Bizon:
   Karienn Montgomery
   Cristina Banuelos
   Blanca Sofia Beas

   Dr. Dawn Bowers:
   Michelle Prosje, Psy.D. (Clinical post-doc, 2009-2011)
   Caleb Peck, Psy.D. (Clinical post-doc, 2011-ongoing)
   Dr. Michael Marsiske:
   Patricia Belchior, PhD. (NIA-funded post-doc, 2009-2010)

19. Did all activities during the report period further the Purpose?

Yes

20. Please describe any negative events (loss of personnel, space, budget, etc.) that occurred during the report period and the possible impact on carrying out the Gift Agreement.

None

21. Please provide any general comments or thoughts not covered elsewhere – a response is not required. Please respond only if you would like to add something not otherwise covered elsewhere.

See attached letter.

22. Signature, date, and title of person submitting the report.

Tetsuo Ashizawa, M.D.
Executive Director
Evelyn F. & William L. McKnight Brain Institute
University of Forida

{M2588587; 1}

Annual Report
McKnight Brain Research Foundation
Sponsored Institutes and Research Programs
(Include activity of all McKnight supported faculty and trainees)
Report Period: January 2011 - January 2012

Some gift agreements require both Institute reports and Chair reports. If applicable, please clearly state whether a particular response relates to a Chair or Institute.

Any capitalized terms used on the template are intended to have the same meaning as the term is defined in the Gift Agreement.

Chair Report

1. **Summary of scientific achievements since last report**

   This year we have seven manuscripts either published or accepted for publication in scientific journals. In addition, I have received a renewal of funding for a grant looking at effect of estrogen on cognition across the lifespan and I received a MERIT award for a grant from the National Institute of Aging to examine signaling cascades and memory deficits during aging.

   Late-life interventions to reverse senescent neurophysiology and cognitive decline: In 2010-2011 we published several papers linking the age-related increase in oxidative stress and altered redox state to physiological markers of memory decline. This past year we attempted to reverse oxidative stress in the hippocampus using viral vector mediated delivery of antioxidant enzymes. We asked the question whether increasing antioxidant enzymes in older animals could reduce oxidative damage and improve cognitive function. We used adeno-associated virus to deliver antioxidant enzymes (superoxide dismutase [SOD1, SOD2], catalase [CAT], and SOD1+CAT) to the hippocampus of young (4 months) and aged (19 months) F344/BN F1 male rats and examined memory-related behavioral performance 1 month and 4 months postinjection. **Results:** Overexpression of antioxidant enzymes reduced oxidative damage; however, memory function was not related to the level of oxidative damage. Increased expression of SOD1, initiated in advanced age, impaired learning. Increased expression of SOD1+CAT provided protection from impairments associated with overexpression of SOD1 alone and appears to guard against cognitive impairments in advanced age. **Conclusion:** Oxidative stress is a likely component of aging; however, it is unclear whether increased production of reactive oxygen species or the accumulation of oxidative damage is the primary cause of functional decline. The results provide support for the idea that altered redox-sensitive signaling rather than the accumulation of damage may be of greater significance in the emergence of age-related learning and memory deficits.

   A second series of studies examined the effects of environmental enrichment (e.g. engaged lifestyle) or exercise on senescent physiology and memory function. **Results:** Spatial discrimination learning and memory consolidation, tested on the water maze, were enhanced in environmentally-enriched compared with sedentary animals. Animals in the exercise group exhibited improved and impaired performance on the cue and spatial task, respectively. Impaired spatial learning was likely due to a bias in response selection associated with exercise training, as object recognition memory improved for exercised rats. An examination of senescent hippocampal physiology revealed that enrichment and exercise reversed age-related changes in long-term depression (LTD) and long-term potentiation (LTP). Rats in the enrichment group exhibited an increase in cell excitability compared with the other 2 groups of aged animals. **Conclusion:** The results indicate that factors common across the two conditions, such as increased hippocampal activity associated with locomotion, contribute to reversal of senescent synaptic plasticity. However, differential experience biased the selection of a spatial or response strategy, as such the greatest improvement in cognition was observed for environmental enrichment.

Estrogen and cognition across the lifespan: I published a major review/position paper providing evidence for the idea that the expression of estrogen receptor alpha and beta (ERalpha and ERbeta) interacts with the level of estradiol (E2) to influence the etiology of age-related cognitive decline and responsiveness to E2 treatments. The conclusion is that an age-related shift in the relative expression of ERalpha/ERbeta, combined with declining gonadal E2 levels can impact transcription, cell signaling, neuroprotection, and neuronal growth. Finally, the role of ERalpha/ERbeta on rapid E2 signaling and synaptogenesis as it relates to hippocampal aging was discussed.

My lab engaged in a number of collaborations with others at the University of Florida looking at genes involved in age-related cognitive decline (Muzyczka lab), late life intervention for sarcopenia (Carter lab), and influence of caloric restriction on age-related oxidative stress in the hypothalamus (Tumer lab).

2. Publications in peer reviewed journals

Carter, C. S., Marzetti, E., Leeuwenburgh, C., Manini, T., **Foster**, T. C., Groban, L., Scarpace, P. J. and Morgan, D. Usefulness of Preclinical Models for Assessing the Efficacy of Late-Life Interventions for Sarcopenia. *J Gerontol A Biol Sci Med Sci.*

Foster, T. C. Role of estrogen receptor alpha and beta expression and signaling on cognitive function during aging. *Hippocampus*.

Kumar, A., Rani, A., Tchigranova, O., Lee, W. H. and **Foster**, T. C. Influence of late-life exposure to environmental enrichment or exercise on hippocampal function and CA1 senescent physiology. *Neurobiol Aging*.

Lee, W. H., Kumar, A., Rani, A., Herrera, J., Xu, J., Someya, S. and **Foster**, T. C. Influence of Viral Vector-Mediated Delivery of Superoxide Dismutase and Catalase to the Hippocampus on Spatial Learning and Memory During Aging. *Antioxid Redox Signal.*

Whidden, M. A., Kirichenko, N., Halici, Z., Erdos, B., **Foster**, T. C. and Tumer, N. Lifelong caloric restriction prevents age-induced oxidative stress in the sympathoadrenal system of Fischer 344 x Brown Norway rats. *Biochem Biophys Res Commun* **408,** 454-458.

Wu, K., Li, S., Bodhinathan, K., Meyers, C., Chen, W., Campbell-Thompson, M., McIntyre, L., Foster, T. C., Muzyczka, N. and Kumar, A. Enhanced expression of Pctk1, Tcf12 and Ccnd1 in hippocampus of rats: Impact on cognitive function, synaptic plasticity and pathology. *Neurobiol Learn Mem.*

Zhou, F. W., Rani, A., Martinez-Diaz, H., **Foster**, T. C. and Roper, S. N. Altered behavior in experimental cortical dysplasia. *Epilepsia.*

3. Publications (other)

4. Presentations at scientific meetings

Speisman RB, Kumar A, Rani A, **Foster** TC, and Ormerod BK (2011) Circulating and central inflammatory cytokines linked to hippocampal neurogenesis; both modified by running in aged rats. Soc for Neurosci.

M. Guidi, A. Rani, G. Prado, A Kumar, T C. **Foster** (2011) Biomarkers of age-related memory syndrome: Differentiating between learning and memory using a spatial discrimination task. Soc for Neurosci.

A. Kumar, A Rani, and T.C. **Foster** (2011) Memory consolidation deficit is associated with decreased NMDA receptor synaptic responses at CA3-CA1 hippocampal synapses. Soc for Neurosci.

{M2588587;1}

X. Han, K. K. Aenlle, A. Kumar, A. Rani, T. C. **Foster** (2011) Role of estrogen receptor alpha and beta in preserving hippocampal function during aging. Soc for Neurosci.

5. Presentations at public (non-scientific) meetings or events

Brain and behavior: Contemplative practices and the brain. Jacksonville, FL. Riverside Presbyterian Church 2/24/2011.

NIH Grant Application Workshop, Department of Neurology, Gainesville, FL. Response to prior review. 5/31/2011.

6. Awards (other)

University of Florida, College of Medicine Exemplary Teacher

University of Florida, College of Medicine Doctoral Mentoring Award

National Advisory Council on Aging NIH Method to Extend Research in Time (MERIT) Award (8/2/2011)

7. Faculty. Please include abbreviated CV with publications for previous 12 months

8. Trainees

a) Post doctoral:
Ashok Kumar (Research Associate)

b) Pre-doctoral
Wei-Hua Lee, Ph.D. program
Xiaoxia Han, Ph.D. program
Mike Guidi, Ph.D. program
Linda Bean, Ph.D. program

c) Other
Asha Rani
Olga Tchigrinova

9. Clinical/translational programs

a) New programs

b) Update on existing clinical studies

In 2009 I took over as Chair for the committee overseeing the Age-Related Memory Loss (ARML) Program. Other members of the committee include Drs. Lucia Notterpek, Tetsua Ashizawa, and Christiaan Leeuwenburg.

i. During the past year Dr Jen Bizon moved to the University of Florida as a new member of the ARML Program. We are collaborating on several projects examining executive function and GABA-B receptors during aging. A grant proposal on this work has been submitted to NIH. In addition, Dr. Bizon is currently the Chair for a search committee to find another researcher to join the ARML program and has participated as a member of the McKnight Cognitive Battery Working group.

ii. The committee provided funding, guidelines and goals for the Village Wellness Study. This study under the direction of Drs Dawn Bowers and Michael Marsiske is investigating the effects of exercise pre-dosing on the cognitive training gains

of older adults. The funding has enabled the researchers to establish a collaborative relationship with The Village of Gainesville and its owner, Santa Fe Healthcare Corporation. An on-site testing and learning laboratory has been established. This site includes spaces for aerobic exercise training (4 stations), training via a Nintendo Wii platform (4 stations), and computerized training in speeded visual processing (6 stations). The committee has requested an interim report and data analysis for February 2012.

iii. The committee provided pilot funding to Dr. Brandi Ormerod. This funding is near completion and resulted in NSF funding for a graduate student (Rachel Speisman) working on biomarkers of cognitive decline, a funded R01 to Drs Ormerod and Foster (Signaling cascades and memory deficits during aging), and multiple presentations at scientific conferences. A manuscript has been submitted to Neurobiology of Aging and is currently under review.

iv. In 2010 the committee put out a request for applications and in 2011 the committee provided pilot grant funding for three projects.

Dr. Vonetta Dotson is characterizing the effect of exercise on memory in geriatric depression. This is an fMRI pilot study to examine whether aerobic exercise improves memory functioning and alters memory-related brain functioning in depressed older adults. The project has received IRB approval, has started enrolling subjects and has started exercise intervention on the first cohort.

Dr. Leonid Moroz is using cutting edge technology characterize the regulation of transcription associated with synaptic plasticity and brain aging. As part of his work he published two papers in 2011 in the highly prestigious journal *Nature*. The goal of this project is to determine whether there is and epigenomic basis of age-related memory loss. This work has evolved into collaborations between Drs Moroz, Frazier, and Foster. An R21 for this work has been submitted to NIH. In addition, the College of Medicine has invited the researchers to submit a full proposal for the 2012 UF Research Opportunity Seed Fund competition.

Dr Jason Frazier's work uses calcium imaging and electrophysiology techniques to examine age-related changes in cellular mechanisms that are thought to regulate memory formation. This work will test the hypothesis that increased calcium activated potassium channel activity during aging effectively reduce cellular excitability and increases the threshold for synaptic plasticity. A postdoc has been hired and, together with a graduate student, have started the studies. An NIH grant proposal, based on this work, should be submitted in 2012.

10. Technology transfer

a) Patents applications
b) Revenue generated from technology

11. Budget update (last year's budget and actual results - with an explanation of material variances)

a) Status of matching funds, if applicable
b) Projected budget for coming year
c) Extramural funding

12. Educational programs focusing on age related memory loss

a) Scientific
b) Public

{M2588587;1}

13. **Collaborative programs with other McKnight Institutes, institutions and research programs.**

    I am a member of a working group examining a library of age-sensitive tasks that can be used to translate findings across different levels of analysis, between humans and animal models of aging. I am acting in my capacity as an Associated Editor and as an author on several of the manuscripts, to publish this body of work (7 manuscripts) in the Journal *Frontiers in Aging Neuroscience*.

14. **Collaborative program with non McKnight Institutes, institutions and research programs**

    I have a collaboration with Jill Daniel at Tulane University to examination over expression of estrogen receptor alpha as a mechanism to prevent age-related cognitive decline. A manuscript has been submitted (Dec 14).

15. **Briefly describe plans for future research and/or clinical initiatives**

    a) We will be examining the effect of non-steroidal anti-inflammatory drugs on age-related cognitive decline and brain aging. It is hypothesized that neuroinflammation contributes to oxidative stress, which mediates senescent physiology and memory decline.

    b) Examination of the effects of altering the expression of estrogen receptor alpha and beta on cognition and gene regulation in the hippocampus. It is hypothesized that the alpha receptor promotes growth and cell health, maintaining hippocampal function during aging.

    c) Gene markers of aging in individual cells. It is hypothesized that there is variability between brain regions and between individual cells in vulnerability to aging. We will initiate the preliminary studies for this work.

    d) We will be collecting preliminary data for our grant on mechanisms of altered synaptic function during aging. This work focuses on the hypothesis that a change in redox state mediates Ca^{2+} dysregulation to alter mechanisms for synaptic plasticity.

16. **If applicable, please provide endowment investment results for the report period.**

17. **Where any funds used for a Prohibited Purpose during the report period?** No.

18. **Do you recommend any modification to the Purpose or mandates in the Gift Agreement?** No.

19. **Did all activities during the report period further the Purpose?** Yes.

20. **Please describe any negative events (loss of personnel, space, budget, etc.) that occurred during the report period and the possible impact on carrying out the Gift Agreement.**

21. **Please provide any general comments or thoughts not covered elsewhere – a response is not required. Please respond only if you would like to add something not otherwise covered elsewhere.**

22. **Signature, date, and title of person submitting the report.**

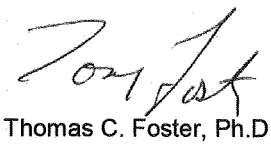

Thomas C. Foster, Ph.D.
Professor and Evelyn F. McKnight Chair for Research on Cognitive Aging and Memory

{M2588587;1}

University of Florida Health Science Center

2011 Annual Report

Age Related Memory Loss (ARML) Program
& Cognitive Aging and Memory Clinical and
Translational Research Program (CAM-CTRP)

Prepared for the McKnight Brain Research Foundation
by the University of Florida
McKnight Brain Institute and Insitute on Aging

CAM-CTRP

UF | Health Science Center
UNIVERSITY of FLORIDA

UF UNIVERSITY of FLORIDA

Institute on Aging
Department on Aging and Geriatric Research
College of Medicine

PO Box 100107
Gainesville, FL 32610-0107
352-265-7227
352-265-7228 Fax

January 9, 2012

Dear McKnight Brain Research Foundation Trustees:

Thank you for the opportunity to present a progress report to the McKnight Brain Research Foundation (MBRF) for the period January 1, 2011 to December 31, 2011. Activity during this timeframe has involved ongoing recruitment of the Director of the Cognitive Aging and Memory Clinical Translational Research Program (CAM-CTRP). In early October, 2009, a national search committee was established, chaired by Tom Foster, PhD. Committee members include Michael Marsiske, PhD.; Herb Ward, MD; Stephen Anton, PhD; Tony Yachnis, MD and Ken Heilman, MD. This original search committee remains intact and continues to serve the recruitment.

Recruiting a Director for the CAM-CTRP continues to be our highest priority. Committee members sent personal invitations to colleagues announcing the opportunity, and in addition, advertisements for the position were placed in six premier medical journals. At the recommendation of the search committee, advertisements to recruit an Associate Director were placed in these premier journals in 2010.

To date, we have identified twelve (12) candidates who have demonstrated significant accomplishments in the field and who, we believe, would be an asset to the Institute. These candidates include Anna Mariya Barrett, MD; Ronald A. Cohen, PhD, ABPP, APCN; Charles DeCarli, MD; Yonas Geda, MD, MSc; Keith Josephs, MST, MD, MS; Kenneth Langa, MD, PhD; Eric J. Lenze, MD; Paul A. Newhouse, M.D.; Caterina Rosano, MD, MPH; Steven L. Small, PhD, MD; Warren D. Taylor, MD, MHSc; and Madhav Thambisetty, MD, PhD. The attached candidate list contains more complete information including dates of interviews and status of recruitment. Successful recruitment of the Director has been more challenging than we originally anticipated.

The search is particularly challenging because of the highly specific position requirements. Despite the challenges, we have narrowed the search down to two very highly qualified candidates, and hope to secure a commitment in the next few months.

In 2010 the NIH NCRR C06RR029852, Construction Grant, Institute on Aging Clinical Translational Research Building was funded (Principal Investigator: Pahor, M, 4/1/2010-1/31/2015, $14,995,000), which will host the CAM-CTRP. The latter and the MBRF support played a pivotal role for the successful funding of that grant.

Please find attached a projected budget for the use of the MBRF funds. To date, we have received funding of $2,590,984. During the period of October – December 2009, we expended approximately $10,852. During the period of January 1 – December 31, 2010,

we expended approximately $50,829. During the period of January 1 – December 31, 2011, we anticipate expending $40,825, leaving approximately $2,488,478 unencumbered for the current reporting period. In addition we anticipate annual endowment income of approximately $470,845. The attached projected budget will be negotiated and updated once the director is successfully recruited to lead the CAM-CRTP. We anticipate substantial escalation on expenses once the program begins to take shape. You will also find attached a MBRF endowment report.

We deeply appreciate our partnership with the MBRF in the development of an interdisciplinary research program, which translates basic science discoveries regarding cognitive aging and memory into clinical applications to slow, avert or restore the age-related cognitive decline and memory loss.

Sincerely,

Marco Pahor, MD
Professor and Chair,
Department of Aging and Geriatric Research
Director, Institute on Aging

COGNITIVE AGING and MEMORY CLINICAL TRANSLATIONAL RESEARCH PROGRAM (CAM-CTRP) DIRECTOR/ASSOCIATE DIRECTOR CANDIDATES

The search for the CAM-CTRP director or associate director is actively proceeding. Among a large pool of potential candidates who have been screened, to date a total of 12 qualified candidates, who are listed below, have been interviewed for the position. The search is particularly challenging because of the position requirements, including the highly specific research focus, the track record in NIH funding, and the career rank.

Anna Mariya Barrett, MD
Program Director, Kessler Foundation Research Center
Stroke Rehabilitation Research
Professor, University of Medicine and Dentistry
New Jersey—the New Jersey Medical School
West Orange, New Jersey
First visit: February 22-24, 2010

Ronald A. Cohen, PhD, ABPP, APCN
Professor, Department of Psychiatry and Human Behavior
Brown University
Providence, RI
First Visit: November 17-18, 2011
Second Visit: December 12-13, 2011

Charles DeCarli, MD
Director of Faculty Development in the Department of Neurology
University of California at Davis
Sacramento, CA
First visit: February 1-3, 2010

Yonas Geda, MD, MSc
Associate Professor of Neurology and Psychiatry
College of Medicine, Mayo Clinic
Rochester, MN
First visit: June 21-22, 2010
Second visit: September 7-9, 2010

Keith A. Josephs, MST, MD, MS
Associate Professor of Neurology
College of Medicine, Mayo Clinic
Rochester, MN
Phone interview: December 16, 2010
To be scheduled in January or February 2011

Kenneth Langa, MD, PhD
Professor, Department of Internal Medicine
Division of General Medicine
University of Michigan
First visit: August 12-13, 2010

Eric J. Lenze, MD
Professor, Department of Psychiatry
Washington University School of Medicine
St. Louis, MO
First visit: September 29-30, 2011

Paul A. Newhouse, MD
Director, Clinical Neuroscience Research Unit and Brain Imaging Program
Professor, Department of Psychiatry
University of Vermont College of Medicine
Burlington, VT
First visit: January 19-21, 2010
Second visit: June 10-13, 2010

Caterina Rosano, MD, MPH
Associate Professor of Epidemiology
Center for Healthy Aging and Population
Graduate School of Public Health
University of Pittsburgh
Pittsburgh, PA
First visit: February 10-12, 2010

Steven L. Small, PhD, MD
Associate Chair for Research
Department of Neurology
The University of Chicago
Chicago, IL
First visit: November 17-19, 2009

Warren D. Taylor, MD, MHSc
Associate Professor, Department of Psychiatry
Chair, DUHS Institutional Review Board
Duke University School of Medicine
Durham, NC
First visit: December 15-16. 2011

Madhav Thambisetty, MD, PhD
Neurology Staff Clinician
Clinical Research Branch
National Institutes of Health
Adjunct Assistant Professor
Department of Neurology
Johns Hopkins University School of Medicine
Baltimore, MD
First visit: September 22-24, 2010
Second visit: December 8-10, 2010

University of Florida Health Science Center

2011 Annual Report

Age Related Memory Loss (ARML) Program
& Cognitive Aging and Memory Clinical and
Translational Research Program (CAM-CTRP)

Prepared for the McKnight Brain Research Foundation
by the University of Florida
McKnight Brain Institute and Insitute on Aging

Financials

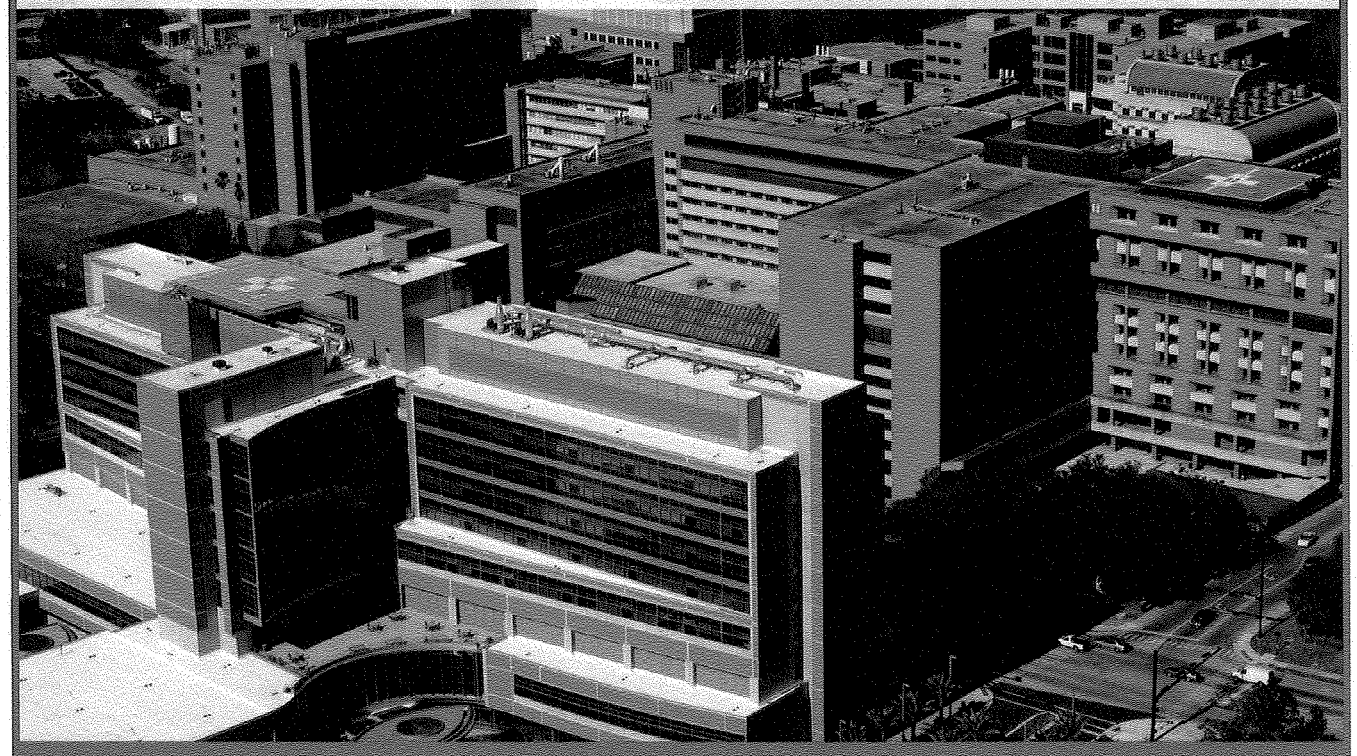

UF | Health Science Center
UNIVERSITY of FLORIDA

UF | UNIVERSITY of FLORIDA

Office of the Senior Vice President, Health Affairs
President, UF & Shands Health System

1600 SW Archer Road
PO Box 100014
Gainesville, FL 32610-0014
352-273-5600 Tel
352-392-9395 Fax

January 9, 2012

The McKnight Brain Research Foundation
The SunTrust Bank
Mail Code FL-ORL-2160
300 South Orange Avenue, Suite 1600
Orlando, FL 32801

Dear Trustees:

Enclosed are the following summary Income and Expenditure statements for the year ended December 31, 2011:

- McKnight Brain Research Grant (F008057/58)
- McKnight Chair (F007889/90)
- CAM-CTRP Budget (F016327)

These reports have been prepared by the respective units and reviewed by me. I believe they represent their financial activities for the 2011 calendar year.

Thank you for the opportunity to work with you in our efforts to understand the mechanisms of age-related memory loss and to aid in its prevention. Let me know if you have any questions about this information.

Sincerely,

Russell E. Armistead, MBA, CPA
Associate Vice President for Finance & Planning
UF Health Science Center

McKnight Brain Research Grant
F008057/58
January 1, 2011 to December 31, 2011

Foundation Spendable Account		Amount	
Endowment income transferred in:			
March 31, 2011		$ 245,926	
June 30,2011		253,330	
Sept 30, 2011		256,575	
Dec 31, 2011		256,576	
Total endowment income transferred in		1,012,407	
Transferred out:			
Transferred to the Institute on Aging, Feb 16, 2011		470,844	
Funding established for pilot studies:			
Dr. Manini, Jan 21, 2011	$ 65,000		
Dr. Bowers (VITAL Project), Apr 18, 2011	77,855		
Dr. Frazier, Apr 18, 2011	100,000		
Dr. Moroz, June 22, 2011	100,000		
Dr. Dotson, July 15, 2011	100,000		
Dr. Bowers (VITAL Project), Sept 21, 2011	30,000	472,855	
Dr. Bizon (FY11 startup and salary support)		372,287	
Transferred to UF Peoplesoft spendable accounts[1]		714,799	[1]
Total transferred out		2,030,785	
Net change in foundation spendable account		(1,018,378)	
Beginning balance, January 1, 2011		1,418,320	
Ending balance, December 31, 2011		**399,942**	
Allocation of ending balance:			
Amount due to the Institute on Aging	$ 271,654		
Remaining funds for Age Related Memory Loss	128,288	**$ 399,942**	

UF PeopleSoft Accounts	Amount	
Received from foundation spendable account	$ 714,799	[1]
Expenditures and transfers:		
Dr. Bizon salary	52,219	
Dr. Sarkisian salary	93,529	
Dr. Foster commitment	135,207	
Dr. Ormerod commitment	11,055	
Dr. Moroz commitment	9,825	
Dr. Bowers (VITAL Project)	25,000	
Advertising and other	633	
Total expenditures	327,468	
Net change in UF Peoplesoft accounts	387,331	
Beginning balance, January 1, 2011	365,732	
Ending balance, Dec 31, 2011	**$ 753,063**	

McKnight Chair
F007889/90
Financial Summary
January 1, 2011 to December 31, 2011

Foundation Spendable Account		Amount	
Endowment income transferred in:			
March 31, 2011	$	37,498	
June 30,2011		38,626	
Sept 30, 2011		39,121	
Dec 31, 2011		39,122	
Total endowment income transferred in		154,367	
Transferred to UF Peoplesoft spendable accounts[1]		200,000	[1]
Net change in foundation spendable account		(45,633)	
Beginning balance, January 1, 2011		179,997	
Ending balance, December 31, 2011	**$**	**134,364**	

UF PeopleSoft Accounts		Amount	
Received from foundation spendable account	$	200,000	[1]
Expenditures:			
Faculty and research staff salaries		109,530	
Research equipment, supplies, and services		22,968	
Travel and other		4,435	
Total expenditures		136,933	
Net change in UF Peoplesoft accounts		63,067	
Beginning balance, January 1, 2011		188,573	
Ending balance, Dec 31, 2011	**$**	**251,640**	

Budget - CAM-CTRP

Personnel Name	1/1/12-12/31/12 Year 4	1/1/13-12/31/13 Year 5	1/1/14-12/31/14 Year 6	1/1/15-12/31/15 Year 7	1/1/16-12/31/16 Year 8			10/1/09-12/31/09 Year 1	1/1/10-12/31/10 Year 2	1/1/11-12/31/11 Year 3	1/1/12-12/31/12 Year 4	1/1/13-12/31/13 Year 5	1/1/14-12/31/14 Year 6	1/1/15-12/31/15 Year 7	1/1/16-12/31/16 Year 8	TOTALS
TBA MD	100%	100%	75%	50%	50%	$ 265,000	Salary	$ -	$ -	$ -	$ 140,569	$ 289,573	$ 223,695	$ 149,130	$ 149,130	$ 952,097
Program Director	6 mos					0.2342	Fringe	$ -	$ -	$ -	$ 32,921	$ 67,818	$ 52,389	$ 34,926	$ 34,926	$ 222,981
Professor							Total Sal	$ -	$ -	$ -	$ 173,491	$ 357,391	$ 276,084	$ 184,056	$ 184,056	$ 1,175,078
TBA MD	100%	100%	75%	50%	50%	$ 225,680	Salary	$ -	$ -	$ -	$ 119,712	$ 246,607	$ 190,504	$ 127,002	$ 127,002	$ 810,827
Associate Professor	6 mos					0.2342	Fringe	$ -	$ -	$ -	$ 28,037	$ 57,755	$ 44,616	$ 29,744	$ 29,744	$ 189,896
							Total Sal	$ -	$ -	$ -	$ 147,748	$ 304,362	$ 235,120	$ 156,746	$ 156,746	$ 1,000,723
TBA MD	100%	100%	75%	50%	50%	$ 176,800	Salary	$ -	$ -	$ -	$ 93,784	$ 193,194	$ 149,242	$ 99,495	$ 99,495	$ 635,210
Assistant Professor	6 mos					0.2342	Fringe	$ -	$ -	$ -	$ 21,964	$ 45,246	$ 34,953	$ 23,302	$ 23,302	$ 148,766
							Total Sal	$ -	$ -	$ -	$ 115,748	$ 238,440	$ 184,195	$ 122,797	$ 122,797	$ 783,976
TBA MD	100%	100%	75%	50%	50%	$ 42,204	Salary	$ -	$ -	$ -	$ 22,387	$ 46,117	$ 35,626	$ 23,750	$ 23,750	$ 151,631
Post Doc Fellow	6 mos					0.1825	Fringe	$ -	$ -	$ -	$ 4,086	$ 8,416	$ 6,502	$ 4,334	$ 4,334	$ 27,673
							Total Sal	$ -	$ -	$ -	$ 26,473	$ 54,534	$ 42,127	$ 28,085	$ 28,085	$ 179,304
TBA MD	100%	100%	75%	50%	50%	$ 42,204	Salary	$ -	$ -	$ -	$ 22,387	$ 46,117	$ 35,626	$ 23,750	$ 23,750	$ 151,631
Post Doc Fellow	6 mos					0.1825	Fringe	$ -	$ -	$ -	$ 4,086	$ 8,416	$ 6,502	$ 4,334	$ 4,334	$ 27,673
							Total Sal	$ -	$ -	$ -	$ 26,473	$ 54,534	$ 42,127	$ 28,085	$ 28,085	$ 179,304
TBA	100%	100%	100%	100%	100%	$ 45,000	Salary	$ -	$ -	$ -	$ 23,870	$ 49,173	$ 50,648	$ 50,648	$ 50,648	$ 224,987
Admininstrative Mgr	6 mos					0.3286	Fringe	$ -	$ -	$ -	$ 7,844	$ 16,158	$ 16,643	$ 16,643	$ 16,643	$ 73,931
							Total Sal	$ -	$ -	$ -	$ 31,714	$ 65,331	$ 67,291	$ 67,291	$ 67,291	$ 298,917
TBA	25%	25%	25%	25%	25%	$ 58,000	Salary	$ -	$ -	$ -	$ 7,692	$ 15,845	$ 16,320	$ 16,320	$ 16,320	$ 72,496
Clinical res. study mgr	6 mos					0.3286	Fringe	$ -	$ -	$ -	$ 2,527	$ 5,207	$ 5,363	$ 5,363	$ 5,363	$ 23,822
							Total Sal	$ -	$ -	$ -	$ 10,219	$ 21,051	$ 21,683	$ 21,683	$ 21,683	$ 96,318
TBA	50%	25%	25%	25%	25%	$ 40,000	Salary	$ -	$ -	$ -	$ 10,609	$ 10,927	$ 11,255	$ 11,255	$ 11,255	$ 55,302
Res. Study Coordinator	6 mos					0.3286	Fringe	$ -	$ -	$ -	$ 3,486	$ 3,591	$ 3,698	$ 3,698	$ 3,698	$ 18,172
							Total Sal	$ -	$ -	$ -	$ 14,095	$ 14,518	$ 14,954	$ 14,954	$ 14,954	$ 73,474
Total FTE	675%	650%	525%	400%	400%		Salary	$ -	$ -	$ -	$ 441,010	$ 897,553	$ 712,915	$ 501,351	$ 501,351	$ 3,054,180
							Fringe	$ -	$ -	$ -	$ 104,951	$ 212,607	$ 170,665	$ 122,345	$ 122,345	$ 732,913
Personnel							Total	**$ -**	**$ -**	**$ -**	**$ 545,960**	**$ 1,110,160**	**$ 883,581**	**$ 623,696**	**$ 623,696**	**$ 3,787,093**

Personnel	Total	$ -	$ -	$ -	$ 545,960	$ 1,110,160	$ 883,581	$ 623,696	$ 623,696	$ 3,787,093
Consultants										
External Advisory Board members (4@1500 honorarium)		$ -	$ -	$ -	$ 6,000	$ 6,000	$ 6,000	$ 6,000	$ 6,000	$ 30,000
External Advisory Board members (4@1250 travel funds)		$ -	$ -	$ -	$ 5,000	$ 5,000	$ 5,000	$ 5,000	$ 5,000	$ 25,000
Expert Speakers @2 per year)		$ -	$ -	$ -	$ 5,000	$ 5,000	$ 5,000	$ 5,000	$ 5,000	$ 25,000
	Sub Consultants	$ -	$ -	$ -	$ 16,000	$ 16,000	$ 16,000	$ 16,000	$ 16,000	$ 80,000
Equipment										
Computers/printers (8@3000)		$ -	$ -	$ -	$ -	$ 24,000	$ -	$ -	$ -	$ 24,000
Info Services		$ -	$ -	$ -	$ 27,000	$ 27,000	$ 27,000	$ 27,000	$ 27,000	$ 135,000
	Sub Equipment	$ -	$ -	$ -	$ 27,000	$ 51,000	$ 27,000	$ 27,000	$ 27,000	$ 159,000
Travel										
Recruitment costs		$ 1,089	$ 20,018	$ 8,072	$ 5,000	$ 5,000	$ 5,000	$ 5,000	$ 5,000	$ 54,179
Professional Travel (specialty conferences, collaborators, etc.)		$ -	$ -	$ -	$ 15,000	$ 15,000	$ 15,000	$ 15,000	$ 15,000	$ 75,000
	sub travel	$ 1,089	$ 20,018	$ 8,072	$ 20,000	$ 20,000	$ 20,000	$ 20,000	$ 20,000	$ 129,179
Supplies										
Software & administrative supplies		$ -	$ -	$ -	$ 10,000	$ 10,000	$ 10,000	$ 10,000	$ 10,000	$ 50,000
Publications Cost (slides, posters)		$ -	$ -	$ -	$ 2,500	$ 2,500	$ 2,500	$ 2,500	$ 2,500	$ 12,500
	sub supplies	$ -	$ -	$ -	$ 12,500	$ 12,500	$ 12,500	$ 12,500	$ 12,500	$ 62,500
Other Cost										
Meals, entertainment (faculty recruitment, consultants, other mtg costs)		$ -	$ -	$ -	$ 5,000	$ 5,000	$ 5,000	$ 5,000	$ 5,000	$ 25,000
Relocation Costs (faculty recruitment)		$ -	$ -	$ -	$ -	$ 15,000	$ -	$ -	$ -	$ 15,000
Program supervision, coordination and administration		$ 6,197	$ 20,584	$ 25,327	$ 26,086	$ 26,869	$ 27,675	$ 28,505	$ 29,360	$ 190,604
License, insurance, dues, subscriptions		$ -	$ -	$ -	$ 25,000	$ 25,000	$ 25,000	$ 25,000	$ 25,000	$ 125,000
Advertising		$ 3,565	$ 10,227	$ 7,426	$ 5,000	$ 5,000	$ 5,000	$ 5,000	$ 5,000	$ 46,218
Start-up Packages (faculty recruitment)		$ -		$ -	$ 20,000	$ -	$ 20,000	$ 20,000	$ 20,000	$ 80,000
Pilot Projects		$ -	$ -	$ -	$ 100,000	$ 100,000	$ 100,000	$ 100,000	$ 100,000	$ 500,000
	Sub total Other	$ 9,762	$ 30,811	$ 32,753	$ 181,086	$ 176,869	$ 182,675	$ 183,505	$ 184,360	$ 981,822
Total Annual Costs		$ 10,852	$ 50,829	$ 40,825	$ 802,547	$ 1,386,529	$ 1,141,756	$ 882,701	$ 883,556	$ 5,199,595
Available Funds- Beginning of Year:										
Initial Transfer from UFF (50% of accumulated non-endowed funds, approx. $3.2 million)		$ 1,634,217								$ 1,634,217
Anticipated Annual Endowment Income		$ -	$ 470,844	$ 470,845	$ 470,845	$ 470,845	$ 470,845	$ 470,845	$ 470,845	$ 3,295,912
Transferred to PeopleSoft Account at UF		$ (200,000)	$ -	$ -	$ (800,000)	$ (1,400,000)	$ (1,200,000)	$ (900,000)	$ (699,595)	$ (5,199,595)
	Funds at UF Foundation	$ 1,434,217	$ 1,905,061	$ 2,375,906	$ 2,046,751	$ 1,117,595	$ 388,440	$ (40,716)	$ (269,466)	$ (269,466)
Less Actual expenditures		$ 10,852	$ 50,829	$ 40,825	$ 802,547	$ 1,386,529	$ 1,141,756	$ 882,701	$ 883,556	$ 5,199,595
Funds in PeopleSoft Account at UF		$ 189,148	$ 138,319	$ 97,495	$ 94,948	$ 108,419	$ 166,663	$ 183,962	$ 0	$ (0)
	Available Funds- End of Year	$ 1,623,365	$ 2,043,381	$ 2,473,401	$ 2,141,698	$ 1,226,014	$ 555,103	$ 143,246	$ (269,466)	$ (269,466)

* Note: Expenses in years 1-3 were for recruitment, advertising, and coordination.

University of Florida Health Science Center

2011 Annual Report

Age Related Memory Loss (ARML) Program
& Cognitive Aging and Memory Clinical and
Translational Research Program (CAM-CTRP)

Prepared for the McKnight Brain Research Foundation
by the University of Florida
McKnight Brain Institute and Insitute on Aging

UF Foundation Endowment Reports

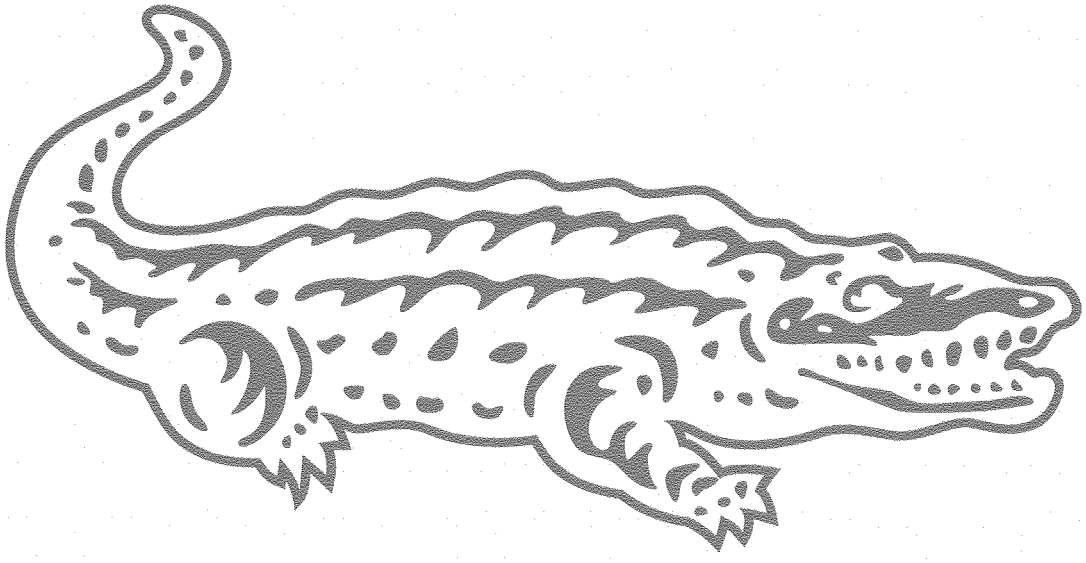

UF | Health Science Center
UNIVERSITY of FLORIDA

Evelyn F. McKnight Brain Research Grant

We would like to take this opportunity to express our gratitude for your generous support of UF through this endowment. University of Florida endowments are a vital asset to the ongoing success and sustainability of future research, teaching, and service programs. By establishing predictable, recurring revenue streams, endowments impact programs that cultivate growth in our students and faculty for generations to follow. We are pleased to provide you with the following financial report for Fiscal Year 2011.

BOOK VALUE as of 09/30/11	**$25,967,781**
MARKET VALUE as of 09/30/11	**$28,388,335**
PROJECTED SPENDABLE INCOME for 2011/12	**$1,026,301**

ENDOWMENT MANAGEMENT

Endowment assets are invested through the University of Florida Investment Corporation (UFICO), created in 2004 to manage UF's investment portfolios. UFICO is headed by a Chief Investments Officer who reports to a volunteer Board of Directors and to the President of the University of Florida.

FOR MORE INFORMATION, CONTACT:
Thomas J. Mitchell
Vice President, Development and Alumni Affairs
(352) 392-5407 (tmitchell@uff.ufl.edu)

Cindy Belknap
Director of Stewardship and Donor Relations
(352) 846-3444 (cbelknap@uff.ufl.edu)

(Fund # 008057)

Evelyn F. McKnight Chair for Brain Research in Memory Loss

We would like to take this opportunity to express our gratitude for your generous support of UF through this endowment. University of Florida endowments are a vital asset to the ongoing success and sustainability of future research, teaching, and service programs. By establishing predictable, recurring revenue streams, endowments impact programs that cultivate growth in our students and faculty for generations to follow. We are pleased to provide you with the following financial report for Fiscal Year 2011.

BOOK VALUE as of 09/30/11	**$3,995,677**
MARKET VALUE as of 09/30/11	**$4,328,512**
PROJECTED SPENDABLE INCOME for 2011/12	**$156,485**

ENDOWMENT MANAGEMENT

Endowment assets are invested through the University of Florida Investment Corporation (UFICO), created in 2004 to manage UF's investment portfolios. UFICO is headed by a Chief Investments Officer who reports to a volunteer Board of Directors and to the President of the University of Florida.

FOR MORE INFORMATION, CONTACT:
Thomas J. Mitchell
Vice President, Development and Alumni Affairs
(352) 392-5407 (tmitchell@uff.ufl.edu)

Cindy Belknap
Director of Stewardship and Donor Relations
(352) 846-3444 (cbelknap@uff.ufl.edu)

(Fund # 007889)

McKnight Brain Research Foundation

Evelyn F. McKnight Brain Research Grant (008057)

Spendable Fund Transfers since endowment inception

FY 2011/2012	**$256,575**	**(09/30/11 YTD)**
FY 2010/2011	**$971,846**	
FY 2009/2010	**$941,689**	
FY 2008/2009	**$1,086,475**	
FY 2007/2008	**$1,172,824**	
FY 2006/2007	**$1,056,031**	
FY 2005/2006	**$881,347**	
FY 2004/2005	**$843,131**	
FY 2003/2004	**$729,335**	
FY 2002/2003	**$651,801**	
FY 2001/2002	**$657,852**	
FY 2000/2001	**$648,384**	
TOTAL	**$9,897,290**	

Evelyn F. McKnight Chair for Brain Research in Memory Loss (007889)

Spendable Fund Transfers since endowment inception

FY 2011/2012	**$39,121**	**(09/30/11 YTD)**
FY 2010/2011	**$148,182**	
FY 2009/2010	**$143,584**	
FY 2008/2009	**$165,660**	
FY 2007/2008	**$178,827**	
FY 2006/2007	**$161,019**	
FY 2005/2006	**$134,384**	
FY 2004/2005	**$127,813**	
FY 2003/2004	**$124,127**	
FY 2002/2003	**$125,768**	
FY 2001/2002	**$100,869**	
FY 2000/2001	**$99,417**	
FY 1999/2000	**$3,438**	
TOTAL	**$1,552,209**	

FOR MORE INFORMATION, CONTACT:
Thomas J. Mitchell
Vice President, Development and Alumni Affairs
(352) 392-5407 (tmitchell@uff.ufl.edu)

Cindy Belknap
Director of Stewardship and Donor Relations
(352) 846-3444 (cbelknap@uff.ufl.edu)

University of Florida Fund Report
Prepared for the McKnight Foundation

F007889/90 Evelyn F. McKnight Chair for Brain Research in Memory Loss
Fund Administrator: Thomas C. Foster, Ph.D.

F007889	
Balance in Endowment	**$4,328,511.53**
F007890	
Spendable Income Beginning Balance	**$ 179,996.55**
Endowment transfers	$ 154,366.74
Transferred to UF	$ (200,000.00)
Spendable Income Balance	**$ 134,363.29**

Estimated Annual Transfers $ 156,485.27 *

* estimated based on spending base (spending base is adjusted quarterly).

F008057/58 Evelyn F. McKnight Brain Research Grant
Fund Administrator: Tetsuo Ashizawa, M.D.

F008057	
Balance in Endowment	**$28,388,334.59**
F008058	
Spendable Income Beginning Balance	**$ 1,418,320.46**
Endowment transfer	$ 1,012,406.81
Transferred to UF	$ (1,559,941.25)
Transferred to F016327	$ (470,844.50)
Spendable Income Balance	**$ 399,941.52**

Estimated Annual Transfers $ 1,026,301.14 *

* estimated based on spending base (spending base is adjusted quarterly).

F016327 McKnight Brain Research Foundation Cognitive Aging and Memory Program
Fund Administrator: Marco Pahor, M.D.

F016327	
Beginning balance in Fund	$1,905,061.10
Transferred from 8058	$ 470,844.50
Current Fund balance	**$2,375,905.60**

Data as of 12/31/2011
Prepared 1/8/2012

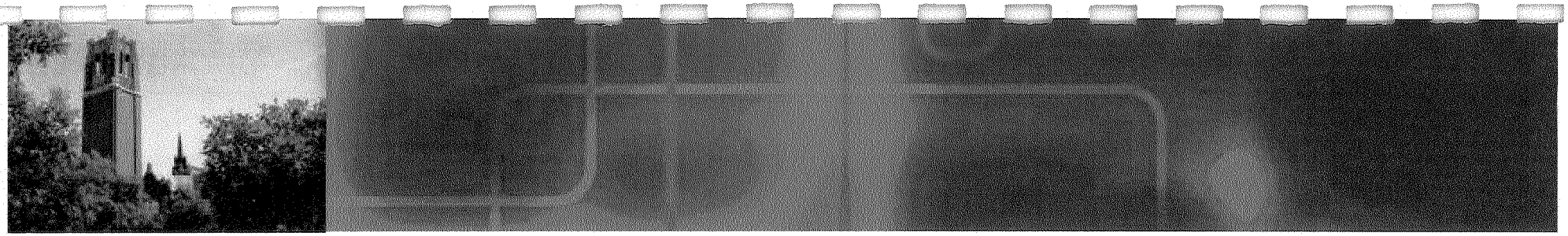

McKnight Brain Research Foundation

UF Investment Corporation Update
January 2012

UF | UNIVERSITY of FLORIDA INVESTMENT CORPORATION

UFF Endowment Portfolio
Asset Allocation

Actual
11/30/2011

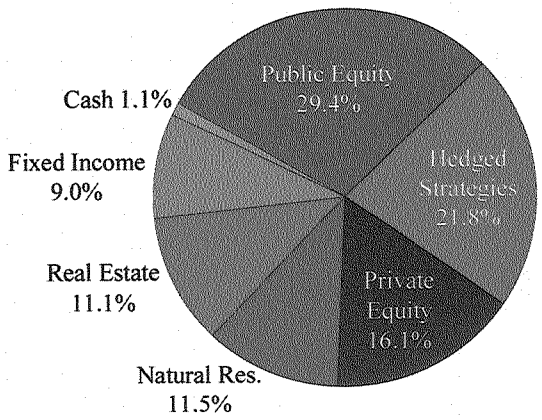

Active Target

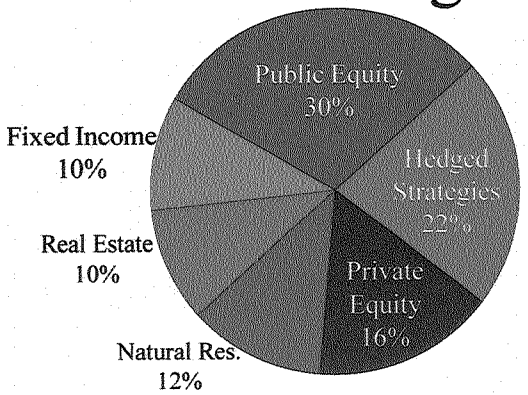

Strategic Target

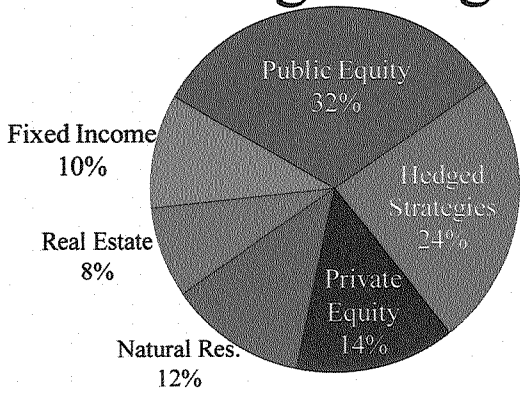

	Actual 11/30/2011	Active Target	Strategic Target
Public Equity	29.4%	30.0%	32.0%
Hedged Strategies	21.8%	22.0%	24.0%
Private Equity	16.1%	16.0%	14.0%
Natural Resources	11.5%	12.0%	12.0%
Real Estate	11.1%	10.0%	8.0%
Fixed Income	9.0%	10.0%	10.0%
Opportunistic	0.0%	0.0%	0.0%
Cash	1.1%	0.0%	0.0%
Total	100.0%	100.0%	100.0%

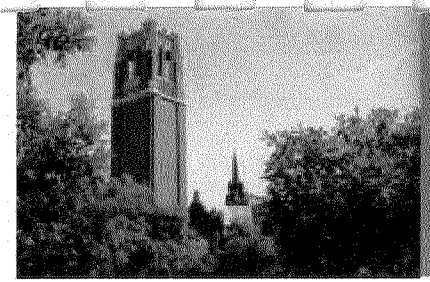

Endowment Portfolio Positioning

- Public Equity
  - Underweight strategic and active target allocations
  - Overweight US, underweight Europe
  - Value bias
- Hedged Strategies
  - Underweight strategic target allocation
  - Low use of leverage
  - Overweight Equity Long/Short
- Fixed Income
  - Underweight strategic target allocation
  - Biased toward passive, liquid and sovereign investments
- Private Markets
  - Overweight strategic allocation to PE and RE
- Overall Defensive Position

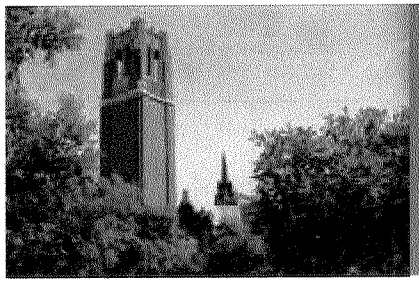

UFF Endowment Performance Review

Periods Ending
November 30, 2011

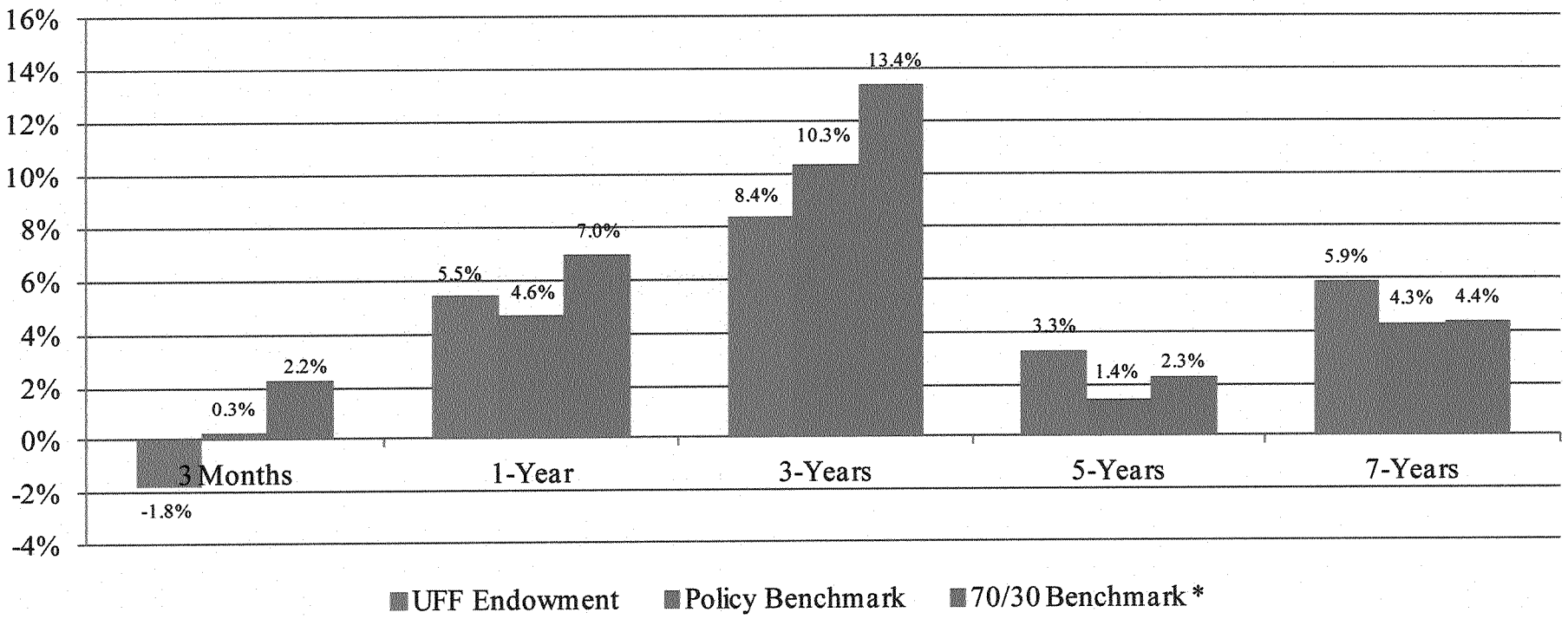

* 70%Russell 3000 Index / 30% Barclays Aggregate Bond Index

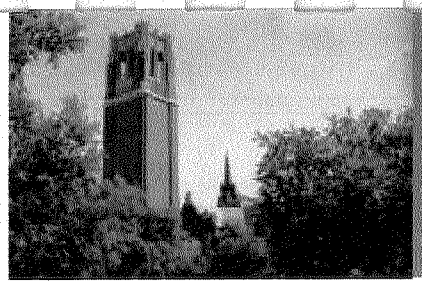

UFF Endowment Performance Review

Fiscal Year 2011

As of November 30, 2011

	(000's) NAV	Allocation Actual %	Allocation Target %	Last 3 Months	Fiscal YTD	Calendar YTD	1 Year	Annualized 3 Year	Annualized 5 Year	Annualized 7 Year
UFF Endowment Total Pool	**$1,232,993**	**100.0%**	**100.0%**	**-1.76%**	**-3.39%**	**3.02%**	**5.45%**	**8.39%**	**3.29%**	**5.86%**
UFF Endowment Policy Benchmark				*0.27%*	*-4.44%*	*-0.30%*	*4.64%*	*10.33%*	*1.43%*	*4.30%*
70% Russell 3000/30% Barcap Aggregate				*2.23%*	*-2.72%*	*2.42%*	*6.95%*	*13.42%*	*2.27%*	*4.35%*
Public Equity	**$362,206**	**29.4%**	**30.0%**	**-3.76%**	**-11.97%**	**-6.99%**	**-1.38%**	**16.94%**	**0.85%**	**5.06%**
MSCI ACWI Free				*-2.73%*	*-11.31%*	*-7.16%*	*-0.36%*	*13.43%*	*-1.46%*	*3.42%*
Hedged Strategies	**$268,782**	**21.8%**	**22.0%**	**-1.25%**	**-5.18%**	**-3.74%**	**-1.42%**	**7.37%**	**2.32%**	**4.58%**
Hedged Strategies Benchmark				*-1.96%*	*-4.00%*	*-4.11%*	*-2.03%*	*3.48%*	*-0.07%*	*2.35%*
Fixed Income	**$111,120**	**9.0%**	**10.0%**	**0.43%**	**6.05%**	**9.63%**	**8.77%**	**13.47%**	**5.75%**	**5.46%**
Fixed Income Benchmark				*1.96%*	*6.56%*	*9.66%*	*8.69%*	*9.83%*	*6.74%*	*6.12%*
Private Equity	**$197,904**	**16.1%**	**16.0%**	**-0.04%**	**2.68%**	**18.68%**	**25.43%**	**5.90%**	**10.89%**	**13.01%**
Private Equity Benchmark				*3.66%*	*-3.47%*	*3.85%*	*11.05%*	*17.52%*	*2.82%*	*6.06%*
Natural Resources	**$142,268**	**11.5%**	**12.0%**	**-3.80%**	**-0.23%**	**14.00%**	**19.04%**	**5.26%**	**6.98%**	**8.09%**
Natural Resources Benchmark				*3.66%*	*-3.47%*	*3.85%*	*11.05%*	*17.52%*	*2.82%*	*6.06%*
Real Estate	**$137,020**	**11.1%**	**10.0%**	**0.53%**	**6.73%**	**11.63%**	**16.65%**	**-5.09%**	**0.15%**	**3.21%**
Real Estate Benchmark				*3.30%*	*8.10%*	*12.03%*	*16.10%*	*-1.45%*	*3.40%*	*7.48%*
Opportunistic	**$525**	**0.0%**	**0.0%**	*n/m*	*n/m*	*n/m*	*n/m*	*n/m*	*n/m*	*n/m*
Cash	**$13,168**	**1.1%**	**0.0%**	**0.01%**	**0.05%**	**0.29%**	**0.29%**	**0.75%**	**1.93%**	**2.44%**
Citi 3 Month Treasury Bill				*0.01%*	*0.02%*	*0.08%*	*0.09%*	*0.14%*	*1.45%*	*2.10%*

Current Benchmark Composites

UFF Endowment: 32% MSCI ACWI, 24% HFRI FOF Diversified, 26% S&P 500 + 3%, 8% NCREIF Property Index, 5% Barclays Government Index, 5% Barclays US Inflation-Linked Bond Index
Hedged Strategies Benchmark: 100% HFRI FOF Diversified
Fixed Income Benchmark: 7/1/04-6/30/11 - 100% Barclays Universal; As of 7/1/11 - 50% Barclays Gov't Index / 50% Barclays US Inflation Protected
Private Equity Benchmark: S&P 500 + 3%
Natural Resources Benchmark: S&P 500 + 3%
Real Estate Benchmark: NCREIF Property Index
Note: Total Pool Returns are net of all fees / Asset Class Returns are gross of UFICO fees & net of manager fees

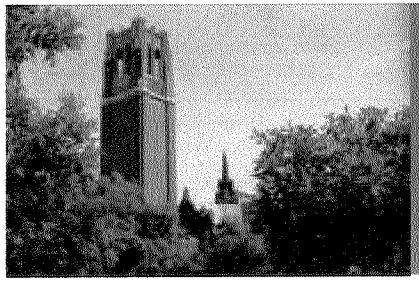

UFF Endowment Portfolio
Peer Comparison

Callan Associates
Mid-size Endowment & Foundation Universe
As of September 30, 2011

Rolling One-Year Percentile Rank

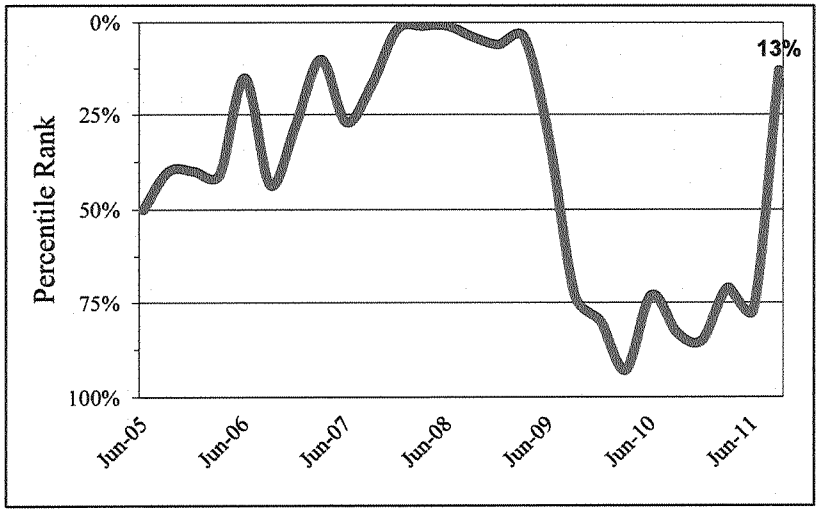

Rolling Three-Year Percentile Rank

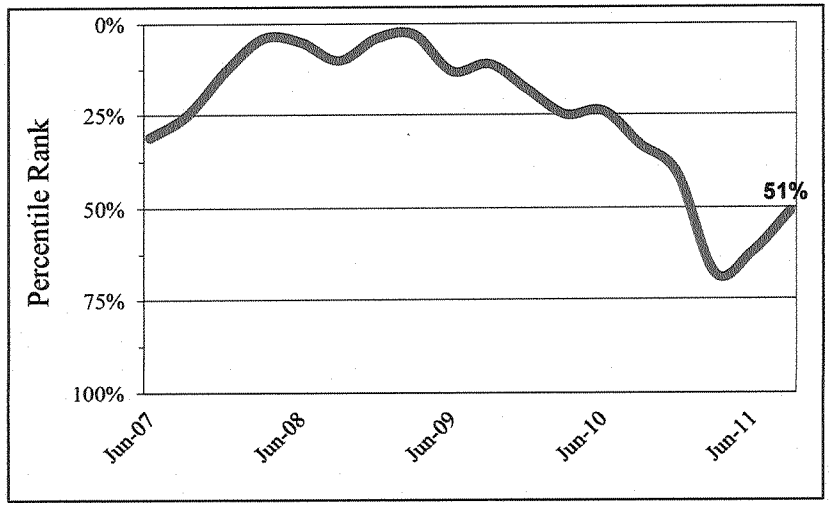

UFICO Inception-to-Date*

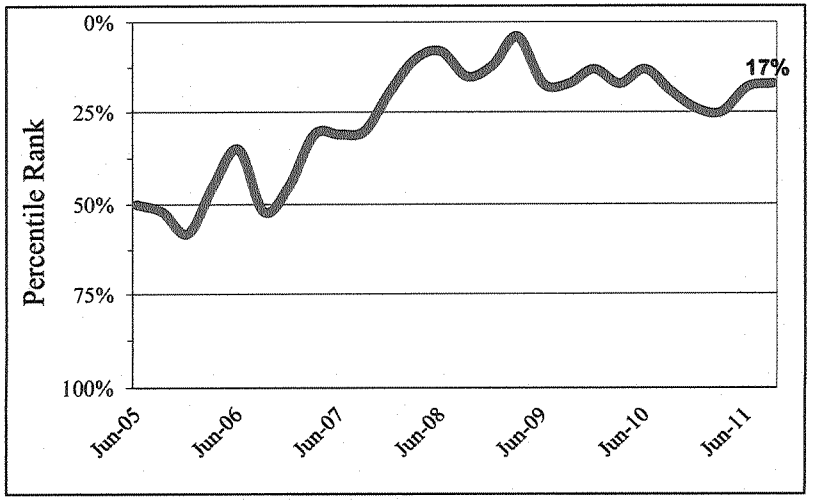

* UFICO Inception date of 7/1/2004

UFF Endowment Portfolio
SEC Comparison

SEC Endowment Performance
as of 09-30-11

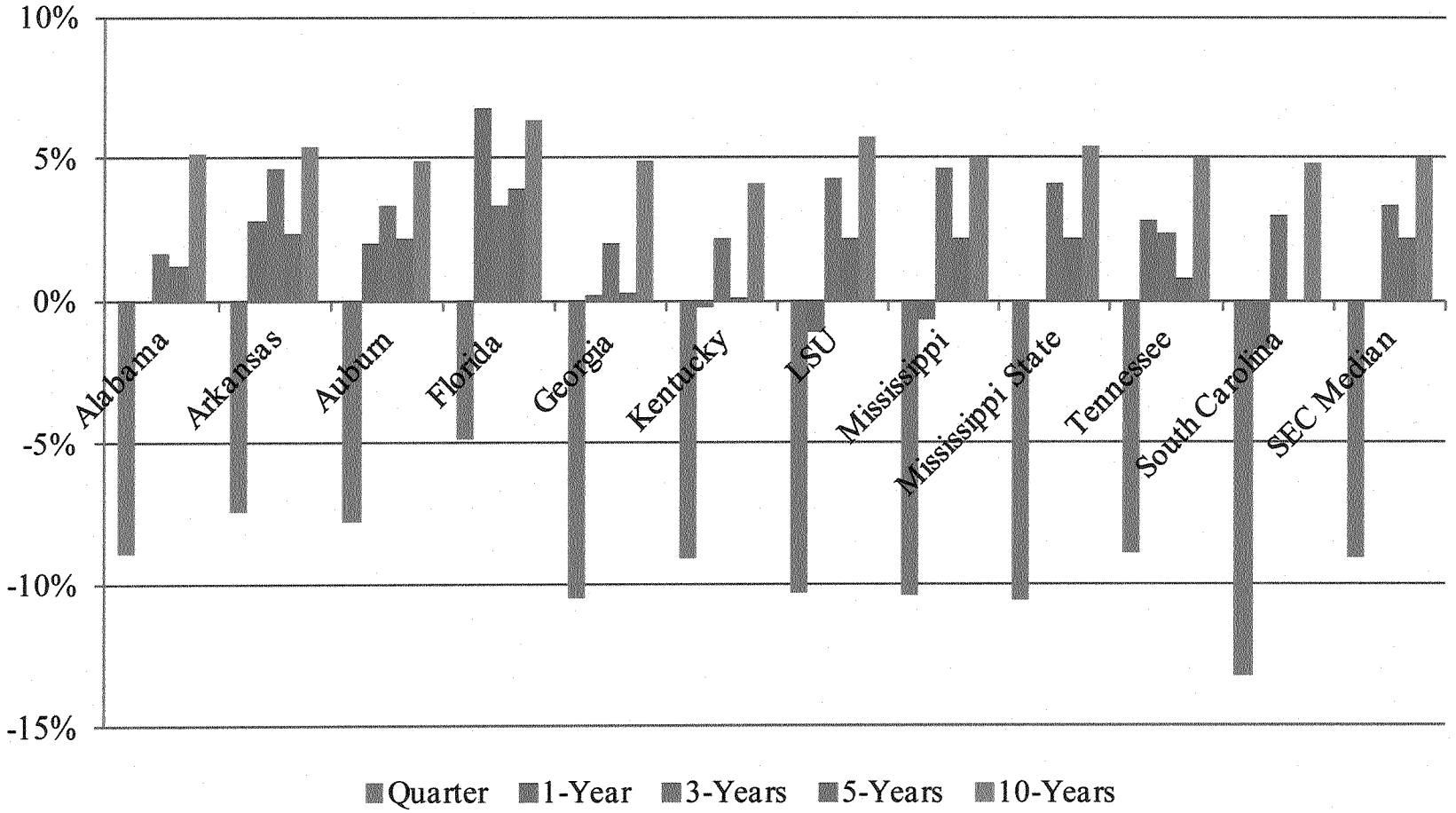

Vanderbilt elected not to participate

University of Florida Health Science Center

2011 Annual Report

Age Related Memory Loss (ARML) Program
& Cognitive Aging and Memory Clinical and
Translational Research Program (CAM-CTRP)

Prepared for the McKnight Brain Research Foundation
by the University of Florida
McKnight Brain Institute and Insitute on Aging

Faculty Biography / Curriculum Vitae

UF | Health Science Center
UNIVERSITY of FLORIDA

D. Research Support

Ongoing

1RC1NS068897-01; Ashizawa (PI) 09/30/2009-09/29/2012
(no-cost extension)
Clinical Research Consortium for Spinocerebellar Ataxias
The goal of this grant is to establish infrastructure and resources for clinical research on spinocerebellar ataxias. This application is to continue this project.
Role: PI

National Ataxia Foundation: S.H. Subramony (PI) 07/01/2009-06/30/2012
New initiative for clinical research on ataxia
The goal of this grant is to establish and maintain the National Ataxia Registry, which supplements the DMCC's Contact Registry by verifying the diagnosis of the specific type of spinocerebellar ataxias by medical documents.
Role: Co-PI

Completed

2R01NS041547-06: Ashizawa (PI) 05/01/2006-03/30/2010
Pathogenic Mechanism of Spinocerebellar Ataxia Type 10
The goal of this grant was to investigate the molecular mechanism of spinocerebellar ataxia type 10 in patient-derived tissues/cells, transgenic mouse models and transfected cell culture models. The project is closed, and a new translational proposal is being prepared.
Role: PI

1U01NS050733-01A1; Newsom-Davis (PI) 09/24/2005-08/31/2010
Thymectomy in non-thymomatous MG patients on Prednisone.
The goal of this study was to determine the efficacy of thymectomy in reducing the dose of oral prednisone that is required to adequately treat patients with myasthenia gravis.
Role: site PI

5U01NS052592-05; Cudkowicz (PI) 09/30/2005-11/30/2011
Coenzyme Q10 in Huntington's Disease
The goal of this study was to determine the efficacy of coenzyme Q10 in Huntington's disease. When I left UTMB for UF on 03/31/2009, I transferred the site-PI from me to Dr. George Jackson at UTMB.
Role: site PI

Muscular Dystrophy Association: Ashizawa (PI) 09/01/2009-03/31/2010
7th Internatinal Myotonic Dystrophy Consortium meeting (IDCM7)
The goal of this grant is to support the 7th International Myotonic Dystrophy Consortium meeting held in Wuertzberg, Germany in September 10-12, 2009.
Role: PI

BIOGRAPHICAL SKETCH

Provide the following information for the Senior/key personnel and other significant contributors in the order listed on Form Page 2.
Follow this format for each person. **DO NOT EXCEED FOUR PAGES.**

NAME	POSITION TITLE
Jennifer L. Bizon	Associate Professor
eRA COMMONS USER NAME (credential, e.g., agency login) jbizon	

EDUCATION/TRAINING *(Begin with baccalaureate or other initial professional education, such as nursing, include postdoctoral training and residency training if applicable.)*

INSTITUTION AND LOCATION	DEGREE *(if applicable)*	MM/YY	FIELD OF STUDY
University of North Carolina at Chapel Hill	BS	1993	Psychology
University of California, Irvine	PhD	1998	Neurobiology and Behavior
Johns Hopkins University	Post-doc	1998-2002	Neuroscience

A. Personal Statement

My primary research program broadly focuses on understanding brain aging as it relates to cognitive processes, with an emphasis on modulatory neurotransmitter systems. Our approach involves the integration of neuroanatomical, biochemical, and pharmacological variables with novel cognitive/behavioral assays, with the goal of identifying those factors that contribute to loss of cognitive function across the lifespan. My NIH-funded research program is focused on understanding basal forebrain-hippocampal systems and specifically the effects of age on both cholinergic and GABAergic systems. In addition to our work investigating learning and memory functions supported by hippocampus/ medial temporal lobe, my laboratory also has a strong interest in understanding the neural and behavioral mechanisms associated with age-related changes in executive function, including working memory, cognitive flexibility and decision making.

B. Positions and Honors

1993 Research Assistant at University of North Carolina at Chapel Hill
1993-1998 Graduate Student Assistant, University of California, Irvine, Laboratory of Dr. Christine Gall
1998-2003 Postdoctoral Fellow, Johns Hopkins University, Laboratory of Dr. Michela Gallagher
2002-2004 Assistant Research Scientist, Dept. of Psychology, Johns Hopkins University
2004-2010 Assistant Professor of Psychology, Texas A&M University
2004-2010 Faculty of Neuroscience, Texas A&M University
2010-present Associate Professor of Neuroscience and Psychiatry, University of Florida College of Medicine

Honors and Professional Activities

Graduated with Highest Honors (Psychology) UNC-Chapel Hill
Individual NRSA, NIMH F31 pre-doctoral award, (1995-1998)
Individual NRSA, NIA F32 post-doctoral award (2001-2003)
Leadership and Service Award (2008), Faculty of Neuroscience, Texas A&M University

Montague Center for Teaching Excellence Award (2008), College of Liberal Arts, Texas A&M University

Editor, Animal Models of Human Cognitive Aging (2008), *Humana (Wiley) Press*

Editorial Board, *Neurobiology of Aging* (2008-present)

Advisory Board, Alzheimer's Drug Discovery Foundation (2010-present)

NSF Review Panel (Modulatory Brain Systems), Rockville MD (2011)

NIH Review Panel (CNNT) Washington DC (2010)

NIH Special Emphasis Review Panel (ZAG1 ZIJ-5), Bethesda, MD (2009)

Ad Hoc Reviewer for National Science Foundation (2009)

McKnight Cognitive Test Battery Working Group (2011)

Co-Director of Neuroscience Graduate Program, University of Florida, College of Medicine (2011)

C. *Selected* Peer-reviewed Publications:

Recent (2011) and Most Relevant:

McQuail, JA, Bañuelos, LaSarge, CL, Nicolle, MM, Bizon, JL GABAB receptor GTP-binding is decreased in the prefrontal cortex butmnot the hippocampus of aged rats. *Neurobiology of Aging. In Press.*

Gilbert, RJ, Mitchell, M, Simon, NW, Bañuelos, C, Setlow, S, & Bizon, JL, Risk, reward, and decision-making in a rodent model of cognitive aging Frontiers Neuroscience. *In Press.*

Simon NW, Montgomery KS, Beas BS, Mitchell MR, Lasarge CL, Mendez IA, Bañuelos C, Vokes CM, Taylor AB, Haberman RP, Bizon JL, Setlow B. Dopaminergic Modulation of Risky Decision-Making. J Neurosci. 2011 Nov 30;31(48):17460-17470.

Bañuelos C, Gilbert RJ, Montgomery KS, Fincher AS, Wang H, Frye GD, Setlow B, Bizon JL. Altered spatial learning and delay discounting in a rat model of human third trimester binge ethanol exposure. Behav Pharmacol. 2011 Nov 29. [Epub ahead of print]

Huie JR, Garraway SM, Baumbauer KM, Hoy KC Jr, Beas BS, Montgomery KS, Bizon JL, Grau JW. Brain-derived neurotrophic factor promotes adaptive plasticity within the spinal cord and mediates the beneficial effects of controllable stimulation. Neuroscience. 2011 Oct 25. [Epub ahead of print]

Shineman DW, Basi GS, Bizon JL, Colton CA, Greenberg BD, Hollister BA, Lincecum J, Leblanc GG, Lee LB, Luo F, Morgan D, Morse I, Refolo LM, Riddell DR, Scearce-Levie K, Sweeney P, Yrjänheikki J, Fillit HM. Accelerating drug discovery for Alzheimer's disease: best practices for preclinical animal studies. Alzheimers Res Ther. 2011 Sep 28;3(5):28. [Epub ahead of print]

Lim, C-S Kim, Y-J ,Hwang,Y-K, Bañuelos, C., Bizon, J.L. and Han, J-S (2011) Decreased interactions in PKA-GR signaling in the hippocampus after selective removal of the basal forebrain cholinergic input. *Learning and Memory.* doi: 10.1002/hipo.20912. [Epub ahead of print]

Lim CS, Hwang YK, Kim D, Cho SH, Bañuelos C, Bizon JL, Han JS. Increased interactions between PKA and NF-κB signaling in the hippocampus following loss of cholinergic input. Neuroscience. 2011 Sep 29;192:485-93.

Montgomery, K. S., Simmons, R.K., Edwards, G. 3rd, Nicolle, M. M., Meyers, C. A., Gluck, M., & Bizon, J. L. (2011). Novel age-dependent learning deficits in a mouse model of Alzheimer's disease: Implications for translational research. *Neurobiology of Aging.* 32(7):1273-85.

Simon, N.W., LaSarge, C.L., Montomery, K.S., Williams, M.T., Mendez, I.A., Setlow, B., Bizon, J.L. (2010) Good things come to those who wait: attenuated discounting of delayed rewards in aging. *Neurobiology of Aging.* 31(5):853-62.

LaSarge, C.L., Bañuelos C, Mayse, J.R., & Bizon, J. L. (2009). Blockade of GABA(B) receptors completely reverses age-related learning impairment. *Neuroscience*.164(3):941-7.

Murchison, D., Armstrong, G., Mieckowski, A.N., LaSarge, C.L., Bizon, J.L., Griffith, W.H. (2009). Cognitive performance in a spatial learning task is correlated with altered calcium homeostasis in basal forebrain neurons of aged Fischer 344 rats. *Journal of Neurophysiology.* 102(4):2194-207.

Bizon, J.L., LaSarge, C.L., Montgomery, K.S., McDermott, A.N., Setlow, B., & Griffith, W.G. (2009). Spatial reference and working memory across the lifespan of Fischer 344 rats. *Neurobiology of Aging* 30(4): 645-55.

Simon, N. W., Gilbert, R. J., Mayse, J. D., Bizon, J. L., & Setlow, B. (2009). Balancing risk and reward: A rat model of risky decision-making. *Neuropsychopharmacology.* 34, 2208-2217.

LaSarge, C.L., Montgomery, K.S., Tucker, C., Slaton, S.G.., Griffith, W.H., Setlow, B., & Bizon, J. L. (2007) Deficits across multiple cognitive domains in a subset of aged Fischer 344 rats. *Neurobiology of Aging,* 28(6):928-36.

Bizon, J., Prescott, S., & Nicolle, M. M. (2007). Intact spatial learning in adult Tg2576 mice. *Neurobiology of Aging.* 28(2): 440-6.

Bizon, J.L., Gallagher, M. (2005) More is less: Neurogenesis and age-related cognitive decline in Long-Evans rats. *Science of Aging Knowledge Environment.* 16(7):re2.

Bizon, J.L., Lee, H-J, Gallagher, M. (2004) Neurogenesis in a cognitive model of aging. *Aging Cell* 3(4):227-34.

Bizon, J. L., Gallagher, M. (2003) Production of new cells in the rat dentate gyrus over the lifespan: relation to cognitive decline. *European Journal of Neuroscience.* 18:215-9.

Nicolle, M., Prescott, S., Bizon, J.L. (2003) Emergence of a cue strategy on the water maze task in aged B6XSJL F1 hybrid mice. *Learning and Memory.* 10 (6): 520-4

Bizon, J. L., Helm, K.A., Han, J.-S., Chun, H.-J., Pucilowski, J., Lund, P. K., Gallagher, M. (2001) Hypothalamic-pituitary-adrenal axis function and corticosterone receptor expression in behaviorally characterized young and aged rats. *European Journal of Neuroscience.* 14:1739-51.

Bizon, J. L., Lauterborn, J. Gall, C. (1999) Trophic factors are expressed by distinct populations of striatal interneurons. *Journal of Comparative Neurology,* 408(2): 283-98.

Nicolle, M. M., Bizon, J. L., Gallagher, M. (1996) In vitro autoradiography of ionotropic glutamate receptors in hippocampus and striatum of aged Long-Evans rats: relationship to spatial learning. *Neuroscience,* 74(3) 741-756

Bizon, J. L., Lauterborn, J, Isacson, P., Gall, C. (1996) Acidic fibroblast growth factor is expressed by basal forebrain and striatal cholinergic neurons. *Journal of Comparative Neurology,* 366: 379-389.

Ongoing:

R01 AG02942 (Jennifer L. Bizon, PI) 8/1/07-6/30/12 35% effort
National Institute on Aging $226,359direct/year
"Basal Forebrain and Cognitive Aging: Novel Experimental and Therapeutic Avenues"
The goal of this project is to determine how changes in cholinergic and GABAergic basal forebrain neuron structure and function relate to cognitive decline in aging, and to ameliorate such decline by pharmacologically targeting these neurons. No overlap.

R01 DA024671 (B. Setlow PI, Bizon co-PI) 4/1/09-3/31/14 15% effort
National Institute on Drug Abuse $205,000 direct/year
"Neural mechanisms of enduring cocaine effects on impulsive choice"
The goal of this project is to understand the long-term effects of cocaine use on decision making and to begin to elucidate the neurobiology associated with impulsivity resulting from psychostimulant drug use. No overlap.

F31-AG037286-01 (Karienn Montgomery student. Bizon Sponsor) 8/1/10-8/1/13 n/a
National Institute of Aging $102,294 direct/total

Transfer Learning in Mice: Implications for improved diagnosis and treatment of Alzheimer's Disease
The goal of this study is to design novel behavioral assessments that are very sensitive to age-related pathology and tat are highly translational.

Completed:

R01-NS041548 (Grau PI, Bizon, co-I) 4/07-3/11 15% effort
National Institute of Neurological Disorder and Diseases $246,948 direct/yr
"Learning within the spinal cord: clinical implications"
The goal of this grant is to study the role of BDNF in spinal cord learning. No overlap.

R01-DA13188 (PJ Wellman PI, Bizon co-I) 8/01/07-6/30/10 15% effort
National Institute of Drug Abuse
"Heavy Metal and Drug Self-Administration: Mechanisms"
The goal of this project is to determine how exposure to heavy metals (lead, cadmium) during development affects vulnerability to drug abuse during adulthood.

F31- NS059324 (Candi Lynn LaSarge student, Bizon Sponsor) 6/1/08- 12/1/10 n/a
National Institute of Neurological Disorders and Stroke $92,123 direct/total
"The Role of Basal Forebrain in Mild Cognitive Impairment"
The goal of the project under this training fellowship is to determine how changes in basal forebrain anatomy are related to cognitive dysfunction in aging.

R01-AA012386 (G Frye PI, Bizon co-I) 8/1/08-8/1/10 10% effort
National Institute on Alcohol Abuse and Alcoholism
"CNS Development GABAARs and Vulnerability to Ethanol"
The goal of this project is to determine how developmental exposure to alcohol affects basal forebrain neuronal function and cognition later in life.

F31- DA023331 (NW Simon student, Bizon co-sponsor) 2/1/08-2/1/10 n/a
National Institute on Drug Abuse
"Long-term cocaine effects on impulsive choice and orbitofrontal cortex activity"
The goal of the project under this training fellowship is to determine how chronic cocaine exposure affects impulsive decision-making and orbitofrontal cortex function.

BIOGRAPHICAL SKETCH

Provide the following information for the Senior/key personnel and other significant contributors in the order listed on Form Page 2.
Follow this format for each person. **DO NOT EXCEED FOUR PAGES.**

NAME	POSITION TITLE
Dawn Bowers, Ph.D.	Professor, Clinical & Health Psychology and Neurology
eRA COMMONS USER NAME (credential, e.g., agency login) dbowers	

EDUCATION/TRAINING *(Begin with baccalaureate or other initial professional education, such as nursing, include postdoctoral training and residency training if applicable.)*

INSTITUTION AND LOCATION	DEGREE *(if applicable)*	MM/YY	FIELD OF STUDY
Emory University, Atlanta GA		1968-1970	Psychology
University of Florida, Gainesville FL	B.A.	08/1972	Psychology
University of Florida, Gainesville FL	M.S.	12/1974	Clinical Psych/Neuropsy
University of Florida, Gainesville FL	Ph.D.	12/1978	Clinical Psych/Neuropsy
University of Florida, Gainesville FL	Post-doc	12/1979	Behavioral Neurology

A. Personal Statement

I have longstanding research and clinical expertise in non-motor symptoms of Parkinson disease, particularly emotion (apathy, depression), neurocognitive changes associated with disease progression and deep brain stimulation, and clinical heterogeneity of PD cognitive subtypes. I have been a funded researcher for many years, including two recently completed clinical trials, one for treatment of apathy using rTMS and another for treatment of "'masked faces" in individuals with Parkinson disease, as well as other collaborative studies related to dual task processing, and psychophysiology of motivated behavior in Parkinson disease. I have served as a primary sponsor for 6 pre-doctoral NRSA recipients, 1 post-doctoral NRSA recipient, 1 post-doctoral minority supplement, and 1 current K23 trainee. I have a keen understanding of the cognitive and emotional sequalae of DBS along with statistical methods inherent in conducting reliable change analyses over time. As lead neuropsychologist for the UF Movement Disorders Center, I oversee the neurocognitive module of the INFORM database. We currently have neurocognitive data on over 1200 movement disorder patients. Initial statistical modeling from this database is supportive of PD cognitive subtypes which appears to map closely to onto neuroimaging parameters (i.e., DTI FA and tractography). As Co-PI of the VITAL study, we are examining the interactive effects of cognitive training and exercise in a unique cohort of community living older adults.

B. Positions and Honors

Positions & Employment

1976-1977: Teaching Fellow in Neurology, Boston University College of Medicine
1976-1977: Internship in Clinical Psychology/Neuropsychology, Boston VAMC
1976-1977 Externship in Geriatric Neuropsychology, Framingham Heart Study, MA
1979 Post-doctoral Fellowship, Behavioral Neurology, UF College of Medicine
1980- 1998 Associate Professor in Neurology [Assistant 1980-85], UF College of Medicine
1984-1998 Neuropsychologist, State of Florida Memory Disorders Clinic
1998- Professor of Clinical & Health Psychology [Associate 1998-2002]
1998- Director, Cognitive Neuroscience Laboratory, UF McKnight Brain Institute
2006- Division Chief, Neuropsychology Area, Dept. Clinical & Health Psychology
2006- UF Foundation Research Professor

Other Experience & Professional Memberships

2009-10 Ad hoc Member, NIH Adult Psychopathology & Disorders of Aging Study Section
2006 Member, NIH Special Emphasis Panel (ZRR1 BT-801), Interdisciplinary Research Consortium
2005 Member, NIH Special Emphasis Panel (2006/01) Cognition and Perception Study Section
2004-05 Ad hoc Member, NIH Biobehavioral Mechanisms of Emotion, Stress, and Health Study Section

2000- Editorial Boards, The Clinical Neuropsychologist, Journal of International Neuropsychological Society
1999-2003 Special Review Panel, Minority Research Infrastructure Support Program (MRISP), NIMH
1995-1998: Member, Merit Review Committee, Mental Health &d Behavioral Science, Dept. Veterans Affairs
Membership American Psychological Association (Divisions 12 and 40), International Neuropsychology Society, American Academy of Neurology, Society for Neuroscience, Cognitive Neuroscience Society
Journal Reviews: *Neuropsychologia, Lancet, Neurology, New England Journal of Medicine, Cortex, Movement Disorders, Journal of International Neuropsychological Society, The Clinical Neuropsychologist, J. Neurology, Neuropsychiatry, & Neurosurgery, Neuropsychology, Neuropsychologia, J. Cognitive Neursocience, Brain, JCCP, J.Abnormal Psychology, Archives Clinical Neuropsychologia*

C. Selected Peer-reviewed Publications (out of 155)
(Students in italics)

1. **Bowers, D.,** *Miller, K., Mikos, A., Kirsch-Darrow, L., Springer,* U., Fernandez, H., Foote, K., & Okun, M. (2006). Startling facts about emotion in Parkinson disease: blunted reactivity to aversive stimuli. Brain, 129, 3345-3365
2. **Bowers, D.**, *Miller, K., Bosch, W., Gokcay, D., Pedraza, O, Springer, U.*, & Okun, M. (2006). Faces of emotion in Parkinson"s disease: Microexpressivity and bradykinesia during voluntary expressions. Journal of International Neuropsychological Society, 12, 765-773.
3.
3 . *Kirsch-Darrow, L.*, Fernandez, H., Marsiske, M., Okun, M., & **Bowers, D.** (2006). Dissociating apathy from depression in Parkinson's disease. Neurology. 67(1), 20-27. *[master's thesis]*

4 . *Springer, U.S., Rosas, A., McGettrick, J.,* & **Bowers, D.** (2007). Differences in startle reactivity during the perception of angry and fearful faces. Emotion, 7 (3), 516-525.

5 . *Mikos, A., Springer, U.S., Nisenzon, A., Kellison*, I., Fernandez, H.H., Okun, M.S., & **Bowers, D.** (2009). Awareness of expressivity deficits in non-demented Parkinson disease. The Clinical Neuropsychologist, 25(4),

6. *Miller, K.M.*, Okun, M.S., Marsiske, M., Fennell, E.F., & **Bowers, D.** (2009). Startle reflex hyporeactivity in Parkinson's disease: an emotion specific or arousal modulated deficit? Neuropsychologia, *47, 1917-72.*

7. Zahodne, L., Okun, M.S., Foote, K., Fernandez, H., *Kirsch-Darrow, L.*, **Bowers, D.** (2009). Cognitive declines one year after unilateral deep brain stimulation surgery in Parkinson's disease: A control study using reliable change. The Clinical Neuropsychologist, 23(3):385-405 *[master's]*

8. *Miller, K.M.*, Price, C.C., Okun, M.S., *Montijo, H.*, & **Bowers, D.** (2009). Is the n-back task a clinically useful measure for assessing working memory in Parkinson's disease? Arch. of Neuropsychology. 24, 711-717.

9. *Mikos, A., Zahodne, Z.*, Okun, MS, Foote, K., **Bowers, D.** (2010). Cognitive declines after deep brain stimulation surgery in Parkinson's disease: A controlled study using reliable change. Part II. The Clinical Neuropsychologist, 24, 235-45.

10. *Zahodne, L.*, **Bowers, D.** Price, CC, Bauer, RM, *Nisenzon, A.*, Foote, K., Okun, MS (2011) The case for testing memory with both stories and word lists prior to DBS surgery. The Clinical Neuropsychologist, 25 (3), 348-58.

11. *Dietz, J.*, Bradley, M., Okun, M.S., **Bowers, D.** (2011). Emotion and ocular responses in Parkinson's disease . Neuropsychologia, 49, 3247-53.

12. *Mikos, A.*, **Bowers, D.**, Noecker, A., McIntyre, C, Won, M., Chaturvedi, A., Foote, K.D., Okun, M.S. (2011) Patient-specific analysis of the relationship between the volume of tissue activated during DBS and verbal fluency. Neuroimage, 54 Suppl 1:S238-46.

13. *Kirsch-Darrow,L*, Marsiske, M, Okun, M.S., Bauer, R.M., **Bowers, D.** (2011) Apathy and depression are separate factors in Parkinson Disease: Evidence from confirmatory factor analysis. Journal of International Neuropsychological Society, *17, 1-9.*

Price, C.C., *Cunningham, H., Coronado, N., Freedland, A.*, Cosentino, S., Penney, D., Pensi, A., **Bowers, D.,** Okun, M.S., Libon, D. (2011). Clock drawing in the Montreal Cognitive Assessment (MoCA): Recommendations for dementia assessment. *Dementia and Geriatric Cognitive Disorders,* 31 (3), 179-187.

14. *Zahodne, L*, Marsiske, M., Okun, M.S., Rodriguez, R., Malaty, I, **Bowers, D.** (2011, in press) Naturalistic trajectories of mood and motor symptoms in Parkinson's Disease: a multivariate latent growth curve analysis. Neuropsychology.

15. *Naugle, K.*, Hass, C.J., , **Bowers, D.**, Janelle, C. (2011, in press). Emotional state affects gait initiation in individuals with Parkinson disease. Cognitive, Affective, and Behavioral Neuroscience.

1. Research Support

Current

McKnight Brain Research Foundation PI: Bowers 11/01/2010-10/30/2013
The VITAL Study: A Multimodal Platform for the Enhancement of Cognition in Normal Elderly
This study examines whether exercise predosing improves effects of cognitive training in older adults, the trajectory of change over time, and the extent to which pure "aerobic" vs exergames are more beneficial.

1 F31 NS073331-01 PI: Dietz 5/01/2011-6/30/2013
Psychophysiology of Emotion in Parkinson disease
This predoctoral NRSA examines temporal trajectory of psychophysiological and ERP changes associated with approach and avoidance in Parkinson disease.
Role: Mentor

R21-AG033284 Multiple PI: Altman & Hass 8/2/2010-8/1/2012
Language and Executive function in Parkinson's disease: Effects of dual task and exercise.
This project examines the influence of aerobic exercise and multi-tasking on language processing in patients with Parkinson disease.
Role: Co-I

National Parkinson Foundation PI: Classen 7/01/2010 – 06/30/2012
The Role of Visual Attention in Driving Safety in Parkinson disease
This study examines the relationship between driving and various visuopercpetual/spatial indices of cognition.
Role: Co-I

K23- NS060660 PI: Price 08/31/2007-08/29/2012
White Matter and Cognition in Parkinson Disease
This project examines the role of white matter integrity, as indexed by diffusion tensor imaging, in relationship to cognitive decline in patients with Parkinson disease.
Role: Mentor

1R34MH080764, PI: Okun 08/31/2009 -09/01/2012
Scheduled and Responsive Brain Stimulation for the Treatment of Tourette Syndrome.

This clinical trial examines the effectivess of a scheduled DBS protocol for treatment of symptoms in patients with intractable Tourettes syndrome.
Role: Co-I

Recently Completed

R01-NS50633 PI: Bowers 12/01/05-11/30/10
Masked Facies in Parkinson Disease: Mechanism and Treatment
In this study, we evaluated a behavioral treatment approach for improving facial expressivity in patients with parkinson's disease using a double-blind sham-controlled randomized clinical.
Role: PI

Michael J. Fox Foundation PI: Fernandez 10/31/2006-9/30/2009
Repetitive Transcranial Magnetic Stimulation for the Treatment of Apathy in Parkinson's Disease
The purpose of this study was to learn whether rTMS improved symptoms of apathy and depression in nondemented patients with idiopathic Parkinson disease. To do so, we conducted a double-blind placebo controlled randomized parallel group study.
Role: Co-PI

R01 MH62539 PI: Bowers 06/01/02 – 05/31/06
Digitizing the Face: Priming, TMS, and Hemispheric Asymmetries
This project examined three hypotheses regarding the basis forr hemifacial movement asymmetries using cognitive priming, single pulse transcranial magnetic stimulation, and computer based systems for digitizing dynamic facial signals.
Role: PI

F31- NRSA NS059142 PI: Kirsch 7/1/2007-8/30/2009
Apathy, neurocognitive functioning, and Parkinson disease
This predoctoral fellowship examined dissociation and overlap between depression and apathy in a large sample of nondemented Parkinson patients (N=300) using confirmatory factor analysis. The effects of apathy and depression on neurocognitive measures were examined using multiple hierarchical regression techniques.
Role: Primary Mentor

F31- NRSA NS53403 PI: Kim Miller 07/01/05-06/30/07
Parkinson's Disease, Psychophysiology, and the Amygdala
This predoctoral training grant examined whether PD patients have reduced emotional reactivity to threatening stimuli, as measured by psychophysiologic measures (startle, SCR), and whether this defect related to reduced amygdalar volume in PD.
Role: Primary Mentor

R01-NS50633-Supplement PI: Bowers; Trainee: Lopez
Diversity Supplement: Masked Facies in Parkinson Disease: 08/01/05-07/31/07
This project involved research and training of a post-doctoral fellow in studies of Parkinson's disease.
Role: PI/Mentor

2010-present Member, Baylor College of Medicine Alumni Executive Committee
2011-present Member, Advisory Board, University of Texas Medical Branch – University of Florida Rehabilitation Research Career Development Program (K12)

Honors

2004 "Promoting Excellence In End-of –Life-Care": the Huntington's Disease Peer Workgroup, The Robert Wood Johnson Foundation
2005 "The Team Hope Award" for Medical Leadership: the Huntington's Disease Society of America
2006 "Medical Research Award": the Myotonic Dystrophy Assistance & Awareness Support Group
2009 "Steinert Medal": the IDMC7
2011 "Faculty member": Alpha Omega Alpha (AOA)
2011 "Best Doctors in America"
2011 MDA-MMDSG Award: Muscular Dystrophy Association

C. Selected Peer-reviewed publications (in chronological order). From 143 peer-reviewed papers.

1. Zhuchenko O, Bailey J, Bonnen P, Ashizawa T, Stockton DW, Amos C, Dobyns WB, Subramony SH, Zoghbi HY, Lee CC. Autosomal dominant cerebellar ataxia (SCA6) associated with small polyglutamine expansions in the α 1A-voltage-dependent calcium channel. Nature Genet 1997;15:62-69
2. Monckton DG, Cayuela ML, Gould FK, Brock GJR, de Silva R, Ashizawa T: Massive (CAG)n DNA repeat expansions in the sperm of spinocerebellar ataxia type 7 males. Hum Mol Genet 1999;8:2473-2478
3. Matsuura, T., Yamagata, T., Burgess, D.L., Rasmussen, A., Grewal, R.P., Watase, K., Khajavi, M., McCall, A., Caleb F. Davis, C.F., Zu, L., Achari, M., Pulst, S.M., Alonso, E., Noebels, J.L., Nelson, D.L., Zoghbi, H.Y., Ashizawa, T. Large Expansion of ATTCT Pentanucleotide Repeat in Spinocerebellar Ataxia Type 10. Nat Genet 2000;26:191-194
4. Matsuura T, Fang P, Lin X, Khajavi M, Tsuji K, Rasmussen A, Grewal RP, Achari M, Alonso ME, Pulst SM, Zoghbi HY, Nelson DL, Roa BB, Ashizawa T. Somatic and germline instability of the ATTCT repeat in spinocerebellar ataxia type 10. Am J Hum Genet 2004:74;1216-1224.
5. Teive HAG, Roa BB, Raskin S, Fang P, Arruda WO, Neto YC, Gao, R., Werneck LW, Ashizawa T. Clinical Phenotype of Brazilian Families with Spinocerebellar Ataxia 10. Neurology 2004;63:1509-1512
6. Wakamiya M, Matsuura T, Liu Y, Schuster GC, Gao R, Xu W, Sarkar PS, Lin X, Ashizawa T. The role of ataxin 10 in the pathogenesis of spinocerebellar ataxia type 10. Neurology 2006;67:607-613.
7. Gatto EM, Gao R, White MC, Uribe Roca MC, Etcheverry JL, Persi G, Poderoso JJ, Ashizawa T. Ethnic origin and extrapyramidal signs in an Argentinean spinocerebellar ataxia type 10 family. Neurology 2007;69:216-218.
8. Gao R, Matsuura T, Coolbaugh M, et al., Ashizawa T, Lin X. Instability of expanded CAG/CAA repeats in spinocerebellar ataxia type 17. Eur J Hum Genet 2007; 16:215-222. [PMC Journal – in process]
9. White MC, Gao R; Xu W, Mandal SM, Lim JG, Hazra TK, Wakamiya M, Edwards SF, Raskin S, Teive HAG, Zoghbi HY, Sarkar PS, Ashizawa T. Inactivation of hnRNP K by Expanded Intronic AUUCU Repeat Induces Apoptosis via Translocation of PKCδ to Mitochondria in Spinocerebellar Ataxia 10. PLoS Genet 2010; 6:e1000984.
10. Teive HA, Munhoz RP, Raskin S, Arruda WO, et al. and Ashizawa T. Spinocerebellar ataxia type 10: Frequency of epilepsy in a large sample of Brazilian patients. Mov Disord 2010; 25:2875-2878.
11. White M, Xia G, Gao R, Wakamiya M, Sarkar PS, Ashizawa T. Transgenic mice with SCA10 pentanucleotide repeats show motor phenotype and susceptibility to seizure. J Neruosci Res 2011 *in press.*
12. Teive HA, Munhoz RP, Ashizawa T. New gene of spinocerebellar ataxia. Brain 2011 Feb 26. [Epub ahead of print] [PMID:21357611]
13. Cherng N, Shishkin AA, Schlager LI, Tuck RH, Sloan L, Matera R, Sarkar PS, Ashizawa T, Freudenreich CH, Mirkin SM. Expansions, contractions, and fragility of the spinocerebellar ataxia type 10 pentanucleotide repeat in yeast. Proc Natl Acad Sci U S A 2011;108:2843-2848. [PMC Journal – in process]
14. Teive HA, Arruda WO, Raskin S, Munhoz RP, Zavala JA, Werneck LC, Ashizawa T. Symptom onset of spinocerebellar ataxia type 10 in pregnancy and puerperium. J Clin Neurosci 2011;18:437-438.
15. Subramony SH, Ashizawa T, Langford L, McKenna R, Avvaru B, Siddique T, Vedanarayanan V. Confirmation of the severe phenotypic effect of serine at codon 41 of the superoxide dismutase 1 gene. Muscle Nerve 2011;44:499-502.

D. Research Support

Ongoing

1RC1NS068897-01; Ashizawa (PI) 09/30/2009-09/29/2012
(no-cost extension)
Clinical Research Consortium for Spinocerebellar Ataxias
The goal of this grant is to establish infrastructure and resources for clinical research on spinocerebellar ataxias. This application is to continue this project.
Role: PI

National Ataxia Foundation: S.H. Subramony (PI) 07/01/2009-06/30/2012
New initiative for clinical research on ataxia
The goal of this grant is to establish and maintain the National Ataxia Registry, which supplements the DMCC's Contact Registry by verifying the diagnosis of the specific type of spinocerebellar ataxias by medical documents.
Role: Co-PI

Completed

2R01NS041547-06: Ashizawa (PI) 05/01/2006-03/30/2010
Pathogenic Mechanism of Spinocerebellar Ataxia Type 10
The goal of this grant was to investigate the molecular mechanism of spinocerebellar ataxia type 10 in patient-derived tissues/cells, transgenic mouse models and transfected cell culture models. The project is closed, and a new translational proposal is being prepared.
Role: PI

1U01NS050733-01A1; Newsom-Davis (PI) 09/24/2005-08/31/2010
Thymectomy in non-thymomatous MG patients on Prednisone.
The goal of this study was to determine the efficacy of thymectomy in reducing the dose of oral prednisone that is required to adequately treat patients with myasthenia gravis.
Role: site PI

5U01NS052592-05; Cudkowicz (PI) 09/30/2005-11/30/2011
Coenzyme Q10 in Huntington's Disease
The goal of this study was to determine the efficacy of coenzyme Q10 in Huntington's disease. When I left UTMB for UF on 03/31/2009, I transferred the site-PI from me to Dr. George Jackson at UTMB.
Role: site PI

Muscular Dystrophy Association: Ashizawa (PI) 09/01/2009-03/31/2010
7th Internatinal Myotonic Dystrophy Consortium meeting (IDCM7)
The goal of this grant is to support the 7th International Myotonic Dystrophy Consortium meeting held in Wuertzberg, Germany in September 10-12, 2009.
Role: PI

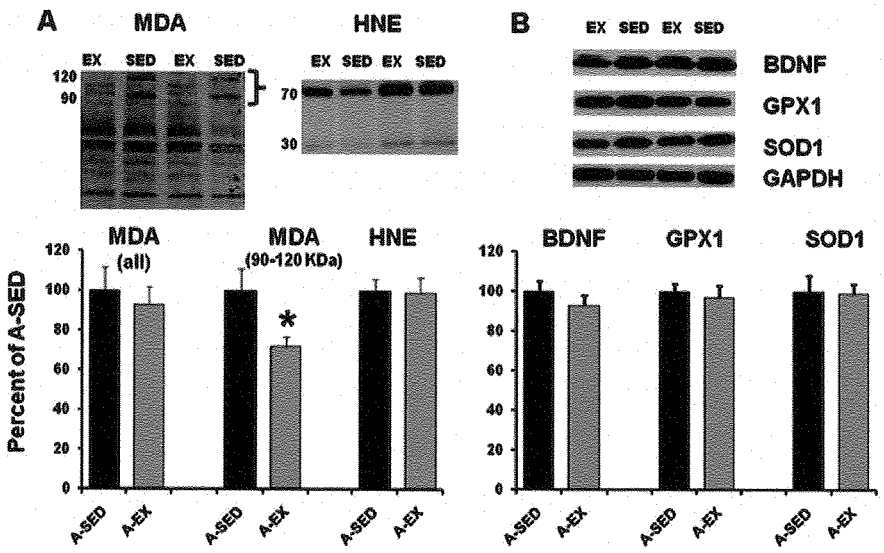

Fig. 11. Protein analysis of lipid oxidation. Western blots for sedentary (A-SED) (filled bars) and exercise (A-EX) (gray bars) showing the mean expression of (A) malondialdehyde (MDA) and HNE or (B) brain-derived neurotrophic factor (BDNF), glutathione peroxidase 1 (GPX1), and superoxide dismutase 1 (SOD1). Densitometry readings for each protein of interest were standardized by the corresponding reading for GAPDH. Inserts provide example blots. All measures were normalized to the A-SED group. MDA measured between 90 and 120 kDa (bracket on the blot insert) was decreased in the A-EX group. * Significant ($p < 0.05$) difference.

ited superior performance on the cue discrimination task, suggesting enhanced reliance on systems other than the hippocampus (McDonald and White, 1994; Packard and McGaugh, 1992). In older humans, exercise may promote more general attentional processes with limited influence specific to spatial processing (Colcombe and Kramer, 2003). The object recognition task requires attentional processing (Levin et al., 2011) and minimizes the need for spatial orientation. Furthermore, performance on this task declines with advanced age (Blalock et al., 2003; Dellu et al., 1992; Ennaceur and Meliani, 1992; Hauser et al., 2009). We observed that exercise increased object recognition memory in older rats, a result similar to that observed in young animals (García-Capdevila et al., 2009; Griffin et al., 2009; O'Callaghan et al., 2007), suggesting that exercise can improve memory in older animals. Together, the results suggest that the exercise conditions altered the response selection, such that when presented with the option of using a spatial or a response strategy in the water maze, animals with a history of 10–12 weeks of exercise biased their behavior to employ an egocentric response strategy.

The results on physiology confirm an age-related increase in the susceptibility to induction of LTD (Foster and Kumar, 2007; Foy et al., 2008; Hsu et al., 2002; Norris et al., 1996), impaired LTP induction (Coultrap et al., 2008; Deupree et al., 1993; Eckles-Smith et al., 2000; Moore et al., 1993; O'Callaghan et al., 2009; Shankar et al., 1998), and an increase in the AHP (Bodhinathan et al., 2010b; Disterhoft et al., 1996; Gant and Thibault, 2009; Kumar and Foster, 2002, 2007; Landfield and Pitler, 1984; Tombaugh et al., 2005). Consistent with a number of studies, mainly in young animals, environmental enrichment decreased LTD and improved LTP (Artola et al., 2006; Duffy et al., 2001; O'Callaghan et al., 2009; Yang et al., 2006, 2007). Similarly, we confirmed that exposure to novelty decreases the AHP in aged rats (Kumar and Foster, 2007). The fact that the AHP was larger in A-SED and A-EX, groups that performed poorly on the water maze, is consistent with the idea that learning reduces the AHP amplitude (Oh et al., 2010). Previous work indicates that exercise in young animals does not enhance LTP in region CA1 (Lange-Asschenfeldt et al., 2007; Tartar et al., 2006; van Praag et al., 1999). In contrast, we observed that the influence of exercise on synaptic plasticity was qualitatively similar to environmental enrichment, reducing the susceptibility to induction of LTD and enhancing LTP. The difference may be due to baseline differences in the threshold or susceptibility to LTP induction, such that exercise improved LTP induction only in aged animals that normally exhibit impaired LTP.

The rejuvenation of senescent physiology by environmental enrichment and exercise has important implications for our understanding of brain aging. The improvement in synaptic plasticity is likely due to factors that are common across the 2 conditions including increased hippocampal activity associated with locomotion (Bland, 1986; Buzsáki, 2002; Czurkó et al., 1999; Foster et al., 1989). The idea that neural activity modifies Ca^{2+}-dependent processes is consistent with gene microarry studies (Molteni et al., 2002; Stranahan et al., 2010; Tong et al., 2001). This work indicates that exercise increases the expression of genes linked

to neural activity and synaptic plasticity and reduces the expression of genes linked to oxidative stress. In some cases, the increase in neural activity due to exercise results in increased expression of BDNF (Berchtold et al., 2005; Griffin et al., 2009; Molteni et al., 2002; O'Callaghan et al., 2009) and protection against oxidative stress (Nakajima et al., 2010; Rodrigues et al., 2010; Stranahan et al., 2010; Vaynman et al., 2006). We did not observe an increase in BDNF expression, which is consistent with several other studies (Cechetti et al., 2008; Lou et al., 2008; Marais et al., 2009; Vaynman et al., 2004). Taken together, the results indicate that the ability to observe an increase in BDNF is related to the specific region of the hippocampus examined and a number of ancillary factors associated with the exercise treatment including the age of the animal, intensity, and duration of the exercise.

Exercise can shift the redox state of the brain (Radak et al., 2007). It might be expected that a shift in redox state would influence oxidative damage. We observed a decrease in lipid peroxidation, which was limited to certain bands on the Western blot. The results are consistent with other studies that observed minimal changes in lipid peroxidation in the hippocampus after exercise training (Acikgoz et al., 2006; Cechetti et al., 2008; Devi and Kiran, 2004; Jolitha et al., 2006). Thus, it is possible that a shift in redox state has large effects on the activity of signaling cascades that are important for hippocampal function (Bodhinathan et al., 2010a, 2010b) with limited effects on oxidative damage.

In summary, the data indicate that both exercise and environmental enrichment ameliorated the physiological markers of hippocampal aging including synaptic plasticity (Figs. 8 and 9). In contrast, the results indicate that only environmental enrichment improved hippocampal-dependent spatial discrimination learning (Fig. 4C), ameliorated the memory consolidation deficit observed in older animals (Fig. 5C), and improved cell excitability (Fig. 10). Taken together with other studies comparing the effects of exercise and experience on age-related cognitive decline, our results suggest that neural activity associated with locomotion, exploration, and novelty may rejuvenate hippocampal neural plasticity processes; however, the history of experience may predispose the animal to employ a limited behavioral repertoire. Thus, exercise appears to provide a means to promote healthy brain aging; nevertheless, in the absence of concomitant cognitive training, the benefits may not be fully realized. Consequently, physical activity and the associated activation of hippocampal circuits may be useful as an adjunct to various cognitive training programs.

Disclosure statement

The authors have no actual or potential conflicts of interest.

Procedures involving animals have been reviewed and approved by the Institutional Animal Care and Use Committee and were in accordance with guidelines established by the U.S. Public Health Service Policy on Humane Care and Use of Laboratory Animals.

Acknowledgements

This work was supported by National Institutes of Aging grants AG14979, AG037984, AG036800, and the Evelyn F. McKnight Brain Research Foundation.

Thanks to Prasanna Durairaj, Jose Herrera, and Vijay Parekh for technical assistance.

References

Acikgoz, O., Aksu, I., Topcu, A., Kayatekin, B.M., 2006. Acute exhaustive exercise does not alter lipid peroxidation levels and antioxidant enzyme activities in rat hippocampus, prefrontal cortex and striatum. Neurosci. Lett. 406, 148–151.

Artola, A., von Frijtag, J.C., Fermont, P.C., Gispen, W.H., Schrama, L.H., Kamal, A., Spruijt, B.M., 2006. Long-lasting modulation of the induction of LTD and LTP in rat hippocampal CA1 by behavioural stress and environmental enrichment. Eur. J. Neurosci. 23, 261–272.

Asl, N.A., Sheikhzade, F., Torchi, M., Roshangar, L., Khamnei, S., 2008. Long-term regular exercise promotes memory and learning in young but not in older rats. Pathophysiology 15, 9–12.

Barnes, C.A., Forster, M.J., Fleshner, M., Ahanotu, E.N., Laudenslager, M.L., Mazzeo, R.S., Maier, S.F., Lal, H., 1991. Exercise does not modify spatial memory, brain autoimmunity, or antibody response in aged F-344 rats. Neurobiol. Aging 12, 47–53.

Berchtold, N.C., Chinn, G., Chou, M., Kesslak, J.P., Cotman, C.W., 2005. Exercise primes a molecular memory for brain-derived neurotrophic factor protein induction in the rat hippocampus. Neuroscience 133, 853–861.

Bizon, J.L., LaSarge, C.L., Montgomery, K.S., McDermott, A.N., Setlow, B., Griffith, W.H., 2009. Spatial reference and working memory across the lifespan of male Fischer 344 rats. Neurobiol. Aging 30, 646–655.

Blalock, E.M., Chen, K.C., Sharrow, K., Herman, J.P., Porter, N.M., Foster, T.C., Landfield, P.W., 2003. Gene microarrays in hippocampal aging: statistical profiling identifies novel processes correlated with cognitive impairment. J. Neurosci. 23, 3807–3819.

Bland, B.H., 1986. The physiology and pharmacology of hippocampal formation theta rhythms. Prog. Neurobiol. 26, 1–54.

Bodhinathan, K., Kumar, A., Foster, T.C., 2010a. Intracellular redox state alters NMDA receptor response during aging through Ca2+/calmodulin-dependent protein kinase II. J. Neurosci. 30, 1914–1924.

Bodhinathan, K., Kumar, A., Foster, T.C., 2010b. Redox sensitive calcium stores underlie enhanced after hyperpolarization of aged neurons: role for ryanodine receptor mediated calcium signaling. J. Neurophysiol. 104, 2586–2593.

Buzsáki, G., 2002. Theta oscillations in the hippocampus. Neuron 33, 325–340.

Carter, C.S., Leeuwenburgh, C., Daniels, M., Foster, T.C., 2009. Influence of calorie restriction on measures of age-related cognitive decline: role of increased physical activity. Gerontol. A Biol. Sci. Med. Sci. 64, 850–859.

Cechetti, F., Fochesatto, C., Scopel, D., Nardin, P., Goncalves, C.A., Netto, C.A., Siqueira, I.R., 2008. Effect of a neuroprotective exercise protocol on oxidative state and BDNF levels in the rat hippocampus. Brain Res. 1188, 182–188.

Chang, H.C., Yang, Y.R., Wang, S.G., Wang, R.Y., 2009. Effects of treadmill training on motor performance and extracellular glutamate level in striatum in rats with or without transient middle cerebral artery occlusion. Behav. Brain Res. 205, 450–455.

Colcombe, S., Kramer, A.F., 2003. Fitness effects on the cognitive function of older adults: a meta-analytic study. Psychol. Sci. 14, 125–130.

Coultrap, S.J., Bickford, P.C., Browning, M.D., 2008. Blueberry-enriched diet ameliorates age-related declines in NMDA receptor-dependent LTP. Age. (Dordr.) 30, 263–272.

Countryman, R.A., Gold, P.E., 2007. Rapid forgetting of social transmission of food preferences in aged rats: relationship to hippocampal CREB activation. Learn. Mem. 14, 350–358.

Cracchiolo, J.R., Mori, T., Nazian, S.J., Tan, J., Potter, H., Arendash, G.W., 2007. Enhanced cognitive activity—over and above social or physical activity—is required to protect Alzheimer's mice against cognitive impairment, reduce Abeta deposition, and increase synaptic immunoreactivity. Neurobiol. Learn. Mem. 88, 277–294.

Cui, L., Hofer, T., Rani, A., Leeuwenburgh, C., Foster, T.C., 2009. Comparison of lifelong and late life exercise on oxidative stress in the cerebellum. Neurobiol. Aging 30, 903–909.

Czurkó, A., Hirase, H., Csicsvari, J., Buzsáki, G., 1999. Sustained activation of hippocampal pyramidal cells by "space clamping" in a running wheel. Eur. J. Neurosci. 11, 344–352.

Davis, H.P., Small, S.A., Stern, Y., Mayeux, R., Feldstein, S.N., Keller, F.R., 2003. Acquisition, recall, and forgetting of verbal information in long-term memory by young, middle-aged, and elderly individuals. Cortex 39, 1063–1091.

DeCoteau, W.E., Kesner, R.P., 2000. A double dissociation between the rat hippocampus and medial caudoputamen in processing two forms of knowledge. Behav. Neurosci. 114, 1096–1108.

Dellu, F., Mayo, W., Cherkaoui, J., Le Moal, M., Simon, H., 1992. A two-trial memory task with automated recording: study in young and aged rats. Brain Res. 588, 132–139.

Deupree, D.L., Bradley, J., Turner, D.A., 1993. Age-related alterations in potentiation in the CA1 region in F344 rats. Neurobiol. Aging 14, 249–258.

Devi, S.A., Kiran, T.R., 2004. Regional responses in antioxidant system to exercise training and dietary vitamin E in aging rat brain. Neurobiol. Aging 25, 501–508.

Ding, Y., Li, J., Lai, Q., Azam, S., Rafols, J.A., Diaz, F.G., 2002. Functional improvement after motor training is correlated with synaptic plasticity in rat thalamus. Neurol. Res. 24, 829–836.

Diniz, D.G., Foro, C.A., Rego, C.M., Gloria, D.A., de Oliveira, F.R., Paes, J.M., de Sousa, A.A., Tokuhashi, T.P., Trindade, L.S., Turiel, M.C., Vasconcelos, E.G., Torres, J.B., Cunnigham, C., Perry, V.H., Vasconcelos, P.F., Diniz, C.W., 2010. Environmental impoverishment and aging alter object recognition, spatial learning, and dentate gyrus astrocytes. Eur. J. Neurosci. 32, 509–519.

Disterhoft, J.F., Thompson, L.T., Moyer, J.R., Mogul, D.J., 1996. Calcium-dependent afterhyperpolarization and learning in young and aging hippocampus. Life Sci. 59, 413–420.

Driscoll, I., Howard, S.R., Stone, J.C., Monfils, M.H., Tomanek, B., Brooks, W.M., Sutherland, R.J., 2006. The aging hippocampus: a multi-level analysis in the rat. Neuroscience 139, 1173–1185.

Duffy, P.H., Feuers, R.J., Leakey, J.A., Nakamura, K., Turturro, A., Hart, R.W., 1989. Effect of chronic caloric restriction on physiological variables related to energy metabolism in the male Fischer 344 rat. Mech. Ageing Dev. 48, 117–133.

Duffy, P.H., Feuers, R.J., Pipkin, J.L., Turturro, A., Hart, R.W., 1997a. Age and temperature related changes in behavioral and physiological performance in the Peromyscus leucopus mouse. Mech. Ageing Dev. 95, 43–61.

Duffy, P.H., Leakey, J.E., Pipkin, J.L., Turturro, A., Hart, R.W., 1997b. The physiologic, neurologic, and behavioral effects of caloric restriction related to aging, disease, and environmental factors. Environ. Res. 73, 242–248.

Duffy, S.N., Craddock, K.J., Abel, T., Nguyen, P.V., 2001. Environmental enrichment modifies the PKA-dependence of hippocampal LTP and improves hippocampus-dependent memory. Learn. Mem. 8, 26–34.

During, M.J., Cao, L., 2006. VEGF, a mediator of the effect of experience on hippocampal neurogenesis. Curr. Alzheimer Res. 3, 29–33.

Eckles-Smith, K., Clayton, D., Bickford, P., Browning, M.D., 2000. Caloric restriction prevents age-related deficits in LTP and in NMDA receptor expression. Brain Res. Mol. Brain Res. 78, 154–162.

Ennaceur, A., Meliani, K., 1992. A new one-trial test for neurobiological studies of memory in rats. III. Spatial vs. non-spatial working memory. Behav. Brain Res. 51, 83–92.

Fernandez, C.I., Collazo, J., Bauza, Y., Castellanos, M.R., Lopez, O., 2004. Environmental enrichment-behavior-oxidative stress interactions in the aged rat: issues for a therapeutic approach in human aging. Ann. N. Y. Acad. Sci. 1019, 53–57.

Foster, T.C., 1999. Involvement of hippocampal synaptic plasticity in age-related memory decline. Brain Res. Rev. 30, 236–249.

Foster, T.C., Barnes, C.A., Rao, G., McNaughton, B.L., 1991. Increase in perforant path quantal size in aged F-344 rats. Neurobiol. Aging 12, 441–448.

Foster, T.C., Castro, C.A., McNaughton, B.L., 1989. Spatial selectivity of rat hippocampal neurons: dependence on preparedness for movement. Science 244, 1580–1582.

Foster, T.C., Dumas, T.C., 2001. Mechanism for increased hippocampal synaptic strength following differential experience. J. Neurophysiol. 85, 1377–1383.

Foster, T.C., Gagne, J., Massicotte, G., 1996. Mechanism of altered synaptic strength due to experience: relation to long-term potentiation. Brain Res. 736, 243–250.

Foster, T.C., Kumar, A., 2007. Susceptibility to induction of long-term depression is associated with impaired memory in aged Fischer 344 rats. Neurobiol. Learn. Mem. 87, 522–535.

Foster, T.C., Sharrow, K.M., Kumar, A., Masse, J., 2003. Interaction of age and chronic estradiol replacement on memory and markers of brain aging. Neurobiol. Aging 24, 839–852.

Foy, M.R., Baudry, M., Foy, J.G., Thompson, R.F., 2008. 17beta-estradiol modifies stress-induced and age-related changes in hippocampal synaptic plasticity. Behav. Neurosci. 122, 301–309.

Frick, K.M., Fernandez, S.M., 2003. Enrichment enhances spatial memory and increases synaptophysin levels in aged female mice. Neurobiol. Aging 24, 615–626.

Gagné, J., Gélinas, S., Martinoli, M.G., Foster, T.C., Ohayon, M., Thompson, R.F., Baudry, M., Massicotte, G., 1998. AMPA receptor properties in adult rat hippocampus following environmental enrichment. Brain Res. 799, 16–25.

Gant, J.C., Thibault, O., 2009. Action potential throughput in aged rat hippocampal neurons: regulation by selective forms of hyperpolarization. Neurobiol. Aging 30, 2053–2064.

García-Capdevila, S., Portell-Cortés, I., Torras-Garcia, M., Coll-Andreu, M., Costa-Miserachs, D., 2009. Effects of long-term voluntary exercise on learning and memory processes: dependency of the task and level of exercise. Behav. Brain Res. 202, 162–170.

Goodrick, C.L., Ingram, D.K., Reynolds, M.A., Freeman, J.R., Cider, N.L., 1983a. Differential effects of intermittent feeding and voluntary exercise on body weight and lifespan in adult rats. J. Gerontol. 38, 36–45.

Goodrick, C.L., Ingram, D.K., Reynolds, M.A., Freeman, J.R., Cider, N.L., 1983b. Effects of intermittent feeding upon growth, activity, and lifespan in rats allowed voluntary exercise. Exp. Aging Res. 9, 203–209.

Griffin, E.W., Bechara, R.G., Birch, A.M., Kelly, A.M., 2009. Exercise enhances hippocampal-dependent learning in the rat: evidence for a BDNF-related mechanism. Hippocampus 19, 973–980.

Hall, C.B., Lipton, R.B., Sliwinski, M., Katz, M.J., Derby, C.A., Verghese, J., 2009. Cognitive activities delay onset of memory decline in persons who develop dementia. Neurology 73, 356–361.

Hansalik, M., Skalicky, M., Viidik, A., 2006. Impairment of water maze behaviour with ageing is counteracted by maze learning earlier in life but not by physical exercise, food restriction or housing conditions. Exp. Gerontol. 41, 169–174.

Harburger, L.L., Lambert, T.J., Frick, K.M., 2007a. Age-dependent effects of environmental enrichment on spatial reference memory in male mice. Behav. Brain Res. 185, 43–48.

Harburger, L.L., Nzerem, C.K., Frick, K.M., 2007b. Single enrichment variables differentially reduce age-related memory decline in female mice. Behav. Neurosci. 121, 679–688.

Hauser, E., Tolentino, J.C., Pirogovsky, E., Weston, E., Gilbert, P.E., 2009. The effects of aging on memory for sequentially presented objects in rats. Behav. Neurosci. 123, 1339–1345.

Holloszy, J.O., Smith, E.K., Vining, M., Adams, S., 1985. Effect of voluntary exercise on longevity of rats. J. Appl. Physiol. 59, 826–831.

Hori, N., Hirotsu, I., Davis, P.J., Carpenter, D.O., 1992. Long-term potentiation is lost in aged rats but preserved by calorie restriction. Neuroreport 3, 1085–1088.

Hsu, K.S., Huang, C.C., Liang, Y.C., Wu, H.M., Chen, Y.L., Lo, S.W., Ho, W.C., 2002. Alterations in the balance of protein kinase and phosphatase activities and age-related impairments of synaptic transmission and long-term potentiation. Hippocampus 12, 787–802.

Jolitha, A.B., Subramanyam, M.V., Asha Devi, S., 2006. Modification by vitamin E and exercise of oxidative stress in regions of aging rat brain: studies on superoxide dismutase isoenzymes and protein oxidation status. Exp. Gerontol. 41, 753–763.

Kumar, A., Foster, T., 2007. Environmental enrichment decreases the afterhyperpolarization in senescent rats. Brain Res. 1130, 103–107.

Kumar, A., Foster, T.C., 2002. 17beta-Estradiol benzoate decreases the AHP amplitude in CA1 pyramidal neurons. J. Neurophysiol. 88, 621–626.

Kumar, A., Thinschmidt, J.S., Foster, T.C., King, M.A., 2007. Aging Effects on the Limits and Stability of Long-Term Synaptic Potentiation and Depression in Rat Hippocampal Area CA1. J. Neurophysiol. 98, 594–601.

Lambert, T.J., Fernandez, S.M., Frick, K.M., 2005. Different types of environmental enrichment have discrepant effects on spatial memory and synaptophysin levels in female mice. Neurobiol. Learn. Mem. 83, 206–216.

Landfield, P.W., Pitler, T.A., 1984. Prolonged Ca2+-dependent afterhyperpolarizations in hippocampal neurons of aged rats. Science 226, 1089–1092.

Lange-Asschenfeldt, C., Lohmann, P., Riepe, M.W., 2007. Spatial performance in a complex maze is associated with persistent long-term potentiation enhancement in mouse hippocampal slices at early training stages. Neuroscience 147, 318–324.

Leal-Galicia, P., Castañeda-Bueno, M., Quiroz-Baez, R., Arias, C., 2008. Long-term exposure to environmental enrichment since youth prevents recognition memory decline and increases synaptic plasticity markers in aging. Neurobiol. Learn. Mem. 90, 511–518.

Levin, E.D., Bushnell, P.J., Rezvani, A.H., 2011. Attention-modulating effects of cognitive enhancers. Pharmacol. Biochem. Behav. 99, 146–154.

Lores-Arnaiz, S., Bustamante, J., Arismendi, M., Vilas, S., Paglia, N., Basso, N., Capani, F., Coirini, H., Costa, J.J., Arnaiz, M.R., 2006. Extensive enriched environments protect old rats from the aging dependent impairment of spatial cognition, synaptic plasticity and nitric oxide production. Behav. Brain Res. 169, 294–302.

Lou, S.J., Liu, J.Y., Chang, H., Chen, P.J., 2008. Hippocampal neurogenesis and gene expression depend on exercise intensity in juvenile rats. Brain Res. 1210, 48–55.

Marais, L., Stein, D.J., Daniels, W.M., 2009. Exercise increases BDNF levels in the striatum and decreases depressive-like behavior in chronically stressed rats. Metab. Brain Dis. 24, 587–597.

Markowska, A.L., Mooney, M., Sonntag, W.E., 1998. Insulin-like growth factor-1 ameliorates age-related behavioral deficits. Neuroscience 87, 559–569.

Marques, J.M., Alonso, I., Santos, C., Silveira, I., Olsson, I.A., 2009. The spatial learning phenotype of heterozygous leaner mice is robust to systematic variation of the housing environment. Comp. Med. 59, 129–138.

McDonald, R.J., White, N.M., 1993. A triple dissociation of memory systems: hippocampus, amygdala, and dorsal striatum. Behav. Neurosci. 107, 3–22.

McDonald, R.J., White, N.M., 1994. Parallel information processing in the water maze: evidence for independent memory systems involving dorsal striatum and hippocampus. Behav. Neural Biol. 61, 260–270.

Mohammed, A.H., Henriksson, B.G., Söderström, S., Ebendal, T., Olsson, T., Seckl, J.R., 1993. Environmental influences on the central nervous system and their implications for the aging rat. Behav. Brain Res. 57, 183–191.

Molteni, R., Ying, Z., Gómez-Pinilla, F., 2002. Differential effects of acute and chronic exercise on plasticity-related genes in the rat hippocampus revealed by microarray. Eur. J. Neurosci. 16, 1107–1116.

Moore, C.I., Browning, M.D., Rose, G.M., 1993. Hippocampal plasticity induced by primed burst, but not long-term potentiation, stimulation is impaired in area CA1 of aged Fischer 344 rats. Hippocampus 3, 57–66.

Mora, F., Segovia, G., del Arco, A., 2007. Aging, plasticity and environmental enrichment: structural changes and neurotransmitter dynamics in several areas of the brain. Brain Res. Rev. 55, 78–88.

Nakajima, S., Ohsawa, I., Ohta, S., Ohno, M., Mikami, T., 2010. Regular voluntary exercise cures stress-induced impairment of cognitive function and cell proliferation accompanied by increases in cerebral IGF-1 and GST activity in mice. Behav. Brain Res. 211, 178–184.

Nguyen, P.V., Woo, N.H., 2003. Regulation of hippocampal synaptic plasticity by cyclic AMP-dependent protein kinases. Prog. Neurobiol. 71, 401–437.

Norris, C.M., Korol, D.L., Foster, T.C., 1996. Increased susceptibility to induction of long-term depression and long-term potentiation reversal during aging. J. Neurosci. 16, 5382–5392.

O'Callaghan, R.M., Griffin, E.W., Kelly, A.M., 2009. Long-term treadmill exposure protects against age-related neurodegenerative change in the rat hippocampus. Hippocampus 19, 1019–1029.

O'Callaghan, R.M., Ohle, R., Kelly, A.M., 2007. The effects of forced exercise on hippocampal plasticity in the rat: A comparison of LTP, spatial- and non-spatial learning. Behav. Brain Res. 176, 362–366.

Oh, M.M., Oliveira, F.A., Disterhoft, J.F., 2010. Learning and aging related changes in intrinsic neuronal excitability. Front. Aging Neurosci. 2, 2.

Olson, A.K., Eadie, B.D., Ernst, C., Christie, B.R., 2006. Environmental enrichment and voluntary exercise massively increase neurogenesis in the adult hippocampus via dissociable pathways. Hippocampus 16, 250–260.

Packard, M.G., McGaugh, J.L., 1992. Double dissociation of fornix and caudate nucleus lesions on acquisition of two water maze tasks: further evidence for multiple memory systems. Behav. Neurosci. 106, 439–446.

Pardon, M.C., Sarmad, S., Rattray, I., Bates, T.E., Scullion, G.A., Marsden, C.A., Barrett, D.A., Lowe, J., Kendall, D.A., 2009. Repeated novel cage exposure-induced improvement of early Alzheimer's-like cognitive and amyloid changes in TASTPM mice is unrelated to changes in brain endocannabinoids levels. Neurobiol. Aging 30, 1099–1113.

Pietropaolo, S., Feldon, J., Alleva, E., Cirulli, F., Yee, B.K., 2006. The role of voluntary exercise in enriched rearing: a behavioral analysis. Behav. Neurosci. 120, 787–803.

Potegal, M., 1972. The caudate nucleus egocentric localization system. Acta Neurobiol. Exp. (Wars.) 32, 479–494.

Radak, Z., Kumagai, S., Taylor, A.W., Naito, H., Goto, S., 2007. Effects of exercise on brain function: role of free radicals. Appl. Physiol. Nutr. Metab. 32, 942–946.

Rapp, P.R., Rosenberg, R.A., Gallagher, M., 1987. An evaluation of spatial information processing in aged rats. Behav. Neurosci. 101, 3–12.

Rodrigues, L., Dutra, M.F., Ilha, J., Biasibetti, R., Quincozes-Santos, A., Leite, M.C., Marcuzzo, S., Achaval, M., Gonçalves, C.A., 2010. Treadmill training restores spatial cognitive deficits and neurochemical alterations in the hippocampus of rats submitted to an intracerebroventricular administration of streptozotocin. J. Neural Transm. 117, 1295–1305.

Schrijver, N.C., Bahr, N.I., Weiss, I.C., Würbel, H., 2002. Dissociable effects of isolation rearing and environmental enrichment on exploration, spatial learning and HPA activity in adult rats. Pharmacol. Biochem. Behav. 73, 209–224.

Schrijver, N.C., Pallier, P.N., Brown, V.J., Würbel, H., 2004. Double dissociation of social and environmental stimulation on spatial learning and reversal learning in rats. Behav. Brain Res. 152, 307–314.

Shankar, S., Teyler, T.J., Robbins, N., 1998. Aging differentially alters forms of long-term potentiation in rat hippocampal area CA1. J. Neurophysiol. 79, 334–341.

Soffié, M., Hahn, K., Terao, E., Eclancher, F., 1999. Behavioural and glial changes in old rats following environmental enrichment. Behav. Brain Res. 101, 37–49.

Stranahan, A.M., Lee, K., Becker, K.G., Zhang, Y., Maudsley, S., Martin, B., Cutler, R.G., Mattson, M.P., 2010. Hippocampal gene expression patterns underlying the enhancement of memory by running in aged mice. Neurobiol. Aging 31, 1937–1949.

Sweatt, J.D., 2009. Experience-dependent epigenetic modifications in the central nervous system. Biol. Psychiatry 65, 191–197.

Tartar, J.L., Ward, C.P., McKenna, J.T., Thakkar, M., Arrigoni, E., McCarley, R.W., Brown, R.E., Strecker, R.E., 2006. Hippocampal synaptic plasticity and spatial learning are impaired in a rat model of sleep fragmentation. Eur. J. Neurosci. 23, 2739–2748.

Tombaugh, G.C., Rowe, W.B., Rose, G.M., 2005. The slow afterhyperpolarization in hippocampal CA1 neurons covaries with spatial learning ability in aged Fisher 344 rats. J. Neurosci. 25, 2609–2616.

Tong, L., Shen, H., Perreau, V.M., Balazs, R., Cotman, C.W., 2001. Effects of exercise on gene-expression profile in the rat hippocampus. Neurobiol. Dis. 8, 1046–1056.

van Groen, T., Kadish, I., Wyss, J.M., 2002. Old rats remember old tricks; memories of the water maze persist for 12 months. Behav. Brain Res. 136, 247–255.

van Praag, H., Christie, B.R., Sejnowski, T.J., Gage, F.H., 1999. Running enhances neurogenesis, learning, and long-term potentiation in mice. Proc. Natl. Acad. Sci. U. S. A. 96, 13427–13431.

van Uffelen, J.G., Chin A Paw, M.J., Hopman-Rock, M., van Mechelen, W., 2008. The effects of exercise on cognition in older adults with and without cognitive decline: a systematic review. Clin. J. Sport Med. 18, 486–500.

Vaynman, S., Ying, Z., Gómez-Pinilla, F., 2004. Exercise induces BDNF and synapsin I to specific hippocampal subfields. J. Neurosci. Res. 76, 356–362.

Vaynman, S.S., Ying, Z., Yin, D., Gomez-Pinilla, F., 2006. Exercise differentially regulates synaptic proteins associated to the function of BDNF. Brain Res. 1070, 124–130.

Veyrac, A., Sacquet, J., Nguyen, V., Marien, M., Jourdan, F., Didier, A., 2009. Novelty determines the effects of olfactory enrichment on memory and neurogenesis through noradrenergic mechanisms. Neuropsychopharmacology 34, 786–795.

Weed, J.L., Lane, M.A., Roth, G.S., Speer, D.L., Ingram, D.K., 1997. Activity measures in rhesus monkeys on long-term calorie restriction. Physiol. Behav. 62, 97–103.

Winocur, G., 1998. Environmental influences on cognitive decline in aged rats. Neurobiol. Aging 19, 589–597.

Yang, C.H., Huang, C.C., Hsu, K.S., 2006. Novelty exploration elicits a reversal of acute stress-induced modulation of hippocampal synaptic plasticity in the rat. J. Physiol. 577, 601–615.

Yang, J., Hou, C., Ma, N., Liu, J., Zhang, Y., Zhou, J., Xu, L., Li, L., 2007. Enriched environment treatment restores impaired hippocampal synaptic plasticity and cognitive deficits induced by prenatal chronic stress. Neurobiol. Learn. Mem. 87, 257–263.

Yu, B.P., Masoro, E.J., McMahan, C.A., 1985. Nutritional influences on aging of Fischer 344 rats: I. Physical, metabolic, and longevity characteristics. J. Gerontol. 40, 657–670.

Original Research Communication

Influence of viral vector-mediated delivery of superoxide dismutase and catalase to the hippocampus on spatial learning and memory during aging

Wei-Hua Lee[1], Ashok Kumar[1], Asha Rani[1], Jose Herrera[1], Jinze Xu[2], Shinichi Someya[2], and Thomas C. Foster[1]*

Department of Neuroscience, McKnight Brain Institute[1],
Departments of Aging and Geriatric Research Division of Biology of Aging[2],
University of Florida, Gainesville, FL 32610

Total number of words: 4485
Reference numbers: 47
Gray scale illustrations: 3
Color illustration: 6 (online 5 and hardcopy 1)

Running title: Oxidative stress during senescence

Corresponding author:
Thomas Foster, Ph.D.
University of Florida Brain Institute
PO Box 100244
Gainesville, FL 32610-0244
Tel (352) 294-0033
Fax (352) 392-8347
Email: foster@mbi.ufl.edu

Abstract

Aims: Studies employing transgenic mice indicate overexpression of superoxide dismutase 1 (SOD1) improves memory during aging. It is unclear whether the improvement is due to a lifetime of overexpression, decreasing the accumulation of oxidized molecules, or if increasing antioxidant enzymes in older animals could reduce oxidative damage and improve cognitive function. We used adeno-associated virus (AAV) to deliver antioxidant enzymes (SOD1, SOD2, CAT and SOD1+CAT) to the hippocampus of young (4-month) and aged (19-month) F344/BN F1 male rats and examined memory-related behavioral performance one month and four months post injection.

Results: Overexpression of antioxidant enzymes reduced oxidative damage; however, memory function was not related to the level of oxidative damage. Increased expression of SOD1, initiated in advanced age, impaired learning. Increased expression of SOD1+CAT provided protection from impairments associated with overexpression of SOD1 alone and appears to guard against cognitive impairments in advanced age.

Innovation: Viral vector gene delivery provides a novel approach to test the hypothesis that increased expression of antioxidant enzymes, specifically in hippocampal neurons, will provide protection from age-related cognitive decline. Further, expression of multiple vectors permits more detailed investigation of mechanistic pathways.

Conclusion: Oxidative stress is a likely component of aging; however, it is unclear whether increased production of ROS or the accumulation of oxidative damage is the primary cause of functional decline. The results provide support for the idea that altered redox sensitive signaling

rather than the accumulation of damage may be of greater significance in the emergence of age-related learning and memory deficits.

Introduction

The brain is highly sensitive to oxidative stress (22), and the accumulation of damaged molecules may contribute to age-related memory impairments (8, 14, 30, 37, 38). Antioxidant molecules and enzymes balance the biological activity of reactive oxygen species (ROS), superoxide ($O_2^{\cdot-}$) and hydrogen peroxide (H_2O_2). Superoxide dismutase (SOD) catalyzes $O_2^{\cdot-}$ into H_2O_2 and catalase (CAT) or glutathione peroxidase (GPx) convert H_2O_2 to water and oxygen. SODs are classified according to their metal cofactors and cellular localization. The Cu/Zn-SOD1 (SOD1) is distributed throughout the cytoplasm, nucleus, and inner membrane space of mitochondria, Cu/Zn-SOD3 (SOD3) is located in the extracellular space, and Mn-SOD (SOD2) is restricted to the mitochondrial matrix (11, 18, 28).

SOD1 overexpression differentially influences brain function over the course of aging (23). Enhanced long-term potentiation (LTP) and spatial memory are observed in aged transgenic SOD1 (tg-SOD1) mice (25, 27). In contrast, tg-SOD2 mice do not exhibit altered synaptic plasticity or memory (23). It is unclear if increased SOD1 activity is required over the lifespan in order to prevent the accumulation of oxidative damage; or whether enhanced SOD1 activity, initiated in aged animals, might be therapeutic. To test this hypothesis, we used adeno-associated virus (AAV) to deliver antioxidant enzymes (SOD1, SOD2, CAT, or SOD1+CAT) to the hippocampus of young and aged rats. The results demonstrate a dissociation of learning from measures of oxidative stress and suggest that changes in redox sensitive signaling may mediate cognitive impairment.

Results

Efficiency-specificity of the viral vectors

Following behavioral testing (see below) a subset of animals was killed for examination of vector expression. Figure 1 illustrates the pattern of AAV-mediated transfection. Strong expression was observed throughout the dorsal hippocampus, extending > 3,000 μm along the anterior-posterior axis and included all major cell layers (Fig. 1A). Transfection was limited to the hippocampus in confirmation of our previous work (17) and mainly observed in neurons. Immunostaining for the myc tag of SOD1-myc revealed transfection in neurons identified by NeuN (Fig. 1B) or MAP2 (Fig. 1C) staining. Myc immunofluorescence was not localized to astrocytes or microglia, assessed by immunostaining for GFAP (Fig. 1D) and Iba1 (Fig. 1E). Injections of SOD1+CAT resulted in co-localization within the soma and dendrites of neurons (Fig. 1F). SOD2 was observed in the soma, but not the nucleus and co-localized with COX consistent with mitochondrial localization (Fig. 1G).

Figure 2 shows the increase in enzyme expression and decrease in oxidative damage associated with viral vector treatment. For quantification, band intensities were normalized to GAPDH, and then normalized to the mean value for young animals. Two SOD1 bands were observed for young and aged SOD1-myc injected rats (Fig. 2A). The band representing endogenous SOD1 was observed at 19 kDa and a larger band representing the myc tagged human SOD1 was located at 23 kDa. Densitometry indicated that rats injected with SOD1-myc exhibited a fourfold increase in total SOD1 [$F(1,16)=45.59$, $p<0.0001$) (Fig. 2E). Measurement of the 19 kDa band indicated that SOD1-myc expression did not modify the level of endogenous SOD1 (data not shown). An increase in the relevant vector was observed for SOD2 [$F(1,11)=7.9$,

$p<0.05$] (Figs. 2B, 2F) and CAT [$F(1,8)=7.14$, $p<0.05$] (Figs. 2C, 2G). Finally, injection of SOD1+CAT increased the expression of SOD1 [$F(1,10)=14.54$, $p<0.01$] and CAT [$F(1,12)=7.83$, $p<0.05$] (Figs. 2D, 2H). It should be noted that the level of expression for SOD1 under this condition was reduced relative to injection of SOD1-myc (i.e. 2 versus 4 fold).

As shown in Figure 2, SOD1, SOD2, CAT, or SOD1+CAT overexpression was associated with reduced HNE-staining. Quantification confirmed a decrease in HNE-reactive protein for SOD1 [$F(1,8)=9.26$, $p<0.05$], SOD2 [$F(1,12)=11.45$, $p<0.01$, CAT [$F(1,8)=18.53$, $p>0.01$], and SOD1+CAT [$F(1,8)=16.53$, $p<0.01$]. A decrease in protein S-glutathionylation was observed for rats overexpressing SOD1 [$F(1,12)=15.17$, $p<0.005$], SOD2 [$F(1,12)=7.83$, $p<0.05$], CAT [$F(1,8)=22.54$, $p<0.01$], and SOD1+CAT [$F(1,8)=7.3$, $p<0.05$]. Examination of SOD activity indicated that SOD1-myc rats exhibited a two-fold increase in SOD activity compared to GFP-injected rats ($p<0.05$; n = 4/group, data not shown).

SOD overexpression can increase the level of H_2O_2 and the expression of downstream antioxidant enzymes (13, 19, 29, 33). Western blots indicate that GPx4 and CAT levels did not differ among groups; however, there was a tendency for a treatment effect for GPx1 [$F(1,15)=3.46$, $p=0.08$] and post hoc comparisons indicated GPx1 expression significantly increased in aged SOD1 rats (Fig. 2E).

Age-dependent influence of enzyme overexpression on spatial learning

Spatial learning in the water maze was tested one month following virus injections. Figure 3 shows the mean escape latency and escape path length across the five training blocks during cue discrimination training. All groups exhibited a decrease in escape latency and path length during training, and young animals exhibited superior latency and path length relative to

aged rats. An ANOVA on latency indicated an effect of training [$F(4,404 = 107.21$, $p<0.0001$] and an age effect [$F(1,404)=34.71$, $p<0.0001$] in the absence of a treatment effect (Figs. 3A, 3B). Similarly, an ANOVA on path length indicated an effect of training [$F(4,404)=71.23$, $p<0.0001$] and age [$F(1,404)=40.084$, $p<0.0001$] in the absence of a treatment effect (Figs. 3C, 3D).

For spatial discrimination, an ANOVA on escape latency indicated significant main effects of training [$F(5,505)=68.03$, $p<0.0001$] and age [$F(1,505)=37.35$, $p<0.0001$], with a tendency for a treatment effect [$F(4,505)=2.10$, $p=0.08$] (Figs. 4A, 4B). Analysis of escape path length indicated effects of training [$F(5, 505)=81.19$, $p<0.0001$] and age [$F(1,505)=28.83$, $p<0.0001$], with a tendency for a treatment effect [$F(4,505)=2.27$, $p=0.06$] (Figs. 4C, 4D). To localize treatment effects, the data for the last two training blocks were averaged and an ANOVA was run within each age group. No treatment effects were found in young rats. A tendency [$F(4,50)=1.92$, $p=0.12$] for a treatment effect on latency was observed for aged rats, and post hoc analyses indicated that aged SOD1+CAT rats exhibited significantly less time to reach platform compared to aged rats expressing SOD2 or SOD1 alone (Fig. 4E). The results were confirmed for distance (Fig. 4F). An ANOVA on the mean for the last two blocks revealed tendency for a treatment effect in aged rats [$F(4,50)=2.5$, $p=0.05$] and post hoc analysis indicated that aged SOD1+CAT rats had a shorter path length compared to aged SOD2 or SOD1 rats.

A 60 sec probe trial was delivered between training blocks 5 and 6. Analyses were performed on two consecutive 30 sec segments. An ANOVA on the percent time in the goal quadrant during the first 30 seconds indicated young spent more time in the goal quadrant than aged rats [$F(1,100)=4.82$, $p<0.05$] and there was a tendency for a treatment effect [$F(4,100)=2.07$, $p=0.08$] (Figs. 5A, 5B). ANOVAs within each age group revealed a treatment effect for aged animals [$F(4,50)=3.07$, $p<0.05$] and post hoc comparisons indicated that aged control rats spent

more time in the goal quadrant compared to aged rats with SOD1 or CAT overexpression. Aged SOD1+CAT rats spent significantly more time in the goal quadrant relative to aged SOD1 rats. The percent time in the goal quadrant was compared to that expected by chance (i.e. 25%). For the first 30 seconds of the probe trial, all groups except for aged SOD1 or CAT performed above chance. Examination of time spent searching the goal quadrant for the last 30 sec of the probe trial indicated a tendency for an age effect [$F(1,100)=5.06$, $p=0.08$] in the absence of a treatment effect (Figs. 5C, 5D). An examination of the percent time in the goal quadrant indicated that all groups except aged controls and aged SOD1 rats spent significantly greater time in the goal quadrant relative to chance (Figs. 5C, 5D). The fact that aged SOD1 rats did not spend a significant portion of their search behavior in the goal quadrant for either segment of the probe trial indicates that these animals did not acquire a spatial search strategy.

The aged SOD1 impairment was confirmed by measuring the latency to the first platform crossing (Figs. 5E, 5F). An ANOVA indicated an age [$F(1,100)=10.95$, $p<0.01$] and treatment [$F(4,100)=2.52$, $p<0.05$] effect. ANOVAs within each age group indicated a tendency for a treatment effect in aged animals [$F(4,49)=2.38$, $p=0.06$] and post hoc comparisons indicated that aged SOD1 rats required a longer time to cross the platform location compared to age matched controls, CAT, and SOD1+CAT expressing groups. There was a tendency ($p=0.08$) for a difference between SOD1 and SOD2 groups. An ANOVA on the total number of platform crossing indicated an age difference [$F(1,100)=13.15$, $p<0.001$] (Figs. 5G, 5H), in the absence of a treatment effect. In sum, the results indicate that SOD1 overexpression for one month was associated with impaired spatial learning in aged rats. The fact that the SOD1+CAT exhibited superior performance relative to SOD1 group indicates that the impairment may be rescued to co-overexpressing CAT.

Overexpression of SOD1+CAT for 4 months improves spatial learning

Our results contrast with studies in tg-SOD1 mice, which indicate that young tg-SOD1 mice exhibit impaired spatial learning while aged tg-SOD1 mice show enhanced spatial memory (20, 27). The difference may result from an interaction of age and the duration of overexpression. To examine this possibility, a subset of animals tested at one month was retested at four months post-injection. The experimental groups included young rats (8 mo) injected with SOD1 (n = 6), SOD1+CAT (n = 10), GFP (n = 2), no surgery controls (n = 4), and aged rats (23 mo) injected with SOD1 (n = 6), SOD1+CAT (n = 10), GFP (n = 2) or no surgery controls (n = 4).

For examination of spatial learning 4 months after viral vector injections, the platform location in the maze was shifted to a new quadrant. An ANOVA on escape latency across training blocks indicated main effects of training [$F(5,185)=40.53$, $p<0.0001$] and age [$F(1,185)=5.19$, $p<0.05$], with a tendency for a treatment effect [$F(2,185)=5.19$, $p=0.07$] (Figs. 6A, 6B). Analysis of escape path length indicated effects of training [$F(5, 185)=36.12$, $p<0.0001$] and age [$F(1,185)=5.20$, $p<0.05$] (Figs. 6C, 6D). To localize treatment effects, the data for the last two training blocks were averaged and an ANOVA for treatment effects was run within each age group. An ANOVA for young animals indicated a tendency for a treatment effect [$F(2,18)=7.12$, $p=0.14$], however; post hoc comparisons did not reach significance; although there was a trend for young SOD1 rats to exhibit an increase in the escape latency relative to young control rats ($p=0.05$). An ANOVA for aged animals indicated a tendency for a treatment effect [$F(2,19)=3.24$, $p=0.06$] and post hoc comparisons indicated that aged SOD1+CAT rats required less time to reach platform compared to aged SOD1 rats (Fig. 6B). Analysis of the mean distance for the last two training blocks also indicated a tendency for a treatment effect in aged rats [$F(2,19)=2.67$,

p=0.09) (Figs. 6C, 6D) and post hoc comparisons confirmed that aged SOD1+CAT rats had a shorter path length to escape compared to aged SOD1 rats (Fig. 6D).

Examination of the first 30 seconds of the probe trial delivered between blocks 5 and 6, indicated a tendency for young rats to spend more time in the goal quadrant relative to aged rats [$F(1,37)=3.33$, $p=0.07$] in the absence of a treatment effect (Figs. 7A, 7B). The percent time searching the goal quadrant was significantly above chance for all groups, indicating that all groups had acquired a spatial search strategy. A tendency for a treatment effect [$F(2, 37)=2.47$, $p=0.09$] in the absence of an age difference was observed for the second half-minute of the probe trial (Figs. 7C, 7D). Again, all groups spent a significantly longer time in goal quadrant than expected by chance (Figs. 7C, 7D). An ANOVA on the latency to the first platform crossing indicated a significant age effect [$F(1,37)=12.73$, $p<0.01$], and a tendency for a treatment effect [$F(2,37)=2.24$, $p=0.1$]. An ANOVA within each age group indicated a tendency for a treatment effect only in the aged group [$F(2,19)=3.29$, $p=0.05$]. Post hoc comparison indicated that aged SOD1+CAT rats required less time for the first platform crossing compared to aged SOD1 rats and there was a tendency ($p=0.08$) for SOD1+CAT rats to cross quicker than aged controls. Finally, an ANOVA on total platform crossing indicated an age effect [$F(1,37)=12.67$, $p<0.005$] and a tendency for a treatment effect [$F(2,37)=2.54$, $p=0.09$]. An ANOVA within each age group indicated a tendency for a treatment effect in aged rats [$F(2,19)=3.45$, $p=0.05$] and post hoc comparisons indicated that aged SOD1+CAT rats exhibited significantly more platform crossings than aged controls (Fig. 7H). In fact, aged SOD1+CAT rats exhibited performance similar to young animals.

Figure 8 shows western blot data on enzyme expression and lipid peroxidation in the hippocampus for animals that overexpressed viral vectors for ~5 months. As shown in Figure 8A,

the two SOD1 bands (19 and 23 kDa) were observed for SOD1-myc injected rats. Densitometry confirmed that rats injected with SOD1-myc exhibited ~3 fold increase in total SOD1 [$F(1,12)=133.08$, $p<0.0001$] (Figs. 8A, 8C). Again, the 19 kDa band was not influenced by SOD1-myc expression (data not shown). Injection of SOD1+CAT increased the expression of SOD1 [$F(1,12)=31.31$, $p<0.001$] and CAT [$F(1,8)=10.40$, $p<0.05$] (Figs. 8B, 8D). Similar to 2-month overexpression, the level of expression for SOD1 under this condition was reduced relative to injection of SOD1-myc alone (i.e. 2 versus 2.5 fold).

A decrease in HNE-reactive protein was observed for rats that overexpress SOD1 [$F(1,12)=24.23$, $p<0.001$] or SOD1+CAT [$F(1,12)=7.63$, $p<0.05$] (Fig. 8). For SOD1 rats, there was an age effect on CAT expression [$F(1,12)=6.58$, $p<0.05$] in the absence of a treatment effect. Post hoc tests within each treatment group indicated an age-related decrease in expression in animals overexpressing SOD1 (Fig. 8C). Examination of GPx1 indicated no effect of age or treatment for SOD1 animals and SOD1+CAT animals exhibited an effect of age [$F(1,16)=15.00$, $p<0.005$] and treatment [$F(1,16)=4.27$, $p<0.05$]. Post hoc analyses indicated that GPx1 expression was reduced in aged rats that overexpressed SOD1+CAT [$F(1,8)=7.9$, $p<0.05$] compared to aged controls (Figs. 8B, 8D). Levels of protein carbonyls were measured; however, the results did not reveal any information concerning the effect of SOD1 overexpression, possibly due to the lack of specificity of carbonyl measures (1) or the fact that H_2O_2 is a poor mediator of stable oxidative damage for protein carbonyls (43). Furthermore, previous research indicates that lipid peroxidation may be more sensitive since SOD overexpression in mice markedly reduces lipid peroxidation in the absence of a significant effect on protein carbonyls (24). Consistent with the lipid peroxidation results, overexpression of SOD1 resulted in a

Rats were anesthetized with ketamine/xylazine (90/10 mg/kg) and virus was stereotactically injected at 2 sites bilaterally in the hippocampus using glass pipettes. Each injection consisted of 2 µl of GFP (dot blot titer: 1.02 x 10^{13} vg/mL), SOD1 (dot blot titer: 1.14 x 10^{13} vg/mL), SOD2 (dot blot titer: 6.99 x 10^{12} vg/mL), CAT (dot blot titer: 2.53 x 10^{13} vg/mL), or 3 ul 2:1 mix of SOD1 and CAT.

Behavior Testing

Methods for water maze testing have been published previously (16). Rats were first trained to find a visible platform using 15 trials separated to 5 blocks. Rats that did not reach the platform within 60 seconds on all trials during the 5th block were removed from the experiment. Standard water maze testing across several days is insensitive to cognitive decline across this age span in Fischer 344/Brown Norway F1 rats (46). Therefore, the task difficulty was increased by employing a single day massed training protocol, which is sensitive to age (9). Spatial discrimination testing occurred three days later and consisted of 18 trials separated into 6 blocks. A free swim probe trial was inserted between blocks 5 and 6. For the probe trial, the number of platform crossings was counted and the time spent in both goal and opposite quadrants was recorded.

Western Immunoblotting

The hippocampi were frozen in liquid nitrogen, and stored at -80°C. Tissue was prepared in RIPA buffer supplemented with protease inhibitor, phosphatase inhibitor and EDTA (Thermo scientific, Rockford, IL). The lysates were assayed for protein content using BCA kit (Pierce, Rockford, IL) and then separated on polyacrylamide gels (Bio-Rad Laboratories, Hercules, CA) and transferred to PVDF membranes (GE Healthcare) for western blotting. Primary antibodies

[SOD1, 1:5000; SOD2, 1:6000; 4-hydroxy-2-nonenal (HNE), 1:100; CAT, 1:1000; glutathione peroxidase 1 (GPx1), 1:600; glutathione peroxidase 4 (GPx4), 1:1000 (abcam Inc. Cambridge, MA); glyceraldehyde 3-phosphate dehydrogenase (GAPDH), 1:6000 (EnCor Biotechnology Inc., Gainesville, FL); glutathione (GSH), 1:1000 (Arbor Assays, Ann Arbor, MI] were diluted in blocking buffer (5% milk in Tris-Buffered Saline Tween-20 [TBST]) and applied to the membrane overnight at 4°C. Membranes were then incubated with horseradish peroxidase-conjugated secondary antibodies directed against the primary antibody (Cell Signaling technology, Inc, Danvers, MA). Membranes were reacted with and enhanced chemiluminescent substrate (Pierce Biotechnology, Rockford, IL). A medical film processor (SRX-101A, Konica Minolta Medical Imaging U.S.A., Inc.) was used to image the film.

Immunohistochemistry

Brains were postfixed in 4% paraformaldehyde followed by 30% sucrose in PBS (4°C). Sections (10-20 μm) were incubated with primary antibodies [SOD1, 1:1000; MAP2, 1:10000; CAT, 5 μg/ml; SOD2, 1:500 (abcam Inc. Cambridge, MA); myc-tag, 1:2000 (Cell Signaling Technology, Beverly, MA); neuronal nuclei (NeuN), 1:1000 (Chemicon/Millipore, Billerica, MA); Iba1, 1-2 μg/mL (Wako, Richmond, VA); glial fibrillary acidic protein (GFAP), 1:500 (DakoCytomation, Carpinteria, CA); anti-OxPhos complex IV subunit I (COX), 1:300 (Invitrogen, Camarillo, CA)] overnight at 4°C. The brain sections were then washed and incubated in corresponding Alexa 488 or 594 secondary antibodies (Molecular Probes, Eugene, OR) for 1 hour at room temperature. Sections were washed and counterstained with 4'-6-Diamidino-2-phenylindole (DAPI) solution (0.1 μg/ml in PBS) before mounting. Expression was confirmed using fluorescent microscopy (Zeiss Axioplan 2 upright fluorescent microscope, equipped with a QImaging Retiga 4000R Camera with RGB-HM-5 Color Filter and QImaging QCapture Pro 6.0

software; QImaging Surrey, BC Canada).

SOD activity was measured using the HT superoxide dismutase assay kit (Trevigen Inc, Gaithersburg, MD) and protein carbonyls were measured using a commercial ELISA (Zentech PC Test, Protein Carbonyl Enzyme Immuno-Assay Kit, Biocell Corp, Papatoetoe, NZ) according to the manufacturer's instructions. 8-oxo-7,8-dihydro-2-deoxyguanosine (8-oxodGuo) levels were determined according to our previously published methods (12).

Statistical analysis

Analyses of variance (ANOVAs) were used to establish main effects and interactions. Follow-up ANOVAs and/or Fisher's PLSD post hoc comparisons with $p < 0.05$ were employed to determine specific differences. Student *t* tests were used to determine whether quadrant search behavior was different than that expected by chance.

Acknowledgement

This work was supported by National Institutes of Aging Grants AG014979, AG037984, AG036800, and the Evelyn F. McKnight Brain Research Foundation. Special thanks to Katrina Velez, Marvin Servanez, and Christiaan Leeuwenburgh for technical support and advice.

Author Disclosure Statement

No competing financial interests exist.

Abbreviations Used

8-oxodGuo = 8-oxo-7,8-dihydro-2-deoxyguanosine

AAV = adeno-associated virus

ANOVAs = Analyses of variance

CAT = catalase

COX = OxPhos complex IV subunit I

GAPDH = glyceraldehyde 3-phosphate dehydrogenase

GFAP = glial fibrillary acidic protein

GFP = green fluorescence protein

GPx = glutathione peroxidase

GSH = glutathione

HNE = 4-hydroxy-2-nonenal

H_2O_2 = hydrogen peroxide

LTP = long-term potentiation

ROS = reactive oxygen species

SOD = superoxide dismutase

tg-SOD = SOD transgenic mice

Figure Legends

Figure 1. Neurons are the primary cell type transduced by the AAV vectors. (**A**) Panels show that transfection of myc (green) for SOD1-myc extended at least 3,000 μm though the hippocampus, was observed in all three cell layers, and was limited to the hippocampus. The distance is calculated relative to bregma. (**B**) Merged images showing co-localization (yellow) of myc (green) for SOD1-myc and NeuN (red) in neuron cell bodies, and (**C**) in dendrites determined by MAP2 (red). Myc did not co-localize with (**D**) GFAP (red) or (**E**) Iba1 (red). (**F**) Merged figure for the hippocampus of a rat injected with SOD1+CAT and immunostained for myc (green) for SOD1-myc and CAT (red) and co-localization (yellow). (**G**) Merged figure of a cell in the CA1 pyramidal cell layer of a rat injected with the SOD2 vector showing co-localization of SOD2 (green) with the OxPhos Complex IV subunit I (COX) (red). Note the expression is not observed in the nucleus (N) consistent with mitochondrial localization. Cell nuclei in **A**, **D** and **E** were stained with DAPI (blue). Calibration bars represent 500 μm (**A**), 100 μm (**B-F**) and 10 μm (**G**).

Figure 2. Overexpression of antioxidant enzymes in the hippocampus reduces markers of oxidative stress. Western blot analysis of hippocampal lysates from young and aged rats injected with viral vectors to express (**A, E**) SOD1-myc, (**B, F**) SOD2, (**C, G**) CAT, or (**D, H**) SOD1+CAT. For quantification, band intensities were normalized to expression of GAPDH and this value was normalized to the mean value of young controls from the same blot. In each case, transfection resulted in an increase in the expression of the antioxidant enzyme. For SOD1-myc (**A, D**), two bands were observed representing endogenous rat SOD1 (rSOD1) and the human myc tagged SOD1 (hSOD1). Lipid peroxidation (HNE) and S-glutathionylated proteins (GSH) were decreased by enzyme overexpression. To determine whether overexpression of antioxidant

enzymes would influence expression of downstream antioxidant enzymes, immunostaining was performed for glutathione peroxidase 1 (GPx1), glutathione peroxidase 4 (GPx4), and CAT. Overexpression of SOD1-myc was associated with an increase in GPx1 (**E**). Each bar represents the normalized mean + SEM (n = 3-6). Asterisks indicate significant ($p < 0.05$) differences determined by post hoc Fisher PLSD.

Figure 3. Overexpression of antioxidant enzymes did not affect cue discrimination in water maze. All groups learned to reach the visible platform, as indicated by a significant overall decrease in latency (**A, B**) and distance (**C, D**) across blocks. Y = 5-month and A = 20-month old rats injected with SOD1, SOD2, CAT, or SOD1+CAT. Age matched controls (Cont) included rats injected with GFP and no surgery controls. (To see this illustration in color the reader is referred to the web version of this article at www.liebertonline.com/ars).

Figure 4. Overexpression of SOD1 impaired spatial learning in aged rats. Behavioral measures for young and aged rats during training on the spatial version of the water escape task. Mean latency (**A, B**) and mean path length (**C, D**) to escape during spatial discrimination training. No treatment effects were found for young rats. Examination of the mean latency (**E**) and mean path length (**F**) averaged across the last two training blocks in aged animals indicated an effect of treatment. Due to better performance by the SOD1+CAT group relative to the SOD1 and SOD2 groups. Asterisk indicates a significant ($p < 0.05$) difference. (To see this illustration in color the reader is referred to the web version of this article at www.liebertonline.com/ars).

Figure 5. Overexpression of SOD1 impaired acquisition of a spatial search strategy in aged rats. A single probe trial was given between block 5 and block 6 of spatial training. Percent time spent searching the goal quadrant during the first 30 seconds of for (**A**) young and (**B**) aged rats.

The search behavior of aged rats with overexpression of SOD1 or CAT was not different from chance levels (25% dashed line). Aged SOD1 rats spent significant less time compared to aged control and aged rats with overexpression of SOD1+CAT. Aged rats with overexpression of CAT spent significant less time than aged control. Examination of the percent of time spent in goal quadrant during the second 30 seconds of probe trial for (**C**) young and (**D**) aged rats indicated that aged rats with overexpression of SOD1 continued to perform at chance levels. Examination of the latency for first platform crossing for (**E**) young and (**F**) aged rats indicated a treatment effect for aged animals due to an extended latency for the SOD1 group. Age differences were observed for total number of platform crossings between (**G**) young and (**H**) aged rats. Asterisk = $p < 0.05$ group difference. Pound sign indicates a significance ($p < 0.05$) difference from chance. (To see this illustration in color the reader is referred to the web version of this article at www.liebertonline.com/ars).

Figure 6. Long-term overexpression of SOD1+CAT improved learning in spatial trials in aged rats. Behavioral measures for young and aged rats during training on the spatial version of the water escape task four months after viral injections. Mean latency (**A, B**) and mean path length (**C, D**) to escape during spatial discrimination training. The bar graphs represent the means latency averaged across the last two training blocks. For aged animals better performance was observed for the SOD1+CAT group relative to the SOD1 group. Asterisk indicates a significant ($p < 0.05$) difference. (To see this illustration in color the reader is referred to the web version of this article at www.liebertonline.com/ars).

Figure 7. Overexpression of SOD1+CAT for four months improves spatial learning in probe test. A single probe trial was given between block 5 and block 6 of spatial training. Mean percent time spent searching the goal quadrant during the first 30 seconds of for (**A**) young and

(**B**) aged rats. Mean percent of time spent in goal quadrant during the second 30 seconds of probe trial for (**C**) young and (**D**) aged rats. Examination of the latency for first platform crossing for (**E**) young and (**F**) aged rats indicated a treatment effect for aged animals due to an superior performance by the SOD1+CAT group compared to the SOD1 group. Asterisk = $p < 0.05$ group difference. Pound sign indicates a significance ($p < 0.05$) difference from chance. (To see this illustration in color the reader is referred to the web version of this article at www.liebertonline.com/ars).

Figure 8. Antioxidant enzymes and oxidative stress markers in hippocampus with 5-month SOD1 and SOD1+CAT overexpression. Western blot analysis of hippocampal lysates from young and aged rats injected with viral vectors to express (**A**) SOD1, and (**B**) SOD1+CAT. For SOD1 (**A, C**), two bands were observed representing endogenous rat SOD1 (rSOD1) and the human myc tagged SOD1 (hSOD1). CAT level did not change in SOD1 rats but increased in SOD1+CAT rats. Lipid peroxidation measured with anti-4-hydroxy-2-nonenal (HNE) antibody was decreased by SOD1 and SOD1+CAT overexpression. Expression of SOD1 did not change the level of GPx1 but expression of SOD1+CAT in aged rats was associated with a decrease in GPx1 (**D**). GAPDH was used as a loading control. Asterisk indicates a significant ($p < 0.05$) difference in treatment. ω indicates a significant ($p < 0.05$) difference in age.

Figure 9. DNA oxidative damage is reduced by overexpression of SOD1. The level of 8-oxodGuo was measured and normalized by young controls (Y-Cont). Bars represent the mean and SEM.

References

1. Adams S, Green P, Claxton R, Simcox S, Williams MV, Walsh K, and Leeuwenburgh C. Reactive carbonyl formation by oxidative and non-oxidative pathways. *Front Biosci* 6: A17-24, 2001.

2. Aenlle KK, Kumar A, Cui L, Jackson TC, and Foster TC. Estrogen effects on cognition and hippocampal transcription in middle-aged mice. *Neurobiology of aging* 30: 932-945, 2009.

3. Auerbach JM, and Segal M. Peroxide modulation of slow onset potentiation in rat hippocampus. *J Neurosci* 17: 8695-8701, 1997.

4. Blalock EM, Chen KC, Sharrow K, Herman JP, Porter NM, Foster TC, and Landfield PW. Gene microarrays in hippocampal aging: statistical profiling identifies novel processes correlated with cognitive impairment. *J Neurosci* 23: 3807-3819, 2003.

5. Bodhinathan K, Kumar A, and Foster TC. Intracellular redox state alters NMDA receptor response during aging through Ca2+/calmodulin-dependent protein kinase II. *J Neurosci* 30: 1914-1924, 2010.

6. Bodhinathan K, Kumar A, and Foster TC. Redox sensitive calcium stores underlie enhanced after hyperpolarization of aged neurons: role for ryanodine receptor mediated calcium signaling. *Journal of neurophysiology* 104: 2586-2593, 2010.

7. Bosco DA, Morfini G, Karabacak NM, Song Y, Gros-Louis F, Pasinelli P, Goolsby H, Fontaine BA, Lemay N, McKenna-Yasek D, et al. Wild-type and mutant SOD1 share an aberrant conformation and a common pathogenic pathway in ALS. *Nat Neurosci* 13: 1396-1403, 2010.

8. Butterfield DA, and Sultana R. Redox proteomics identification of oxidatively modified brain proteins in Alzheimer's disease and mild cognitive impairment: insights into the progression of this dementing disorder. *Journal of Alzheimer's disease : JAD* 12: 61-72, 2007.

9. Carter CS, Leeuwenburgh C, Daniels M, and Foster TC. Influence of calorie restriction on measures of age-related cognitive decline: role of increased physical activity. *The journals of gerontology. Series A, Biological sciences and medical sciences* 64: 850-859, 2009.

10. Catala A. A synopsis of the process of lipid peroxidation since the discovery of the essential fatty acids. *Biochemical and biophysical research communications* 399: 318-323, 2010.

11. Chang LY, Slot JW, Geuze HJ, and Crapo JD. Molecular immunocytochemistry of the CuZn superoxide dismutase in rat hepatocytes. *The Journal of cell biology* 107: 2169-2179, 1988.

12. Cui L, Hofer T, Rani A, Leeuwenburgh C, and Foster TC. Comparison of lifelong and late life exercise on oxidative stress in the cerebellum. *Neurobiology of aging* 30: 903-909, 2009.

13. de Haan JB, Cristiano F, Iannello R, Bladier C, Kelner MJ, and Kola I. Elevation in the ratio of Cu/Zn-superoxide dismutase to glutathione peroxidase activity induces features of cellular senescence and this effect is mediated by hydrogen peroxide. *Human molecular genetics* 5: 283-292, 1996.

14. Forster MJ, Dubey A, Dawson KM, Stutts WA, Lal H, and Sohal RS. Age-related losses of cognitive function and motor skills in mice are associated with oxidative protein

damage in the brain. *Proceedings of the National Academy of Sciences of the United States of America* 93: 4765-4769, 1996.

15. Foster TC. Calcium homeostasis and modulation of synaptic plasticity in the aged brain. *Aging cell* 6: 319-325, 2007.

16. Foster TC, Sharrow KM, Masse JR, Norris CM, and Kumar A. Calcineurin links Ca2+ dysregulation with brain aging. *J Neurosci* 21: 4066-4073, 2001.

17. Foster TC, Rani A, Kumar A, Cui L, and Semple-Rowland SL. Viral vector-mediated delivery of estrogen receptor-alpha to the hippocampus improves spatial learning in estrogen receptor-alpha knockout mice. *Mol Ther* 16: 1587-1593, 2008.

18. Fridovich I. Superoxide dismutases: regularities and irregularities. *Harvey lectures* 79: 51-75, 1983.

19. Fullerton HJ, Ditelberg JS, Chen SF, Sarco DP, Chan PH, Epstein CJ, and Ferriero DM. Copper/zinc superoxide dismutase transgenic brain accumulates hydrogen peroxide after perinatal hypoxia ischemia. *Annals of neurology* 44: 357-364, 1998.

20. Gahtan E, Auerbach JM, Groner Y, and Segal M. Reversible impairment of long-term potentiation in transgenic Cu/Zn-SOD mice. *The European journal of neuroscience* 10: 538-544, 1998.

21. Gonzalez A, Granados MP, Pariente JA, and Salido GM. H2O2 mobilizes Ca2+ from agonist- and thapsigargin-sensitive and insensitive intracellular stores and stimulates glutamate secretion in rat hippocampal astrocytes. *Neurochemical research* 31: 741-750, 2006.

22. Halliwell B. Reactive oxygen species and the central nervous system. *Journal of neurochemistry* 59: 1609-1623, 1992.

23. Hu D, Klann E, and Thiels E. Superoxide dismutase and hippocampal function: age and isozyme matter. *Antioxidants & redox signaling* 9: 201-210, 2007.

24. Jang YC, Perez VI, Song W, Lustgarten MS, Salmon AB, Mele J, Qi W, Liu Y, Liang H, Chaudhuri A, et al. Overexpression of Mn superoxide dismutase does not increase life span in mice. *The journals of gerontology* 64: 1114-1125, 2009.

25. Kamsler A, and Segal M. Paradoxical actions of hydrogen peroxide on long-term potentiation in transgenic superoxide dismutase-1 mice. *J Neurosci* 23: 10359-10367, 2003.

26. Kamsler A, and Segal M. Hydrogen peroxide modulation of synaptic plasticity. *J Neurosci* 23: 269-276, 2003.

27. Kamsler A, Avital A, Greenberger V, and Segal M. Aged SOD overexpressing mice exhibit enhanced spatial memory while lacking hippocampal neurogenesis. *Antioxidants & redox signaling* 9: 181-189, 2007.

28. Keller GA, Warner TG, Steimer KS, and Hallewell RA. Cu,Zn superoxide dismutase is a peroxisomal enzyme in human fibroblasts and hepatoma cells. *Proceedings of the National Academy of Sciences of the United States of America* 88: 7381-7385, 1991.

29. Kelner MJ, Bagnell R, Montoya M, Estes L, Uglik SF, and Cerutti P. Transfection with human copper-zinc superoxide dismutase induces bidirectional alterations in other antioxidant enzymes, proteins, growth factor response, and paraquat resistance. *Free radical biology & medicine* 18: 497-506, 1995.

30. Knoferle J, Koch JC, Ostendorf T, Michel U, Planchamp V, Vutova P, Tonges L, Stadelmann C, Bruck W, Bahr M, et al. Mechanisms of acute axonal degeneration in the

optic nerve in vivo. *Proceedings of the National Academy of Sciences of the United States of America* 107: 6064-6069, 2010.

31. Leutner S, Eckert A, and Muller WE. ROS generation, lipid peroxidation and antioxidant enzyme activities in the aging brain. *J Neural Transm* 108: 955-967, 2001.

32. Linden A, Gulden M, Martin HJ, Maser E, and Seibert H. Peroxide-induced cell death and lipid peroxidation in C6 glioma cells. *Toxicol In Vitro* 22: 1371-1376, 2008.

33. Liochev SI, and Fridovich I. The effects of superoxide dismutase on H2O2 formation. *Free radical biology & medicine* 42: 1465-1469, 2007.

34. Liu R, Liu IY, Bi X, Thompson RF, Doctrow SR, Malfroy B, and Baudry M. Reversal of age-related learning deficits and brain oxidative stress in mice with superoxide dismutase/catalase mimetics. *Proceedings of the National Academy of Sciences of the United States of America* 100: 8526-8531, 2003.

35. Malinska D, Kudin AP, Debska-Vielhaber G, Vielhaber S, and Kunz WS. Chapter 23 Quantification of superoxide production by mouse brain and skeletal muscle mitochondria. *Methods Enzymol* 456: 419-437, 2009.

36. Massaad CA, and Klann E. Reactive oxygen species in the regulation of synaptic plasticity and memory. *Antioxidants & redox signaling* 14: 2013-2054, 2011.

37. Navarro A, Sanchez Del Pino MJ, Gomez C, Peralta JL, and Boveris A. Behavioral dysfunction, brain oxidative stress, and impaired mitochondrial electron transfer in aging mice. *American journal of physiology. Regulatory, integrative and comparative physiology* 282: R985-992, 2002.

38. Nicolle MM, Gonzalez J, Sugaya K, Baskerville KA, Bryan D, Lund K, Gallagher M, and McKinney M. Signatures of hippocampal oxidative stress in aged spatial learning-impaired rodents. *Neuroscience* 107: 415-431, 2001.

39. Noack H, Lindenau J, Rothe F, Asayama K, and Wolf G. Differential expression of superoxide dismutase isoforms in neuronal and glial compartments in the course of excitotoxically mediated neurodegeneration: relation to oxidative and nitrergic stress. *Glia* 23: 285-297, 1998.

40. Pellmar TC, Hollinden GE, and Sarvey JM. Free radicals accelerate the decay of long-term potentiation in field CA1 of guinea-pig hippocampus. *Neuroscience* 44: 353-359, 1991.

41. Perez VI, Bokov A, Van Remmen H, Mele J, Ran Q, Ikeno Y, and Richardson A. Is the oxidative stress theory of aging dead? *Biochimica et biophysica acta* 1790: 1005-1014, 2009.

42. Rohrdanz E, Schmuck G, Ohler S, Tran-Thi QH, and Kahl R. Changes in antioxidant enzyme expression in response to hydrogen peroxide in rat astroglial cells. *Archives of toxicology* 75: 150-158, 2001.

43. Shacter E. Quantification and significance of protein oxidation in biological samples. *Drug metabolism reviews* 32: 307-326, 2000.

44. Shetty PK, Huang FL, and Huang KP. Ischemia-elicited oxidative modulation of Ca2+/calmodulin-dependent protein kinase II. *The Journal of biological chemistry* 283: 5389-5401, 2008.

45. Wijeratne SS, Cuppett SL, and Schlegel V. Hydrogen peroxide induced oxidative stress damage and antioxidant enzyme response in Caco-2 human colon cells. *Journal of agricultural and food chemistry* 53: 8768-8774, 2005.

46. Wu K, Meyers CA, Guerra NK, King MA, and Meyer EM. The effects of rAAV2-mediated NGF gene delivery in adult and aged rats. *Mol Ther* 9: 262-269, 2004.

47. Zeier Z, Madorsky I, Xu Y, Ogle WO, Notterpek L, and Foster TC. Gene expression in the hippocampus: regionally specific effects of aging and caloric restriction. *Mechanisms of ageing and development* 132: 8-19, 2011.

Antioxidants & Redox Signaling

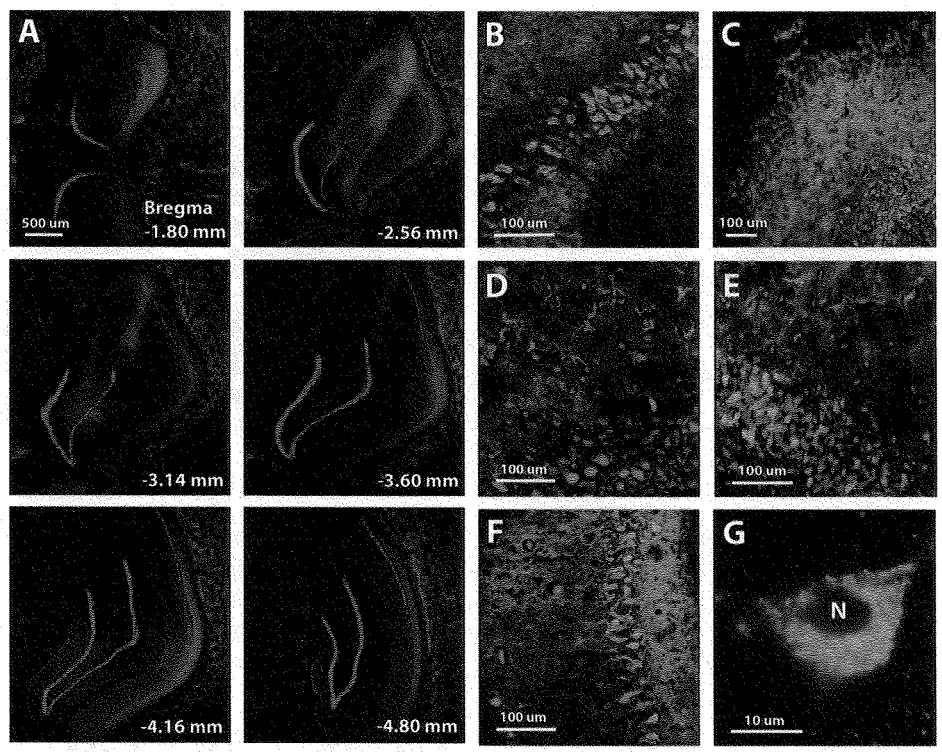

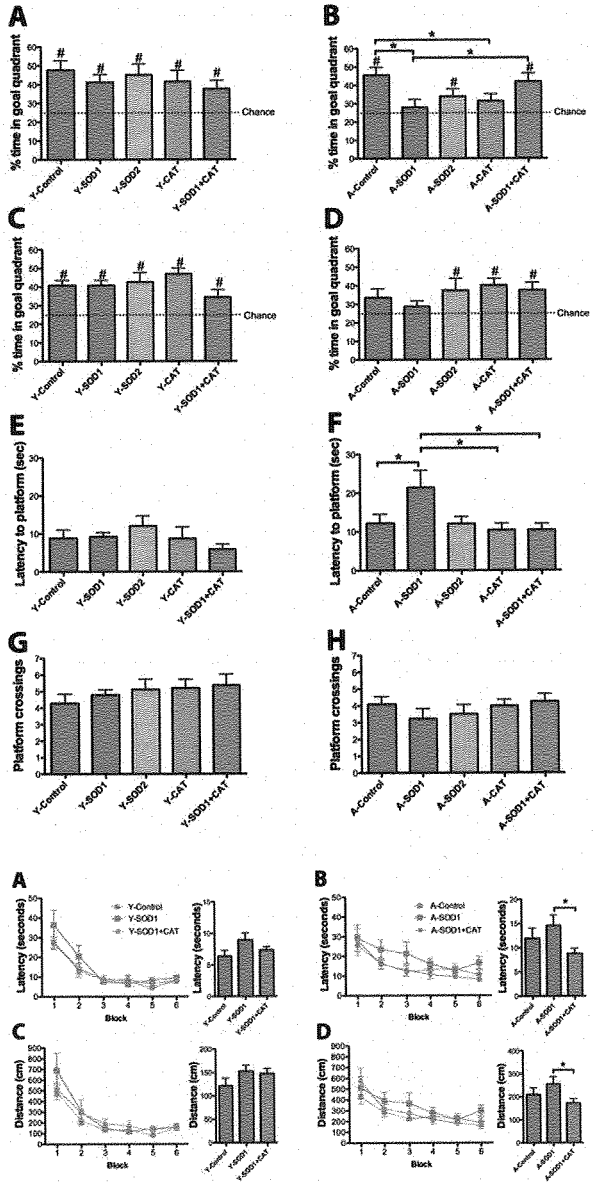

Antioxidants & Redox Signaling

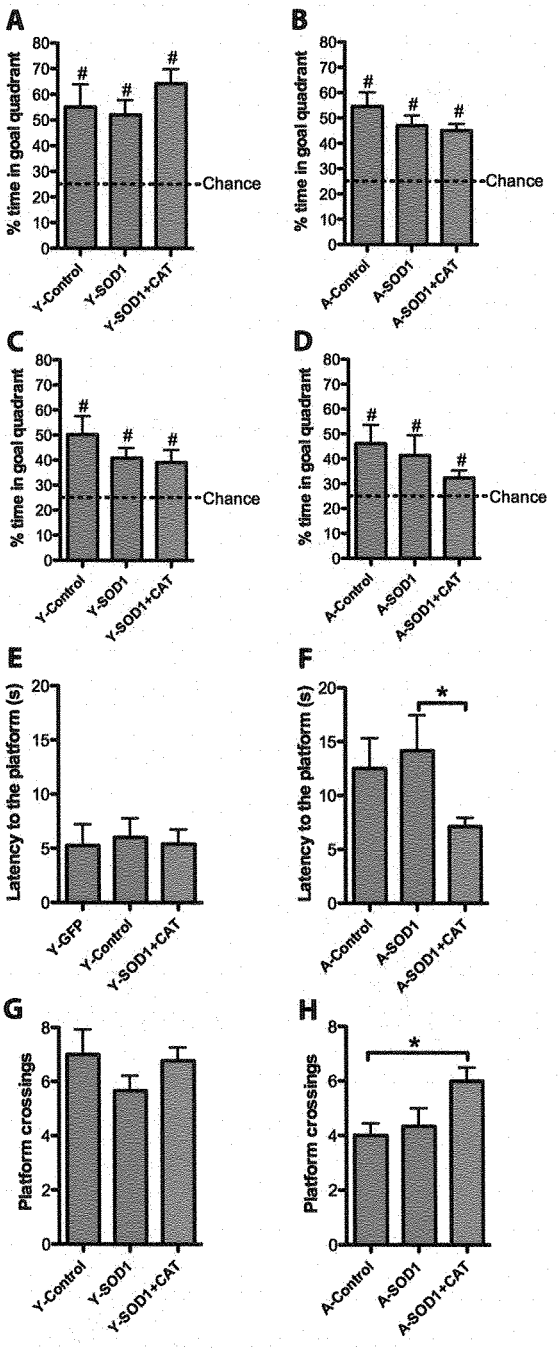

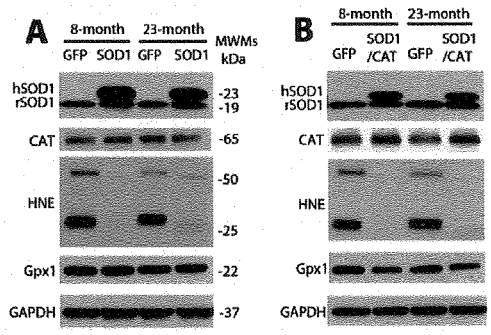

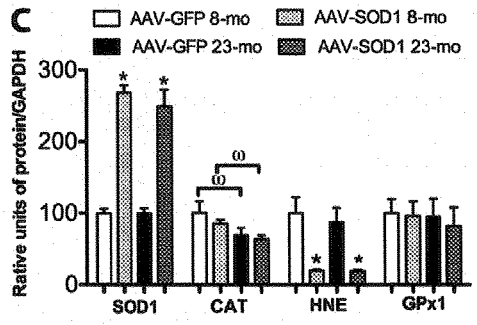

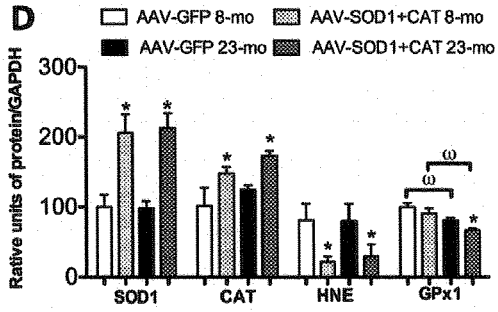

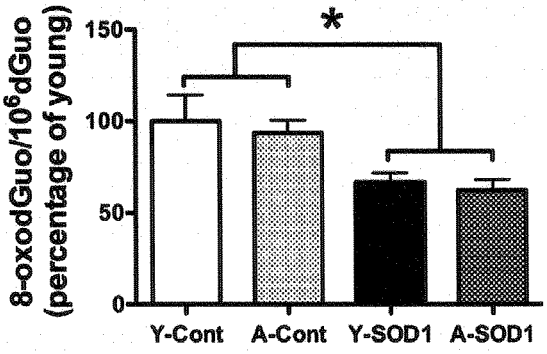

Neurobiology of Learning and Memory xxx (2011) xxx–xxx

Contents lists available at SciVerse ScienceDirect

Neurobiology of Learning and Memory

journal homepage: www.elsevier.com/locate/ynlme

Enhanced expression of Pctk1, Tcf12 and Ccnd1 in hippocampus of rats: Impact on cognitive function, synaptic plasticity and pathology

Ke Wu [a,c,1], Shoudong Li [a,c,1], Karthik Bodhinathan [f], Craig Meyers [a,c], Weijun Chen [a,c], Martha Campbell-Thompson [e], Lauren McIntyre [a,c], Thomas C. Foster [b,d], Nicholas Muzyczka [a,c,d,*], Ashok Kumar [b,d,*]

[a] Department of Molecular Genetics and Microbiology, University of Florida, Gainesville, FL 32610, United States
[b] Department of Neuroscience, University of Florida, Gainesville, FL 32610, United States
[c] Powell Gene Therapy Center, UF Genetics Institute, Gainesville, FL 32610, United States
[d] McKnight Brain Institute, University of Florida, Gainesville, FL 32610, United States
[e] Department of Pathology, University of Florida, Gainesville, FL 32610, United States
[f] Peptide Biology Labs, Salk Institute for Biological Studies, La Jolla, CA 92037, United States

ARTICLE INFO

Article history:
Received 9 May 2011
Revised 24 August 2011
Accepted 14 September 2011
Available online xxxx

Keywords:
Hippocampus
Gene expression
Learning and memory
Synaptic plasticity
LTP
LTD

ABSTRACT

We previously identified a set of 50 genes that were differentially transcribed in the hippocampal CA1 region of aged, learning-impaired rats compared to aged, superior learning animals during a Morris water maze paradigm. In the current study, we expressed three of these genes (Pctk1, Tcf12 and Ccnd1), which had shown increased transcription in aged, learning impaired rats, in the hippocampus of young rats using viral gene transfer and tested for learning and memory deficits at age 7–14 months. Pctk1 injected animals displayed a modest deficit in acquiring latency in both the Morris water maze and the reverse Morris maze. In the radial arm water maze paradigm, Pctk1, Tcf12 and Ccnd1 expressing animals all showed significant deficits in spatial working memory compared to controls. Rats injected with Ccnd1 and Tcf12, but not Pctk1, also showed a significant deficit in spatial reference memory in the radial arm water maze. Electrophysiological experiments revealed no difference in LTP in Ccnd1 and Pctk1 animals. However, LTD induced by low frequency stimulation was observed in control and Ccnd1 animals, but not in Pctk1 treated animals. In addition, neither Ccnd1 nor Pctk1 expression produced any detectable neuropathology. In contrast Tcf12 expressing animals displayed significant neurodegeneration in both CA1 and dentate gyrus. Several Tcf12 animals also developed tumors that appeared to be glioblastomas, suggesting that aberrant Tcf12 expression in the hippocampus is tumorigenic. Thus, behavioral experiments suggested that overexpression of Pctk1 and Ccnd1 produce a deficit in learning and memory, but electrophysiological experiments do not point to a simple mechanism. In contrast, the learning and memory deficits in Tcf12 animals are likely due to neuropathology associated with Tcf12 gene expression.

1. Introduction

Aging is associated with cognitive declines in both humans and rodents. Humans, as well as rodents, display a large variability between individuals in age-related impairments in learning and memory. The underlying causes for this variability remain unknown. The formation of long term memory requires transcription and synthesis of new proteins (Hernandez & Abel, 2008). We have hypothesized that differential changes in gene expression between individuals may be responsible for the variability in memory-related behaviors in aged rodents. We previously used the Morris water maze (MWM) to segregate aged learning-competent and aged learning-impaired animals, and used microarray analysis to investigate the genome-wide transcriptional changes that occurred in both CA1 and dentate gyrus of rats that showed age-related learning impairment (AI) in MWM compared to rats that showed less cognitive impairment (superior learners (SL). We identified two sets of genes that are differentially expressed in CA1 and dentate gyrus, respectively, in AI and SL rats (Burger, Lopez, et al., 2007, 2008). Several genes that we identified

* Corresponding authors. Address: Department of Neuroscience, University of Florida, Gainesville, FL 32610, United States.
E-mail address: kash@mbi.ufl.edu (A. Kumar).
[1] These authors contributed equally.

1074-7427/$ - see front matter © 2011 Elsevier Inc. All rights reserved.
doi:10.1016/j.nlm.2011.09.006

had already been validated for their roles in learning and memory processes by other studies, but most remained to be investigated. In this study, we focus on validating the roles of three genes identified by differential transcription in CA1, which may play a role in cognition. The three genes were PCTAIRE protein kinase 1 (Pctk1, Cdk16), G1/S-specific cyclin D1 (Ccnd1), and Transcription factor 12 (Tcf12, HEB, HTF4). The messenger RNA levels for all three genes were upregulated in the CA1 region in aged, learning-impaired rats, suggesting that their elevated expression might contribute to learning impairment (Burger, Lopez, et al., 2007).

Pctk1 is a member of the serine/threonine protein kinase family with a conserved cyclin-dependent kinase-like kinase domain and variable N- and C-terminal domains (Meyerson, Enders, et al., 1992; Okuda, Cleveland, et al., 1992). Although originally identified as a cdc2-like kinase, Pctk1 is not involved in the regulation of cell cycle progression, nor does it require cyclins for its activity (Graeser, Gannon, et al., 2002). The expression of Pctk1 is ubiquitous in mammalian tissue with particular abundance in pyramidal neurons in the hippocampus (Besset, Rhee, et al., 1999).

Ccnd1 (cyclin D1) is a key regulator of cell cycle progression that functions as a mitogenic sensor and allosteric activator of cyclin dependent kinases 4 and 6 (CDK4/6) (Kozar & Sicinski, 2005; Sherr & Roberts, 1999). Ccnd1/CDK4/6 holoenzyme phosphorylates the retinoblastoma protein (Rb) and promotes progression through the G1-S phase of the cell cycle. Ccnd1 is important for normal development of retina, mammary gland and cerebellum as homozygous deletion of Ccnd1 results in impaired development of these tissues (Fantl, Stamp, et al., 1995; Kim, Pomeroy, et al., 2000; Kozar & Sicinski, 2005). Interestingly, Ccnd1 is also expressed abundantly in adult brain neurons such as pyramidal cells in the CA1 region of the hippocampal formation and SGZ zone of dentate gyrus. These regions are known to be sites of neurogenesis in adult brain; alternatively, Ccnd1 may have functions independent of promoting cell cycle progression in brain.

Tcf12 is believed to be a transcription factor. It is a member of the basic helix-loop-helix family of proteins that recognizes the DNA E-box motif (Hu, Olson, & Kingston, 1992; Zhang et al., 1991). It has been shown to form homooligomers or heterooligomers with myogenin, E12 and ITF2, and interacts with PTF-1 and RUNX1T1 and the Tcf12 regulator, ID1. Tcf12 has been shown to have a role in neuron differentiation and is upregulated in some tumors (O'Neil et al., 2004; Uittenbogaard & Chiaramello, 2002; Zhuang, Cheng, & Weintraub, 1996). All three of the genes we chose to study (Tcf12, Ccnd1 and Pctk1) are abundantly expressed in hippocampal neurons (Allen, 2004).

To investigate the potential involvement of these genes in learning and memory, we used targeted overexpression in the hippocampus with recombinant Adeno-associated virus (rAAV)-mediated gene transfer, an approach that had previously worked successfully for determining gene function in the hippocampus as well as the substantia nigra (Kirik, Rosenblad, et al., 2002; Rex, Gavin, et al., 2010). Our results showed that rAAV-mediated gene expression in hippocampus caused deficits in spatial working memory (SWM) performance in a radial arm water maze (RAWM) task in animals injected with Ccnd1, Tcf12 or Pctk1. Overexpression of Ccnd1 or Tcf12, but not Pctk1, also resulted in impairments in spatial reference memory (SRM) in the same task. Overexpression of Pctk1 had a significant effect on LTD but not on LTP, while Ccnd1 did not significantly affect neuronal plasticity in hippocampus of aged animals. In addition, expression of Pctk1 (but not Ccnd1 or Tcf12) produced deficits in the MWM and reverse MWM. Finally, although neither Ccnd1 nor Pctk1 produced significant pathology or neurodegeneration in the hippocampus, the third gene, Tcf12, induced measurable neurodegeneration that was accompanied by the formation of tumors.

2. Materials and methods

2.1. rAAV vectors

The coding sequences for Pctk1, Tcf12 and Ccnd1 were cloned from a rat brain cDNA library (Biochain). The primers for Pctk1 cloning were TCCAAGCTTCCACCATGGATCGGATGAAGAAGATCA AACG and ATCAAGCTTTCAAGCGTAGTCTGGGACGTCGTATGGGTA GAACTCGGTATCCACCACACGG. Pctk1 was tagged with hemagglutinin (HA) at its C-terminal. Pctk1 tagged with HA retains its kinase activity. The primers for Ccnd1 cloning were CGTTGGCGG CCGCCACCATGGAACAACAGCTCCTGTGCTGCGAAG and GGATGGTC GACTCAGATGTCCACATCTCGGACGTCGG. Ccnd1 was not tagged. The Tcf12 primers were: TCCAAGCTTCCACCATGAATCCCCAGC AGCAGCGCAT and ATCAAGCTTTCAAGCGTAGTCTGGGACGTCGTA TGGGTACAGATGACCCATAGGGTTGGTTGTCT. Tcf12 was HA-tagged at its C-terminal end.

Coding sequences for Pctk1 and Tcf12 were cloned into an AAV cloning vector plasmid called pTR2 MCS at the HindIII site; Ccnd1 sequences were cloned into the NotI and SalI sites. Constructs were verified by DNA sequencing and immunoblotting using anti-Pctk1, anti-Tcf12 and anti-Ccnd1 antibodies against HEK 293 cell extracts from cells transfected with the constructs (not shown). An empty pTR2 MCS was used as null control construct. The pTR2 MCS (tr2), HA-tagged Pctk1 and Tcf12 constructs were serotyped with AAV8 capsid and the Ccnd1 construct was serotyped with AAV5 capsid during virus production as previously described (Zolotukhin et al., 2002). The recombinant viruses were generated and purified as described (Hauswirth, Lewin, et al., 2000; Zolotuk-hin, Potter, et al., 2002). rAAV particles are expressed as vector genomes (Vg.ml). Vector genomes were quantitated using the dot plot protocol, with a probe for the chicken β-actin promoter, as described by Hauswirth, Lewin et al. (2000) and Zolotukhin, Potter, et al. (2002). The titers were 3.4×1012, 2.3×1012, 2.4×1013, and 8.8×10^{12} Vg/ml for tr2 null, Pctk1, Tcf12, and Ccnd1 and vectors, respectively.

2.2. Subjects and surgery

Three month old male Sprague–Dawley rats were injected with rAAV vector bilaterally in the hippocampus. Specifically, each animal was injected at two positions on each side of the brain with a total of 3 μl of vector at each position. At each position, 1 μl of vector was injected at each depth for a total of three depths. The coordinates for injection at the first position were AP −3.48 mm; ML ±2.2 mm; DV −3.7 mm, −3 mm, and −2.8 mm. The coordinates for the injection at the second position were AP −5.28 mm; ML ±5 mm; DV −7.5 mm, −6 mm, and −4 mm. All surgical procedures were performed by using aseptic techniques and isoflurane gas anesthesia. Procedures involving animal subjects have been reviewed and approved by the Institutional Animal Care and Use Committee, and were in accordance with guidelines established by the US Public Health Service Policy on Humane Care and Use of Laboratory Animals. Animals were group housed (2 per cage), maintained on a 12:12 h light schedule, and provided *ad lib* access to food and water. Behavioral tests and electrophysiological experiments were carried out as shown in the timeline in Fig. 1A. Additional 3 month old rats were injected with Ccnd1, Tr2 and Pctk1 vector and taken for electrophysiological measurements at 1 month post-injection.

2.3. Morris water maze

Four months after vector injections, animals received 8 days of three training sessions/day beginning in the morning of each day.

Please cite this article in press as: Wu, K., et al. Enhanced expression of Pctk1, Tcf12 and Ccnd1 in hippocampus of rats: Impact on cognitive function, synaptic plasticity and pathology. *Neurobiology of Learning and Memory* (2011), doi:10.1016/j.nlm.2011.09.006

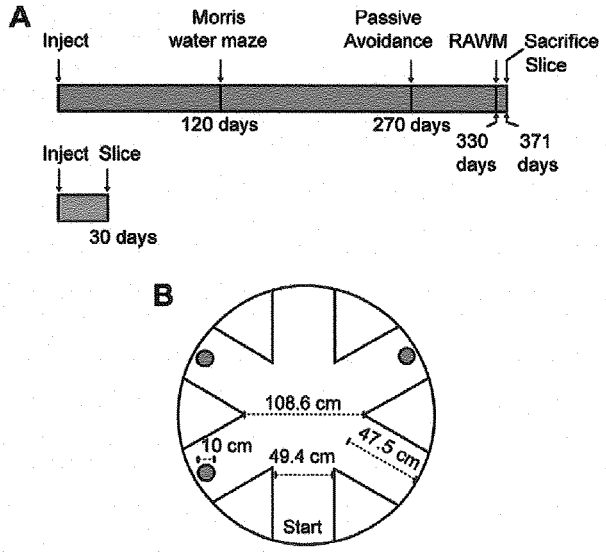

Fig. 1. (A) Timeline for study. (B) Schematic and dimensions of three platform radial arm water maze used in the study.

Twenty-four hours after the last training session, animals received a probe trial in which the hidden platform was removed. During training, escape latencies were measured for each session. During training, animals were hand-guided to the platform if they did not find it by 90 s; these training intervals were given a 90 s value. Swimming distance was measured for the entire 24 trials for each animal. During the probe trial, percentage time in target vs. non-target quadrants was determined over a 60-s interval. Paths swum by animals were recorded and analyzed using a computerized video monitoring system (EthoVision, Noldus Information Technology).

2.4. Passive avoidance behavior

Animals were trained in a two-chamber passive avoidance paradigm. They were placed in the lit compartment and allowed to enter the dark adjoining chamber. Animals that entered the second chamber received a mild foot shock (0.8 mA) for 1 s. Rats were tested for latency to enter the dark chamber 24 h later for up to 5 min. Statistical analyses used rank order nonparametric comparisons of latencies.

2.5. Radial arm water maze

Rats were tested in the radial-arm maze shown in Fig. 1B. The maze was constructed of aluminum, and was placed in a large pool of water in a black tank 2 m in diameter. No dye was added. It had black escape platforms (2 cm below the water surface) placed at the ends of three of the six arms. The distance from the water level to the top of the maze was approximately 20 cm. The temperature of water was 25 °C. Each subject had different platform locations that were randomly determined, and that remained fixed throughout the experiment. There was no platform in the arm from which the rats was released. The testing room had salient extra-maze cues, including a door, solid black panels on a wall, black and white stripped panels on the opposite wall.

In each trial, the rat was introduced into the start arm with its head pointing towards the tank wall. The rat had 90 s to locate a platform. If the allotted time expired, the subject was guided to the nearest available platform. Once a platform was found, the animal remained on it for 20 s, and was returned to its heated cage for 30 s. During the interval, the just-chosen platform was removed from the maze. The animal was then placed back into the start arm and allowed to locate another platform. A session consisted of this sequence of events repeated until all three platforms were located, resulting in a total of three trials per session. After the first day of training, rats were tested for nine more days using the same procedure as day one. Behavioral testing took place between 9:30 am and 3:30 pm.

An arm entry is counted when the tip of a rat's snout reaches a mark on the outside of the arm (~11 cm into the arm), or all four paws enter the arm. Working memory errors are the number of first and repeat entries into any arm from which a platform has been removed previously during the session and the number of entries into any arm with an existing platform that is not located by rats. Reference memory errors are the number of first entry into any arm that never contains a platform. In order to determine whether rats employed non-spatial strategies similar to thigmotaxis in MWM by simply going from one arm to an adjacent arm (chaining) during the RAWM task, a radial index was calculated. A radial index is defined as the mean of the angles formed by successively chosen arms (Roullet, Lassalle, et al., 1993). When a rat swims out of an arm, it can enter the adjacent arm (60°), the second arm (120°), the third arm (180°), or it can reenter the same arm (0°). If a rat developed chaining behavior, its radial index would approach 60°. When it had no preference for a particular angle, the radial index would remain 90°.

2.6. Stereology

The unbiased stereological estimation of the total number of the cresyl violet stained neurons in hippocampus was performed by using the optical fractionator method, as described (Tran & Kelly, 2003) with the MicroBrightfield Stereo Investigator System. Hippocampal subregions were outlined according to the atlas published in The Rat Brain (Paxinos, Watson, et al., 1985). The estimate of the total number of neurons and coefficient of error due to the estimation was calculated according to the optical fractionator formula as described (Tran & Kelly, 2003).

2.7. Immunoblotting and real-time PCR

Tissues were suspended in 300 μl of lysis buffer (50 mM Tris, pH 7.5, 0.15 M NaCl) containing protease mixture (0.1 mM PMSF, 0.5 μg/ml leupeptin, 0.7 μg/ml pepstatin A) (Roche) and homogenized for 10 s. Each aliquot was adjusted to a final concentration of 1% Nonidet P-40, 0.1% SDS, incubated on ice for 30 min, and centrifuged for 15 min at 4 °C. Protein concentrations were determined by the Bradford protein assay. Fifty micrograms of each protein pool was separated on Bio-Rad precast 4–20% SDS/PAGE gradient gel, transferred to PVDF-LFP (Amersham) membranes, and immunoblotted. Mouse anti-Pctk1 (sc-53410, Santa Cruz Biotechnology) and rat anti-HA peroxidase high affinity (3F10, Roche) antibodies were used as recommended by the supplier.

For detection of rat Ccnd1 messenger RNA, rat hippocampal tissues were homogenized in TRIzol reagent according to the manufacturer's manual (Invitrogen). After DNase I treatment, 500 ng of RNA was reverse-transcribed in 25 μl reaction using SuperScriptTM III first strand cDNA synthesis kit (Invitrogen). Real time PCR was performed on the MyiQ Single-Color Real-Time PCR Detection System (Bio-Rad) using IQ SYBR Green Supermix (Bio-Rad), 2 μl of cDNA, and Ccnd1 primers. All values obtained were normalized with respect to levels of β-actin mRNA. The primer pairs used for RT-PCR experiments were forward 5′-AGTTGCTGCAAATGGAACTG-3′ and reverse 5′-TGGAGAGGAAGTGTTCGA G-3′ for Ccnd1 gene, and forward 5′-CACTGCCGCATCCTCTTCCT-3′ and reverse

Please cite this article in press as: Wu, K., et al. Enhanced expression of Pctk1, Tcf12 and Ccnd1 in hippocampus of rats: Impact on cognitive function, synaptic plasticity and pathology. *Neurobiology of Learning and Memory* (2011), doi:10.1016/j.nlm.2011.09.006

5′-AACCGCTCATTGCCGATAGTG-3′ for β-actin gene. All real-time PCR s were performed in duplicate using RNA from individual rats to give an average value for each animal. Serial dilutions of plasmid DNA containing Ccnd1 gene were used as standard templates. Relative quantification was performed using the ΔCt method.

2.8. Immunohistochemistry and pathology

Rat brain was harvested and fixed in 4% paraformaldehyde followed by freezing in optimal cutting temperature media. Frozen sections (40 μm) were stained by immunohistochemistry and immunofluorescence using minor modifications of previously published methods (Campbell-Thompson, Dixon, et al., 2009). Primary antibodies included anti-GFAP (Novus Biologicals, NB300141), anti-HA (sc-7932, Santa Cruz Biotechnology), Pctk1 (sc-53410, Santa Cruz Biotechnology) and Tcf12 (sc-23128, Santa Cruz Biotechnology). Secondary fluorescent antibodies were conjugated with Alexa Fluor (Invitrogen) fluorochromes (488 and 594); DAPI was used to counter stain nuclei (blue).

2.9. Electrophysiological recordings

The methods for hippocampal slice preparation have been published previously (Bodhinathan, Kumar, et al., 2010; Kumar, 2010; Kumar & Foster, 2004; Kumar & Foster, 2007; Kumar, Thinschmidt, et al., 2007). Briefly, rats were anesthetized with isoflurane (Halocarbon Laboratories, River Edge, NJ) and swiftly decapitated. The brains were rapidly removed and the hippocampi were dissected. Hippocampal slices (~400 μm) were cut parallel to the alvear fibers using a tissue chopper. The slices were incubated in a holding chamber (room temperature) containing standard artificial cerebrospinal fluid (ACSF) (in mM): NaCl 124, KCl 2, KH_2PO_4 1.25, $MgSO_4$ 1.5, $CaCl_2$ 2.4, $NaHCO_3$ 26, and glucose 10. Thirty to sixty min before recording, 2–3 slices were transferred to a standard interface recording chamber (Harvard Apparatus, Boston, MA); the chamber was continuously perfused with standard oxygenated (95% O_2, 5% CO_2) ACSF at a flow rate of 2 ml/min. The pH and temperature were maintained at 7.4 and 30 ± 0.5 °C, respectively. Humidified air (95% O_2, 5% CO_2) was continuously blown over the slices.

Extracellular synaptic field potentials from CA3–CA1 synaptic contacts were recorded with glass micropipettes (4–6 MΩ) filled with recording medium (ACSF). Two concentric bipolar stimulating electrodes (outer pole: stainless steel, 200 μm diameter; inner pole: platinum/iridium, 25 μm diameter, FHC, Bowdoinham, ME) were positioned approximately 1 mm from either side of the recording electrode localized in the middle of the stratum radiatum. A single diphasic stimulus pulse of 100 μs was passed via stimulators (SD9 Stimulator, Grass Instrument Co., West Warwick, RI) to the Schaffer collateral commissural pathway, in order to evoke field potentials at 0.033 Hz. The signals were amplified, filtered between 1 Hz and 1 kHz, and stored for off-line analysis. Two cursors were placed around the initial descending phase of the excitatory post synaptic potential (EPSP) waveform, and the maximum slope (mV/ms) of the EPSP was determined by a computer algorithm that found the maximum change across all sets of 20 consecutively recorded points (20 kHz sampling rate) between the two cursors. For examination of synaptic plasticity, the stimulus current was adjusted to produce a response 50–60% of the maximal EPSP slope. Responses were collected for at least 20 min prior to pattern stimulation to insure a stable baseline before induction of synaptic plasticity. LTP was induced by employing four trains of 100 Hz (100 pulses, 10 ms apart, each train 10 s apart). LTD was induced by using 1 Hz paired-pulse (1 Hz PP, with 50 ms inter-pulse interval, total 900 pulses) low frequency stimulation. Changes in transmission properties induced by patterned stimulation were calculated as the percent change from the averaged response collected during baseline. For examination of paired-pulse facilitation (PPF), a 50 ms inter-pulse interval was used. The PPF ratio was calculated by dividing the slope of the second synaptic response by the slope of the first response.

2.10. Statistical analysis

Analyses of variance (ANOVAs) were used with treatment effects and interactions as independent varaibles. For electrophysiological recordings F tests of main effects, t-tests for planned contrasts, and Fisher's PLSD or Bonferroni post hoc comparisons were employed. A p-value of $P < 0.05$, was considered statistically significant when testing changes in synaptic response induced by pattern stimulation, as well as any possible differences between baseline and PPF ratio. The data were log transformed when appropriate. Statistical analyses were performed using StatView 5.0 (SAS Institute) and Prism 5 (GraphPad).

3. Results

3.1. Behavioral experiments

3.1.1. Morris water maze

Three month old rats were injected bilaterally into their hippocampus with rAAV virus expressing Pctk1, Ccnd1 or Tcf12. The timeline for the study is shown in Fig. 1A. Four months after rats were injected with rAAV virus they were tested for their performance in a MWM task along with uninjected, age-matched animals. AAV viral gene transfer has previously been shown to produce no pathology or cell loss when control genes such as green fluorescent protein (GFP) have been expressed in rodent brain at the input doses used in this study (Gorbatyuk, Li, et al., 2008). In addition, previous work has shown that expression of an irrelevant gene such as GFP in the hippocampus using rAAV mediated transduction had no effect on memory formation in rats (Rex, Gavin, et al., 2010). To be certain that virus injection itself did not induce behavioral deficits, we compared uninjected animals with animals that had been injected with virus carrying a null gene, tr2. Tr2 was an empty cloning vector with multiple stop codons in all possible reading frames that was driven by the same CMV/β-actin hybrid promoter that was used to drive expression of Ccnd1, Pctk1 and Tcf12. Although it was expected to make mRNA at the same rate as the experimental constructs, no protein product could be made from tr2. Thus, tr2 injection controlled for effects from the surgery, injection of virus and production of a foreign RNA.

When the data were analyzed by two-way ANOVA, there was a significant main effect of treatment for latency between experimental groups (Table 1, $Fs_{4,42} = 2.87$, $P = 0.0346$), with no interaction between treatment and day of treatment ($Fs_{28,294} = 0.81$, $P = 0.7378$). A two-way repeated measures ANOVA analysis showed no difference in performance between animals from the uninjected, age-matched group and those receiving the tr2 null vector (Fig. 2A and Table 1, for gene $Fs_{1,112} = 0.8968$, $P = 0.358$). Because there was no difference in performance between animals from the uninjected, age-matched group and those receiving the tr2 null vector, they were combined as a single control group to simplify subsequent comparison with each experimental group. See Supplementary Table 1 for additional comparisons between each experimental group (Pctk1, Ccnd1, Tcf12) and each control group (uninjected, tr2).

Comparison of each of the experimental groups (Pctk1, Ccnd1, and Tcf12) with the control group in a two-way repeated measures ANOVA (Fig. 2B–D) suggested that there was a significant difference for latency between Pctk1 and controls (Fig. 2B,

Please cite this article in press as: Wu, K., et al. Enhanced expression of Pctk1, Tcf12 and Ccnd1 in hippocampus of rats: Impact on cognitive function, synaptic plasticity and pathology. *Neurobiology of Learning and Memory* (2011), doi:10.1016/j.nlm.2011.09.006

Table 1
P values for treatment comparisons*.

Control treatment	Experimental treatment	MWM latency	Reverse MWM latency	RAWM reference memory	RAWM working memory
Control**	Pctk1	0.044	0.004	0.638	0.003
Control	Ccnd1	0.054	0.219	0.009	<0.0001
Control	Tcf12	0.067	0.08	0.019	0.004
Uninjected tr2	Pctk1 ccnd1 tcf12	0.035	0.046	0.001	<0.0001
Uninjected	Tr2	0.358	0.341	0.607	0.882

* Two-way repeated measures ANOVA *P* values for main effect of the four treatment groups (pctk1, ccnd1, tcf12 and tr2) compared to the indicated control groups.
** Control group = uninjected + tr2 animals.

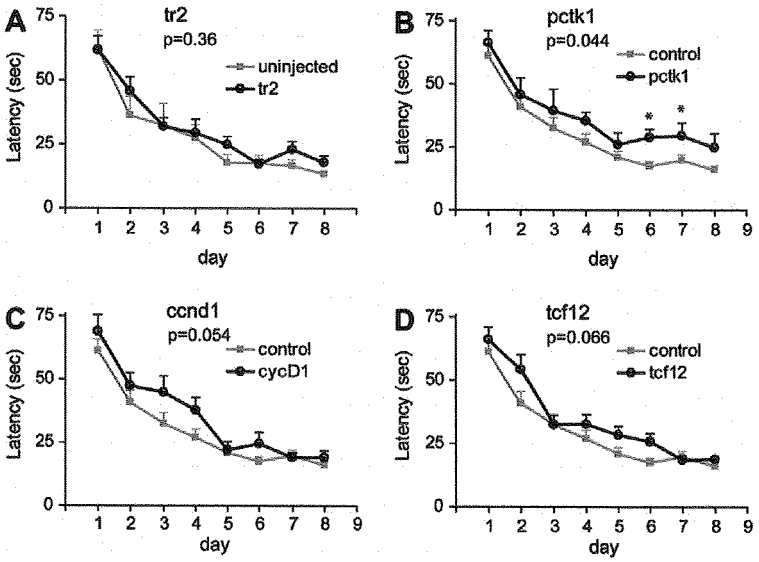

Fig. 2. Morris water maze task performance. Each day block represents the average of three trials. Each data point represents the mean ± SEM of time to find the platform. (A) There was no significant difference between uninjected ($n = 8$) and tr2 vector-injected rats ($n = 10$). For ease of further analysis, these two groups were combined and designated as the control group. (B) A significant difference was found between control ($n = 18$) and Pctk1 ($n = 10$) animals in the acquisition phase of the MWM task. (C and D) Comparison of control and Ccnd1 ($n = 9$) or control and Tcf12 animals ($n = 10$) did not reach significance. Asterisks indicate a significant difference between control and treatment animals on a particular day by Bonferroni post hoc comparison (*$P < 0.05$). See text and Table 1 for additional details.

$Fs_{1,175} = 4.494$, $P = 0.044$), but not between Ccnd1 and controls (Fig. 2C, $Fs_{1,168} = 4.14$, $P = 0.054$) or between Tcf12 and controls (Fig. 2D, $Fs_{1,175} = 3.709$, $P = 0.066$). In addition, during the MWM probe trial, all treatment groups were able to recall the position of the platform. There was no difference in the time spent in the target quadrant among treatment groups (one-way ANOVA, $F_{3,46} = 0.5317$, $P = 0.663$, Supplementary Fig. 1A) or in the number of target crossings ($F_{3,43} = 2.034$, $P = 0.123$, Supplementary Fig. 1B). In addition, there was no difference in the swimming speed between groups (Supplementary Fig. 2).

3.1.2. Reverse Morris water maze

A subsequent reverse MWM test also showed a significant difference between all groups for the gene in a two-way ANOVA (Table 1, $F_{4,42} = 2.65$, $P = 0.046$) and a significant interaction between time and gene ($F_{12,126} = 1.97$, $P = 0.032$). As in the MWM above, two-way ANOVA comparison of the two control groups revealed no significant difference between animals that had been uninjected or injected with the null tr2 gene (Supplementary Fig. 3A and Table 1, $Fs_{1,48} = 0.9635$, $P = 0.341$), and these groups were pooled and used as the control group for further comparisons. Comparison of the control group with individual genes (Supplementary Fig. 3B–D and Table 1) in the reverse MWM showed a significant difference for Pctk1 ($Fs_{1,78} = 9.966$, $P = 0.004$), but Tcf12 ($Fs_{1,78} = 5.28$, $P = 0.08$) and Ccnd1 ($Fs_{1,75} = 1.593$, $P = 0.219$) were not significant. Additionally, during the probe trial, there was no significant difference between groups in target crossings (one-way ANOVA, $F_{3,38} = 1.265$, $P = 0.300$, Supplementary Fig. 1C) or time spent in the target quadrant ($F_{3,38} = 1.51$, $P = 0.341$, Supplementary Fig. 1D).

Finally, 5 months after the MWM task, the animals were evaluated for their performance in the hippocampus-dependent passive avoidance task. One day after training, animals from all groups spent a similar amount of time in the light chamber (data not shown).

3.1.3. Radial arm water maze

Taken together, the data suggested that Pctk1 animals had a deficit in acquiring the platform in the MWM. The failure to detect a robust difference in MWM and passive avoidance tasks between control groups and the Ccnd1 and Tcf12 groups raised the possibility that the difference between these treatment groups might be small, and that it might only be revealed in a more sensitive behavioral performance test. We, therefore, tested the same rats in a radial arm water maze that contained six arms in a water tank with three hidden platforms in three arms other than the start arm (Fig. 1B). The platform was removed after being located by the rats in each session. To perform well in this task, the rats needed to remember the position of each hidden platform (reference memory) as well as whether they had visited a platform in

Please cite this article in press as: Wu, K., et al. Enhanced expression of Pctk1, Tcf12 and Ccnd1 in hippocampus of rats: Impact on cognitive function, synaptic plasticity and pathology. *Neurobiology of Learning and Memory* (2011), doi:10.1016/j.nlm.2011.09.006

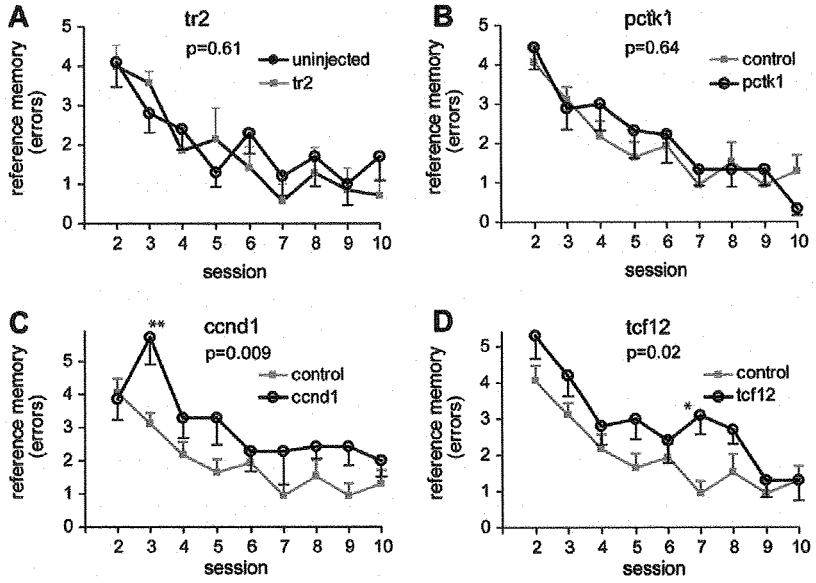

Fig. 3. Spatial reference memory performance in radial arm water maze. Each data point represents the mean ± SEM of spatial reference memory errors committed in each session. (A) There was no difference between tr2 vector ($n = 10$) injected and uninjected animals ($n = 7$). These two groups were combined as a control group. (B) No significant difference was found between Pctk1 ($n = 10$) and control animals ($n = 17$). (C and D) A significant difference was found between control animals and the Ccnd1 ($n = 7$, panel C) or Tcf12 ($n = 10$, panel D) treatment groups. Asterisks indicate a significant difference between control and treatment animals on a particular day by Bonferroni post hoc comparison (*$P < 0.05$; **$P < 0.01$). See text and Table 1 for additional details.

previous sessions (working memory). Therefore, this testing scheme allowed us to measure the SWM as well as SRM performance by rats in a single task.

Analysis of reference memory errors of all groups in a two-way ANOVA revealed a significant effect of gene ($F_{4,38} = 5.59$, $P = 0.001$, Table 1) with no interaction between gene and session day ($F_{32,304} = 1.26$, $P = 0.1613$). Two-way (treatment and sessions) repeated measures ANOVA comparison of the two control groups (tr2 and uninjected) confirmed that there was no significant difference between the two controls (Fig. 3A and Table 1, $Fs_{1,120} = 0.2760$, $P = 0.607$) and these two groups were pooled to simplify further comparisons. (See Supplementary Table 1 for separate comparisons with each control group.)

Direct comparison between each gene and the control group (Fig. 3B–D, Table 1) revealed that there was a significant difference in the number of reference memory errors between control and Ccnd1 rats ($Fs_{1,176} = 8.117$, $P = 0.009$) or control and Tcf12 rats ($Fs_{1,200} = 6.323$, $P = 0.019$), but surprisingly, not between control and Pctk1 rats ($Fs_{1,192} = 0.2276$, $P = 0.638$). For each of the genes there was no significant interaction between gene and session day.

3.1.4. Working memory correct errors

Analysis of working memory correct errors of all groups in a two-way ANOVA revealed a significant effect of gene (Table 1, $F_{4,38} = 8.33$, $P < 0.0001$) with no interaction between gene and session day ($F_{32,304} = 0.93$, $P = 0.5838$). Two-way (treatment and sessions) repeated measures ANOVA comparison of the two control groups (tr2 and uninjected) confirmed that there was no significant difference between the two controls (Fig. 4A, $Fs_{1,120} = 0.0227$, $P = 0.882$) and these two groups again were pooled for further comparisons. Comparison of each experimental group with the control revealed a significant difference between the control group and each of the experimental groups, Pctk1 (Fig. 4B, $Fs_{1,192} = 10.77$; $P = 0.003$), Ccnd1 (Fig. 4C, $Fs_{1,176} = 25.42$; $P < 0.0001$), and Tcf12 (Fig. 4D, $Fs_{1,200} = 10.10$; $P = 0.004$). (See Supplementary Table 1 for separate comparisons with each control group.)

All groups significantly reduced the number of errors with number of sessions in all memory categories ($Fs_{8,312} = 20.36$, and 14.10 for reference memory and working memory errors, respectively; Ps for session <0.0001 for both reference and working memory correct). We concluded that all three genes had an effect on working memory but only Ccnd1 and Tcf12 had an effect on reference memory.

To determine if the rats were solving the maze by simply moving from one arm to the next adjacent arm (chaining), we calculated the radial index scores over sessions for each treatment (Supplementary Fig. 4). The radial index was 90° or greater for both control groups and for Pctk1 and Ccnd1, suggesting that chaining was not occurring. There was no significant main effect of treatment ($Fs_{2,248} = 1.061$, $P = 0.358$). There also was no significant main effect of sessions ($Fs_{8,248} = 0.5596$, $P = 0.810$), nor was there a significant main effect of treatment × sessions interaction ($Fs_{16,248} = 0.9821$, $P = 0.476$).

Taken together, the RAWM data suggested that all three genes produced a learning deficit when overexpressed in hippocampus. Ccnd1 and Tcf12 produced robust deficits in both working and reference memory; in contrast, Pctk1 affected only working memory.

3.2. Gene expression and pathology

One week after RAWM, rats were sacrificed to confirm gene expression in the injected tissue, for electrophysiology assays and for pathological examination. Gene delivery of Pctk1 resulted in expression of the HA tagged Pctk1 and a significant increase in the total level of Pctk1 protein in rat hippocampus as judged by immunoblotting of tissues with HA and Pctk1 antibodies (Supplementary Fig. 5). The level of expression was constant over a broad region of the hippocampus and was similar between animals (Supplementary Fig. 6A). Interestingly, we could not detect endogenous Pctk1 expression under current experimental conditions, probably due to the low endogenous protein levels (Supplementary Figs. 5 and 6A). Attempts to detect Ccnd1 protein in rat hippocampus after gene delivery were not successful due to high backgrounds (not

Please cite this article in press as: Wu, K., et al. Enhanced expression of Pctk1, Tcf12 and Ccnd1 in hippocampus of rats: Impact on cognitive function, synaptic plasticity and pathology. *Neurobiology of Learning and Memory* (2011), doi:10.1016/j.nlm.2011.09.006

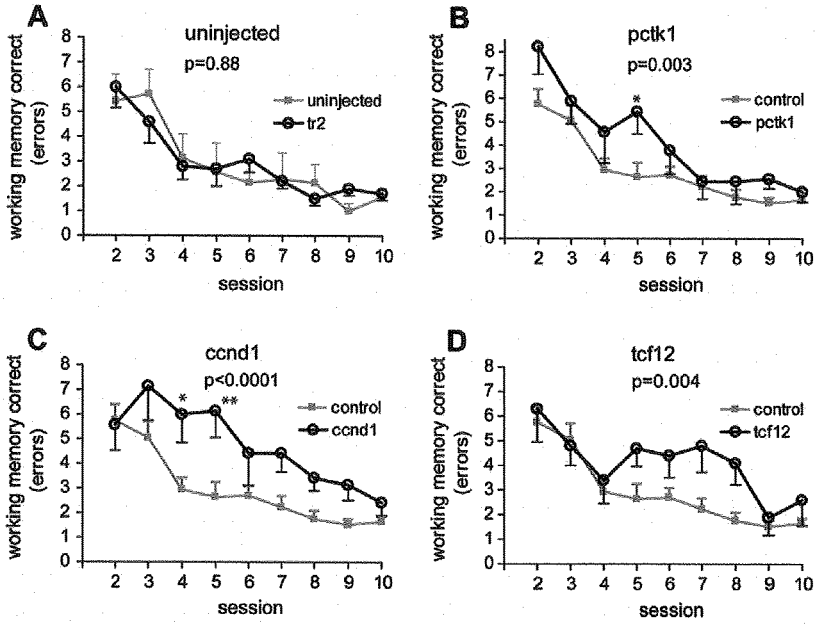

Fig. 4. Spatial working memory performance in radial arm water maze. Each data point represents the mean ± SEM of spatial working memory correct errors committed in each session. (A) There was no difference between tr2 vector ($n = 10$) injected and uninjected animals ($n = 7$). These two groups were combined as control group. (B–D) Significant differences were found between control animals ($n = 17$) and Pctk1 ($n = 9$, panel B), or Ccnd1 ($n = 7$, panel C), or Tcf12 ($n = 10$, panel D). Asterisks indicate a significant difference between control and treatment animals on a particular day by Bonferroni post hoc comparison (*$P < 0.05$; **$P < 0.01$). See text and Table 1 for additional details.

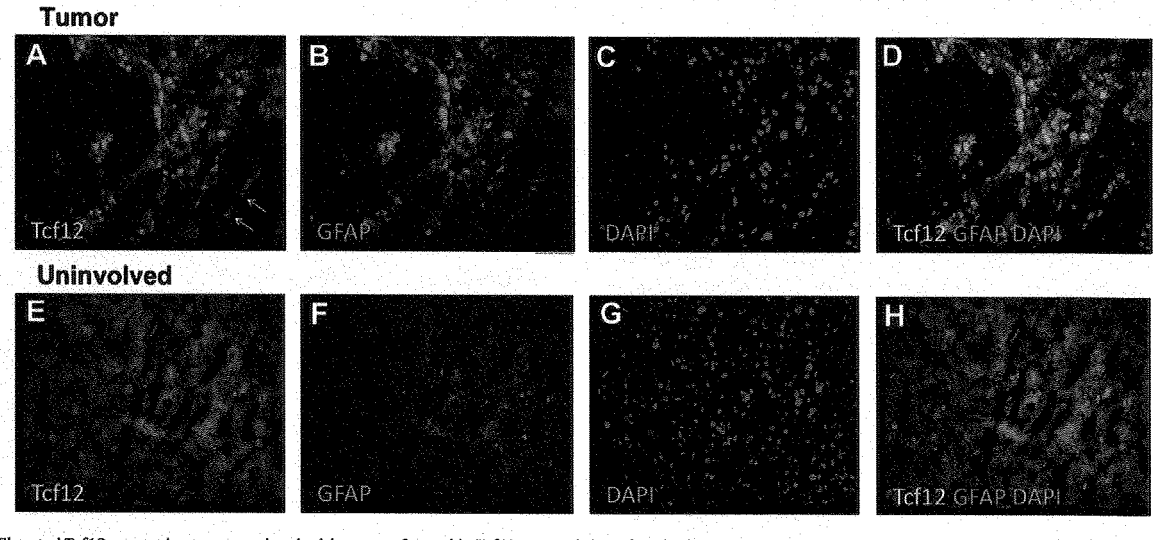

Fig. 5. Elevated Tcf12 expression was associated with tumors formed in Tcf12 vector-injected rat brains. Tumor tissue (A–D) and nearby non-tumor (uninvolved) tissue (E–H) was stained with Tcf12 antibody (A, E, green), GFAP antibody (B, F, red), DAPI (C, G, blue) or merged (D, H). Increased Tcf12 expression appeared to be localized inside nuclei (panels A, C, D compared to E, F, H) and was associated with activation of astrocytes as shown by strong GFAP staining (panels B and D). In contrast, there was no detectable Tcf12 expression that colocalized with GFAP staining in normal brain tissues (panels E–H) and Tcf12 staining did localize to nuclei (panels E, G, H).

shown). However, real-time PCR using primers specific for Ccnd1 mRNA, showed a sevenfold increase in the levels of Ccnd1 transcript in the hippocampus of Ccnd1-injected animals compared to controls (Supplementary Fig. 6C). Immunoblots of horse fibroblast cells transduced with Ccnd1 vector using anti-Ccnd1 antibody confirmed that gene transfer results in Ccnd1 protein expression (Supplementary Fig. 6B and C).

When we examined tissues at 1 year post injection, both the Ccnd1 and Pctk1 expressing vectors showed no overt pathology (not shown). In contrast, three of 10 rats that had been injected with Tcf12 expressing virus developed tumors in the area of injection. All three tumors were located between hippocampus and thalamus. Although the injection site was hippocampus, there were cystic epithelial features in one rat. All three tumors showed

Please cite this article in press as: Wu, K., et al. Enhanced expression of Pctk1, Tcf12 and Ccnd1 in hippocampus of rats: Impact on cognitive function, synaptic plasticity and pathology. *Neurobiology of Learning and Memory* (2011), doi:10.1016/j.nlm.2011.09.006

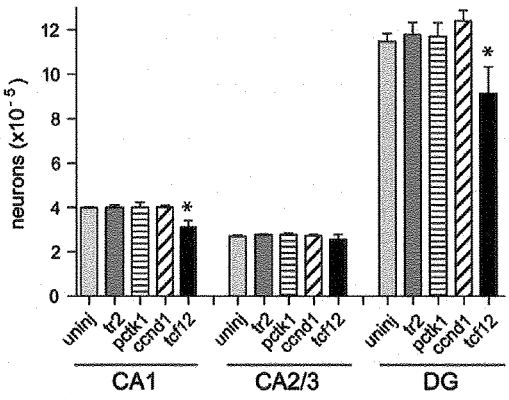

Fig. 6. Unbiased stereological estimate of the total number of cresyl violet stained (mean ± SEM) pyramidal neurons in CA1 and CA2/3, and granule cells in dentate gyrus (DG) of uninjected rats ($n = 5$), and tr2 ($n = 4$), Pctk1 ($n = 5$), Ccnd1 ($n = 4$) and Tcf12 ($n = 4$) injected rats. Each bar represents the mean ± SEM for each group. In a one way ANOVA analysis, Tcf12 was significantly different from either control in CA1 and DG (*$P < 0.05$).

varying degree of vascularization/hemorrhage, with cells primarily neuronal and with no to very infrequent mitotic bodies observed. Immunohistological staining of the tumors with Tcf12 antibody revealed that they were expressing Tcf12. Two of the rat brain tumors were positive for glial fibrillary acidic protein (GFAP) indicating glial cell-origin and therefore glioma or astrocytoma are the likely tumor type (Fig. 5). In contrast to nearby non-tumor tissue, Tcf12 expression appeared to localize to nuclei in tumor tissue (which is its normal location) and resulted in the accumulation of autofluorescent material. One tumor was not positive for GFAP (not shown), yet was positive for Tcf12 indicating some heterogeneity, most likely at the level of transduced cells and subsequent tumorgenesis.

The occurrence of tumors raised the question of whether gene expression of Tcf12 or the other two genes, Ccnd1 or Pctk1, might be exerting their effect by reducing the number of viable cells in the injected hippocampus. To determine this we used non-biased methods to count the number of neuronal cells in the CA1, CA2/3 and dentate gyrus regions of uninjected, tr2 injected and experimental animals (Fig. 6). There was no significant difference in the number of surviving neurons when Pctk1and Ccnd1 injected animals were compared to uninjected and tr2 animals (one-way ANOVA: $P = 0.999$ for CA1; $P = 0.743$ for CA2/3; $P = 0.719$ for DG). In contrast, animals expressing Tcf12 had lost approximately 20–25% of their neurons in CA1 and dentate gyrus (Fig. 6) and were significantly different from the tr2 and uninjected controls (one-way ANOVA: $Fs_{3,18} = 10.89$, $P = 0.001$ for CA1 and $F_{3,18} = 4.024$, $P = 0.024$ for DG).

We concluded that the behavioral deficits seen for Tcf12 injected animals could at least in part be the result of the pathology (tumors and loss of cells) that resulted from Tcf12 gene expression. In contrast, the absence of pathology in Ccnd1 and Pctk1 animals suggested that behavioral deficits in these animals were the result of a functional defect due to gene expression. These animals, therefore, were chosen for further electrophysiological analyses.

3.3. Synaptic transmission and plasticity

To evaluate the influence of enhanced expression of Ccnd1 and Pctk1 genes on synaptic function, 3 month old rats were injected with null, Pctk1 or Ccnd1 vectors. One month after injection, when gene expression reaches a maximum plateau (Reimsnider, Manfredsson, et al., 2007), the input–output synaptic response and level of LTP and LTD were examined in slices near the injection site. Examination of input–output curves of the synaptic response indicated no group difference in baseline synaptic strength (Fig. 7A). Furthermore, paired-pulse stimulation resulted in a similar level of PPF for controls (155.9 ± 34.2, $n = 8$), Ccnd1 (150.9 ± 4.5, $n = 9$), and Pctk1 (152.2 ± 5.8, $n = 11$) treated animals (Fig. 7B), suggesting that expression of Ccnd1 or Pctk1did not influence short-term plasticity mechanisms. Pattern stimulation to induce LTP resulted in an increase in the synaptic response compared to the control path ($P < 0.05$) in each group and the level of LTP was similar across the three groups: control (131.4 ± 3.5, $n = 23$, $P < 0.0001$), Ccnd1 (124.5 ± 6.1, $n = 11$, $P < 0.0002$), and Pctk1 (127.3 ± 7.6, $n = 15$, $P < 0.0001$) (Fig 7C and D). Similar to young animals, middle aged animals, (13–15 months, 12–13 months post injection) showed no group differences in LTP induced by theta burst pattern stimulation; the magnitude of LTP between control and experimental animals were not different (Supplementary Fig. 7).

In contrast, when we analyzed LTD-inducing stimulation in middle aged animals (13–15 months, 12–13 months post injection), we found decreased synaptic responses of controls (88.9 ± 3.9, $n = 10$, $P \leqslant 0.007$) and animals injected with Ccnd1 (87.9 ± 5.2, $n = 4$, $P < 0.03$), when examined 45 min following induction (Fig 7E and F). In contrast, the synaptic response of Pctk1 (101.4 ± 6.8, $n = 5$) treated animals was not different from the non-tetanized control path (100.3 ± 1.7, $n = 19$). The results suggest that enhanced expression of Pctk1 prevents induction of LTD, while Ccnd1 over expression has no influence on this form of synaptic plasticity.

4. Discussion

The genes studied in this report were originally identified by microarray studies; they showed elevated expression in aged (24 months) learning impaired rats compared to aged learning superior animals. That study identified a limited number of genes in CA1 (~50), many of which had not previously been associated with learning and memory deficits, and none of which were elevated in the nearby dentate gyrus region (Burger, Lopez, et al., 2007, 2008). We reasoned that an increase in expression of these genes might also produce a learning deficit at younger ages (7–14 months). To see if we could validate these genes, we used a vector transfer protocol that has previously been successful in studies of learning and memory and Parkinson Disease (Gorbatyuk, Li, et al., 2008; Klugmann, Wymond Symes, et al., 2005). AAV vectors quantitatively transduce the neurons near the site of injection and then slowly ramp up expression of the transferred gene until expression plateaus at 1 month post-injection. Expression then remains constant for the lifetime of the animal (Peel & Klein, 2000; Reimsnider, Manfredsson, et al., 2007). Expression levels are typically 2–4 times endogenous levels (Gorbatyuk, Li, et al., 2008; Gorbatyuk, Li, et al., 2010), which is two to three times higher than the elevations detected in aged animals by microarray in our previous study (Burger, Lopez, et al., 2007). Thus, this approach allowed us to independently evaluate the effect of overexpressing each gene on learning and memory.

All three of the genes chosen for this study displayed significant deficits in learning and memory in some but not all of the behavioral tests that were tried, and each of the three genes revealed a unique behavioral profile (Table 1). Pctk1 showed a significant difference in latency to learn the position of the platform in the conventional MWM and reverse MWM, and also showed a defect in working memory in the RAWM (Table 1). Pctk1 did not, however, display any significant difference in RAWM reference memory. The effect of Pctk1 is likely due to hippocampal

Please cite this article in press as: Wu, K., et al. Enhanced expression of Pctk1, Tcf12 and Ccnd1 in hippocampus of rats: Impact on cognitive function, synaptic plasticity and pathology. *Neurobiology of Learning and Memory* (2011), doi:10.1016/j.nlm.2011.09.006

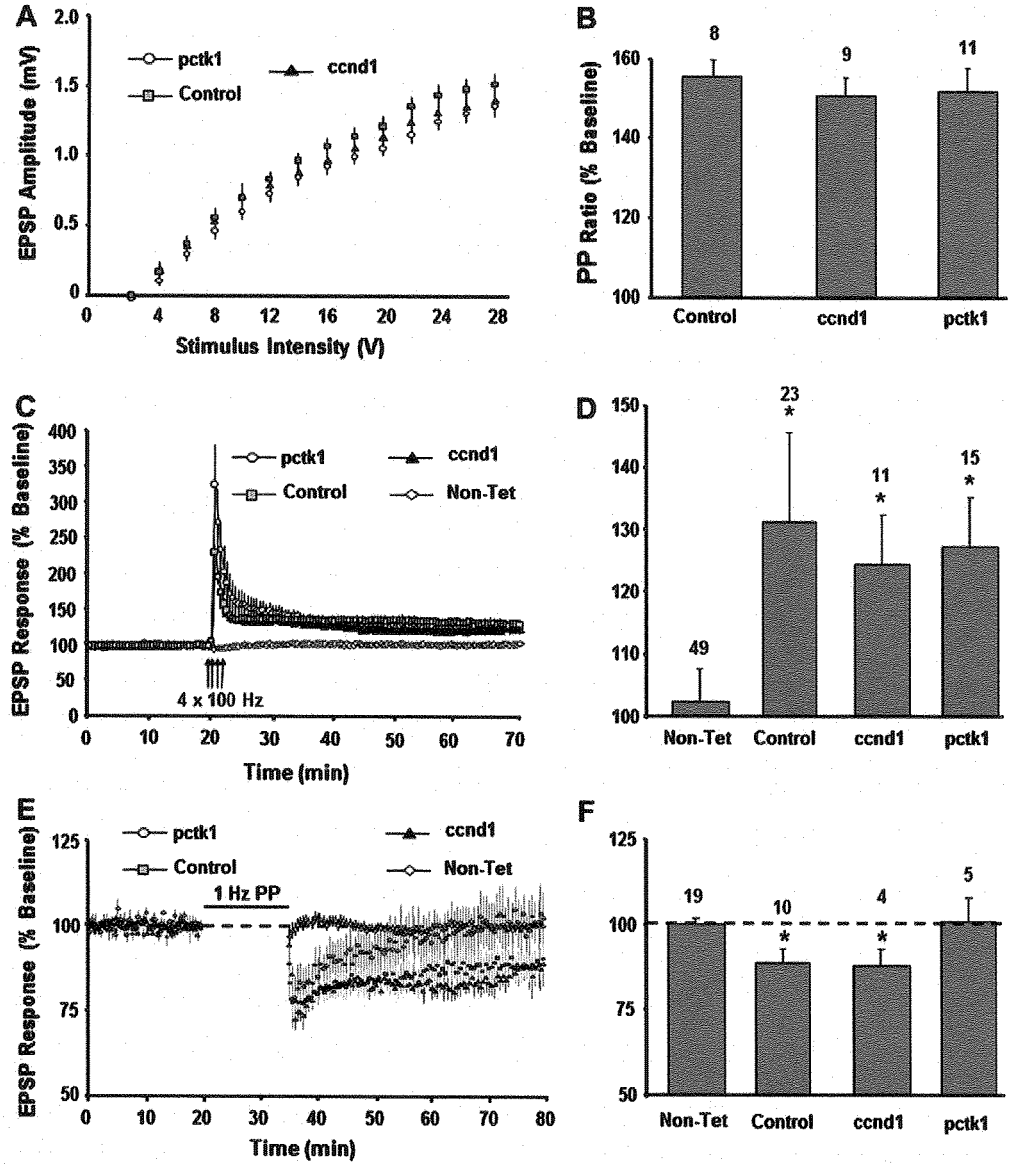

Fig. 7. Effect of expression of Ccnd1 and Pctk1 on hippocampal synaptic function. (A) Input–output curves of the baseline EPSP response vs. stimulus intensity for control (filled square, $n = 45$ slices), Ccnd1 (filled triangle, $n = 23$ slices), and Pctk1 (filled circle, $n = 25$ slices) treated rats. Each point represents the mean ± the SEM. (B) The bar diagram shows the mean PPF ratio for control, Ccnd1, and Pctk1 treated rats. (C) Time course of changes in the field EPSP obtained from hippocampal slices 20 min before and 50 min after stimulation to induce LTP for the control (gray square, Ccnd1 (filled triangle), and Pctk1 (open circle) treated slices. A non-tetanized control path (Non-Tet, open diamond) was used to insure that changes in EPSP were specific to pattern stimulation and not due to change in slice health. (D) Bar diagram showing the average magnitude of LTP during the last 5 min of recording for control non-tetanized path, control, Ccnd1, and Pctk1 treated animals. The number above each bar indicates number of animals recorded for each group at each point. (E) Time course of the field EPSP measurements obtained from hippocampal slices 20 min before and 45 min after stimulation to induce LTD for the control, Ccnd1, and Pctk1 treated slices. (F) Bar diagram showing the average magnitude of LTD during the last 5 min of recording for control non-tetanized path, controls, Ccnd1 and Pctk1 treated animals. Asterisk represents significant difference between tetanized and not-tetanized control paths. For each panel, error bars equal SEM.

dysfunction rather than a sensorimotor deficit. In general, sensorimotor deficits result in thigmotaxis and increased latencies, primarily during the early acquisition trials (Devan & White, 1999; Dolleman-van der Weel et al., 2009). In contrast, deficits in Pctk1 animals emerged during later trials, suggesting impaired hippocampal-dependent spatial learning (Morris et al., 1990). In contrast to Pctk1, both Ccnd1 and Tcf12 both showed robust defects in RAWM reference and working memory, but did not reach significance when tested in the conventional MWM. Finally, Pctk1 and Ccnd1 expressing animals were tested for LTP and LTD. The results suggested that Pctk1 overexpression may result in reduced LTD, but no other significant differences for Pctk1 or Ccnd1 expressing groups compared to control groups was found.

The deficits in MWM, SWM and SRM are not likely the results of sensorimotor deficit because all rats had similar swimming speed (Supplementary Fig. 2) and learned the task as indicated by the decreasing number of errors in both working and reference memory during sessions. Further, the radial index scores for all groups in the RAWM were well above 60°, indicating a lack of chaining behavior (Roullet, Lassalle, et al., 1993) and supporting the notion that behavioral deficits were the results of learning and memory impairments (Supplementary Fig. 4).

Please cite this article in press as: Wu, K., et al. Enhanced expression of Pctk1, Tcf12 and Ccnd1 in hippocampus of rats: Impact on cognitive function, synaptic plasticity and pathology. *Neurobiology of Learning and Memory* (2011), doi:10.1016/j.nlm.2011.09.006

We note that although there was a clear effect of Pctk1 on latency in the MWM, there was no significant difference in the subsequent probe tests for any group, suggesting that all groups successfully learned the platform position (Supplementary Fig. 1). Additionally, none of the genes showed an effect in the passive avoidance test (not shown). In contrast, many previous experiments with aged animals, including our own (Burger, Lopez, et al., 2007; Burger, Lopez, et al., 2008) have shown an effect on memory acquisition in the probe trials and in passive avoidance tests. The most likely explanation is that learning deficits in aged animals are the result of multiple gene expression changes. Our previous microarray studies identified at least 135 genes whose expression pattern was significantly modified in aged rodents in CA1 or DG. In contrast, the study described here changed the expression of only one gene at a time, and only at an earlier age, when all other genes were likely to be expressed at normal levels, and possibly compensated for the engineered defect. In spite of this limitation, the effect of Ccnd1 and Pctk1 on memory in some of the behavioral tests was quite robust.

4.1. Tcf12

Tcf12. is a basic helix loop helix (bHLB) transcription factor that binds to E box sequences (Hu, Olson, et al., 1992; Zhang, Babin, et al., 1991). It forms homo and heteroduplex complexes with other bHLB factors (Tcf3, E12, myogenin, ITF2, RUNX1T1 and TAL1) and can act both as a repressor and activator of transcription depending on the cellular context. A family of proteins (Id1–Id3) retain the protein interaction loop but not the DNA binding domain and act as inhibitors of the Tcf proteins. Tcf12 has been extensively characterized as a key factor controlling B and T cell progenitor expansion and differentiation as well as myogenesis (Parker, Perry, et al., 2006; Quong, Romanow, et al., 2002). In T cells, it is involved in TCRα and TCRβ rearrangement. Tcf12 knockout mice die shortly after birth (Uittenbogaard & Chiaramello, 2002). Relatively little is known about Tcf12 in neuronal tissues. Its pattern of expression suggests that it may be involved in neuronal stem cell and progenitor cell proliferation or may be necessary to maintain an undifferentiated state (Uittenbogaard & Chiaramello, 2002). In knockout mice heterozygous for Tcf12, Tal1 induced T cell acute lymphoblastic leukemia was accelerated, suggesting that Tcf12 normally inhibited genes that lead to leukemia induction (O'Neil, Shank, et al., 2004). In contrast, our results suggest that its expression may lead to neurodegeneration and tumor formation in the adult rodent brain. AAV has been used to deliver genes in many animal models, and has been used in several clinical trials that address neurodegenerative diseases (Manfredsson & Mandel, 2010). To date, there has been no evidence of vector related toxicity in the brain. Tcf12 is the first example of an AAV delivered gene product that induced brain tumors.

Clearly, the loss of neurons in CA1 and dentate gyrus and possibly tumor formation are the most likely mechanisms for the learning deficits seen in the RAWM with Tcf12 injected animals. However, since we did not determine the time course of neurodegeneration, we cannot rule out a direct effect on learning and memory. In PC12 cells, overexpression of Tcf12 has been shown to repress the expression of the low-affinity neurotrophin receptor p75 gene (Uittenbogaard & Chiaramello, 2002), which could be responsible for the neurodegeneration observed in CA1 and dentate gyrus.

4.2. Pctk1. and Ccnd1

Gene transfer of Pctk1 and Ccnd1 into rat hippocampus did not cause neurodegeneration, as indicated by the unaltered numbers of hippocampal neurons between treatment groups (Fig. 6). The gross morphology of pyramidal neurons in CA1, CA2/3 subregions and granule cells in dentate gyrus was also unaltered in Pctk1 and Ccnd1 rats compared to control animals (unpublished observation). These results suggest that the memory deficits that we observed in Pctk1 and Ccnd1 rats were due to altered gene expression and an apparent functional role for Pctk1 and Ccnd1 in learning and memory. Our results validate our previous microarray study that showed elevated transcript levels of Pctk1 and Ccnd1 in the hippocampus of aged, learning-impaired rats. The fact that increased levels of these genes also induce a learning deficit in young and middle-aged animals suggests that they are likely to play a role in learning and memory at all ages.

4.3. Pctk1

Pctk1. is abundantly expressed in pyramidal neurons (Besset, Rhee, et al., 1999) and has been shown to be a negative regulator of N-ethylmaleimide-sensitive fusion (NSF) protein (Liu, Cheng, et al., 2006). NSF is required for the disassembly and recycling of SNARE proteins during the interval between exocytosis and endocytosis, an event important for maintaining normal neurotransmitter release in presynaptic termini (Littleton, Barnard, et al., 2001; Parnas, Rashkovan, et al., 2006; Schweizer, Dresbach, et al., 1998). NSF is also important for synaptic plasticity, which is believed to be the cellular mechanism for the formation of memory. NSF binds to the glutamate receptor subunit 2 (GluR2) of the postsynaptic α-amino-3-hydroxy-5-methyl-4-isoxazolepropionic acid receptor (AMPAR). This interaction promotes trafficking and stabilization of AMPAR at the postsynaptic membrane (Hanley, 2007; Lee, Liu, et al., 2002; Luscher, Xia, et al., 1999). The NSF-GluR2 interaction is thought to be essential for the expression of LTD, a form of synaptic plasticity in the hippocampus (Lei & McBain, 2004; Steinberg, Huganir, et al., 2004). Pctk1 binds to NSF at the D2 domain, and phosphorylates NSF at serine 569 (Liu, Cheng, et al., 2006). This inhibits oligomerization of NSF, which is required for normal NSF function. Expression of a kinase-dead mutant of Pctk1 or NSF-S569A in PC12 cells significantly increases high K(+)-stimulated growth hormone release, whereas expression of wild type Pctk1 had the opposite effect. These data suggest that Pctk1 may be involved in the formation of memory by modulating the activity of NSF at presynaptic or postsynaptic termini. Our result that Pctk1 inhibits induction of LTD is consistent with the Pctk1 interaction with NSF.

Pctk1 also interacts with the coat protein II (COPII) complex (Palmer, Konkel, et al., 2005), which mediates the export of secretory cargo from the endoplasmic reticulum. Pctk1 interacts specifically with Sec23Ap, and inhibition of Pctk1 kinase activity produces a defect in cargo transport in the endoplasmic reticulum.

Pctk1 can be phosphorylated by protein kinase A (PKA). Phosphorylation of S153 inhibits Pctk kinase activity and kinase active forms of Pctk stimulate neurite outgrowth in Neuro-2A cells (Graeser, Gannon, et al., 2002). Pctk1 can also be phosphorylated by cyclin dependent kinase 5 (Cdk5)/p35 complex. Like Cdk5, Pctk1 does not bind a cyclin; instead both Cdk5 and Pctk1 bind the same regulatory protein, p35. Whereas PKA phosphorylation of Pctk1 inhibits its kinase activity, phosphorylation of Pctk1 by Cdk5/p35 activates Pctk1 kinase activity (Graeser, Gannon, et al., 2002). Pctk1 kinase activity in Cdk5 null mice is significantly reduced in brain and muscle.

The fact that Pctk1 rats showed a deficit in only SWM and not SRM lends support to the notion that SWM and SRM are encoded by different information processing mechanisms in hippocampus. However, it is not clear whether one of the interactions described above between Pctk1 and other neuronal complexes is responsible for the behavioral effect on learning and memory, or if some unknown interaction is essential. The present demonstration of

Please cite this article in press as: Wu, K., et al. Enhanced expression of Pctk1, Tcf12 and Ccnd1 in hippocampus of rats: Impact on cognitive function, synaptic plasticity and pathology. *Neurobiology of Learning and Memory* (2011), doi:10.1016/j.nlm.2011.09.006

impaired SWM but intact SRM in Pctk1 rats shows some parallels with the behavioral phenotypes of transgenic mice with functional loss of *N*-methyl-D-aspartate (NMDA) glutamate receptors in dentate gyrus or CA3 subregions (Niewoehner, Single, et al., 2007).

4.4. Ccnd1

Ccnd1 rats displayed both SRM and SWM deficits in RAWM, but unlike Pctk1 injected animals, Ccnd1 rats did not show a significant deficit in the MWM. It is unclear whether the deficit in RAWM performance by Ccnd1 animals was due to an increase in memory load required in this paradigm or the difference in age of the animals during the two behavioral tests, 14 months old vs. 7 months old for RAWM and MW, respectively.

Ccnd1 is a key regulator of the transition from G1 to S phase in all cells (Weinberg, 1995). It activates cdk4/6, which in turn phosphorylates Rb and releases E2f transcription factors. These then activate a variety of enzyme pathways essential for DNA synthesis. Despite its presence in adult dentate gyrus neurons, Ccnd1 does not appear essential for neurogenesis during development or in adults, because its ablation had little or no effect on the growth of neurons (Fantl, Stamp, et al., 1995; Kowalczyk, Filipkowski, et al., 2004; Sicinski, Donaher, et al., 1995). However, overexpression of Ccnd1/cdk4 during development promoted the expansion of neural progenitors and inhibited neuron maturation leading to larger cortical and subventricular cell layers (Lange, Huttner, et al., 2009; Simpson, Moon, et al., 2007). Conversely, reduction of Cdnd1 had the opposite effect. Thus, the increase in Ccnd1 expression in mature adult brains might be expected to expand the pool of neuroprogenitors and delay their differentiation to mature neurons. It is worth noting that Ccnd1 expresses exclusively in neurons in adult brains and that it appears to be sequestered in cytoplasm in terminally differentiated neurons. In differentiated progenitor cells, nuclear localization of ectopic Ccnd1 induced apoptosis, and the DNA-damaging compound camptothecin caused nuclear accumulation of endogenous Ccnd1, accompanied by Rb phosphorylation (Sumrejkanchanakij, Tamamori-Adachi, et al., 2003).

Ccnd1 may also influence learning and memory performance through its effect on several nuclear receptors/transcription factors (Ewen & Lamb, 2004). Ccnd1 is a ligand-independent co-repressor of thyroid hormone receptor β1 (TRβ1) (Lin, Zhao, et al., 2002; Petre-Draviam, Williams, et al., 2005). Transgenic mice carrying a mutant TRβ1 that reduces its ligand binding activity (and, therefore, its activity) display hyperactivity and learning deficits, suggesting that the normal function of TRβ1 may be important for cognition (McDonald, Wong, et al., 1998). Repression of TRβ1 by overexpression of Ccnd1 may lead to similar learning deficits.

Ccnd1 also modulates the activities of sex hormone receptors such as androgen receptors (ARs) and estrogen receptors (ERs). Ccnd1 selectively inhibits ligand-dependent AR functions in several cell types (Knudsen, Cavenee, et al., 1999; Petre, Wetherill, et al., 2002; Petre-Draviam, Williams, et al., 2005). The roles of ARs in learning and memory have been controversial. Some studies have shown that adrogens and selective AR modulators enhanced learning and memory, whereas other studies showed that androgens impaired learning and memory (Acevedo, Tittle, et al., 2008; Naghdi, Nafisy, et al., 2001). Finally, Ccnd1 binds to and activates the estrogen receptor α (ERα) both in the presence and absence of estrogen (Neuman, Ladha, et al., 1997; Zwijsen, Wientjens, et al., 1997). Estrogen enhances the spatial memory performance of both male and female rats (Foy, Baudry, et al., 2010; Mukai, Kimoto, et al., 2010). This would suggest that the behavioral learning deficits induced by Ccnd1 expression in this study are independent of ERα.

To our knowledge, the results from the current study provide the first validation of the involvement of Pctk1 and Ccnd1 proteins in learning and memory processes. Further studies are needed to tease out the precise mechanisms by which these two proteins affect cognition. Additionally, 3 out of 3 genes chosen for this study all showed a defect in learning and memory. This validates, the original studies of Burger, Lopez, et al. (2007) and Burger, Lopez et al. (2008) and suggests that other genes identified in those studies should probably be examined as well.

Acknowledgments

The authors were supported by NIH Grants NS36302, HL59412, and NS69574 to N.M. and AG014979, AG037984, AG036800 and the Evelyn F. McKnight Brain Research Foundation to T.C.F. N.M. was also supported by the Edward R. Koger American Cancer Society endowment fund. N.M. is an inventor of AAV patents related to recombinant AAV Technology and owns equity in a gene therapy company that is commercializing AAV for gene therapy applications.

Appendix A. Supplementary material

Supplementary data associated with this article can be found, in the online version, at doi:10.1016/j.nlm.2011.09.006.

References

Acevedo, S. F., Tittle, S., et al. (2008). Transgenic expression of androgen receptors improves spatial memory retention in both sham-irradiated and 137Cs gamma-irradiated female mice. *Radiation Research, 170*(5), 572–578.

Allen (2004). Allen Brain Atlas (Internet). <http://www.brain-map.org> Accessed 12.12.10.

Besset, V., Rhee, K., et al. (1999). The cellular distribution and kinase activity of the Cdk family member Pctaire1 in the adult mouse brain and testis suggest functions in differentiation. *Cell Growth and Differentiation, 10*(3), 173–181.

Bodhinathan, K., Kumar, A., et al. (2010). Intracellular redox state alters NMDA receptor response during aging through Ca^{2+}/calmodulin-dependent protein kinase II. *Journal of Neuroscience, 30*(5), 1914–1924.

Burger, C., Lopez, M. C., et al. (2007). Changes in transcription within the CA1 field of the hippocampus are associated with age-related spatial learning impairments. *Neurobiology of Learning and Memory, 87*(1), 21–41.

Burger, C., Lopez, M. C., et al. (2008). Genome-wide analysis of aging and learning-related genes in the hippocampal dentate gyrus. *Neurobiology of Learning and Memory, 89*(4), 379–396.

Campbell-Thompson, M., Dixon, L. R., et al. (2009). Pancreatic adenocarcinoma patients with localised chronic severe pancreatitis show an increased number of single beta cells, without alterations in fractional insulin area. *Diabetologia, 52*(2), 262–270.

Ewen, M. E., & Lamb, J. (2004). The activities of cyclin D1 that drive tumorigenesis. *Trends in Molecular Medicine, 10*(4), 158–162.

Fantl, V., Stamp, G., et al. (1995). Mice lacking cyclin D1 are small and show defects in eye and mammary gland development. *Genes and Development, 9*(19), 2364–2372.

Foy, M. R., Baudry, M., et al. (2010). Regulation of hippocampal synaptic plasticity by estrogen and progesterone. *Vitamins and Hormones, 82*, 219–239.

Gorbatyuk, O. S., Li, S., et al. (2008). The phosphorylation state of Ser-129 in human alpha-synuclein determines neurodegeneration in a rat model of Parkinson disease. *Proceedings of the National Academy of Sciences, USA, 105*(2), 763–768.

Gorbatyuk, O. S., Li, S., et al. (2010). Alpha-Synuclein expression in rat substantia nigra suppresses phospholipase D2 toxicity and nigral neurodegeneration. *Molecular Therapy, 18*(10), 1758–1768.

Graeser, R., Gannon, J., et al. (2002). Regulation of the CDK-related protein kinase PCTAIRE-1 and its possible role in neurite outgrowth in Neuro-2A cells. *Journal of Cell Science, 115*(Pt 17), 3479–3490.

Hanley, J. G. (2007). NSF binds calcium to regulate its interaction with AMPA receptor subunit GluR2. *Journal of Neurochemistry, 101*(6), 1644–1650.

Hauswirth, W. W., Lewin, A. S., et al. (2000). Production and purification of recombinant adeno-associated virus. *Methods in Enzymology, 316*, 743–761.

Hernandez, P. J., & Abel, T. (2008). The role of protein synthesis in memory consolidation: Progress amid decades of debate. *Neurobiology of Learning and Memory, 89*(3), 293–311.

Hu, J. S., Olson, E. N., et al. (1992). HEB, a helix-loop-helix protein related to E2A and ITF2 that can modulate the DNA-binding ability of myogenic regulatory factors. *Molecular and Cellular Biology, 12*(3), 1031–1042.

Kim, H. A., Pomeroy, S. L., et al. (2000). A developmentally regulated switch directs regenerative growth of Schwann cells through cyclin D1. *Neuron, 26*(2), 405–416.

Kirik, D., Rosenblad, C., et al. (2002). Parkinson-like neurodegeneration induced by targeted overexpression of alpha-synuclein in the nigrostriatal system. *Journal of Neuroscience, 22*(7), 2780–2791.

Klugmann, M., Wymond Symes, C., et al. (2005). AAV-mediated hippocampal expression of short and long Homer 1 proteins differentially affect cognition and seizure activity in adult rats. *Molecular and Cellular Neurosciences, 28*(2), 347–360.

Knudsen, K. E., Cavenee, W. K., et al. (1999). D-type cyclins complex with the androgen receptor and inhibit its transcriptional transactivation ability. *Cancer Research, 59*(10), 2297–2301.

Kowalczyk, A., Filipkowski, R. K., et al. (2004). The critical role of cyclin D2 in adult neurogenesis. *Journal of Cell Biology, 167*(2), 209–213.

Kozar, K., & Sicinski, P. (2005). Cell cycle progression without cyclin D-CDK4 and cyclin D-CDK6 complexes. *Cell Cycle, 4*(3), 388–391.

Kumar, A. (2010). Carbachol-induced long-term synaptic depression is enhanced during senescence at hippocampal CA3–CA1 synapses. *Journal of Neurophysiology, 104*(2), 607–616.

Kumar, A., & Foster, T. C. (2004). Enhanced long-term potentiation during aging is masked by processes involving intracellular calcium stores. *Journal of Neurophysiology, 91*(6), 2437–2444.

Kumar, A., & Foster, T. C. (2007). Shift in induction mechanisms underlies an age-dependent increase in DHPG-induced synaptic depression at CA3–CA1 synapses. *Journal of Neurophysiology, 98*(5), 2729–2736.

Kumar, A., Thinschmidt, J. S., et al. (2007). Aging effects on the limits and stability of long-term synaptic potentiation and depression in rat hippocampal area CA1. *Journal of Neurophysiology, 98*(2), 594–601.

Lange, C., Huttner, W. B., et al. (2009). Cdk4/cyclinD1 overexpression in neural stem cells shortens G1, delays neurogenesis, and promotes the generation and expansion of basal progenitors. *Cell Stem Cell, 5*(3), 320–331.

Lee, S. H., Liu, L., et al. (2002). Clathrin adaptor AP2 and NSF interact with overlapping sites of GluR2 and play distinct roles in AMPA receptor trafficking and hippocampal LTD. *Neuron, 36*(4), 661–674.

Lei, S., & McBain, C. J. (2004). Two Loci of expression for long-term depression at hippocampal mossy fiber-interneuron synapses. *Journal of Neuroscience, 24*(9), 2112–2121.

Lin, H. M., Zhao, L., et al. (2002). Cyclin D1 is a ligand-independent co-repressor for thyroid hormone receptors. *Journal of Biological Chemistry, 277*(32), 28733–28741.

Littleton, J. T., Barnard, R. J., et al. (2001). SNARE-complex disassembly by NSF follows synaptic-vesicle fusion. *Proceedings of the National Academy of Sciences, USA, 98*(21), 12233–12238.

Liu, Y., Cheng, K., et al. (2006). Pctaire1 phosphorylates N-ethylmaleimide-sensitive fusion protein: Implications in the regulation of its hexamerization and exocytosis. *Journal of Biological Chemistry, 281*(15), 9852–9858.

Luscher, C., Xia, H., et al. (1999). Role of AMPA receptor cycling in synaptic transmission and plasticity. *Neuron, 24*(3), 649–658.

Manfredsson, F. P., & Mandel, R. J. (2010). Development of gene therapy for neurological disorders. *Discovery Medicine, 9*(46), 204–211.

McDonald, M. P., Wong, R., et al. (1998). Hyperactivity and learning deficits in transgenic mice bearing a human mutant thyroid hormone beta1 receptor gene. *Learning & Memory, 5*(4–5), 289–301.

Meyerson, M., Enders, G. H., et al. (1992). A family of human cdc2-related protein kinases. *EMBO Journal, 11*(8), 2909–2917.

Mukai, H., Kimoto, T., et al. (2010). Modulation of synaptic plasticity by brain estrogen in the hippocampus. *Biochimica et Biophysica Acta, 1800*(10), 1030–1044.

Naghdi, N., Nafisy, N., et al. (2001). The effects of intrahippocampal testosterone and flutamide on spatial localization in the Morris water maze. *Brain Research, 897*(1–2), 44–51.

Neuman, E., Ladha, M. H., et al. (1997). Cyclin D1 stimulation of estrogen receptor transcriptional activity independent of cdk4. *Molecular and Cellular Biology, 17*(9), 5338–5347.

Niewoehner, B., Single, F. N., et al. (2007). Impaired spatial working memory but spared spatial reference memory following functional loss of NMDA receptors in the dentate gyrus. *European Journal of Neuroscience, 25*(3), 837–846.

Okuda, T., Cleveland, J. L., et al. (1992). PCTAIRE-1 and PCTAIRE-3, two members of a novel cdc2/CDC28-related protein kinase gene family. *Oncogene, 7*(11), 2249–2258.

O'Neil, J., Shank, J., et al. (2004). TAL1/SCL induces leukemia by inhibiting the transcriptional activity of E47/HEB. *Cancer Cell, 5*(6), 587–596.

Palmer, K. J., Konkel, J. E., et al. (2005). PCTAIRE protein kinases interact directly with the COPII complex and modulate secretory cargo transport. *Journal of Cell Science, 118*(Pt 17), 3839–3847.

Parker, M. H., Perry, R. L., et al. (2006). MyoD synergizes with the E-protein HEB beta to induce myogenic differentiation. *Molecular and Cellular Biology, 26*(15), 5771–5783.

Parnas, I., Rashkovan, G., et al. (2006). Role of NSF in neurotransmitter release: A peptide microinjection study at the crayfish neuromuscular junction. *Journal of Neurophysiology, 96*(3), 1053–1060.

Paxinos, G., Watson, C., et al. (1985). Bregma, lambda and the interaural midpoint in stereotaxic surgery with rats of different sex, strain and weight. *Journal of Neuroscience Methods, 13*(2), 139–143.

Peel, A. L., & Klein, R. L. (2000). Adeno-associated virus vectors: Activity and applications in the CNS. *Journal of Neuroscience Methods, 98*(2), 95–104.

Petre, C. E., Wetherill, Y. B., et al. (2002). Cyclin D1: Mechanism and consequence of androgen receptor co-repressor activity. *Journal of Biological Chemistry, 277*(3), 2207–2215.

Petre-Draviam, C. E., Williams, E. B., et al. (2005). A central domain of cyclin D1 mediates nuclear receptor corepressor activity. *Oncogene, 24*(3), 431–444.

Quong, M. W., Romanow, W. J., et al. (2002). E protein function in lymphocyte development. *Annual Review of Immunology, 20*, 301–322.

Reimsnider, S., Manfredsson, F. P., et al. (2007). Time course of transgene expression after intrastriatal pseudotyped rAAV2/1, rAAV2/2, rAAV2/5, and rAAV2/8 transduction in the rat. *Molecular Therapy, 15*(8), 1504–1511.

Rex, C. S., Gavin, C. F., et al. (2010). Myosin IIb regulates actin dynamics during synaptic plasticity and memory formation. *Neuron, 67*(4), 603–617.

Roullet, P., Lassalle, J. M., et al. (1993). A study of behavioral and sensorial bases of radial maze learning in mice. *Behavioral and Neural Biology, 59*(3), 173–179.

Schweizer, F. E., Dresbach, T., et al. (1998). Regulation of neurotransmitter release kinetics by NSF. *Science, 279*(5354), 1203–1206.

Sherr, C. J., & Roberts, J. M. (1999). CDK inhibitors: Positive and negative regulators of G1-phase progression. *Genes and Development, 13*(12), 1501–1512.

Sicinski, P., Donaher, J. L., et al. (1995). Cyclin D1 provides a link between development and oncogenesis in the retina and breast. *Cell, 82*(4), 621–630.

Simpson, P. J., Moon, C., et al. (2007). Progressive and inhibitory cell cycle proteins act simultaneously to regulate neurotrophin-mediated proliferation and maturation of neuronal precursors. *Cell Cycle, 6*(9), 1077–1089.

Steinberg, J. P., Huganir, R. L., et al. (2004). N-ethylmaleimide-sensitive factor is required for the synaptic incorporation and removal of AMPA receptors during cerebellar long-term depression. *Proceedings of the National Academy of Sciences, USA, 101*(52), 18212–18216.

Sumrejkanchanakij, P., Tamamori-Adachi, M., et al. (2003). Role of cyclin D1 cytoplasmic sequestration in the survival of postmitotic neurons. *Oncogene, 22*(54), 8723–8730.

Tran, T. D., & Kelly, S. J. (2003). Critical periods for ethanol-induced cell loss in the hippocampal formation. *Neurotoxicology and Teratology, 25*(5), 519–528.

Uittenbogaard, M., & Chiaramello, A. (2002). Expression of the bHLH transcription factor Tcf12 (ME1) gene is linked to the expansion of precursor cell populations during neurogenesis. *Brain Research: Gene Expression Patterns, 1*(2), 115–121.

Weinberg, R. A. (1995). The retinoblastoma protein and cell cycle control. *Cell, 81*(3), 323–330.

Zhang, Y., Babin, J., et al. (1991). HTF4: A new human helix-loop-helix protein. *Nucleic Acids Research, 19*(16), 4555.

Zhuang, Y., Cheng, P., et al. (1996). B-lymphocyte development is regulated by the combined dosage of three basic helix-loop-helix genes, E2A, E2-2, and HEB. *Molecular and Cellular Biology, 16*(6), 2898–2905.

Zolotukhin, S., Potter, M., et al. (2002). Production and purification of serotype 1, 2, and 5 recombinant adeno-associated viral vectors. *Methods, 28*(2), 158–167.

Zwijsen, R. M., Wientjens, E., et al. (1997). CDK-independent activation of estrogen receptor by cyclin D1. *Cell, 88*(3), 405–415.

Please cite this article in press as: Wu, K., et al. Enhanced expression of Pctk1, Tcf12 and Ccnd1 in hippocampus of rats: Impact on cognitive function, synaptic plasticity and pathology. *Neurobiology of Learning and Memory* (2011), doi:10.1016/j.nlm.2011.09.006

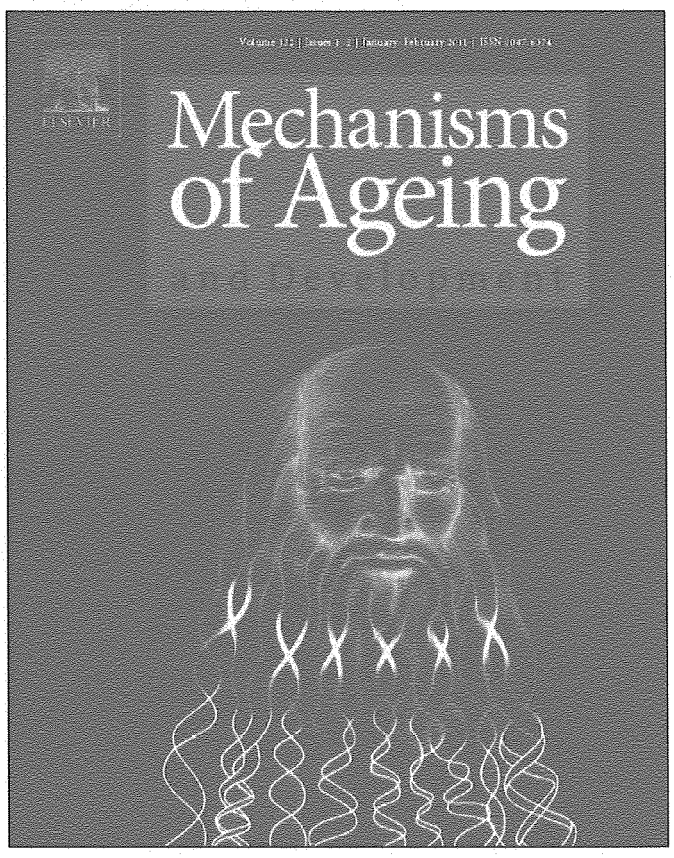

Mechanisms of Ageing and Development 132 (2011) 8–19

Contents lists available at ScienceDirect

Mechanisms of Ageing and Development

journal homepage: www.elsevier.com/locate/mechagedev

Gene expression in the hippocampus: Regionally specific effects of aging and caloric restriction

Zane Zeier[a], Irina Madorsky[a], Ying Xu[b], William O. Ogle[b], Lucia Notterpek[a], Thomas C. Foster[a,*]

[a] Department of Neuroscience, McKnight Brain Institute, University of Florida, P.O. Box 100244, Gainesville, FL 32610-0244, USA
[b] Department of Biomedical Engineering, University of Florida, Gainesville, FL 32611, USA

ARTICLE INFO

Article history:
Received 3 February 2010
Received in revised form 13 October 2010
Accepted 21 October 2010
Available online 3 November 2010

Keywords:
Aging
Diet
Hippocampus
Transcription
Proteosome
Ubiquitin

ABSTRACT

We measured changes in gene expression, induced by aging and caloric restriction (CR), in three hippocampal subregions. When analysis included all regions, aging was associated with expression of genes linked to mitochondrial dysfunction, inflammation, and stress responses, and in some cases, expression was reversed by CR. An age-related increase in ubiquintination was observed, including increased expression of ubiquitin conjugating enzyme genes and cytosolic ubiquitin immunoreactivity. CR decreased cytosolic ubiquitin and upregulated deubiquitinating genes. Region specific analyses indicated that CA1 was more susceptible to aging stress, exhibiting a greater number of altered genes relative to CA3 and the dentate gyrus (DG), and an enrichment of genes related to the immune response and apoptosis. CA3 and the DG were more responsive to CR, exhibiting marked changes in the total number of genes across diet conditions, reversal of age-related changes in p53 signaling, glucocorticoid receptor signaling, and enrichment of genes related to cell survival and neurotrophic signaling. Finally, CR differentially influenced genes for synaptic plasticity in CA1 and CA3. It is concluded that regional disparity in response to aging and CR relates to differences in vulnerability to stressors, the availability of neurotrophic, and cell survival mechanisms, and differences in cell function.

1. Introduction

Brain aging processes are enormously complex affecting multiple systems, cell types, and cellular pathways. Gene expression studies attempt to estimate the status of critical parameters for multiple cellular processes that change with age. Examination of gene expression in brain tissue over the lifespan indicates alterations in general aging processes including inflammation, oxidative stress, Ca^{2+} regulation, and cell growth/structural organization (Aenlle et al., 2009; Blalock et al., 2003; Erraji-Benchekroun et al., 2005; Prolla, 2002; Terao et al., 2002).

Caloric restriction (CR) is the most accepted approach to slow the aging process and delay or prevent many age-related diseases (Mattson and Wan, 2005; Weindruch et al., 1988). A review of transcription changes associated with CR indicates that there are no common genes or groups of genes which are influenced by CR across different species (Han and Hickey, 2005). Indeed, for studies that examine gene changes across tissues, even in the same animal, only a handful of genes may emerge as sensitive to treatment (Fu et al., 2006; Selman et al., 2006; Swindell, 2008). Differences may be related to whether the cells in the tissue are post-mitotic (Spindler and Dhahbi, 2007), the function of the tissues examined, and the effects of aging on the tissue (Weindruch et al., 2002).

While much work has focused on peripheral organs and lifespan, little is known concerning the effects of CR on the nervous system. There are some indications that CR improves motor and cognitive function in aged animals (Carter et al., 2009; Fontan-Lozano et al., 2007; Ingram et al., 1987; Pitsikas and Algeri, 1992) and in models of neurodegeneration (Bruce-Keller et al., 1999; Halagappa et al., 2007). The hippocampus is a region that is particularly sensitive to aging, resulting in impaired synaptic plasticity and memory deficits (Foster, 1999, 2007). The three main regions of the hippocampus include the CA1, CA3, and dentate gyrus (DG). These regions differ in terms of efferents, afferents and major cell types (Knowles, 1992), neurogenesis (Ormerod et al., 2008; Pawluski et al., 2009), vulnerability to stressors (Jackson and Foster, 2009; Jackson et al., 2009; McEwen, 2001), and synaptic plasticity mechanisms (Hussain and Carpenter, 2005; McBain, 2008; Zalutsky and Nicoll, 1990). In addition, differences have been noted concerning biological markers of aging within these regions, including altered synaptic function and response to stress (Foster, 2002; Jackson et al., 2009; McEwen, 2001; Patrylo and Williamson, 2007; Rosenzweig and Barnes, 2003). The current study was designed to determine whether CR had a similar effect in these

* Corresponding author. Tel.: +352 392 4359; fax: +352 392-8347.
E-mail address: Foster@mbi.ufl.edu (T.C. Foster).

0047-6374/$ – see front matter © 2010 Elsevier Ireland Ltd. All rights reserved.
doi:10.1016/j.mad.2010.10.006

three closely linked regions and whether CR would act on genes related to biological markers of aging in the hippocampus such as inflammation, stress, and mitochondrial dysfunction.

2. Materials and methods

2.1. Animals

All procedures involving animals were approved by the Institutional Animal Care and Use Committee of the University of Florida. *Ad libitum* (AL) fed and calorie restricted (CR) male F344xBN rats were obtained from the National Institute on Aging (NIA) rodent colony. Reduction of calorie intake began at 14 weeks of age starting with 10%, 25%, and finally 40% restriction at 17 weeks until the end of the experiment. Animals were maintained in our facility for approximately one month prior to tissue collection. All animals had free access to water and AL fed rats had free access to NIH-31 pellets. For CR animals, the dietary regimen of 40% restriction was maintained, with food delivered at 17:00 h each evening. Animals were assessed on a weekly basis for signs of overt health problems including marked weight loss. For gene arrays, middle aged (MA) and old (O) animals (18 and 28 months (mo) of age, respectively) were employed. In general, biological variability increases with advanced age (Busuttil et al., 2007; Foster and Kumar, 2007); therefore, the number of animals in the older groups was increased in order to increase the power of the study. The groups consisted of AL-MA ($n = 3$), AL-O ($n = 6$), and CR-O ($n = 6$). Due to the limited supply of CR rats at specific ages, western blots were performed for 8 mo AL, 38 mo AL and 38 mo CR animals ($n = 3$ per group). Ubiquitin-like immunofluorescence was examined in the brains of an 18 mo AL, 38 mo AL, and 38 mo CR rat.

2.2. RNA isolation and gene chips

On the day of tissue collection, animals were killed using a guillotine. Brains were quickly removed and placed on an ice-cold Petri dish. Brains were then bisected, making a dorsal to ventral incision along the midline such that the two hemispheres were separated. The neocortex of each hemisphere was then resected in order to expose and remove the hippocampus using forceps and a spatula and 2–3 tissue blocks of the dorsal hippocampus were cut parallel to the alvear fibers (~1 mm thick) using a razor blade. The blocks were laid flat and the subiculum was removed. An incision was made from the CA3–CA1 border to the end of the upper and lower blades of the dentate gyrus (DG) in order to isolate the CA3 region, and an incision through the hippocampal fissure was used to separate the DG and CA1 regions. Tissue from each region was placed into separate tubes and immediately snap-frozen in liquid nitrogen. Tissue samples from three regions of the hippocampus (CA1, CA3, DG) were removed from storage at −80 °C and homogenized for 30 s in 600 μL of RLT buffer using a Rotor–stator homogenizer. Following centrifugation for 3 min at maximum speed the supernatant was transferred to a new tube and an equal volume of 70% ethanol was added, the solution was then applied to a Qiagen RNeasy mini column and isolated according to the manufacturer's protocol. Purified RNA was labeled and hybridized to RAE 230 V2.0 gene chips by the NIH core facility. The chips were scanned with an Affymtrix GeneChip Scanner 3000, and the raw data, publicly available through the NIH neuroscience microarray consortium (http://arrayconsortium.tgen.org/np2/viewProject.do?action=viewProject&projectId=522821) and the NCBI gene expression omnibus Accession No. GSE21681, were processed with Affymetrix GCOS software.

2.3. Data analysis

For the 15 animals (AL-MA = 3, AL-O = 6, and CR-O = 6), one chip was hybridized per region (CA1, CA3, DG) per animal, resulting in 45 arrays. Array outliers were identified by dChip and performance in leave-one-out-cross validation studies; two arrays (one CR-O for CA1 and one CR-O for CA3) were removed from the study due to poor hybridization. Probe set filtering was performed according to our previously published work (Aenlle and Foster, 2010; Aenlle et al., 2009; Blalock et al., 2003). Microarray Suite (Affymetrix) was used to determine whether a particular probe was reliably detectable (presence/absence calls). The number of present calls for each probe set was determined across all chips and the probe set was removed if fewer than 80% of the chips exhibited a present call for the probe. Normalization and computation of gene expression values were performed using the perfect-match-only method by inputting data (.cel files) into dChip (Li and Wong, 2001). Unsupervised hierarchical cluster analyses were performed with probe sets that exhibited hybridization signal intensities with a coefficient of variation of greater than 0.5 identified using algorithms implemented in dChip. Statistical algorithms implemented in BRB array tools (version 3.5.0-beta 1, developed by Richard Simon, Amy Peng Lam, Supriya Menezes, NCI and EMMES Corp.) were used to identify probe sets whose hybridization signal intensity values differed between experimental groups (alpha level set at $p < 0.001$) and calculate the false discovery rate (FDR). The ability of significant genes to distinguish between treatment groups was assessed by leave-one-out-cross-validation studies. The ability of gene expression classifiers to correctly predict the class label of the array left out of the analysis was estimated using Monte Carlo simulations. Functional pathways associated with pools of significantly altered probe sets were identified using Ingenuity Pathway Analysis (IPA, Ingenuity Systems, Redwood City, CA). Fischer's exact test was used to calculate a p-value determining the probability that each pathway assigned to that data set is due to chance alone. In addition, BRB array tools was used to calculate the largest observed/expected ratios in specific gene ontology (GO) categories for cellular component, molecular function, and biological process that were associated with the significantly altered probe sets.

2.4. Western blot analyses

For total protein analyses, the CA1, CA3, or DG regions were dissected from hippocampi. Samples were homogenized with an ultrasonic cell disrupter (Misonix Incorporated; Farmingdale, NY) in SDS sample buffer (62.5 mM Tris, pH 6.8, 10% glycerol, 3% SDS) supplemented with complete protease inhibitor (Roche, Indianapolis, IN). A BCA kit (Pierce, Rockford, IL) was used to determine the protein concentration of the supernatant. Samples were fractionated by SDS-gel electrophoresis using Ready Precast Gradient 8–16% SDS-polyacrylamide gels with 20 μg protein loaded per well. Following fractionation, proteins were transferred to a nitrocellulose (0.45 μm pore size) or a PVDF (for pUbi) (Bio-Rad, Hercules, CA) membrane overnight at 4 °C and a constant voltage of 35 V. Blots were blocked for one hour with Tris-buffered saline containing 0.05% Tween (TBST) and 5% nonfat dry milk. After blocking, the blots were incubated overnight at 4 °C with the following primary antibodies: Ubiquitin (rabbit polyclonal; Dako, Carpinteria, CA); UBE2J1 (mouse monoclonal; Santa Cruz Biotechnology Inc, Santa Cruz, CA); HSP90 (rabbit polyclonal; Cell signaling, Danvers, MA); HSP70 (rabbit polyclonal; Stressgen, Ann Arbor, MI); HSP40 (rabbit polyclonal; Stressgen); HSP27 (goat polyclonal; Santa Cruz); Glyceraldehyde-3-phosphate dehydrogenase (GAPDH) (mouse monoclonal; EnCor Biotechnology, Alachua, FL). After incubation with anti-rabbit, anti-mouse (Cell signaling), or anti-goat horseradish peroxidase conjugated secondary antibodies (Sigma-Aldrich, St. Louis, MO), membranes were reacted with an enhanced chemiluminescent substrate (Perkin Elmer Life Sciences; Boston, MA). A GS-710 densitometer (Bio-Rad Laboratories) was then used to digitally image the films. Densitometric analyses were made using the ImageJ 1.42q computer program (Wayne Rasband, National Institutes of Health, USA). Since many endogenous control markers are affected by aging and caloric restriction, fold change values for these experimental variables were calculated by normalizing to the 8 mo AL control signal, however, GAPDH staining is provided in order to illustrate consistency of gel-loading. Films were formatted for printing using Adobe Photoshop. Significant changes in western blot densitometry between groups were determined by two-tailed student's t-tests.

2.5. Immunolabeling

For examination of ubiquitin-like immunofluorescence, the brains were bisected through the central sulcus and half of each brain was immediately frozen in liquid nitrogen. Coronal cryosections (5 μm thickness) were collected on Superfrost Plus glass slides (Fisher), and allowed to air dry for 1 h. Slides were then fixed in 4% paraformaldehyde in PBS for 15 min., permeabilized in ice-cold methanol for 5 min. at −20° C, rinsed with PBS and blocked in 20% goat serum in PBS plus 0.05% Triton X-100 for 1 hour at room temperature. Sections were incubated with the indicated primary antibodies overnight at 4 °C. Bound anti-ubiquitin antibodies were detected with Alexa Fluor 594 (Molecular Probes, Eugene, OR). Hoechst dye (Molecular Probes) was included in the secondary antibody solution to visualize nuclei. Slides were mounted with cover slips using Antifade Kit (Molecular Probes). Samples were imaged with a Spot camera attached to a Nikon Eclipse E800 microscope (Melville, NY) and were formatted for printing by using Adobe Photoshop software.

3. Results

3.1. Gene expression changes induced by aging and CR indicate region-specific sensitivity

Filtering the data resulted in 24,244 probes sets in which at least 80% of the arrays exhibited a present call. To examine generalized gene expression changes throughout the hippocampus with age, we included arrays across all three regions from AL-MA and AL-O animals. This regionally combined analysis revealed 4821 probe sets (FDR = 0.005) that were altered by aging. In addition, we determine the number of probes that exhibited altered expression within each region of the hippocampus. The number of probe sets that change with age ($p < 0.001$) more than double between the DG (898, FDR = 0.027) and CA1 regions (2141, FDR = 0.01) (Fig. 1), suggesting that region CA1 may be more susceptible to the effects of age. The effect of age on region CA3 (1461, FDR = 0.016) was intermediate as compared with the other two.

To determine gene expression changes due to lifelong CR, arrays were analyzed for probe sets that differed between CR-O and AL-O

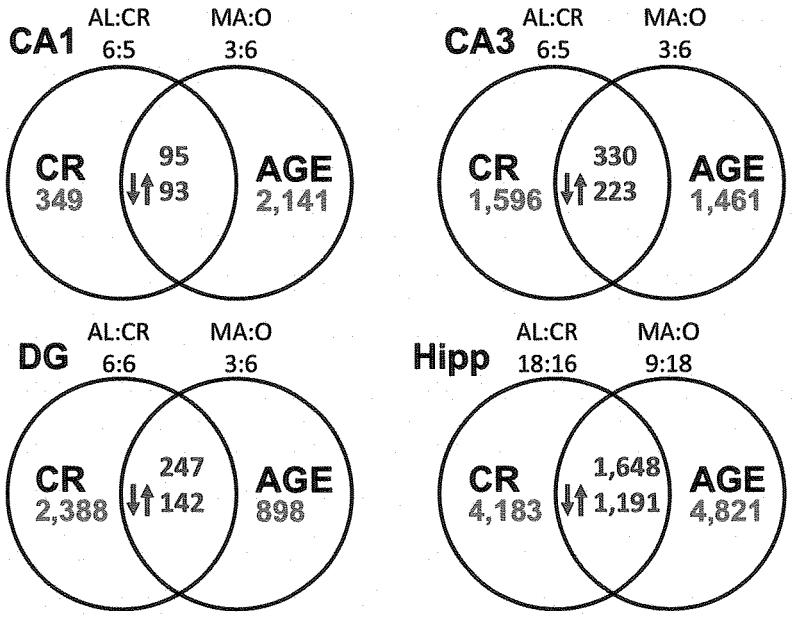

Fig. 1. Number of probe sets altered by CR in the hippocampus of rats aged 28 mo (AL-O versus CR-O) and across age (18 and 28 mo) in ad libitum fed rats (AL-MA versus AL-O). Numbers in the main panels (red) indicate the total probe sets altered by aging and CR in regions CA1 (upper left) and CA3 (upper right), the DG (lower left), and across all regions (Hipp, lower right). Numbers in the overlapping areas (green) indicate the number of probe sets altered by both treatments (i.e. overlapping probe sets). Arrows indicate the number of overlapping probe sets whose expression level was oppositely affected by age and CR. Above each circle is an indication of the number of arrays in each group involved in the analysis.

groups. When all regions were combined, 4183 probe sets (FDR = 0.006) were significantly ($p < 0.001$) altered by CR in the older animals (Fig. 1). Interestingly, while the number of probe sets that changed with age increased between the DG and CA1, CR effects were in the opposite direction. Specifically, CR induced a > 6-fold increase in the number of altered probe sets in the DG (2388, FDR = 0.01) relative to CA1 (349, FDR = 0.07) (Fig. 1). The number of probes altered across the diet conditions for CA3 was 1596 (FDR = 0.015). Thus, age differences, as determined by the number of altered genes, appear to be more pronounced in region CA1, whereas CR effects are magnified in the DG.

3.2. Pathway regulation during aging and CR

Table 1 illustrates the top GO categories for cellular component (CC), molecular function (MF), and biological process (BP), that exhibited gene enrichment in the hippocampus. In general, aging was associated with enrichment of genes in categories linked to energy homeostasis (glucose homeostasis, creatine kinase activity), oxidative stress (superoxide activity, heme oxidation, aconitate hydratase activity), and response to stress (DNA damage, MHC class II protein complex). CR was associated with an enrichment of genes for several metabolic pathways.

In order to examine age and CR influences on signaling pathways, significantly altered gene expression within each region and for the regionally combined analysis was submitted to IPA (Table 2). The results from the regionally combined analysis confirmed previous work indicating that, throughout the hippocampus, aging was associated with altered expression of genes related to inflammation, mitochondrial dysfunction, stress, and neurodegenerative diseases (Aenlle et al., 2009; Blalock et al., 2003; Prolla, 2002; Weindruch et al., 2002). CR was associated with a downregulation of inflammatory marker genes (such as antigen presentation genes) (Morgan et al., 2007; Wu et al., 2008). In addition, aging was associated with an upregulation of genes involved with the protein ubiquitination pathway, while CR resulted in a mixture of up and downregulated genes for this protein quality control mechanism.

Due to the large number of significant genes for age or CR when examined across all regions, these data sets were separated according to genes that were up or downregulated and these selective data sets were submitted to IPA. In order to limit the number of pathways examined, we selected a cut off of $p < 0.001$ for gene enrichment in the signaling pathways. The analysis indicated no significant gene clustering in pathways for downregulated genes associated with age or CR; although nucleotide excision repair and protein ubiquitination pathways for CR approached the cut off ($p = 0.0025$). An examination of upregulated genes during aging confirmed involvement of signaling for Huntington's disease, amyloid processing, mitochondrial dysfunction, NRF2-mediated oxidative stress, and protein ubiquitination. In addition, the analysis indicated gene enrichment in a number of pathways, which was likely due to the common elements in Gβγ signaling rather that increased activity in the specific signaling processes. In this case, the signaling pathways for α-adrenergic receptor, androgen receptor, tubby, FAK, and breast cancer regulation by stathmin1 exhibited an enrichment of upregulated genes. However, notably absent from these pathways was a change in the expression of the adrenergic or androgen receptor, tubby, FAK, or stathmin1. Similarly, an enrichment of upregulated genes was observed for pathways linked to the antigen presentation pathway. Gene enrichment was observed for NFAT in regulation of the immune response, IL-8, and chemokine receptor 5 (CCR5) signaling in macrophages, although, NFAT, the IL-8 receptor and CCR5 were not altered. For CR, selective analysis limited to upregulated genes confirmed an enrichment of long-term potentiation (LTP) signaling. Other pathways with gene enrichment contained elements of LTP signaling including Rac, breast cancer regulation by stathmin1, IL-3, and formyl-Met-Leu-Phe (fMLP) signaling in neutrophils. Again, while many of the elements were increased, major determinants of the pathway (rac, stathmin1, IL-3

Table 1
Results of GO analysis for age and CR.

Effect of Age				Effect of CR			
GO category	GO ID	GO Term	Ratio	GO category	GO ID	GO Term	Ratio
CA1							
CC	42613	MHC class II protein complex	4.46	CC	5891	voltage-gated calcium channel complex	6.76
MF	16527	brain-specific angiogenesis inhibitor activity	7.14	MF	8191	metalloendopeptidase inhibitor activity	19.67
BP	45582	positive regulation of T cell differentiation	4.45	BP	19233	sensory perception of pain	7.07
BP	30330	DNA damage response, signal transduction by p53 class mediator	4.45				
CA3							
CC	30864	cortical actin cytoskeleton	3.24	CC	35253	ciliary rootlet	6.99
MF	16527	brain-specific angiogenesis inhibitor activity	10.35	MF	5093	Rab GDP-dissociation inhibitor activity	9.9
MF	4757	sepiapterin reductase activity	10.35	MF	4740	[pyruvate dehydrogenase (lipoamide)] kinase activity	9.9
BP	48145	regulation of fibroblast proliferation	4.96	BP	6613	cotranslational protein targeting to membrane	4.96
DG							
CC	5802	trans-Golgi network	3.88	CC	35253	ciliary rootlet	4.03
MF	4757	sepiapterin reductase activity	15.99	MF	4965	GABA-B receptor activity	7.23
BP	15802	basic amino acid transport	8.22	MF	4740	[pyruvate dehydrogenase (lipoamide)] kinase activity	7.23
				BP	6596	polyamine biosynthetic process	4.95
Hippocampus							
CC	42613	MHC class II protein complex	3.34	CC	35253	ciliary rootlet	3.07
CC	30669	clathrin-coated endocytic vesicle membrane	3.34	MF	4965	GABA-B receptor activity	4.32
CC	30666	endocytic vesicle membrane	3.34	MF	4658	propionyl-CoA carboxylase activity	4.32
CC	30128	clathrin coat of endocytic vesicle	3.34	MF	4133	glycogen debranching enzyme activity	4.32
CC	30122	AP-2 adaptor complex	3.34	MF	4069	aspartate transaminase activity	4.32
CC	5666	DNA-directed RNA polymerase III complex	3.34	BP	6573	valine metabolic process	4.51
MF	16783	sulfurtransferase activity	3.35				
MF	16527	brain-specific angiogenesis inhibitor activity	3.35				
MF	8526	phosphatidylinositol transporter activity	3.35				
MF	4965	GABA-B receptor activity	3.35				
MF	4757	sepiapterin reductase activity	3.35				
MF	4558	alpha-glucosidase activity	3.35				
MF	4430	1-phosphatidylinositol 4-kinase activity	3.35				
MF	4392	heme oxygenase (decyclizing) activity	3.35				
MF	4111	creatine kinase activity	3.35				
MF	3994	aconitate hydratase activity	3.35				
BP	19430	removal of superoxide radicals	3.53				
BP	6788	heme oxidation	3.53				
BP	1678	cell glucose homeostasis	3.53				
BP	389	nuclear mRNA 3'-splice site recognition	3.53				

For each category; cellular component (CC), molecular function (MF), and biological process (BP), the gene ontology groups with the largest observed/expected ratio (Ratio) are identified according to the GO ID and term.

and fMLP receptors) were not increased. Finally, enrichment was observed for clathrin-mediated endocytosis.

Regional differences associated with aging were observed in the regulation of genes for pathways related to neuroinflammation, cell survival, oxidative phosphorylation, mitochondrial dysfunction, and protein ubiquitination pathways. An age-related increase in genes for antigen presentation and IL-4 signaling was evident only in region CA1 suggesting that CA1 may be more sensitive to the effects of age, at least with regard to processes that increase the expression of genes related to immune responses (Wang et al., 2009).

Similarly, regional specificity was observed for CR influences, such that regions CA1 and CA3 exhibited altered LTP signaling; however, no gene changes were found to be common between the two regions. Several kinases were upregulated in CR animals including calcium/calmodulin-dependent protein kinase IV (CAMK4) in the CA1 region and cAMP dependent protein kinase (PKA) and mitogen-activated protein kinase kinase 1 (MAP2K1) in CA3; protein kinase C gamma and protein kinase C beta increased in CA3 and CA1, respectively. Similarly, calcium/calmodulin dependent protein kinase II (CaMKII) alpha was upregulated in CA3 and CaMKII gamma was upregulated in CA1. In region CA3, the catalytic and regulatory subunits for the phosphatase calcineurin (PPP3CA, PPP3CB), were down and upregulated, respectively. In the CA1 region, alpha-amino-3-hydroxy-5-methyl-4-isoxazole propionate selective glutamate receptor (GRIA2) receptor was upregulated and the NMDA receptor associated protein 1 (GRINA) increased in CA3. The results are consistent with research indicating that CR can improve synaptic plasticity in the hippocampus and suggest the mechanism varies between regions.

Table 3 illustrates the directional changes in genes that were altered in at least two of the three regions for the IGF-1, PI3K/AKT, P53, apoptosis, oxidative phosphorylation, mitochondrial dysfunction, and protein ubiquitination pathways. Several pathways share common molecular members. In some cases, these molecules were similarly influenced across regions during aging; however, notable differences were observed for CR influences.

3.3. Apoptosis and cell survival pathways

Pathways pertinent to apoptosis and viability or cell survival, which share several common molecular members, were found to be altered by aging including IGF-1, PI3K/AKT, P53, and apoptosis signaling (Table 3). In general, aging increased signaling molecules for apoptosis. Gene enrichment was observed for the P53 pathway

Table 2
Pathways altered by caloric restriction or aging in the hippocampus.

Aging				Caloric Restriction			
Pathway	P	Ratio	FC	Pathway	P	Ratio	FC
CA1							
Estrogen Receptor Signaling	0.000567	0.178	+18, −3	Synaptic Long Term Potentiation	0.00635	0.054	+5, −1
NRF2-mediated Oxidative Stress Response	0.000586	0.167	+24, −6	Neuregulin Signaling	0.00927	0.055	+2, −3
Huntington's Disease Signaling	0.000994	0.147	+29, −5	Hepatic Fibrosis/Hepatic Stellate Cell Activation	0.0105	0.046	+4, −2
IL-4 Signaling	0.00322	0.191	+11, −2	Hypoxia Signaling in the Cardiovascular System	0.0157	0.056	+0, −4
Apoptosis Signaling	0.00359	0.184	+13, −3	Notch Signaling	0.018	0.073	+1, −2
Insositol Phosphate Metabolism	0.0137	0.121	+6, −5				
Antigen presentation	0.0169	0.154	+6, −0				
IGF-1 Signaling	0.0204	0.163	+12, −3				
p53 Signaling	0.022	0.149	+12, −1				
CA3							
p53 Signaling	0.00446	0.138	+11, −1	Protein Ubiquitination Pathway	0.00108	0.119	+16, −8
Hypoxia Signaling in the Cardiovascular System	0.0048	0.155	+10, −1	IGF-1 Signaling	0.00116	0.163	+12, −3
Parkinson's signaling	0.0115	0.235	+4, −0	ERK/MAPK Signaling	0.00402	0.122	+16, −6
PI3K/AKT signaling	0.0168	0.113	+10, −4	Hypoxia Signaling in the Cardiovascular System	0.00494	0.155	+8, −3
Biosynthesis of Steroids	0.0309	0.039	+2, −3	Synaptic Long Term Potentiation	0.0109	0.135	+12, −3
Protein Ubiquitinatioin	0.0326	0.094	+17, −2	Cardiac β^2-adrenergic Signaling	0.012	0.115	+13, −2
Amyotrophic Lateral Sclerosis Signaling	0.0389	0.107	+8, −3	Insulin Receptor Signaling	0.0138	0.12	+14, −2
				Oxidative Phosphorylation	0.0155	0.095	+9, −6
				Chemokine Signaling	0.0166	0.147	+9, −2
				Glucocorticoid Receptor Signaling	0.017	0.095	+14, −2
				PI3K/AKT Signaling	0.0186	0.113	+12, −2
DG							
PI3K/AKT signaling	0.000293	0.113	+10, −4	Oxidative Phosphorylation	0.00389	0.133	+14, −7
Oxidative Phosphorylation	0.0019	0.082	+12, −1	IL-2 Signaling	0.0108	0.208	+8, −3
Mitochondrial Dysfunction	0.00251	0.073	+10, −2	PTEN Signaling	0.0154	0.163	+7, −8
Ubiquinone Biosynthesis	0.00416	0.067	+7, −3	Estrogen Receptor Signaling	0.0203	0.144	+8, −9
Ceramide Signaling	0.0115	0.101	+4, −4	EGF Signaling	0.0214	0.191	+6, −3
P53 Signaling	0.0165	0.092	+7, −1	Nucleotide Excision Repair Pathway	0.0254	0.2	+1, −6
				GM-CSF Signaling	0.0339	0.177	+6, −5
Hippocampus							
Antigen Presentation Pathway	0.0000729	0.308	+12, −0	Protein Ubiquitination Pathway	0.0018	0.218	+18, −26
Mitochondrial Dysfunction	0.000192	0.2	+26, −7	GM-CSF Signaling	0.008	0.29	+11, −7
NRF2-mediated Oxidative Stress Response	0.00157	0.244	+38, −6	Nucleotide Excision Repair Pathway	0.0205	0.286	+2, −8
Amyloid Processing	0.002	0.346	+15, −3	Synaptic Long Term Potentiation	0.021	0.243	+19, −8
Integrin Signaling	0.00499	0.24	+34, −12	Antigen Presentation Pathway	0.066	0.179	+1, −6
Huntington's Disease Signaling	0.0063	0.211	+42, −7				
Ubiquinone Biosynthesis	0.00755	0.144	+13, −2				
Protein Ubiquitination Pathway	0.00937	0.208	+32, −10				

Pathways significantly altered (p) by caloric restriction or aging, the ratio of significantly altered pathway genes to total pathway genes members, and the number of genes in the corresponding pathway that were upregulated (+FC) or downregulated (−FC).

in each region (Table 2) and several apoptosis promoting molecules exhibited increased expression in all three regions including p53, BAX, and ACIN1 (Table 3). Differences in expression, particularly between CA1 and the DG were also observed (Table 3), with CA1 exhibiting increased expression of additional p53/apoptosis signaling regulators (BAI1, CASP9, IHPK2, JUN, SFN). In the case of cell survival pathways, aging was associated with gene enrichment for the PI3K/AKT signaling pathway in CA3 and the DG and for IGF-1 signaling in CA1 (Table 2). In addition, AKT, which has anti-apoptotic actions, was increased in all regions (Table 3).

CR influenced cell survival pathways, particularly in region CA3 and the DG. As such, gene enrichment reached significance in region CA3 for IGF-1, insulin, PI3K/AKT, and ERK/MAPK signaling (Table 2). CR reversed an age-related increased expression of the gene encoding the pro-apoptotic molecule, BAX, and increased expression of anti-apoptosis molecule BIRC2, in area CA3 and the DG (Table 3). Interestingly, the expression of genes in these apoptotic and cell survival pathways exhibited minimal CR effects in region CA1 (Table 3). Thus, CR appears to promote cell survival signaling, particularly in regions CA3, while cell survival pathways in region CA1 may be less responsive to CR.

3.4. Mitochondria and oxidative phosphorylation

Aging was associated with an enrichment of genes related to mitochondrial dysfunction across the hippocampus when all regions were combined and specifically in the DG when individual regions were considered (Table 2). The mitochondrial dysfunction pathway shares common molecules with oxidative phosphorylation, and oxidative phosphorylation was influenced by CR in region CA3 and the DG (Table 2). In examining genes that were common across regions, it is clear that the three regions were influenced in the same direction during aging, and that the CA1 region was less responsive to CR (Table 3).

Table 3
Regionally distinct treatment effects.

Molecule	Age Effect			Diet Effect			Pathways			
	CA1	CA3	DG	CA1	CA3	DG	IGF	AKT	P53	Apoptosis
	IGF1-PI3K/AKT and P53-Apoptosis									
ACIN1	1.62	1.53	1.54	NS	NS	NS				X
AKT1	1.61	1.53	1.46	NS	1.32	1.33	X	X	X	
BAI1	1.39	1.61	NS	NS	1.33	1.4			X	
BAX	1.71	1.81	1.93	NS	−1.47	−1.44			X	X
BIRC2	−1.36	NS	NS	NS	1.29	1.26				X
CAPNS1	1.42	NS	1.41	NS	NS	NS				X
CASP9	1.24	1.22	NS	NS	NS	NS	X			X
CTNNB1	NS	1.27	1.24	NS	−1.28	−1.28		X	X	
GRB2	−3.17	−3.45	−2.09	NS	NS	NS	X	X		
IGF1R	NS	NS	NS	1.73	1.68	1.39	X			
IHPK2	1.87	1.61	NS	NS	1.35	1.5			X	
JUN	1.77	1.7	NS	NS	NS	NS	X		X	
NFKBIB	1.55	1.38	1.45	NS	NS	NS		X		X
P53	2.11	2.02	1.89	NS	NS	NS		X	X	X
PIK3CA	NS	NS	NS	NS	1.17	−1.55	X	X	X	
PIK3R2	1.98	−3.13	−3.16	NS	2.75	3.88	X	X	X	
PPKAR1B	NS	NS	NS	NS	1.14	1.23	X			
PRKACB	−4.41	−3.35	−2.65	NS	2.66	2.89	X			
SFN	1.65	1.75	NS	NS	NS	1.32	X	X	X	
YWHAB	1.47	1.46	1.43	NS	NS	NS	X	X		
	Oxidative Phosphorylation and Mitochondrial Dysfunction						OX-Phos		Myto-Dys	
ATP5D	1.26	1.23	1.21	NS	NS	NS	X			
ATP6V0A1	1.59	1.49	NS	NS	1.37	1.5	X			
ATP6V0A2	1.37	NS	1.36	NS	NS	NS	X			
ATP6V0B	NS	NS	NS	NS	6.38	1.24	X			
ATP6V0D1	NS	NS	NS	NS	1.15	1.23	X			
ATP6V1B2	NS	NS	NS	NS	1.17	1.22	X			
ATP6V1G2	NS	NS	NS	NS	1.12	1.18	X			
CASP9	1.24	1.22	NS	NS	NS	NS			X	
COX5B	NS	1.16	1.14	NS	NS	NS	X		X	
COX7B	NS	1.25	1.31	NS	−1.38	−1.36	X		X	
GPX4	1.21	NS	1.23	NS	NS	NS			X	
HCG25731	NS	NS	NS	NS	−1.09	1.12	X			
IHPK2	1.87	1.61	NS	NS	1.35	1.5	X			
MAP2K4	−1.24	NS	−1.27	NS	NS	NS			X	
NDUFA7	−2.3	−1.78	NS	NS	1.9	2.87	X		X	
NDUFS8	1.38	1.35	1.39	NS	NS	NS	X		X	
NDUFV3	1.53	1.58	1.44	NS	−1.26	−1.59	X		X	
UGCRQ	1.32	1.28	NS	NS	NS	NS	X			
UQCRC1	NS	1.15	1.17	NS	NS	1.14	X		X	
	Protein Ubiquitination									
ANAPC2	1.36	1.38	1.44	NS	NS	NS				
ANAPC5	NS	1.15	1.13	NS	NS	NS				
BAG1	NS	1.38	1.27	NS	−1.34	−1.23				
BIRC2	−1.36	NS	NS	NS	1.29	1.26				
BTRC	1.67	1.72	1.75	NS	NS	NS				
FZR1	1.54	1.42	1.53	NS	NS	1.33				
PSMA3	NS	NS	NS	NS	−1.19	−1.26				
PSMB5	NS	1.17	1.21	NS	NS	NS				
PSMD14	NS	NS	NS	NS	1.64	−1.34				
STUB1	NS	NS	1.17	NS	1.14	1.24				
TAP2	5.51	4.83	NS	NS	NS	−3.11				
THOP1	1.93	1.88	1.68	NS	NS	NS				
UBA1	1.37	1.26	NS	NS	1.2	1.4				
UBE2D2	NS	1.38	1.57	NS	2.2	1.4				
UBE2J1	1.31	1.32	NS	NS	NS	NS				
UBE2Q1	NS	1.17	NS	−1.37	−1.22	NS				
UBE2S	1.67	1.94	1.95	NS	NS	NS				
UBE2V1	NS	NS	NS	NS	1.1	1.18				
UCHL3	NS	NS	NS	NS	−1.16	−1.15				
USO1	−1.35	NS	−1.25	NS	NS	NS				
USP11	NS	NS	NS	NS	1.17	1.29				
USP22	NS	NS	NS	NS	1.73	1.53				
USP5	1.27	1.21	NS	NS	1.28	1.33				

Numbers represent significant fold change values; those that were not significant (NS) are indicated. Functional categories with multiple pathways indicate molecular inclusion (X).

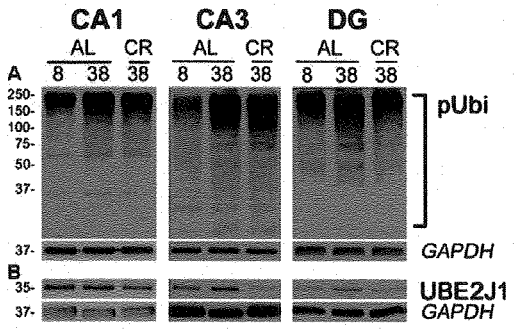

Fig. 2. Polyubiquitination of proteins in the hippocampus. (A) Western blot analysis of total protein (20 μg/lane) from CA1, CA3, and DG regions of the hippocampi of 8 and 38 mo old rats fed AL and 38 mo old rats on 40% CR diet ($n = 3$ per group) probed with an anti-ubiquitin antibody. Slow migrating poly-ubiquitinated (pUbi) protein substrates are marked by a square bracket. (B) Staining against the ubiquitin ligase family member (UBE2J1). GAPDH is shown as a protein loading control. Molecular mass is kDA, on the left.

3.5. Protein ubiquitination

Table 2 indicates that the enrichment of genes for protein ubiquitination associated with aging and CR, which was observed for analysis across all regions, was also observed for region CA3. Furthermore, both conditions were mainly associated with an increase in expression, with 17 genes increased during aging and 16 genes increased in CA3 of older CR animals relative to age matched AL animals. Closer examination of the genes that were altered in at least two of the three regions (Table 3) indicates that aging is associated with an increase in the expression of genes involved in the degradation of antigens (PSMB5, TAP2, THOP1), and genes for proteins that mediate the covalent attachment of ubiquitin to other proteins (UBE2J1, UBE2Q1, UBE2S, BTRC), including those for the E3 ubiquitin ligase of the anaphase promoting complex (ANAPC2, ANAPC5, FZR1). In contrast, CR was associated with increased expression of deubiquitinating enzymes (PSMD14, USP11, USP22, USP5). Finally, age and CR effects were observed for proteins that mediate the interaction between chaperone activity and ubiquitination of misfolded proteins (BAG1, STUB1). Importantly, very few genes exhibited a shift in the opposite direction due to aging and CR, rather it appears that there is an increase in expression for ubiquitinating and deubiquitinating molecules, respectively.

To assess the function of the ubiquitin-proteosome pathway, we analyzed the degree of polyubiquitinated substrates, as well as the expression level of an ubiquitin-conjugating enzyme (UBE2J1) ($n = 3$ per group). In general, the level of polyubiquitinated proteins was increased with age and decreased in CR animals for each hippocampal region (Fig. 2). Densitometric quantification of western blots (Table 4) indicated that, across all regions of the hippocampus, there was a tendency for an increase in the expression of polyubiquitinated proteins (1.31 fold change, $p = 0.066$). In addition, the expression level of UBE2J1 was reduced in CR animals in all regions of the hippocampus (-1.83-fold change, $p < 0.005$) and this decrease was significant for region CA3 (38 mo AL vs 38 mo CR: -2.94-fold change, $p < 0.01$).

Consistent with an age-related increase in polyubiquitinated proteins, immunolabeling of hippocampal sections exhibited

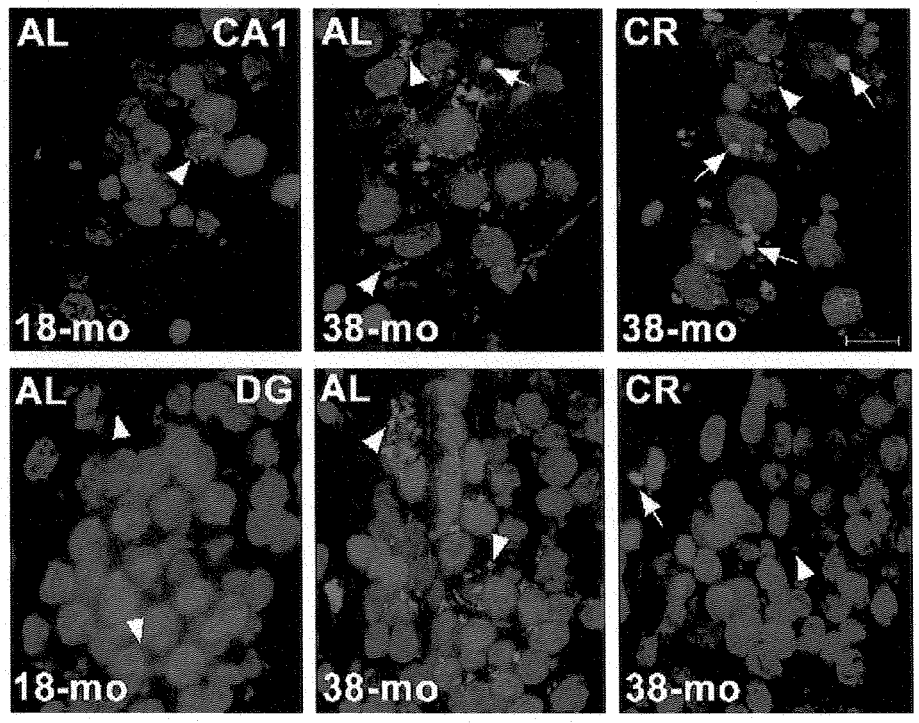

Fig. 3. Immunofluorescence showing ubiquitinated inclusions (red) in CA1 (top row, 60×) and DG (bottom row, 60×) regions for 18 mo AL (left column), 38 mo AL (center column) and 38 mo CR (right column). Nuclei were stained with a Hoechst (blue). There appears to be more ubiquitin staining in 38 AL compared to 18 AL and the ubiquitin was diffuse (arrow heads) and distributed throughout the cell body. In comparison, overall ubiquitin-like immunoreactivity appears reduced by CR and more focal, often limited to inclusions (arrows) adjacent to nuclei. The calibration bar is 10 μM.

Table 4
Western blot analysis of stress response and ubiquitination.

Antigen	CA1				CA3				DG				All			
	AGE		CR		AGE		CR		AGE		CR		AGE		CR	
	FC	P	FC	P	FC	P	FC	P	FC	P	FC	P	FC	P	FC	P
HSP90	1.21	NS	−1.95	0.089	1.23	NS	−1.64	0.098	1.21	NS	−1.76	0.066	1.22	NS	−1.77	0.001
HSP70	1.19	NS	−1.21	NS	−1.05	NS	−1.50	NS	−1.06	NS	−1.44	NS	1.03	NS	−1.35	NS
HSP40	1.15	NS	−1.15	NS	−1.04	NS	−1.42	NS	1.04	NS	−1.15	NS	1.05	NS	−1.22	NS
HSP27	27.03	0.003	1.15	NS	48.12	0.001	1.07	NS	12.66	0.036	−1.38	NS	29.28	0.001	1.05	NS
pUbi	1.24	NS	−1.13	NS	1.47	0.081	−1.01	NS	1.24	NS	1.04	NS	1.31	0.066	−1.03	NS
UBE2J	−1.04	NS	−1.55	NS	1.09	NS	−2.94	0.009	1.02	NS	−1.49	NS	1.02	NS	−1.83	0.005

The fold change for age represents comparisons between 8 mo-AL and 38 mo-AL rats. The fold change for CR represents comparisons between 38 mo-AL and 38 mo-CR rats. NS: not significant.

strong ubiquitin-like reactivity (red) in the hippocampus from a 38 mo AL relative to 18 mo AL animal (Fig. 3). In samples from the AL animal, the ubiquitin was diffuse and distributed throughout the cell body, likely reflecting cytosolic localization. In comparison, it appears that overall ubiquitin-like immunoreactivity was reduced by CR and was more focal, often limited to inclusions adjacent to nuclei (blue).

3.6. CR effects that directly oppose aging effects are associated with stress responses

In addition to compensatory effects of CR, we sought to determine whether CR can directly counteract age effects on specific genes and biological processes, therefore, we examined the genes that were significantly altered during aging and CR, and

Table 5
Pathways associated with genes oppositely affected by aging and CR.

Pathways	*p*-value	Molecules
CA1		
Hypoxia Signaling in the Cardiovascular System	0.027	NFKBIE (1.4, −1.2), UBE2L6 (1.7, −1.4)
CA3		
p53 Signaling	0.001	PRKDC (1.4, −1.3), PIK3R2 (−3.1, 2.8), BAX (1.8, −1.4), CTNNB1 (1.3, −1.3)
RAR Activation	0.010	PRKACB (−3.4, 2.7), NSD1 (1.5, −1.4), RDH10 (−1.2, 1.2), RDH11 (1.3, −1.2), PIK3R2 (−3.1, 2.8)
Oxidative Phosphorylation	0.016	COX7B (−1.3, 1.4), ATP5E (1.2, −1.2), NDUFV3 (1.6, −1.3), NDUFA7 (−1.8, 1.9), UQCRQ (1.3, −1.3)
Glucocorticoid Receptor Signaling	0.020	PRKACB (−3.4, 2.7), HSP90AB1 (−15.7, 2.5), BAG1 (1.4, −1.3), TAF5L (1.2, −1.2), PIK3R2 (−3.1, 2.8), POLR2I (1.4, −1.3)
N-Glycan Biosynthesis	0.023	MAN2A2 (1.5, −1.5), DPM2 (1.2, 1.2)
Mitochondrial Dysfunction	0.044	COX7B (−1.3, 1.4), NDUFV3 (1.6, −1.3), NDUFA7 (−1.8, 1.9)
DG		
p53 Signaling	0.002	PIK3R2 (−3.2, 3.9), BAX (1.9, −1.5), CTNNB1 (1.2, −1.3)
Glucocorticoid Receptor Signaling	0.010	PRKACB (−2.6, 2.9), HSP90AB1 (−10.7, 9.5), BAG1 (1.3, −1.2), POLR2J (1.3, −1.2), PIK3R2 (−3.2, 3.9)
Oxidative Phosphorylation	0.017	ATP7B (−2.1, 1.7), COX7B (1.3, −1.4), NDUFV3 (1.4, −1.3)
Nucleotide Excision Repair Pathway	0.024	XPC (−1.7, 2.5), POLR2J (1.3, −1.2)
Hippocampus		
Oxidative Phosphorylation	0.004	ATP5E (1.2, −1.1), ATP6V1B2 (−1.1, 1.1), COX15 (1.5, −1.4), COX5B (1.2, −1.2), COX6C (−1.5, 1.9), COX7B (1.3, −1.3), FAM63B (−3.4, 2.7), IP6K2 (−1.2, 1.1), NDUFA1 (1.1, −1.1), NDUFA12 (1.1, −1.1), NDUFA7 (−2.0, 1.9), NDUFB10 (1.3, −1.1), NDUFB4 (1.1, −1.1), NDUFS5 (1.2, −1.1), NDUFV3 (1.5, −1.4), UQCRQ (1.3, −1.2)
FcgRIIB Signaling in B Lymphocytes	0.007	BTK (2.1, −1.8), FCGR2B (1.9, −1.6), MAPK8 (−1.1, 1.2), MRAS (1.3, −1.3), PIK3CA (1.4, −1.4), PIK3R2 (−3.3, 2.4), SOS1 (−1.2, 1.3)
Antigen Presentation Pathway	0.010	B2M (1.3, −1.2), CANX (1.1, −1.1), HLA-DQA1 (4.2, −2.6), HLA-DRB1 (4.9, −3.1), TAP2 (4.7, −2.3)
Ubiquinone Biosynthesis	0.012	NDUFA1 (1.1, −1.1), NDUFA12 (1.1, −1.1), NDUFA7 (−2.0, 1.9), NDUFB10 (1.3, −1.1), NDUFB4 (1.1, −1.1), NDUFS5 (1.2, −1.1), NDUFV3 (1.5, −1.4), EDF1 (1.4, −1.1)
Mitochondrial Dysfunction	0.020	NDUFA1 (1.1, −1.1), NDUFA12 (1.1, −1.1), NDUFA7 (−2.0, 1.9), NDUFB10 (1.3, −1.1), NDUFB4 (1.1, −1.1), NDUFS5 (1.2, −1.1), NDUFV3 (1.5, −1.4), COX15 (1.5, −1.4), COX5B (1.2, −1.2), COX6C (−1.5, 1.9), COX7B (1.3, −1.3), MAPK8 (−1.1, 1.2), GPX7 (1.2, −1.2), PSEN1 (1.3, −1.3)
Dendritic Cell Maturation	0.022	B2M (1.3, −1.2), CANX (1.1, −1.1), FCGR2A (1.2, −1.2), FCGR2B (1.9, −1.6), HLA-DQA1 (4.2, −2.6), HLA-DRB1 (4.9, −3.1), IFNAR1 (1.5, −1.3), IRF8 (1.6, −1.6), MAPK8 (−1.1, 1.2), PIK3CA (1.4, −1.4), PIK3R2 (−3.3, 2.4), STAT2 (1.6, −1.2), TREM2 (1.9, −1.5), TYROBP (2.3, −1.4)
Lipid Antigen Presentation by CD1	0.023	B2M (1.3, −1.2), PDIA3 (1.3, −1.2)
Pyrimidine Metabolism	0.034	APOBEC1 (1.6, −1.6), DTYMK (−2.1, 2.1), NME3 (−1.1, 1.1), NME4 (1.3, −1.4), NME6 (1.4, −1.4), POLD4 (1.4, −1.5), POLR2F (1.3, −1.2), POLR2J (1.3, −1.2), POLR3D (1.2, −1.2), POLR3F (−1.5, 1.6), POLR3H (1.2, −1.2), POLRMT (−1.3, 1.5), RPUSD4 (1.2, −1.2), TRUB2 (1.3, −1.2)
NRF2-mediated Oxidative Stress Response	0.047	ACTA1 (1.3, −1.2), DNAJC17 (1.3, −1.3), DNAJC4 (1.4, −1.1), EIF2AK3 (1.2, −1.2), ERP29 (1.3, −1.2), FTL (1.3, −1.1), GSTA1 (1.2, −1.1), HMOX1 (1.4, −1.4), MAPK8 (−1.1, 1.2), MGST1 (1.3, −1.2), MRAS (1.3, −1.3), PIK3CA (1.4, −1.4), PIK3R2 (−3.3, 2.4), PPIB (1.2, −1.1), SCARB1 (1.3, −1.2), SLC35A2 (1.4, −1.2)

The fold change values for aging followed by CR are indicated in the brackets. Some molecules are associated with multiple pathways.

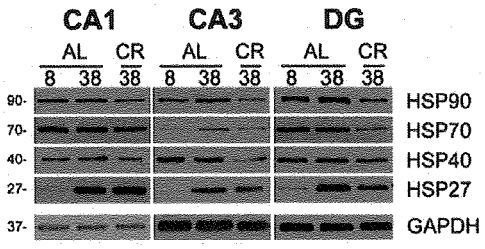

Fig. 4. Expression of heat shock proteins (HSP90, HSP70, HSP40, HSP27) in three regions of the hippocampus from 8 or 38 mo rats fed AL or CR diet ($n = 3$ per group). Note the increased expression of the small heat shock protein HSP27 in samples from the older animals. GAPDH is shown as a protein loading control. Molecular mass is kDa, on the left.

whose expression was oppositely affected by the two treatments. In the CA1, CA3, and DG regions of the hippocampus there were 95, 330, and 247 probe sets sensitive to both aging and CR, respectively (Fig. 1). A large majority of these overlapping probe sets were oppositely affected by aging and CR. Across all regions of the hippocampus, 1191 probe sets were significantly, and oppositely affected by aging and CR (Fig. 1). The probe sets that were oppositely affected by aging and CR, were submitted to IPA to determine enrichment in functional pathways. Table 5 provides the pathways and genes that exhibited significant and opposite alterations in each region. When all regions were considered together, pathways linked to immune responses were revealed including antigen presentation, signaling in B lymphocytes, and dendritic cell maturation. In addition, a significant enrichment of genes was observed for mitochondrial dysfunction and the metabolic pathway for oxidative phosphorylation. IPA analysis within individual regions indicated significant functional enrichment of genes for oxidative phosphorylation in region CA3 and the DG. In addition, we observed regional differences in several pathways involved in responding to stress, including hypoxia signaling in region CA1, p53, and glucocorticoid receptor signaling in CA3 and the DG, and nucleotide excision repair in the DG.

For assessment of the stress response, we measured the expression levels of several heat shock proteins (HSP) including HSP90, HSP70, HSP40, and HSP27 using western blots (Fig. 4). HSPs are induced in response to environmental and pathophysiological stressors, including aging (Kalmar and Greensmith, 2009; Morimoto, 1998). Previous work indicates that the level of HSP expression increases in the hippocampus during aging (Calabrese et al., 2004; Di Domenico et al., 2010; Ghi et al., 2009), and caloric restriction is associated with reduced constitutive HSP expression (for review see Kalmar and Greensmith, 2009). There was a tendency ($p < 0.1$) for age or CR effects within specific regions, which reached significance when examined across all regions, such that aging was associated with upregulation of HSP27 and HSP90 expression was decreased by CR (Table 4, Fig. 4).

4. Discussion

In the present study, we have investigated gene expression in the hippocampus, a brain region that is critical for learning and memory and highly sensitive to aging. Our study was designed to determine whether CR had similar effects in three closely linked regions of the hippocampus and whether CR would act on genes related to biological markers of aging in the hippocampus. Our data revealed several aspects of aging and CR which were common across regions and others that were unique to the CA1, CA3, and DG regions.

Before, considering the interpretation of the results, it is important to recognize the limitations of the study. First, age-related gene changes were examined between 18 and 28 mo and not all gene changes are monotonic with age (Blalock et al., 2003; Xu et al., 2007). It has been suggested that changes in expression from young to middle-age might reflect processes for compensation of increasing stress (Aenlle et al., 2009; Blalock et al., 2003). For example, increased transcription associated with oxidative stress begins in middle-age; however, expression of antioxidant defenses may decline with advanced age (Aenlle et al., 2009; Blalock et al., 2003; Colombrita et al., 2003; Rao et al., 1990; Tsay et al., 2000). Second, due to the limited availability of CR animals at specific ages, the protein assays involved different ages; 8–38 mo for western blots and 18 to 38 mo for immunocytochemistry. Despite the use of different ages, the results from the protein assays support the findings of the gene arrays, indicating aging is associated with increased cellular stress and CR altered protein ubiquitination.

While the western blots indicated changes in HSP expression, the specific HSP genes were not necessarily detected in our array studies. Other researchers have noted that the correlation of mRNA and protein is weak at best (Greenbaum et al., 2003; Gygi et al., 1999; Maier et al., 2009). For the current study, the difference is likely due to the strictness of the statistical filtering, which will limit the number of genes to be examined. Further, the polyclonal antibodies used in the protein expression analysis detect total protein and are not isoform or subunit specific. Finally, the transcription of HSP genes is negatively regulated by expression of heat shock proteins, such that gene expression will be balanced by the level of stress and the level of HSP expression (Morimoto, 1998). Thus, gene changes are likely to provide makers indicating which pathways are important to consider; however, protein expression and the function of the pathway will be determined by several factors including protein translation and degradation processes.

Consistent with previous microarray research on neural tissue, we observed that aging was associated with expression of markers for mitochondrial dysfunction, oxidative phosphorylation, inflammation and oxidative stress (Aenlle et al., 2009; Blalock et al., 2003; Erraji-Benchekroun et al., 2005; Prolla, 2002; Weindruch et al., 2002). While relatively few genes were influenced in the opposite direction by age and CR, the results indicate that CR can reduce some of the markers of aging. Across the three regions, CR had opposing effects for genes related to oxidative phosphorylation, mitochondrial dysfunction, antigen presentation, and the response to oxidative stress. In particular, across the hippocampus, upregulation and downregulation was observed for antigen presentation due to aging and CR, respectively. The gene expression changes for the regionally combined analysis likely reflect the well described increase in microglia activation during aging, which can be reversed by CR (Morgan et al., 2007; Wu et al., 2008). However, it should be pointed out that changes in the immune response may reflect downstream responses to aging mechanisms and compensatory processes mediated by CR.

Other pathways exhibited effects of age and CR which were not necessarily opposite; rather CR induced offsetting or compensatory changes to counterbalance aging. When all regions were combined, effects of age and CR were prominent for the protein ubiquitination pathway (Table 2); however, the two conditions did not have the opposite effect on gene expression (Tables 2 and 3). Rather, the microarray data indicated that, aging was associated an upregulation of genes in this pathway, particularly for ubiquitin conjugating enzymes. The increase in expression of genes for ubiquitin conjugating enzymes and diffuse ubiquitin-like immunoreactivity within hippocampal cells is consistent with the age-related increase in ubiquinated proteins observed in a number of tissues, and is thought to result from proteasome inhibition (Ding et al., 2006; Grune, 2000; Szweda et al., 2003; Yang et al., 2008). CR was marked by an overall downregulation of gene expression in the protein ubiquitination pathway, but an upregulation of

deubiquitinating component genes, suggesting processes for reducing the level ubiquitinated proteins. This idea is further supported by the observation that the CR-mediated increase in deubiquitinating component genes is associated with a reduction in the expression of the ubiquitin conjugating enzyme UBE2J and a decrease in diffuse ubiquitin-like immunoreactivity. The focal, often perinuclear ubiquitin-like immunoreactivity in CR samples likely indicates the sequestration and rerouting of undegraded proteasome substrates to an alternative pathway, namely autophagic-mediated lysosomal degradation (Fortun et al., 2007; Rangaraju et al., 2009).

There are several ways in which a change in protein ubiquitination might influence hippocampal function. For example, a decline in the ubiquitin/proteosome pathway could lead to ubiquitin positive inclusions that manifest in aged or neurodegenerative CNS tissue (Farout and Friguet, 2006; Fortun et al., 2005; Gray et al., 2003; Tydlacka et al., 2008). In turn, these inclusions may precede mitochondrial dysfunction, increased oxidative stress, and the activation of apoptotic pathways (Ding et al., 2006; Paz Gavilan et al., 2006). Finally, protein ubiquitination/proteasome activity has been linked to synaptic plasticity, which is central to learning and memory (Bingol and Schuman, 2006; Li et al., 2008; Patrick, 2006). Thus, aging and CR influences on ubiquitination/proteasome activity could modify the extent of hippocampal-dependent learning and impaired hippocampal LTP (Adams et al., 2008; Carter et al., 2009; Eckles-Smith et al., 2000; Hori et al., 1992). It will be important in future studies to examine the idea that disruption of the ubiquitin/proteosome pathway is a precursor for other markers of aging.

The strategy of combining array samples across regions increased the statistical power and facilitated the detection of genes that were commonly influenced across regions. Not surprising, this strategy accentuates the identification of gene changes that occur in a common cell type among these regions, namely glia. In contrast, analysis within each region can unmask region specific differences in the response or sensitivity to age or CR, which could have been obscured by potentially opposing changes in different regions of the hippocampus. Analysis within each region provided evidence that CA1 was more susceptible to the deleterious effects of aging and region CA3 and the DG were inclined to exhibit enhancement of cell survival signaling pathways associated with age and CR. An examination of the total number of genes influenced by age and CR indicated that more genes were influenced by age in CA1 and the DG exhibited a greater number of genes influenced by CR. Similarly, pathway analysis indicated that region CA1 was particularly sensitive to enhancement of the antigen presentation pathway, oxidative stress, and apoptosis with age (Table 2). In contrast, regions CA3 and the DG exhibited differential expression of genes for PI3/AKT signaling during aging (Table 2). Furthermore, CR was able to reverse aging effects on glucocorticoid signaling in the DG and CA3 (Table 5). The results are consistent with the idea that markers of aging include activation of stress responses and suggest that regional differences in gene expression relate to susceptibility to different stressors. Thus, aging may interact with processes that increase the vulnerability of region CA1 to hypoxia/oxidative stress and mediate glucocorticoid effects specific to region CA3, as well as regional differences in survival pathways including enhanced activity of PI3K/AKT signaling in region CA3 and the DG (Abe et al., 2004; Jackson et al., 2009; Wang et al., 2009).

Cell survival and neurotrophic pathways contribute to CR mediated cell protection in young animals (Katare et al., 2009; Mattson et al., 2004). In the current study, regional differences in gene expression for neurotrophic and cell survival pathways associated with age and CR were noted. In region CA1, aging was associated with gene enrichment for estrogen receptor and IGF-1 signaling and CR was without apparent effect on neurotrophic signaling pathways in this region (Table 2). In contrast, CA3 exhibited CR induced gene expression changes in IGF-1, insulin receptor, PI3K/AKT and ERK/MAPK neurotrophic signaling pathways (Table 2). Again, regional differences in stress may underlie differences in the activation of neurotrophic signaling during aging. For example, expression of AKT was increased across all three regions during aging, with the largest increase in CA1. CR induced an additional, though smaller, increase in AKT expression in CA3 and the DG suggesting that AKT expression may reflect a response to stress associated with aging which overshadows CR effects. CR increased the expression of the IGF receptor (IGF1R) gene in all three regions; however, the CR-mediated reversals of age-related changes in PIK3R2 and PRKACB, which contribute to the IGF-1 signaling cascade, were observed for region CA3 and the DG. The results are consistent with regional differences related to the availability of neurotrophic/cell survival signaling mechanisms (Abe et al., 2004; Jackson et al., 2009) or differential responses to neurotrophic signals (Glasper et al., 2010; Lynch et al., 2001).

Finally, regional differences in CR effects may relate to functional differences between regions. The CA1 and CA3 regions exhibited CR effects on genes within the pathway for LTP. Synaptic plasticity impairments during aging are a common finding in the hippocampus (Foster, 1999, 2002, 2007) and CR is associated with improvements in LTP, although the mechanism for CR effects on LTP is unclear (Adams et al., 2008; Eckles-Smith et al., 2000; Hori et al., 1992). CR resulted in a generalized upregulation of protein kinases; however, no single gene was regulated in the same direction across the two regions. The lack of correspondence between specific genes may result from differences intrinsic to the two regions including the connections, forms of synaptic plasticity, and activity of signaling cascades (Jackson and Foster, 2009). PKC isoforms beta and gamma were differentially expressed in CA1 and CA3 in CR animals. These isoforms contribute to the induction of synaptic plasticity and the regional expression appears to correlate with different forms of synaptic plasticity (Hussain and Carpenter, 2005; Naik et al., 2000). CR resulted in an increase in CAMK4 and PKA in region CA1 and CA3, respectively. CAMK4 is required to initiate transcription for the maintenance of LTP in CA1 (Alzoubi and Alkadhi, 2007; Ho et al., 2000; Kasahara et al., 2001) and PKA in CA3 pyramidal cells contributes to LTP at mossy fiber-CA3 and CA3–CA1 synapses (Nie et al., 2007; Sivakumaran et al., 2009). Similarly, CAMKII alpha, which was increased in region CA3, contributes to synaptic function between CA3 afferent and efferent synapses (Hinds et al., 2003; Lu and Hawkins, 2006). The results indicate that CR enhanced expression of molecules for signaling cascades involved in the specific form of synaptic plasticity observed in each region.

Together the results signify that, across all hippocampal regions, aging is associated with accumulation of ubiquitinated proteins, mitochondrial dysfunction, oxidative stress, and neuroinflammation. Furthermore, these processes are reduced by CR. Gene array studies in younger animals have demonstrated differential gene expression in hippocampal subregions linked to differences in metabolic activity and functional differences in signal transduction, and synaptic plasticity (Greene et al., 2009; Lein et al., 2004). The current study adds to this idea by demonstrating region differences in response to aging and CR. Importantly, the regional response to age-related stressors or CR diverge across hippocampal subregions according to differences in vulnerability of each region to stressors associated with aging, and the availability of neurotrophic or cell survival signaling mechanisms. The results may help to explain regional differences in susceptibility to age-related neurodegenerative disease (Bao et al., 2009; Mattson et al., 1989). Finally, CR is associated with amelioration of age-related deficits in synaptic plasticity and improved memory. The current study indicates that CR, possibly in

combination with a reduction in age-related stressors, permits the expression of genes in signaling pathways which are critical to cellular function, including different forms of synaptic plasticity between hippocampal subregions.

Acknowledgements

This work was supported by NIH grants AG14979 and MH059891 and the Evelyn F. McKnight Brain Research Foundation.

Contributions: Zane Zeier was involved in the conceptual input, planning of the studies, data acquisition, all data analysis, and preparation of the first draft and final editing of the manuscript.

Irina Madorsky was involved in the data acquisition, and data analysis for the protein studies and final editing of the manuscript.

Ying Xu was involved in the acquisition, and preparation of RNA, and final editing of the manuscript.

William O. Ogle was involved in the planning of the studies, acquisition and preparation of RNA and final editing of the manuscript.

Lucia Notterpek was involved in the conceptual input, data analysis related to protein studies and final editing of the manuscript.

Thomas C. Foster was involved in the conceptual input, planning of the studies, all data analysis, and preparation of the first draft and final editing of the manuscript.

Appendix A. Supplementary data

Supplementary data associated with this article can be found, in the online version, at doi:10.1016/j.mad.2010.10.006.

References

Abe, T., Takagi, N., Nakano, M., Furuya, M., Takeo, S., 2004. Altered Bad localization and interaction between Bad and Bcl-xL in the hippocampus after transient global ischemia. Brain Res. 1009, 159–168.

Adams, M.M., Shi, L., Linville, M.C., Forbes, M.E., Long, A.B., Bennett, C., Newton, I.G., Carter, C.S., Sonntag, W.E., Riddle, D.R., Brunso-Bechtold, J.K., 2008. Caloric restriction and age affect synaptic proteins in hippocampal CA3 and spatial learning ability. Exp. Neurol. 211, 141–149.

Aenlle, K.K., Foster, T.C., 2010. Aging alters the expression of genes for neuroprotection and synaptic function following acute estradiol treatment. Hippocampus 20, 1047–1060.

Aenlle, K.K., Kumar, A., Cui, L., Jackson, T.C., Foster, T.C., 2009. Estrogen effects on cognition and hippocampal transcription in middle-aged mice. Neurobiol. Aging 30, 932–945.

Alzoubi, K.H., Alkadhi, K.A., 2007. A critical role of CREB in the impairment of late-phase LTP by adult onset hypothyroidism. Exp. Neurol. 203, 63–71.

Bao, X., Pal, R., Hascup, K.N., Wang, Y., Wang, W.T., Xu, W., Hui, D., Agbas, A., Wang, X., Michaelis, M.L., Choi, I.Y., Belousov, A.B., Gerhardt, G.A., Michaelis, E.K., 2009. Transgenic expression of Glud1 (glutamate dehydrogenase 1) in neurons: in vivo model of enhanced glutamate release, altered synaptic plasticity, and selective neuronal vulnerability. J. Neurosci. 29, 13929–13944.

Bingol, B., Schuman, E.M., 2006. Activity-dependent dynamics and sequestration of proteasomes in dendritic spines. Nature 441, 1144–1148.

Blalock, E.M., Chen, K.C., Sharrow, K., Herman, J.P., Porter, N.M., Foster, T.C., Landfield, P.W., 2003. Gene microarrays in hippocampal aging: statistical profiling identifies novel processes correlated with cognitive impairment. J. Neurosci. 23, 3807–3819.

Bruce-Keller, A.J., Umberger, G., McFall, R., Mattson, M.P., 1999. Food restriction reduces brain damage and improves behavioral outcome following excitotoxic and metabolic insults. Ann. Neurol. 45, 8–15.

Busuttil, R., Bahar, R., Vijg, J., 2007. Genome dynamics and transcriptional deregulation in aging. Neuroscience 145, 1341–1347.

Calabrese, V., Scapagnini, G., Ravagna, A., Colombrita, C., Spadaro, F., Butterfield, D.A., Giuffrida Stella, A.M., 2004. Increased expression of heat shock proteins in rat brain during aging: relationship with mitochondrial function and glutathione redox state. Mech. Ageing Dev. 125, 325–335.

Carter, C.S., Leeuwenburgh, C., Daniels, M., Foster, T.C., 2009. Influence of calorie restriction on measures of age-related cognitive decline: role of increased physical activity. J. Gerontol. A Biol. Sci. Med. Sci. 64, 850–859.

Colombrita, C., Calabrese, V., Stella, A.M., Mattei, F., Alkon, D.L., Scapagnini, G., 2003. Regional rat brain distribution of heme oxygenase-1 and manganese superoxide dismutase mRNA: relevance of redox homeostasis in the aging processes. Exp. Biol. Med. (Maywood) 228, 517–524.

Di Domenico, F., Sultana, R., Tiu, G.F., Scheff, N.N., Perluigi, M., Cini, C., Butterfield, D.A., 2010. Protein levels of heat shock proteins 27, 32, 60, 70, 90 and thioredoxin-1 in amnestic mild cognitive impairment: an investigation on the role of cellular stress response in the progression of Alzheimer disease. Brain. Res. 1333, 72–81.

Ding, Q., Dimayuga, E., Keller, J.N., 2006. Proteasome regulation of oxidative stress in aging and age-related diseases of the CNS. Antioxid. Redox Signal 8, 163–172.

Eckles-Smith, K., Clayton, D., Bickford, P., Browning, M.D., 2000. Caloric restriction prevents age-related deficits in LTP and in NMDA receptor expression. Brain Res. Mol. Brain Res. 78, 154–162.

Erraji-Benchekroun, L., Underwood, M.D., Arango, V., Galfalvy, H., Pavlidis, P., Smyrniotopoulos, P., Mann, J.J., Sibille, E., 2005. Molecular aging in human prefrontal cortex is selective and continuous throughout adult life. Biol. Psychiatry 57, 549–558.

Farout, L., Friguet, B., 2006. Proteasome function in aging and oxidative stress: implications in protein maintenance failure. Antioxid. Redox Signal 8, 205–216.

Fontan-Lozano, A., Saez-Cassanelli, J.L., Inda, M.C., de los Santos-Arteaga, M., Sierra-Dominguez, S.A., Lopez-Lluch, G., Delgado-Garcia, J.M., Carrion, A.M., 2007. Caloric restriction increases learning consolidation and facilitates synaptic plasticity through mechanisms dependent on NR2B subunits of the NMDA receptor. J. Neurosci. 27, 10185–10195.

Fortun, J., Li, J., Go, J., Fenstermaker, A., Fletcher, B.S., Notterpek, L., 2005. Impaired proteasome activity and accumulation of ubiquitinated substrates in a hereditary neuropathy model. J. Neurochem. 92, 1531–1541.

Fortun, J., Verrier, J.D., Go, J.C., Madorsky, I., Dunn, W.A., Notterpek, L., 2007. The formation of peripheral myelin protein 22 aggregates is hindered by the enhancement of autophagy and expression of cytoplasmic chaperones. Neurobiol. Dis. 25, 252–265.

Foster, T.C., 1999. Involvement of hippocampal synaptic plasticity in age-related memory decline. Brain Res. Brain Res. Rev. 30, 236–249.

Foster, T.C., 2002. Regulation of synaptic plasticity in memory and memory decline with aging. Prog. Brain Res. 138, 283–303.

Foster, T.C., 2007. Calcium homeostasis and modulation of synaptic plasticity in the aged brain. Aging Cell 6, 319–325.

Foster, T.C., Kumar, A., 2007. Susceptibility to induction of long-term depression is associated with impaired memory in aged Fischer 344 rats. Neurobiol. Learn. Mem. 87, 522–535.

Fu, C., Hickey, M., Morrison, M., McCarter, R., Han, E.S., 2006. Tissue specific and non-specific changes in gene expression by aging and by early stage CR. Mech. Ageing Dev. 127, 905–916.

Ghi, P., Di Brisco, F., Dallorto, D., Osella, M.C., Orsetti, M., 2009. Age-related modifications of egr1 expression and ubiquitin-proteasome components in pet dog hippocampus. Mech. Ageing Dev. 130, 320–327.

Glasper, E.R., Llorens-Martin, M.V., Leuner, B., Gould, E., Trejo, J.L., 2010. Blockade of insulin-like growth factor-I has complex effects on structural plasticity in the hippocampus. Hippocampus 20, 706–712.

Gray, D.A., Tsirigotis, M., Woulfe, J., 2003. Ubiquitin, proteasomes, and the aging brain. Sci. Aging Knowledge Environ. 2003, RE6.

Greenbaum, D., Colangelo, C., Williams, K., Gerstein, M., 2003. Comparing protein abundance and mRNA expression levels on a genomic scale. Genome Biol. 4, 117.

Greene, J.G., Borges, K., Dingledine, R., 2009. Quantitative transcriptional neuroanatomy of the rat hippocampus: evidence for wide-ranging, pathway-specific heterogeneity among three principal cell layers. Hippocampus 19, 253–264.

Grune, T., 2000. Oxidative stress, aging and the proteasomal system. Biogerontology 1, 31–40.

Gygi, S.P., Rochon, Y., Franza, B.R., Aebersold, R., 1999. Correlation between protein and mRNA abundance in yeast. Mol. Cell Biol. 19, 1720–1730.

Halagappa, V.K., Guo, Z., Pearson, M., Matsuoka, Y., Cutler, R.G., Laferla, F.M., Mattson, M.P., 2007. Intermittent fasting and caloric restriction ameliorate age-related behavioral deficits in the triple-transgenic mouse model of Alzheimer's disease. Neurobiol. Dis. 26, 212–220.

Han, E.S., Hickey, M., 2005. Microarray evaluation of dietary restriction. J. Nutr. 135, 1343–1346.

Hinds, H.L., Goussakov, I., Nakazawa, K., Tonegawa, S., Bolshakov, V.Y., 2003. Essential function of alpha-calcium/calmodulin-dependent protein kinase II in neurotransmitter release at a glutamatergic central synapse. Proc. Natl. Acad. Sci. U. S. A. 100, 4275–4280.

Ho, N., Liauw, J.A., Blaeser, F., Wei, F., Hanissian, S., Muglia, L.M., Wozniak, D.F., Nardi, A., Arvin, K.L., Holtzman, D.M., Linden, D.J., Zhuo, M., Muglia, L.J., Chatila, T.A., 2000. Impaired synaptic plasticity and cAMP response element-binding protein activation in Ca2+/calmodulin-dependent protein kinase type IV/Gr-deficient mice. J. Neurosci. 20, 6459–6472.

Hori, N., Hirotsu, I., Davis, P.J., Carpenter, D.O., 1992. Long-term potentiation is lost in aged rats but preserved by calorie restriction. Neuroreport 3, 1085–1088.

Hussain, R.J., Carpenter, D.O., 2005. A comparison of the roles of protein kinase C in long-term potentiation in rat hippocampal areas CA1 and CA3. Cell Mol. Neurobiol. 25, 649–661.

Ingram, D.K., Weindruch, R., Spangler, E.L., Freeman, J.R., Walford, R.L., 1987. Dietary restriction benefits learning and motor performance of aged mice. J. Gerontol. 42, 78–81.

Jackson, T.C., Foster, T.C., 2009. Regional health and function in the hippocampus: Evolutionary compromises for a critical brain region. Biosci. Hypotheses 2, 245–251.

Jackson, T.C., Rani, A., Kumar, A., Foster, T.C., 2009. Regional hippocampal differences in AKT survival signaling across the lifespan: implications for CA1 vulnerability with aging. Cell Death Differ. 16, 439–448.

Kalmar, B., Greensmith, L., 2009. Induction of heat shock proteins for protection against oxidative stress. Adv. Drug Deliv. Rev. 61, 310–318.
Kasahara, J., Fukunaga, K., Miyamoto, E., 2001. Activation of calcium/calmodulin-dependent protein kinase IV in long term potentiation in the rat hippocampal CA1 region. J. Biol. Chem. 276, 24044–24050.
Katare, R.G., Kakinuma, Y., Arikawa, M., Yamasaki, F., Sato, T., 2009. Chronic intermittent fasting improves the survival following large myocardial ischemia by activation of BDNF/VEGF/PI3K signaling pathway. J. Mol. Cell Cardiol. 46, 405–412.
Knowles, W.D., 1992. Normal anatomy and neurophysiology of the hippocampal formation. J. Clin. Neurophysiol. 9, 252–263.
Lein, E.S., Zhao, X., Gage, F.H., 2004. Defining a molecular atlas of the hippocampus using DNA microarrays and high-throughput in situ hybridization. J. Neurosci. 24, 3879–3889.
Li, C., Wong, W.H., 2001. Model-based analysis of oligonucleotide arrays: expression index computation and outlier detection. Proc. Natl. Acad. Sci. U. S. A. 98, 31–36.
Li, M., Shin, Y.H., Hou, L., Huang, X., Wei, Z., Klann, E., Zhang, P., 2008. The adaptor protein of the anaphase promoting complex Cdh1 is essential in maintaining replicative lifespan and in learning and memory. Nat. Cell Biol. 10, 1083–1089.
Lu, F.M., Hawkins, R.D., 2006. Presynaptic and postsynaptic Ca(2+) and CamKII contribute to long-term potentiation at synapses between individual CA3 neurons. Proc. Natl. Acad. Sci. U. S. A. 103, 4264–4269.
Lynch, C.D., Lyons, D., Khan, A., Bennett, S.A., Sonntag, W.E., 2001. Insulin-like growth factor-1 selectively increases glucose utilization in brains of aged animals. Endocrinology 142, 506–509.
Maier, T., Guell, M., Serrano, L., 2009. Correlation of mRNA and protein in complex biological samples. FEBS Lett. 583, 3966–3973.
Mattson, M.P., Duan, W., Wan, R., Guo, Z., 2004. Prophylactic activation of neuroprotective stress response pathways by dietary and behavioral manipulations. NeuroRx 1, 111–116.
Mattson, M.P., Guthrie, P.B., Kater, S.B., 1989. Intrinsic factors in the selective vulnerability of hippocampal pyramidal neurons. Prog. Clin. Biol. Res. 317, 333–351.
Mattson, M.P., Wan, R., 2005. Beneficial effects of intermittent fasting and caloric restriction on the cardiovascular and cerebrovascular systems. J. Nutr. Biochem. 16, 129–137.
McBain, C.J., 2008. Differential mechanisms of transmission and plasticity at mossy fiber synapses. Prog. Brain Res. 169, 225–240.
McEwen, B.S., 2001. Plasticity of the hippocampus: adaptation to chronic stress and allostatic load. Ann N Y Acad Sci 933, 265–277.
Morgan, T.E., Wong, A.M., Finch, C.E., 2007. Anti-inflammatory mechanisms of dietary restriction in slowing aging processes. Interdiscip Top Gerontol 35, 83–97.
Morimoto, R.I., 1998. Regulation of the heat shock transcriptional response: cross talk between a family of heat shock factors, molecular chaperones, and negative regulators. Genes Dev 12, 3788–3796.
Naik, M.U., Benedikz, E., Hernandez, I., Libien, J., Hrabe, J., Valsamis, M., Dow-Edwards, D., Osman, M., Sacktor, T.C., 2000. Distribution of protein kinase Mzeta and the complete protein kinase C isoform family in rat brain. J Comp Neurol 426, 243–258.
Nie, T., McDonough, C.B., Huang, T., Nguyen, P.V., Abel, T., 2007. Genetic disruption of protein kinase A anchoring reveals a role for compartmentalized kinase signaling in theta-burst long-term potentiation and spatial memory. J Neurosci. 27, 10278–10288.
Ormerod, B.K., Palmer, T.D., Caldwell, M.A., 2008. Neurodegeneration and cell replacement. Philos Trans R Soc Lond B Biol Sci 363, 153–170.
Patrick, G.N., 2006. Synapse formation and plasticity: recent insights from the perspective of the ubiquitin proteasome system. Curr Opin Neurobiol. 16, 90–94.
Patrylo, P.R., Williamson, A., 2007. The effects of aging on dentate circuitry and function. Prog. Brain Res. 163, 679–696.
Pawluski, J.L., Brummelte, S., Barha, C.K., Crozier, T.M., Galea, L.A., 2009. Effects of steroid hormones on neurogenesis in the hippocampus of the adult female rodent during the estrous cycle, pregnancy, lactation and aging. Front. Neuroendocrinol. 30, 343–357.
Paz Gavilan, M., Vela, J., Castano, A., Ramos, B., del Rio, J.C., Vitorica, J., Ruano, D., 2006. Cellular environment facilitates protein accumulation in aged rat hippocampus. Neurobiol. Aging 27, 973–982.
Pitsikas, N., Algeri, S., 1992. Deterioration of spatial and nonspatial reference and working memory in aged rats: protective effect of life-long calorie restriction. Neurobiol. Aging 13, 369–373.
Prolla, T.A., 2002. DNA microarray analysis of the aging brain. Chem. Senses 27, 299–306.
Rangaraju, S., Hankins, D., Madorsky, I., Madorsky, E., Lee, W.H., Carter, C.S., Leeuwenburgh, C., Notterpek, L., 2009. Molecular architecture of myelinated peripheral nerves is supported by calorie restriction with aging. Aging Cell 8, 178–191.
Rao, G., Xia, E., Richardson, A., 1990. Effect of age on the expression of antioxidant enzymes in male Fischer F344 rats. Mech. Ageing Dev. 53, 49–60.
Rosenzweig, E.S., Barnes, C.A., 2003. Impact of aging on hippocampal function: plasticity, network dynamics, and cognition. Prog. Neurobiol. 69, 143–179.
Selman, C., Kerrison, N.D., Cooray, A., Piper, M.D., Lingard, S.J., Barton, R.H., Schuster, E.F., Blanc, E., Gems, D., Nicholson, J.K., Thornton, J.M., Partridge, L., Withers, D.J., 2006. Coordinated multitissue transcriptional and plasma metabonomic profiles following acute caloric restriction in mice. Physiol. Genom. 27, 187–200.
Sivakumaran, S., Mohajerani, M.H., Cherubini, E., 2009. At immature mossy-fiber-CA3 synapses, correlated presynaptic and postsynaptic activity persistently enhances GABA release and network excitability via BDNF and cAMP-dependent PKA. J. Neurosci. 29, 2637–2647.
Spindler, S.R., Dhahbi, J.M., 2007. Conserved and tissue-specific genic and physiologic responses to caloric restriction and altered IGFI signaling in mitotic and postmitotic tissues. Annu. Rev. Nutr. 27, 193–217.
Swindell, W.R., 2008. Comparative analysis of microarray data identifies common responses to caloric restriction among mouse tissues. Mech. Ageing Dev. 129, 138–153.
Szweda, P.A., Camouse, M., Lundberg, K.C., Oberley, T.D., Szweda, L.I., 2003. Aging, lipofuscin formation, and free radical-mediated inhibition of cellular proteolytic systems. Ageing Res. Rev. 2, 383–405.
Terao, A., Apte-Deshpande, A., Dousman, L., Morairty, S., Eynon, B.P., Kilduff, T.S., Freund, Y.R., 2002. Immune response gene expression increases in the aging murine hippocampus. J. Neuroimmunol. 132, 99–112.
Tsay, H.J., Wang, P., Wang, S.L., Ku, H.H., 2000. Age-associated changes of superoxide dismutase and catalase activities in the rat brain. J. Biomed. Sci. 7, 466–474.
Tydlacka, S., Wang, C.E., Wang, X., Li, S., Li, X.J., 2008. Differential activities of the ubiquitin-proteasome system in neurons versus glia may account for the preferential accumulation of misfolded proteins in neurons. J. Neurosci. 28, 13285–13295.
Wang, X., Zaidi, A., Pal, R., Garrett, A.S., Braceras, R., Chen, X.W., Michaelis, M.L., Michaelis, E.K., 2009. Genomic and biochemical approaches in the discovery of mechanisms for selective neuronal vulnerability to oxidative stress. BMC Neurosci. 10, 12.
Weindruch, R., Kayo, T., Lee, C.K., Prolla, T.A., 2002. Gene expression profiling of aging using DNA microarrays. Mech. Ageing Dev. 123, 177–193.
Weindruch, R., Naylor, P.H., Goldstein, A.L., Walford, R.L., 1988. Influences of aging and dietary restriction on serum thymosin alpha 1 levels in mice. J. Gerontol. 43, B40–42.
Wu, P., Shen, Q., Dong, S., Xu, Z., Tsien, J.Z., Hu, Y., 2008. Calorie restriction ameliorates neurodegenerative phenotypes in forebrain-specific presenilin-1 and presenilin-2 double knockout mice. Neurobiol. Aging 29, 1502–1511.
Xu, X., Zhan, M., Duan, W., Prabhu, V., Brenneman, R., Wood, W., Firman, J., Li, H., Zhang, P., Ibe, C., Zonderman, A.B., Longo, D.L., Poosala, S., Becker, K.G., Mattson, M.P., 2007. Gene expression atlas of the mouse central nervous system: impact and interactions of age, energy intake and gender. Genome Biol. 8, R234.
Yang, S., Liu, T., Li, S., Zhang, X., Ding, Q., Que, H., Yan, X., Wei, K., Liu, S., 2008. Comparative proteomic analysis of brains of naturally aging mice. Neuroscience 154, 1107–1120.
Zalutsky, R.A., Nicoll, R.A., 1990. Comparison of two forms of long-term potentiation in single hippocampal neurons. Science 248, 1619–1624.

RESEARCH ARTICLE

Development and Distribution of Neuronal Cilia in Mouse Neocortex

Jon I. Arellano,[1]* Sarah M. Guadiana,[2] Joshua J. Breunig,[3] Pasko Rakic,[1] and Matthew R. Sarkisian[2]*

[1]Department of Neurobiology, Yale University School of Medicine, New Haven, Connecticut 06510
[2]Department of Neuroscience, McKnight Brain Institute, University of Florida, Gainesville, Florida 32610-0244
[3]Department of Biomedical Sciences, Regenerative Medicine Institute and Department of Neurosurgery, Maxine Dunitz Neurosurgical Institute, Cedars-Sinai Medical Center, Los Angeles, California 90048

ABSTRACT

Neuronal primary cilia are not generally recognized, but they are considered to extend from most, if not all, neurons in the neocortex. However, when and how cilia develop in neurons are not known. This study used immunohistochemistry for adenylyl cyclase III (ACIII), a marker of primary cilia, and electron microscopic analysis to describe the development and maturation of cilia in mouse neocortical neurons. Our results indicate that ciliogenesis is initiated in late fetal stages after neuroblast migration, when the mother centriole docks with the plasma membrane, becomes a basal body, and grows a cilia bud that we call a *procilium*. This procilium consists of a membranous protrusion extending from the basal body but lacking axonemal structure and remains undifferentiated until development of the axoneme and cilia elongation starts at about postnatal day 4. Neuronal cilia elongation and final cilia length depend on layer position, and the process extends for a long time, lasting 8–12 weeks. We show that, in addition to pyramidal neurons, inhibitory interneurons also grow cilia of comparable length, suggesting that cilia are indeed present in all neocortical neuron subtypes. Furthermore, the study of mice with defective ciliogenesis suggested that failed elongation of cilia is not essential for proper neuronal migration and laminar organization or establishment of neuronal polarity. Thus, the function of this organelle in neocortical neurons remains elusive. J. Comp. Neurol. 520:848–873, 2012.

INDEXING TERMS: ciliogenesis; forebrain; axoneme; protracted maturation; centrioles; corticogenesis; pyramidal cell; interneuron

The primary cilium of neurons has been mostly overlooked for the last 50 years. Although its presence was occasionally documented in ultrastructural studies using electron microscopy (EM; Dahl, 1963; LeVay, 1973; White and Rock, 1980), the lack of a specific marker for this organelle and intrinsic difficulties with random sampling for cilia with EM did not allow for more extensive studies on their morphology or distribution. More recently, cilia were shown to be enriched with type III adenylyl cyclase (ACIII), a mediator of cAMP signalling typically associated with G-protein-coupled membrane receptors (Bishop et al., 2007). The development of antibodies against ACIII has allowed description of the ubiquitous presence of cilia in neurons in different regions of the brain (Bishop et al., 2007), although confirmation of their presence in specific neuronal cell types is lacking. In addition, little is known about their development and function (for review see Fuchs and Schwark, 2004; Green and Mykytyn, 2010; Whitfield, 2004).

During embryonic development, primary cilia extend from interphase radial glial cells into the lateral ventricles (Cohen et al., 1988; Dubreuil et al., 2007; Li et al., 2011). Loss or reduction in the expression of genes that are important for cilia growth and function (e.g., Ift88, stumpy, and Bardet-Biedl syndrome proteins [BBS]) can lead to cortical morphogenesis defects in mice and human (Bennouna-Greene et al., 2011; Breunig et al., 2008; Rooryck

Grant sponsor: National Institutes of Health; Grant number: DA02399 (to P.R.); Grant sponsor: National Institute of Neurological Disorders and Stroke; Grant number: NS038296-09 (to P.R.); Grant sponsors: Kavli Institute for Neuroscience (to P.R.); McKnight Brain Research Foundation and the Evelyn F. and William L. McKnight Brain Institute at the University of Florida (to M.R.S); Connecticut Stem Cell Research Grants Program (www.ct.gov/dph/cwp/view.aspa=3142&q=389702; to J.J.B.).

*CORRESPONDENCE TO: Matthew R. Sarkisian, Department of Neuroscience, McKnight Brain Institute, University of Florida, Gainesville, FL 32610-0244, E-mail: matt.sarkisian@mbi.ufl.edu; Jon I. Arellano, Department of Neurobiology, Yale University School of Medicine, New Haven, Connecticut, 06510, E-mail: jon.arellano@yale.edu

Received March 16, 2011; Revised July 27, 2011; Accepted October 4, 2011
DOI 10.1002/cne.22793
Published online October 20, 2011 in Wiley Online Library (wileyonlinelibrary.com)

et al., 2007; Willaredt et al., 2008). In the postnatal brain, primary cilia are also found on astrocyte-like neural precursors in the hippocampus that express sonic hedgehog (Shh) signalling machinery and respond to secreted Shh to regulate neurogenesis and differentiation (Breunig et al., 2008; Han et al., 2008).

In addition to ACIII, a few neuronal cilia-specific receptors have been identified, including somatostatin receptor subtype 3 (SSTR3), melanin-concentrating hormone receptor 1 (MchR1), dopamine receptor 1 (D1), and serotonin receptor subtype 6 (5-hydroxytryptamine, 5-HT_6; Berbari et al., 2008; Brailov et al., 2000; Domire et al., 2010; Domire and Mykytyn, 2009; Handel et al., 1999). SSTR3 receptors localize on neuronal cilia in the neocortex, hippocampal CA fields, olfactory bulb, and dentate gyrus neuronal populations (Berbari et al., 2008; Handel et al., 1999). In the hippocampus, SSTR3 appears between postnatal days (P) 0 and 3 in rat (Stanic et al., 2009); however, the neocortical developmental appearance of SSTR3 and other neuronal cilia receptor subtypes is unclear. Recent studies have shown that disruption of these molecules or impairment of ciliogenesis in general can lead to abnormalities in object recognition memory and synaptic plasticity and to obesity (Amador-Arjona et al., 2011; Davenport et al., 2007; Einstein et al., 2010; Wang et al., 2009).

Cilia are composed of a microtubular backbone (the axoneme) surrounded by a specialized membrane that is continuous with the plasma membrane. The axoneme extends from the basal body, a structure derived from the mother centriole (the older of the two centrioles), which can form the cilium in two different ways. In one case, a vesicle from the Golgi apparatus attaches to the mother centriole. The centriole starts growing the cilium inside the vesicle, which eventually fuses with the cell membrane, and the cilium continues growing into the extracellular space. Alternatively, the mother centriole can migrate and anchor to the cell membrane to form the basal body from which the cilium grows into the extracellular space (Sorokin, 1962, 1968; for review see Nigg and Raff, 2009; Pedersen et al., 2008). The process of cilia growth can be rapid upon serum starvation (Ou et al., 2009), whereby the axoneme can quickly disassemble if cells re-enter the cell cycle and subsequently reassemble upon reaching G1/G0 (Tucker et al., 1979a,b).

To our knowledge, there are no studies on the development of cortical neuronal cilia, although it has been shown that failure of neuroblasts to segregate centrioles properly during neurogenesis can result in cortical neurons with multiple centrioles and cilia (Anastas et al., 2011). During neuronal migration, the centrioles are a core component of the centrosome, which aids in guiding neuronal migration (Higginbotham and Gleeson, 2007). Therefore, it would be expected that axoneme extension would occur after cells have completed migration.

This study was designed to address these questions, characterizing the development of cilia in neocortical neurons and their presence in specific neuronal types and describing their morphological features by using different techniques such as Western blot, immunohistochemistry, and ultrastructural analysis.

MATERIALS AND METHODS

Mice

Mice of the CD1 strain (two to four animals per age) were collected on embryonic (E) days (E) 11.5, 13.5, 16, 18.5 and P0, P1, P3, P4, P7, P8, P14, P21, P60, P90, P170, and P365. P0 and older mice were intracardially perfused with saline followed by 4% paraformaldehyde (PFA) in 0.1 M phosphate buffer (PB; pH 7.3). After dissection and fixation, brains were either sectioned (60 μm coronal) in a vibratome or cryoprotected, frozen over liquid N_2, and sectioned (20, 50 or 60 μm coronal) on a cryostat. *Stumpy* mutant brain tissue was generated as previously described (Town et al., 2008). Briefly, a floxed *stumpy* allele was deleted in the presence of Cre under the control of the Nestin promoter. Floxed *stumpy* mice were originally generated on a B6/129 background and then back-crossed onto a B6 background for 10 generations. Floxed mice were then crossed with nestin-Cre deleter mice on a pure B6 background (The Jackson Laboratory). Animal care procedures were performed in accordance with the Laboratory Animal Welfare Act, the *Guidelines for the care and use of laboratory animals* (National Institutes of Health), and the approval of both the University of Florida and the Yale University Institutional Animal Care and Use Committee.

In utero electroporation

We used in utero electroporation to deliver plasmid DNA, pCAGGS-GFP, into fetal cerebral cortices as previously described (Rasin et al., 2007; Sarkisian et al., 2006). Briefly, at E13.5, female CD1 mice were anesthetized by an intraperitoneal injection of ketamine (100 mg/kg) and xylazine (10 mg/kg) diluted in sterile saline. The uterine horns were exposed, and ~1 μl of DNA (0.5 μg/μl) mixed with 0.025% fast green) was microinjected through the uterine wall into the lateral ventricles of the cerebral cortices of the mouse embryos using pulled glass capillaries. Electroporation was achieved by discharging 40 V across the cortex in five 50-msec pulse series spaced 950 msec apart with a BTX ECM 830 Square Wave Electroporator. Following injections, the dams were sutured and allowed to recover on heating pads. Electroporated embryos were harvested at E16.5, and brains

were dissected and processed for immuno-EM as described below.

Immunohistochemistry

Tissue sections were probed 24–48 hours at 4°C using the following primary antibodies (dilutions listed in Table 1): rabbit antiadenylyl cyclase (ACIII), mouse anti-NeuN, mouse antiparvalbumin, goat anti-Foxp2, rabbit anti-CDP (aka Cux1), rabbit antipericentrin, mouse monoclonal anticalretinin, mouse antipericentrin, and chicken antigreen fluorescent protein (GFP). After the sections were rinsed in phosphate-buffered saline (PBS; pH 7.2), appropriate species-specific, fluorescent-conjugated secondary antibodies were used (1:200; Jackson Immunoresearch, West Grove, PA) for each antibody. After a rinse in PBS, immunostained sections were coverslipped using ProLong Gold Antifade media containing 4′,6-diamidino-2-phenylindole dihydrochloride (DAPI; Invitrogen, Carlsbad, CA).

For combination of ACIII and pericentrin rabbit antibodies, tissue was incubated first in ACIII and developed with fluorescein isothiocyanate (FITC)-conjugated monovalent Fab secondary antibodies (1:200; Jackson Immunoresearch), followed by incubation in pericentrin and development in conventional Cy3-conjugated secondary antibodies. No overlapping domains were observed in the cortex, as shown below in Figure 1A.

Antibody characterization

The antibodies used in this study were tested by immunostaining of mouse brain sections or by Western blot analyses of mouse brain lysates. The data that we collected for each antibody were consistent with known information about each protein. Antibody information is detailed in Table 1, with further specificity details listed below.

- Rabbit anti-ACIII was raised against the C-terminal 20 amino acids of mouse ACIII. By Western blot, this antibody can detect bands between ~125 and ~200 kDa depending on the level of glycosylation (Murthy and Makhlouf, 1997; Wei et al., 1996, 1998; Wong et al., 2000). Immunostaining in the brain reveals specific enrichment in neuronal cilia, which was confirmed by the absence of ACIII detection in cilia from ACIII knockout mice (Bishop et al., 2007; Wang et al., 2009). The pattern of staining in our study is consistent with that in the citations given above.
- Mouse monoclonal antibody against β-actin was raised against a modified β-cytoplasmic actin N-terminal peptide (Ac-Asp-Asp-Asp-Ile-Ala-Ala-Leu-Val-Ile-Asp-Asn-Gly-Ser-Gly-Lys) conjugated to KLH. By Western blot, the antibody detects a 42-kDa band (predicted MW of β-actin) from lysates of cultured

TABLE 1.
Primary Antibodies Used in This Study[1]

Antigen	Immunizing antigen	Manufacturer details	Working dilution
Adenylyl cyclase III (ACIII)	Synthetic peptide with the C-terminal 20 amino acids of mouse ACIII (PAAFPNGSSVTLPHQVVDNP)	Santa Cruz Biotechnology; catalog No. sc-588; rabbit polyclonal	1:1,000 (WB) 1:1,000 (IHC)
β-Actin	A modified β-cytoplasmic actin N-terminal peptide (DDDIAALVIDNGSGK, conjugated to KLH)	Sigma; catalog No. A5316; mouse monoclonal	1:10,000 (WB)
Calbindin-D28K	Calbindin D-28k purified from chicken gut	Swant; catalog No. 300; mouse monoclonal	1:4,000 (IHC)
Calretinin	Recombinant human calretinin-22k	Swant; catalog No. 6B3; mouse monoclonal	1:2,000 (IHC)
Green fluorescent protein (GFP)	Recombinant full-length GFP	Abcam; catalog No. ab13970; chicken polyclonal	1:5,000 (IHC)
Neuronal nuclear protein (NeuN)	Cell nuclei purified from mouse brain	Chemicon; catalog No. MAB377; mouse monoclonal	1:1,000 (IHC)
Parvalbumin	Purified parvalbumin from carp muscle	Swant; catalog No. 235; mouse monoclonal	1:4,000 (IHC)
Class IIIβ tubulin (Tuj1)	Purified microtubules from rat brain	Covance; catalog No. MMS-435P mouse monoclonal	1:1,250 (IHC)
Pericentrin	A fusion protein containing T7-Gene10 and ~60kD of pericentrin (amino acids 870–1370 of the mouse protein).	Covance; catalog No. PRB-432C; rabbit polyclonal	1:500 (IHC)
Pericentrin	Amino acids 1692–1814 of mouse pericentrin	BD Biosciences; catalog No. 611815; mouse monoclonal	1:200 (IHC)
Cux-1	Amino acids 1111–1332 of mouse CDP (CCAAT displacement protein)	Santa Cruz Biotechnologies; catalog No. sc-13024; rabbit polyclonal	1:100 (IHC)
FOXP2	Synthetic peptide: REIEEEPLSEDLE, corresponding to amino acids 703–715 of human FOXP2	Abcam; catalog No. ab1307; goat polyclonal	1:100 (IHC)

[1]WB, Western blot; IHC, immunohistochemistry.

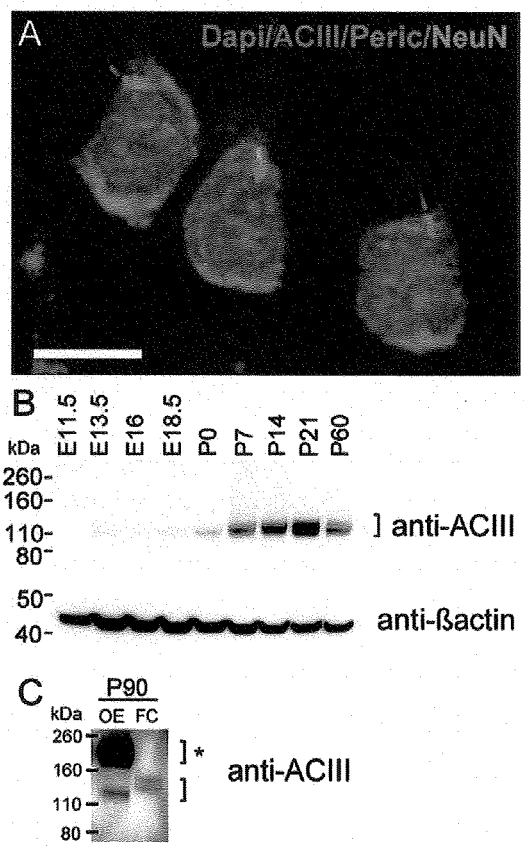

Figure 1. Expression of adenylyl cyclase III during fetal and postnatal cortical development. **A:** Maximum intensity projection of a z-stack of layer 3 pyramidal neurons in the neocortex of a P90 mouse. Cilia were immunostained with ACIII (green), basal bodies with pericentrin (red), neuronal somata with NeuN (purple), and nuclei with DAPI (blue). **B:** Western blot detection of ACIII from mouse cortical lysates from embryonic day 11.5 (E11.5) to young adulthood (~P60). The upper blot for ACIII revealed a band close to the predicted MW of unglycosylated ACIII (MW of ~125 kDa). Generally, ACIII expression significantly increases between P0 and P21. At P60, there is a decrease in the intensity of the ACIII signal. β-Actin (lower blot) was used as a loading control. **C:** Protein lysates of P90 olfactory epithelium (OE) or frontal cortex (FC) were separated by Western blot and probed for ACIII. Very strong expression of ACIII is detected at ~190–200 kDa, which has been shown to reflect high levels of glycosylated ACIII (bracket with asterisk). This higher MW signal was absent in FC sample that revealed only a lower MW signal for ACIII (lower bracket). Scale bar = 10 μm.

mouse, human, or chicken fibroblast extracts. Results described below reveal an identical pattern and molecular weight for β-actin (see Fig. 1).

- Mouse monoclonal antibody against calbindin D-28K was produced by hybridization of mouse myeloma cells with spleen cells isolated from mice immunized with calbindin D-28k purified from chicken gut. This antibody specifically stains the ^{45}Ca-binding domain of calbindin D-28k (MW 28 kDa, IEP 4.8) in a two-dimensional gel. By radioimmunoassay, it detects calbindin D-28k with a sensitivity of 10 ng/assay and an affinity of 1.6×10^{12} L/M. Immunoblots of tissue originating from several species including rodents and primates show a band of 28 kDa, and the antibody does not cross-react with other known calcium-binding proteins (Celio et al., 1990). Antibody CB300 immunolabels a subpopulation of neurons in the normal brain with high efficiency but does not stain in the brain of calbindin D-28k knockout mice (Airaksinen et al., 1997).
- Mouse anticalretinin was produced in mice by immunization with recombinant human calretinin-22k (Zimmermann and Schwaller, 2002), an alternative splice product of the calretinin gene and identical to calretinin up to Arg178. The antibody 6B3 stains a 29-kD band (calretinin MW = 29 kD) on immunoblots of brain extracts from mouse, rat, and macaque. Immunohistochemistry with the antibody stains a subpopulation of nonpyramidal cells in the cortex of mice that is absent in CR-KO mice (Bearzatto et al., 2006). The antibody does not cross-react with calbindin D-28K or other calcium-binding proteins as shown by immunoblots or immunostaining in brain tissue.
- Chicken anti-GFP antibody was raised against the recombinant full-length synthetic peptide of jellyfish *Aequorea victoria*. By Western blot analysis of transgenic mouse spinal cord or mouse carcinoma cell lines expressing GFP, this antibody recognizes a distinct band between 27 and 30 kDa (predicted MW of GFP = 27kDa). Immunostaining of untreated wild-type brain tissue with this antibody showed no detectable staining.
- Mouse monoclonal against neuron-specific nuclear antigen (NeuN) was originally made against cell nuclei purified from mouse brain, and Western blotting with this antibody shows three bands in the 46–48-kDa range (Mullen et al., 1992). The anti-NeuN antibody showed a pattern of neuronal nuclei in the developing mouse brain like that previously described (Mullen et al., 1992). We also observed NeuN in the neuronal cell body, which is consistent not only with previous reports (Kao et al., 2008; Lyck et al., 2007; Saino-Saito et al., 2011) but also with recent identification of NeuN as splicing regulator Fox-3, which appears to have isoforms that localize to the cytoplasm (Dredge and Jensen, 2011; Kim et al., 2009).
- Mouse monoclonal antiparvalbumin reacts specifically with parvalbumin (PV) in cultured nerve cells and in mouse tissue and specifically stains the ^{45}Ca-binding spot of PV (MW = 12 kDa and IEF 4.9) in a two-

dimensional "immunoblot." (Celio and Heizmann, 1981). Staining was located in a subpopulation of nonpyramidal cells in the neocortex as previously described (Cho et al., 2011).

- Rabbit polyclonal antibody anti-pericentrin was raised against a fusion protein containing 60 kDa of pericentrin (amino acids 870–1370 of the mouse protein) and T7-gene10 (Doxsey et al., 1994). This antibody recognizes a single 220-kDa band by immunoblotting and has been extensively characterized in a previous study (Doxsey et al., 1994). Staining in the developing neocortex showed a pattern of pericentrin immunoreactivity that was identical to previous descriptions (Westra et al., 2008).
- Mouse monoclonal anti-pericentrin was raised against amino acids 1692–1814 of mouse pericentrin and purified by affinity chromatography. As described in an original characterization of pericentrin (Doxsey et al., 1994), this antibody detects a band at 220 kDa (MW of pericentrin). The pattern of immunostaining with this antibody is also comparable to other studies showing enrichment in centrioles (Jurczyk et al., 2010) and is also similar to the rabbit pericentrin, with which we found to be localized to the basal body at the cilium base.
- Rabbit polyclonal anti-Cux1 (anti-CDP) was raised against amino acids 1111–1332 of CDP (CCAAT displacement protein) of mouse origin. On Western blot of mouse liver extracts, this antibody detects a band at ~200 kDa, which is knocked down by specific microRNAs (Xu et al., 2010). This antibody has also been shown by multiple investigators to label neurons effectively in upper layers 2/3 of neocortex (Feng and Cooper, 2009; Tury et al., 2011). The pattern of staining in our study is consistent with these earlier studies.
- Goat anti-Foxp2 was raised against a synthetic peptide REIEEEPLSEDLE corresponding to C-terminal amino acids 703–715 of human FOXP2 protein. On Western blot analysis of human cerebellum lysates, this antibody detected a single band at ~ 80kDa (predicted MW = ~79.9 kDa; manufacturer's technical information). Staining for Foxp2 reveals strong expression in neuronal nuclei of deep layers of neocortex (Ferland et al., 2003; Stillman et al., 2009; Waclaw et al., 2010). The patterns of antibody staining in our study resemble those reported in the studies cited above.

Analysis and quantification of cilia

For quantification of cilia length, mice at P0, P4, P7, P14, P60, P90, P170, and P365 were analyzed (two brains/age and two sections/brain) in area S1Tr from the mouse brain atlas (Paxinos and Franklin, 2004), located dorsal to the hippocampus and medial to the barrel field cortex. Vibratome sections (60 μm) were immunostained for ACIII and NeuN and counterstained with DAPI. Mosaic stacks (9–18 images separated ~1 μm in the z axis) were taken from the pial surface to the white matter using a Zeiss Apotome system attached to a Zeiss Axioplan2 microscope with a ×20 objective using Zeiss Axiovision software. Stacks were collapsed to the maximum intensity projection, and the resulting images were adjusted for gray levels for each channel using the same software. Images were imported into Reconstruct software (Fiala, 2005), where they were aligned, layers were delimitated, and cilia were traced and measured. In total 3,756 cilia were measured, averaging ~85 per layer and age studied, in this analysis performed by J.I.A. In addition, a separate analysis was performed by S.M.G. at ages E18.5, P0, P3, P7, P14, P21, P60, P90 using an Olympus IX81-DSU spinning disc confocal microscope. Z-stacks of images (at 0.75 μm steps) of sections immunostained for ACIII (Santa Cruz Biotechnolgy, Santa Cruz, CA) and pericentrin (BD Biosciences, San Jose, CA) were collected and subsequently collapsed to the maximum intensity projection. Resulting images were analyzed in Image J64 (http://rsbweb.nih.gov/ij/), in which cilia lengths were measured from the pericentrin puncta side to the end of the continuous $ACIII^+$ signal in at least two brains and six to eight fields/section for each age. Although not displayed, similar results were obtained in both analyses. For analysis of $ACIII^+$ cilia extending from PV^+ cells, Z-stack images of sections immunostained for ACIII and PV were converted to maximum intensity projection images, and $ACIII^+$ cilia lengths were analyzed in Image J64 as described above. Analyses of cilia length between sexes were compared by Student's *t*-tests (two tailed). In all tests, $P < 0.05$ was considered significant.

Electron microscopy

For the immuno-EM analysis, electroporated brains were fixed at E16.5 by immersion in 4% PFA and 0.3% glutaraldehyde in PB for 24 hours at 4°C. Brains were dissected, embedded in 4% agarose, and sectioned (100 μm thick) with a vibratome (Leica). Sections were collected in PB, cryoprotected with 30% sucrose, and freeze-thawed over liquid nitrogen to permeabilize the tissue. After being rinsed in PB, sections were incubated with antibodies against GFP for 24 hours, rinsed in PB, incubated with biotinylated secondaries (Jackson Immunoresearch) for 2 hours, rinsed in PB, incubated in an ABC Elite kit (Vector, Burlingame, CA), rinsed in PB, and developed with diaminobenzidine (DAB; Vector) as chromogen. From this point, sections were postfixed and processed for EM in the same way as described below.

For the conventional EM analysis, animals were intracardially perfused with saline followed by 4% PFA in PB for P60 brains and 1% PFA and 1.25% glutaraldehyde in PB for the rest of the ages. Brains were dissected and postfixed in the same fixative overnight. After being rinsed in PB, brains were sectioned (60–100 μm thick) coronally with a vibratome. Animals P8 or younger were embedded in 4% agarose before sectioning. P60 sections were collected in PB and postfixed in 2% glutaraldehyde for 1 hour. All sections were postfixed in 1% osmium tetroxide for 40 minutes and then rinsed, dehydrated, embedded in Durcupan (Fluka, Buchs, Switzerland), and cured in an oven for 48 hours at 60°C. Neocortical regions of interest were sectioned at 70 nm in a Reichert ultracut ultramicrotome. Serial sections were collected in slot grids covered with Formvar, counterstained with uranyl acetate and lead citrate, and analyzed in a Jeol JEM-1010. Pictures were taken with a Gatan MSC600W digital camera and adjusted for brightness and contrast in Adobe Photoshop.

Western blots

Protein lysates from mouse cortex were prepared by homogenizing tissue in 1× RIPA buffer (containing 20 mM Tris-HCl, pH 7.5, 150 mM NaCl, 1 mM Na_2EDTA, 1 mM EGTA, 1% vol/vol Triton X-100, 2.5 mM sodium pyrophosphate, 1 mM glycerophosphate, 1 mM Na_3VO_4, 1 mg/ml leupeptin, and 1 mM PMSF; Cell Signaling, Beverly, MA). For developmental time points, similar total amounts (30 μg/lane) were loaded onto 4–12% NuPAGE gel (Invitrogen) and separated by SDS-PAGE. Proteins were transferred onto PVDF membranes using an iBlot (Invitrogen). Blots were blocked in 5% BSA in Tris-buffered saline containing 0.1% Tween (TBST) for 1 hour at RT. The following primary antibodies were diluted in 2.5% BSA in TBST incubated overnight at 4°C: rabbit anti-ACIII or mouse anti-β-actin. Membranes were rinsed in TBST, and incubated with appropriate horseradish peroxidase (HRP)-conjugated secondary antibodies (1;10,000; Bio-Rad, Hercules, CA). Blots were developed using chemiluminescence (ECL-Plus Kit; GE Healthcare, Picataway, NJ), and images were captured with an Alpha Innotech FluorChemQ Imaging System (Cell Biosciences).

RESULTS

Expression of ACIII in fetal and postnatal mouse cortex

Cilia throughout the mature cortex are enriched in ACIII (Bishop et al., 2007), which thus serves as a surrogate ciliial marker (Fig. 1A). To study the expression of ACIII in the developing cortex, we used Western blot analysis to examine protein lysates from mouse cortex at ages E11.5, E13.5, E16, E18.5, P0, P7, P14, P21 and young adult (P60; Fig. 1B). We found low levels of ACIII at ~E13.5 (roughly midcortical neurogenesis), but levels were higher at birth and noticeably increased over the first few postnatal weeks (Fig. 1B). ACIII persisted at P60, but the signal intensity was lower compared with P21 lysates (Fig. 1B). Quantification of ACIII relative to β-actin from the same blot confirmed these observations (data not shown). We found that the signal for ACIII is ~125–130 kDa, suggesting that cortical ACIII might be predominantly in a less glycosylated form (Murthy and Makhlouf, 1997; Wei et al., 1996). To confirm this, we compared lysates isolated from P90 olfactory epithelium and frontal cortex from the same brain. As reported previously (Wong et al., 2000), we observed a very strong signal for glycosylated ACIII between ~190 and ~200 kDa in olfactory epithelium, which was not observed in cortex (Fig. 1C). Taken together, these data suggest that ACIII, a protein enriched in neuronal cilia, is expressed mostly in a less glycosylated form in the neocortex, which increases in the late embryonic stages, becoming more robust in postnatal cortex.

Basal body docking begins in deeper layer cells of the developing cortical plate

To study the possibility of late embryonic growth of neuronal cilia, we analyzed sections of mouse cortex that had been electroporated at embryonic day (E) 13.5 with a plasmid expressing GFP and subsequently fixed at E16.5 and prepared for immuno-EM. We first screened cells localized throughout the cortical plate (CP; Fig. 2A,B) for the presence and location of cilia and centrioles/basal bodies (quantified in Fig. 2C). We found only a few cilia precursors at a very early stage of development (Figs. 2D–F, 3), and most cells exhibited centrioles either free in the cytoplasm (undocked centrioles; Figs. 2G–I, 3A) or located adjacent to the cell membrane with one centriole attached to the plasma membrane (docked centrioles/basal bodies; Figs. 2D–F, 3B,C). The centrioles appeared surrounded by or in close proximity to Golgi apparatus, and in some cases multivesicular bodies were also observed in their vicinity (Fig. 3A,C).

Results of our analysis are summarized in Figure 2C. From among 36 centriole encounters in the deeper CP, 25 were docked with the membrane, whereas 11 were undocked (Fig. 2C). Electroporation of a cohort of neural progenitors from the ventricular zone with GFP cDNA allowed us to track the neural cells derived from them. Cells generated at E13.5 and later are directed mostly to upper layers of the neocortex, so GFP^+ cells located in the deep CP at E16.5 would most likely be migrating cells. In fact, docked centrioles were frequently within non-

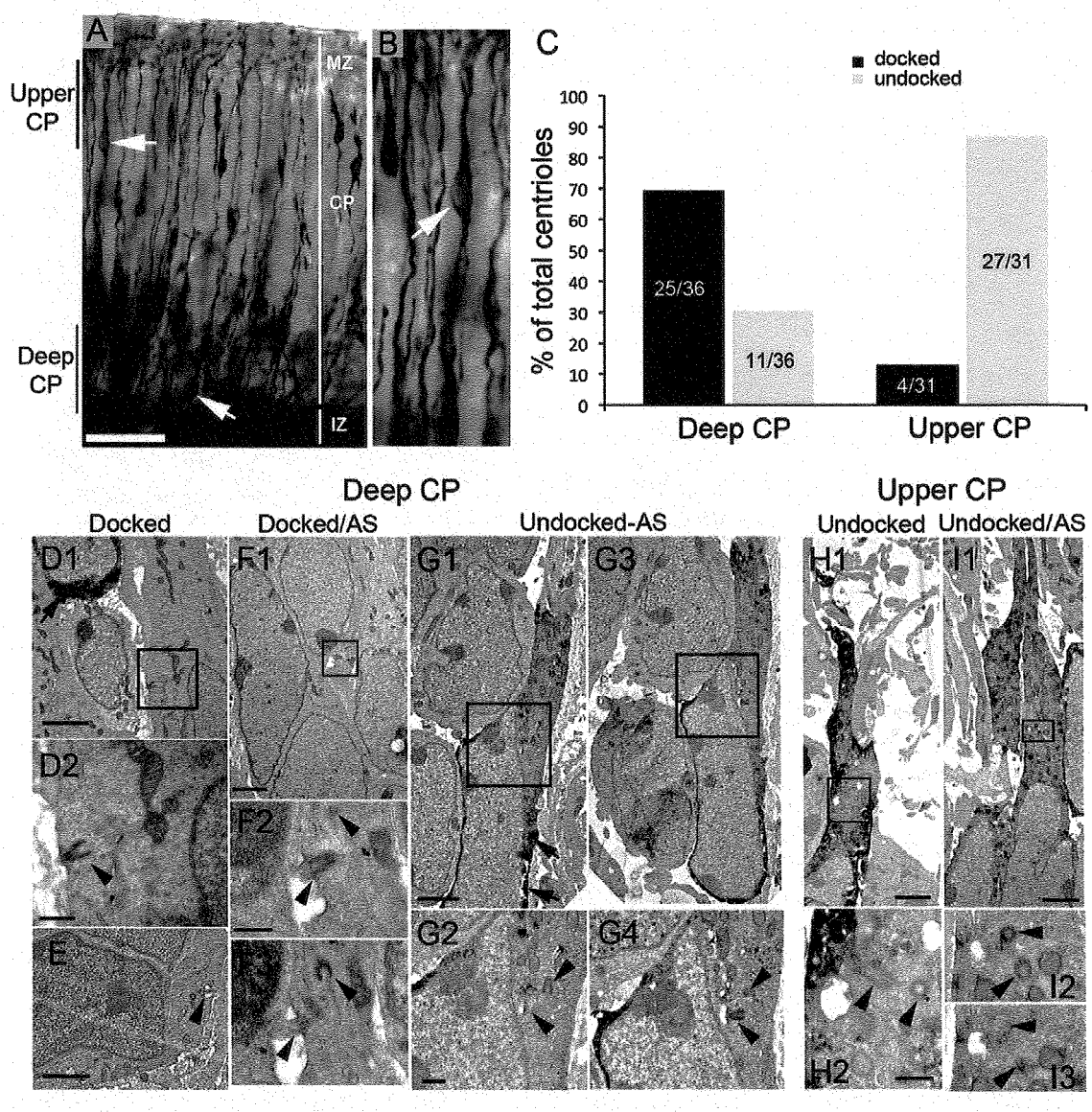

Figure 2. Basal bodies are more prevalent in the deeper cortical plate (CP) at E16.5. E13.5 embryos electroporated with cDNA encoding GFP, killed and fixed for immuno-EM at E16.5. **A:** DAB immunostaining with anti-GFP antibodies shows GFP^+ cells (arrows) with leading and trailing processes in both the deeper layer and the upper layer of the CP. **B:** Higher magnification of the upper CP showing a cell (arrow) with a typical migrating profile. **C:** Bar graph shows a summary of the position of centrioles/basal bodies that were identified in deeper and upper layers of the CP docked (to the plasma membrane) or undocked. In deep CP, ~70% were docked (mostly in cells that were GFP^-). In upper CP, most centrioles (~90%) were undocked. **D–I:** Electron micrographic examples of centrioles and basal bodies in deep (D–G) or upper (H,I) CP. D1: A docked basal body in a GFP^- cell (boxed area is shown in D2). GFP immunoprecipitate is visible in the upper left cell (arrow). E: A docked basal body with a small axoneme extension (arrowhead). F1: Another example of a docked basal body in a GFP^- cell. The boxed region is shown in F2 and an adjacent section (AS) in F3. G1,3: Adjacent sections of a GFP^+ cell (arrows point to GFP precipitate) with a leading process. Boxed regions in G1,3 are magnified in G2,4, respectively. H1: A GFP^+ cell in the upper CP with undocked centrioles (boxed area is magnified in H2, which shows two centrioles (arrowheads). I1: Another example of a GFP^+ cell in the upper CP. The boxed area in I1 is enlarged in I2, with an adjacent section shown in I3. Scale bars = 50 μm in A; 2 μm in D1,E,F1,G1,H1,I1; 0.5 μm in D2,F2,G2 H2.

GFP^+ cells that typically displayed ultrastructural features of nonmigrating cells (e.g., more rounded soma, less elongated nuclei) both in the upper and in the deep CP (e.g., Fig. 2D–F). In contrast, undocked centrioles in the deeper CP were in GFP^+ cells that also typically exhibited leading processes and elongated nuclear

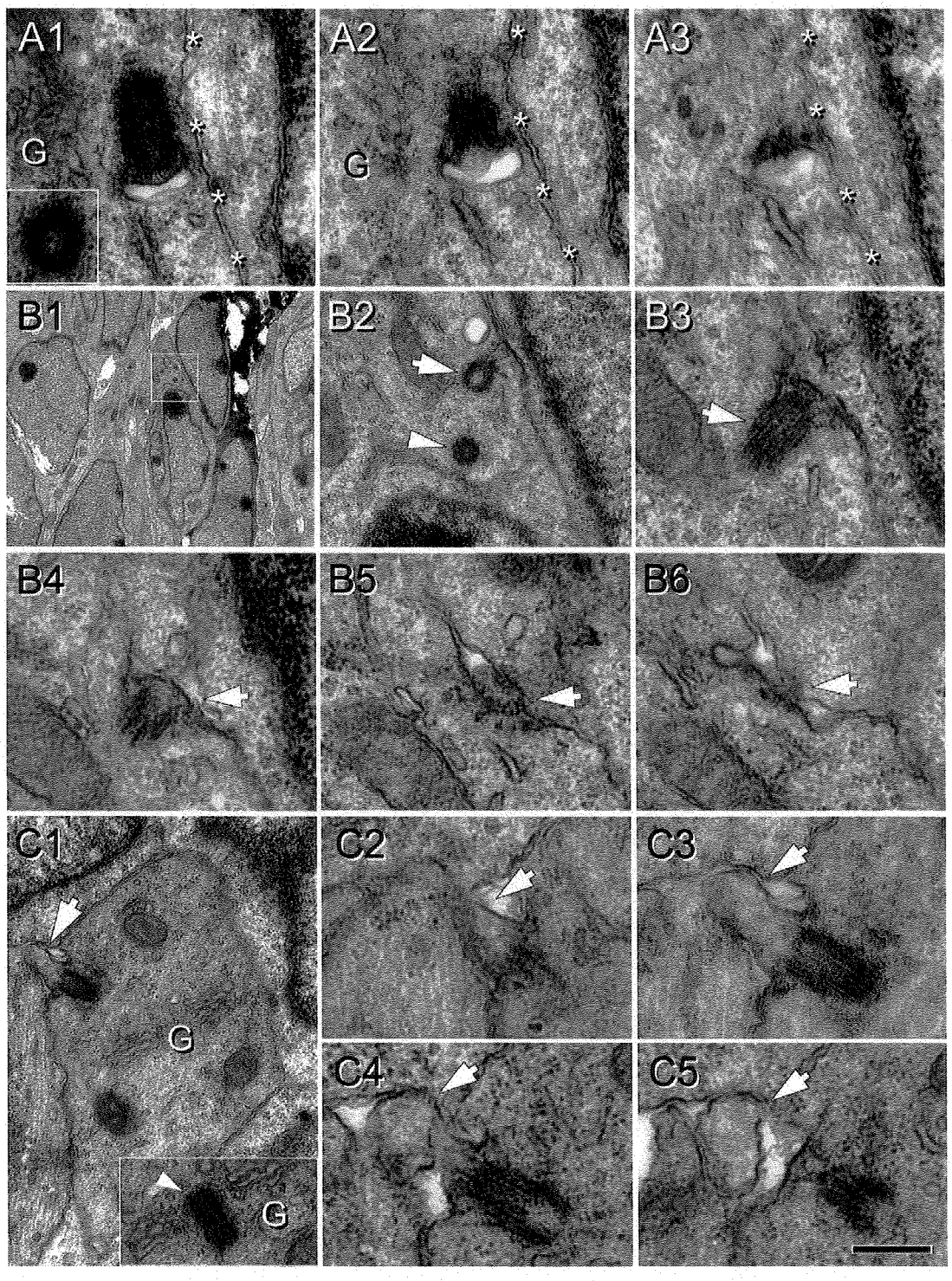

Figure 3. Procilia in the fetal cortical plate at E16.5. Cells of interest and procilia are shaded to help identification. **A:** Serial sections (70 nm thick) illustrating an undocked mother centriole with an attached vesicle located adjacent to the cell membrane (asterisks). **Inset** in A1 shows the daughter centriole found in adjacent sections and (G) indicates Golgi cisterns around the centrosome. A2: A membranous centriolar protrusion, consistent with a procilium budding into the vesicle. This vesicular attachment is predictably the step before docking of the mother centriole to the cell membrane. **B:** Docked basal body with a protruding small procilium. B1: Low magnification image of the cell studied. Boxed area is magnified in B2. B2: Detail of the mother centriole (arrow) and the daughter centriole (arrowhead) located between the nucleus and the pial oriented process. B3–6: Serial sections (70 nm thick) illustrating the short procilium (~0.1 μm long) protruding from the attached mother centriole (arrow). **C:** Docked basal body with developed procilium. C1: Low magnification image of the cell analyzed showing the procilium (~0.3 μm long; arrow) protruding outside the cell. **Inset** shows an adjacent section illustrating the centriole surrounded by Golgi cisterns. C2–5: Serial sections (70 nm thick) illustrating the extent and mushroom shape of the procilium (arrow). Scale bar = 0.25 μm in C5 (applies to A,B3–6,C2–5); 3.6 μm for B1; 0.5 μm for B2; 0.54 μm for C1. [Color figure can be viewed in the online issue, which is available at wileyonlinelibrary.com.]

morphology, suggesting that they were in fact cells migrating to upper layers (e.g., Fig. 2G). Moreover, deep CP cells with docked centrioles sometimes exhibited short (0.1–0.5 μm) protrusions consisting of a membranous bud lacking microtubular organization that we called procilia (e.g., Figs. 2E,F, 3). We found only rare cases of undocked centrioles with a vesicle attached (Figs. 2G, 3A) that could represent the previous step before docking of the centriole to the cell membrane (Pedersen et al., 2008). The relative rarity of these findings suggests that vesicle attachment to the mother centriole could be quickly followed by centriole docking to the cell membrane. According to this model, ciliation of immature neurons would occur at the cell membrane and not inside the vesicle attached to the mother centriole.

In upper CP, 27 of 31 centrioles were undocked (Fig. 2C,H,I). Thus ~70% of deeper layer cells possess a docked centriole, whereas only ~10% of upper CP cells contained similarly docked centrioles. These data suggest that cells initiate docking of the mother centriole in the CP once cells have completed migration and/or reached their appropriate lamina.

Neuronal primary cilia axonemes develop postnatally taking several weeks to reach maximal lengths

In the rodent cortex, the cilia and basal bodies are immunodetectable with ACIII and pericentrin, respectively (Anastas et al., 2011; Bishop et al., 2007; Wang et al., 2011; Fig. 4A–E). To study the development of neocortical cilia, ACIII immunostaining and EM were used at different ages. Cilia length was estimated by tracing ACIII signal on collapsed confocal z-stack images from tissue sections at P0, P4, P7, P14, P60, P90, P170, and P365. Average and maximum cilia lengths were recorded for each age and cortical layer (Table 2, Fig. 4F). ACIII staining revealed regional and laminar differences in the length of cilia in the neocortex. To avoid regional bias, we consistently measured cilia in the dorsal neocortex overlying the hippocampus (for details see Materials and Methods). To distinguish laminar differences, we used DAPI and NeuN to delineate layers 1–6 when possible (Fig. 5). These methods do not allow for the establishment of absolute values of cilia length but provide information about cilia elongation trends in different cortical compartments over time. In total 3,756 cilia were measured, averaging ~85 per layer and age studied. To correspond with our analysis of ACIII, EM studies were performed at P0, P4, P8, and P60 to assess structural developmental characteristics.

At E18.5 and P0, ACIII staining revealed a punctate pattern suggesting slightly elongated growth of cilia compared with E16.5 (Figs. 4A,B, 5A–D, Table 2). NeuN is not fully expressed by all neurons in the region analyzed at P0 and is almost absent in layer 2, upper layer 3, and deep layer 6, although many neurons in the subplate are intensely immunostained. Thus, we only made a distinction between superficial (layers 2–4) and deep (layers 5 and 6) strata based on cytoarchitecture and NeuN expression (Fig. 5A–D). ACIII was found in small specks in all layers, with rare rod-like cilia. Layer 1 had short cilia compared with the CP, in which both superficial and deep strata showed similar lengths (Table 2, Figs. 4F, 5A–D). Ultrastructural analysis at P0 supported those findings and showed the presence of procilia in all cells analyzed ($n = 21$), although with large heterogeneity in their length (Figs. 6, 7). These procilia were similar to some observed at E16.5 (Figs. 2D–I, 3, 6), but they had different ciliar content. Sometimes they exhibited a short axoneme, with doublets of outer microtubules poorly developed and distinguishable only for about 100–200 nm into the procilium. The presence of vesicles was a common finding inside the procilia (see. e.g., Fig. 6B,C), and some procilia appeared to be filled with a number of vesicles of different size (Fig. 7B,C). Interestingly, we found one cell located in the subplate region bearing a short cilium, but with a well-organized axoneme (Fig. 7D).

At P4, NeuN expression is not fully mature and is very weak in layer 2 and deep layer 6 (Fig. 5E,G,J). Layer 1 at P4 showed relatively long cilia compared with upper layers 2–4, where most ACIII staining appeared as thick punctae (0.7–1.5 μm), with few intermingling longer cilia (2–3 μm; Fig. 5F–H). In deeper layers 5 and 6, the heterogeneity was more dramatic, and two clear populations could be distinguished: a majority of short punctae (0.5–2 μm) and a population of longer cilia especially in some cells in layer 5 (up to 6.6 μm) and in the subplate (up to 5.4 μm; Table 2, Figs. 4F,G, 5I–K). These results suggest that most cilia in upper and deep layers remained in a procilia stage, although some specific subpopulations in deeper layers start elongating earlier. Consistently with this, from the EM analysis at P4 in supragranular layers 1–4, we found only procilia in the cells studied ($n = 11$; Fig. 8). The procilia at P4 were slightly longer but similar to those described for P0. They showed occasional vesicle-like structures and diffuse electron-dense material, and sometimes the membrane was expanded in a mushroom-like shape (Fig. 8A–C). Similar to P0, procilia at P4 had short and poorly organized axonemes, extending about 200 nm into the procilium, and in deeper layer cells microtubules were observed but lacked clear axonemal organization (Fig. 8D–F). From P4 to P7, upper layer cilia showed an increase in length to match deeper layers lengths (Figs. 4F,G, 5, 9), and all layers had similar average cilia length between 3 and 4.4 μm, with maximum

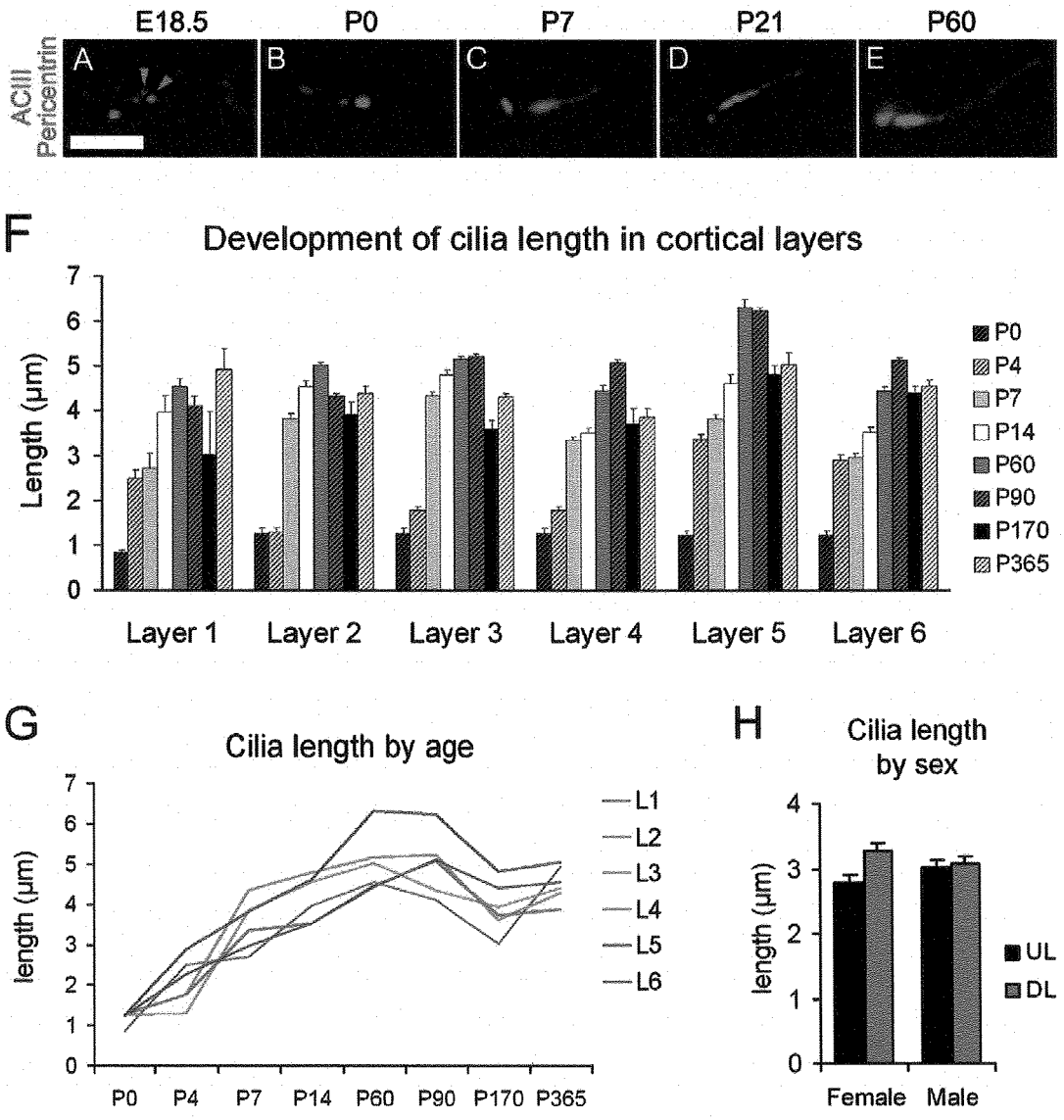

Figure 4. Elongation of neuronal cilia over several postnatal weeks. A–E: Examples of basal bodies (pericentrin^{+}; red; example indicated by red arrowhead) and cilia (ACIII^{+}; green; example indicated by green arrowhead) for the indicated ages. F: Bar graph shows the average ± SEM of cilia length (µm) in the neocortical layers at the indicated ages. Because it was difficult to differentiate neocortical lamina at early ages, average lengths for layers 2–4 and layers 5-6 were pooled for P0, whereas at P4 layers 3 and 4 were also pooled. G: Graphic representation of cilia elongation across age in the cortical layers. Mean values of length are used (SEM values are omitted for clarity but can be found in Table 2). H: Comparison of cilia length in upper layers (2–4; UL) and deep layers (5–6; DL) of the neocortex in male and female P14 mice did not show significant effect of gender. Scale bar = 2.5 µm.

lengths of about 7 µm in layers 2, 3, and 5 (Table 2, Figs. 4F,G, 9). From this age onward, ACIII staining of cilia showed an intense pattern in the proximal segment that tapered toward the tip (Figs. 1A, 4C–E). Consistent with immunohistochemistry results, EM analysis at P8 revealed longer, straighter cilia with a developed axoneme that can be followed several micrometers into the parenchyma (Fig. 10). Unfortunately, the lengthening of cilia creates technical difficulties in following the entire cilium length across a series of EM sections. Thus, for this age onward, we do not have information on the structure of the tip of cilia.

At P14 and P60, there is a progressive elongation of cilia in all layers (Table 2, Figs. 4F,G, 9H–N) and ultrastructural analysis at P60 showed well-developed axonemes and rounded cilia that could be only partially

TABLE 2.
Average Length of Cilia in the Neocortical Lamina at Different Ages[1]

	L1	L2	L3	L4	L5	L6
P0	0.9 ± 0.1 (2)	1.3 ± 0.1 (3.3)	1.3 ± 0.1 (3.3)	1.3 ± 0.1 (3.3)	1.2 ± 0.1 (3.7)	1.2 ± 0.1 (3.7)
P4	2.5 ± 0.2 (4.6)	1.3 ± 0.1 (2.2)	1.8 ± 0.1 (3.1)	1.8 ± 0.1 (3.1)	3.4 ± 0.1 (6.6)	2.9 ± 0.1 (4.5)
P7	2.7 ± 0.3 (4.2)	3.8 ± 0.1 (7.1)	4.4 ± 0.1 (7)	3.4 ± 0.1 (5.3)	3.8 ± 0.1 (6.9)	3 ± 0.1 (5.3)
P14	4 ± 0.4 (6.5)	4.5 ± 0.1 (6.9)	4.8 ± 0.1 (8.3)	3.5 ± 0.1 (5.7)	4.6 ± 0.2 (8.4)	3.5 ± 0.1 (6.9)
P60	4.6 ± 0.2 (7)	5 ± 0.1 (7.7)	5.2 ± 0.1 (9.2)	4.5 ± 0.1 (7.5)	6.3 ± 0.2 (9.7)	4.4 ± 0.1 (7.5)
P90	4.1 ± 0.2 (6.5)	4.3 ± 0.1 (6.1)	5.2 ± 0.1 (7.9)	5.1 ± 0.1 (7.7)	6.2 ± 0.1 (10.8)	5.1 ± 0.1 (8.1)
P170	3 ± 1 (4.9)	3.9 ± 0.3 (6.6)	3.6 ± 0.2 (6)	3.7 ± 0.4 (5.9)	4.8 ± 0.2 (8.3)	4.4 ± 0.1 (8.1)
P365	4.9 ± 0.5 (6.6)	4.4 ± 0.2 (7.3)	4.3 ± 0.1 (6.2)	3.9 ± 0.2 (4.8)	5 ± 0.3 (9.9)	4.6 ± 0.1 (6.5)

[1]Average length (in micrometers) ± SEM and maximum length noted (in parentheses) of cilia in the cortical layers at different ages. At P0, only upper and deep cortical strata were quantified, and those values were used for layers 2-4 (upper) and layers 5-6 (deep). The same applies to layers 3 and 4 at P4. The subplate at P0 was included in layer 6, but at P4 showed marked differences, with a mean cilia length of 3.8 ± 0.1 μm and a maximum of 5.4 μm.

reconstructed (Fig. 11). At P90, ACIII staining showed similar or only slightly longer cilia lengths in all layers compared with P60, suggesting that cilia stop growing by ~P60-P90. Cilia exhibited maximum lengths at these ages, with averages of ~5 μm in layers 2-4 and 6, and ~6 μm in layer 5. Maximum values in each layer varied from ~8 μm in layers 2, 4, and 6 to ~9 μm in layer 3 and to 10.8 μm in layer 5 (Table 2, Fig. 4F,G).

We found a notable shortening of the estimated cilia length at P170 and P365 compared with P60-P90 (Table 2, Fig. 4F,G). This could be due to an actual shortening of cilia, although an alternative possibility is that in aging animals ACIII protein does not fill the cilia completely and is absent from the distal tip. In fact, there were also slight decreases in estimated cilia length in layer 1 and 2 between P60 and P90 that could be due to the same phenomenon (see Discussion).

To determine whether sex had any significant influence on cilia length, we examined the average length in upper and deeper layers of the neocortex of males (n = 2) and females (n = 2) at P14. This analysis did not reveal significant differences in cilia length between sexes (3.06 ± 0.19 μm and 3.03 ± 0.19 μm [mean ± SEM] for males and females, respectively [Fig. 4H]). Taken together, our results suggest that cilia elongation in neocortex is a slow process that starts postnatally with slightly different dynamics depending on cortical layer but is not significantly affected by gender. Maximal cilia length is different depending on cortical layer, and overall it can take up to 3 months to be reached.

Extension of cilia from Ca^{2+} binding protein-containing interneurons

Although $ACIII^{+}$ cilia have been described for cultured hippocampal cells expressing glutamate acid decarboxylase (Berbari et al., 2007), their presence in inhibitory neurons in the neocortex has not been described. Inhibitory neurons migrate tangentially into the neocortex during development to invade the CP (Wonders and Anderson, 2006). Inhibitory interneurons can be identified by the expression of several markers. From those, calcium-binding proteins parvalbumin, calbindin, and calretinin distinguish three large subpopulations of inhibitory interneurons with little overlap (Defelipe et al., 1999). In the mature rodent cortex, parvalbumin-expressing neurons make up ~50% of GABAergic inhibitory interneurons (Wonders and Anderson, 2006). We examined confocal z-stack images of P60 tissue sections immunostained for PV, ACIII, and NeuN and measured cilia from these cells compared with cells that did not express PV (Fig. 12A-G). PV^{+} cells appeared to extend a cilium from the soma (Fig. 12A-F). We found that the lengths of cilia from PV^{+} neurons appeared comparable to those of neighboring PV^{-} neurons (putatively excitatory neurons; mean PV^{+} = 5.12 ± 0.42 μm SEM; PV^{-} = 5.06 ± 0.25 μm; Fig. 12G). In addition, $ACIII^{+}$ cilia were found in other interneuron subtypes expressing calbindin and calretinin (Fig. 12H-R). These results suggest that neocortical interneurons also extend $ACIII^{+}$ cilia that reach lengths similar to those of neighboring excitatory pyramidal neurons.

Neuronal cilia do not appear critical for neuronal polarity or expression of layer-specific markers

On pyramidal neurons, cilia generally extend from the base of the apical dendrite (Anastas et al., 2011). This suggests that cilia could be related to the orientation/polarity of neocortical neurons and particularly to the extension/orientation of the apical dendrite. To analyze this, we examined neocortical neurons in *Stumpy conditional* mutant (Δ*Stumpy; NestinCre;Stumpy*$^{fl/fl}$) mice in which all neural cell types (including neurons) either lack or extend a poorly formed, stunted cilia (Breunig et al., 2008; Town et al., 2008). Although the lack of cilia leads to hydrocephalus and noticeable compression of the neocortex starting at approximately P4 (Fig. 13), we still observed

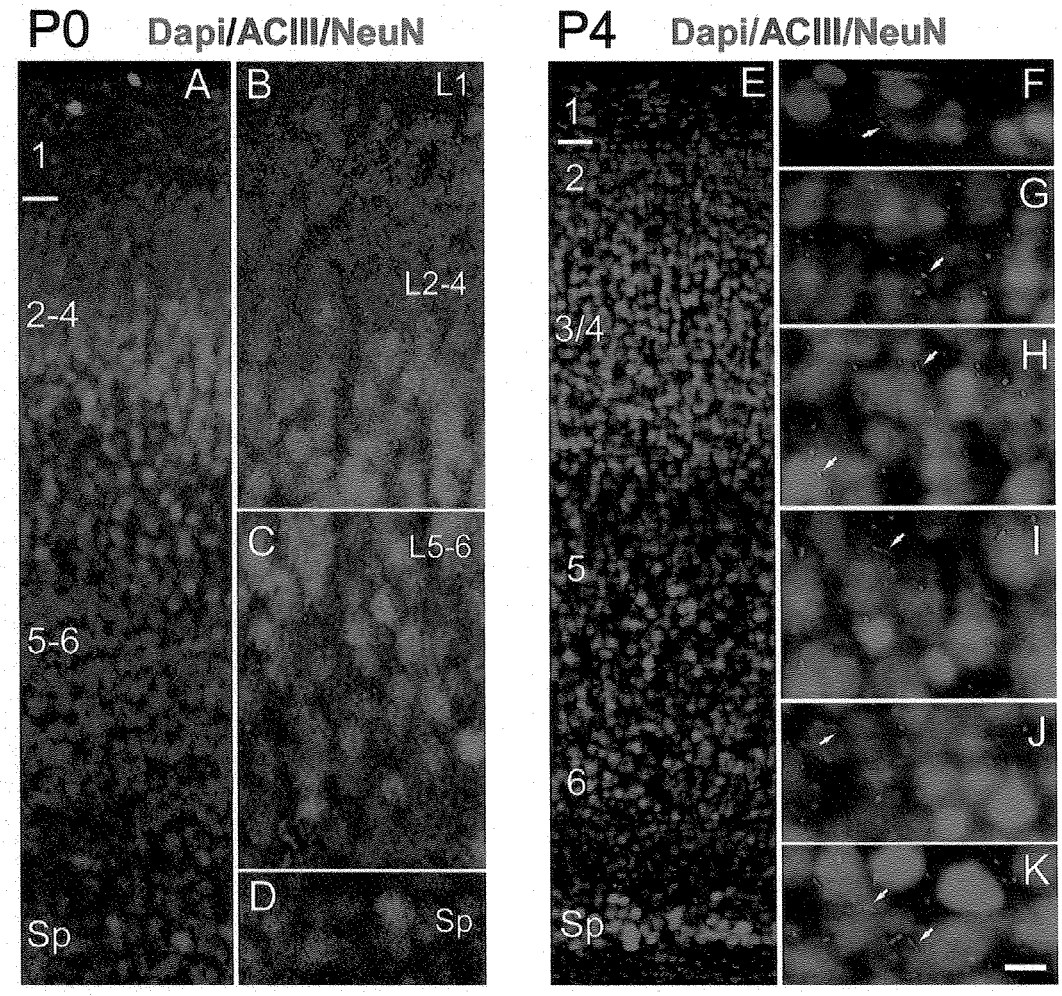

Figure 5. Distribution of procilia in the neocortex at P0 and P4. **A:** Low-magnification view of the P0 neocortex immunostained for ACIII (green) and NeuN (red) and counterstained with DAPI (blue). NeuN is expressed in some cells of layers 2–5, scarce cells in layer 6, and intensely by some cells in the subplate (Sp). **B–D:** Details of the neocortex illustrating approximate layers 1–4 (L1, L2–4) in B, layers 5 and 6 (L5–6) in C, and the Sp in D. $ACIII^{+}$ specks were found in all layers, with rare longer, rod-shaped cilia. **E:** Low-magnification view of the P4 neocortex immunostained for ACIII and NeuN and counterstained with DAPI. **F–K:** High-magnification details of the cortical layers from layer 1 to the Sp. NeuN is still not fully expressed by all neurons, and layer 2 (G) and deep layer 6 (J) have few stained neurons. In contrast, the subplate (K) shows large neurons intensely stained with NeuN. Overall, intense $ACIII^{+}$ puncta are predominant, although scattered longer cilia can be found in all layers (arrows) and particularly in some neurons in layer 5 (I) and in the Sp (K). Scale bar = 10 μm in K (applies to F–K); 15 μm for A; 8 μm for B–D; 30 μm for E.

properly oriented neurons with apical dendrites in Δ*Stumpy* brain (Fig. 13A–C). In addition, laminar-specific marker expression was preserved in Δ*Stumpy* mice (Fig. 13D,E). These data suggest that failure of neurons to extend normal cilia does not dramatically alter polarity or gross laminar pattern of neurons in the neocortex.

DISCUSSION

Previous studies in vitro and in vivo have gone a long way toward characterizing neuronal cilia and the expression of specific proteins within these structures (for review see Green and Mykytyn, 2010; Lee and Gleeson, 2010). Indeed, there is growing evidence that dysgenesis of the primary cilium can be associated with neurological disorders (Sharma et al., 2008). In addition, during the past decade, much has been learned about the cell biology of ciliogenesis (Goetz and Anderson, 2010). However, the genesis of neuronal cilia during brain development has not been well characterized.

Our results suggest that ciliogenesis in mouse cortical neurons initiates after cells complete migration by

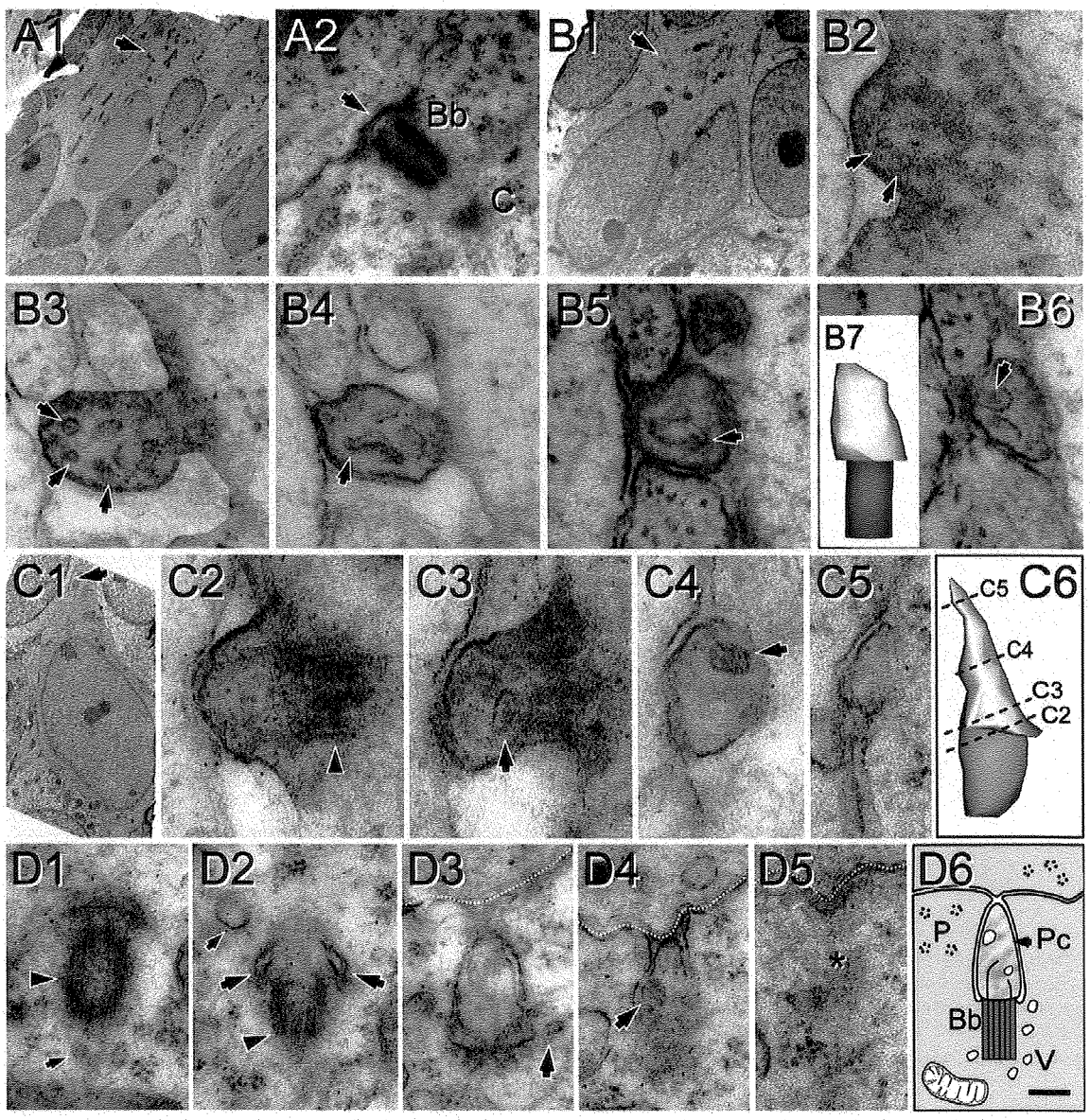

Figure 6. Heterogeneity of procilia at P0 in the upper cortical plate. Cells and procilia of interest are shaded to help with identification. **A1:** Low-magnification view of a cell with neuronal morphology in layer 2; arrow indicates the position of the docked centriole (basal body). **A2** shows higher magnification of the basal body (Bb) and part of the adjacent daughter centriole (C). Note the lack of procilium (arrow) that was also absent in adjacent serial sections. **B:** A procilium in a cell with neuronal morphology in layer 2. B1: Low-magnification view of the cell with an arrow indicating the location of the procilium. B2: Cross-section of the basal body showing microtubular doublets (arrows) in the transitioning basal body/axonemal rudiment. B3–6: Serial sections (70 nm) through the procilium show the lack of axoneme but the presence of a tubular/vesicular network (arrows) inside the procilium. B7: 3D reconstruction of the procilium (white) and basal body (gray). **C:** Procilium in a cell with neuronal morphology. C1: Low-magnification view of a cell with an arrow indicating the location of the procilium. C2: Transition between the basal body (arrowhead) and procilium. C3–5: Serial sections illustrate a short procilium lacking microtubules and containing some vesicular structures (arrows). C6: 3D reconstruction of the basal body (gray) and the procilium (white) indicating the levels of C2–5 sections. **D:** Serial sections showing a procilium growing inside the cytoplasm in a cell in the upper cortical plate. D1: The basal body (arrowhead) and an adjacent vesicle (small arrow). D2: The basal body (arrowhead) and the budding procilium with a vesicle attached (large arrows). D3,4: The procilium is surrounded by the cell membrane and reaching the extracellular space in contact with an adjacent cell (discontinuous white line). Vesicles in and around the procilium are indicated with arrows. D5: Final section containing the procilium (asterisk). D6: Schematic of the procilia (Pc) growing inside the cytoplasm. Bb, basal body; V, vesicles; P, polyribosomes. Scale bar = 90 nm in D6 (applies to D1–5); 4 μm for A1; 0.18 μm for A2; 3 μm for B1; 70 nm for B2–6,C2–5; 0.15 μm for B7; 2 μm for C1; 0.1 μm for C6.

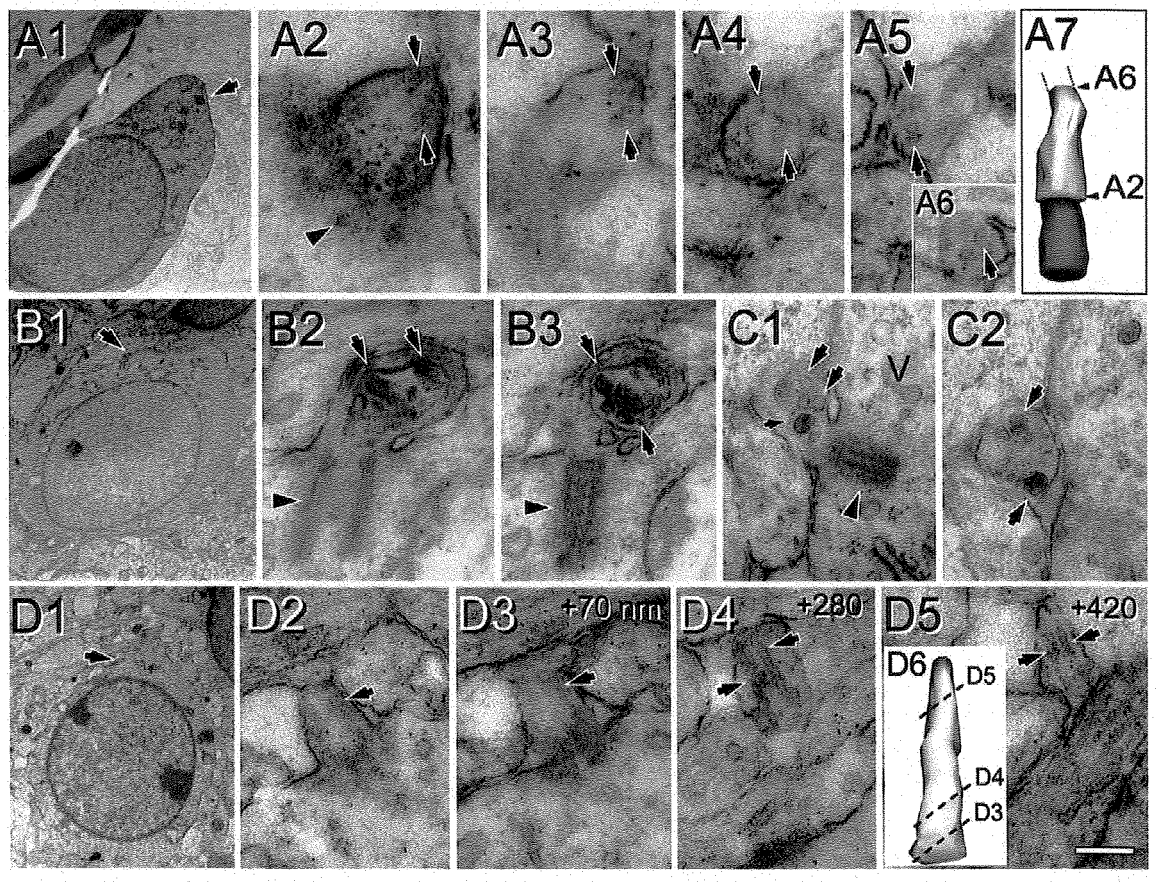

Figure 7. Procilia in the deep cortical plate at P0. Cells and procilia of interest are shaded to help with identification. **A1:** Low-magnification view of a cell with neuronal morphology bearing a procilium (arrow) in its pial aspect. **A2–6:** Serial sections of the procilium from the cell in A1. A2: The transition between the basal body (arrowhead) to the procilium. The procilium lacks an axoneme, but some microtubule-like structures are detectable (arrows in A2–6). **A7:** 3D reconstruction of the basal body (gray) and the (incomplete) procilium (white) indicating the relative positions of sections A2 and A6. **B:** Procilium in the deep cortical plate with "cabbage-like" morphology. B1: Low-magnification image of the cell with neuronal morphology bearing the procilium. B2,3: Serial micrographs showing the basal body (arrowhead) and the procilium with membrane foldings and multiple vesicles (arrows). **C:** Another example of a procilium containing multiple vesicles (arrows) and occasional tubular structures (small arrow). Vesicles (V) were also frequent around the basal body (arrowhead in C1). **D:** A cilium with axoneme in a cell with neuronal morphology in the subplate. D1: Low-magnification image of the cell bearing the cilium (arrow). D2–5: Selected serial oblique sections of the cilium illustrating the presence of parallel microtubules (arrows) forming the axoneme. The distance (nanometers) between sections is indicated at upper right. Surprisingly, the microtubules are more visible in distal sections (D4,5) than in proximal ones (D2,3). D6: 3D reconstruction of the cilium (basal body is not illustrated) showing the levels of sections D3–5. Scale bar = 0.16 μm in D5 (applies to D4,5); 2 μm for A1,B1; 90 nm for A2–6, 0.26 μm for A7; 0.18 μm for B2–3; 0.24 μm for C1,2; 1.8 μm for D1; 0.2 μm for D2,3; 0.25 μm for D6. [Color figure can be viewed in the online issue, which is available at wileyonlinelibrary.com.]

docking of the mother centriole to the cell membrane and growing a procilium: a rudiment of the cilium lacking axonemal organization that will largely develop and elongate postnatally. The elongation of neocortical cilia is a surprisingly protracted process lasting for several weeks that follows different temporal patterns and reaches different final lengths depending on laminar position. In addition to pyramidal neuron cilia, we describe the presence of cilia in interneurons, with lengths comparable to those in pyramidal cells. Collectively, our study provides a comprehensive initial characterization of neuronal ciliogenesis and cilia distribution in the developing and mature mouse neocortex.

Initiation of ciliogenesis in the developing CP

EM analysis of the CP at E16.5 showed frequent undocked centrioles in cells with migratory morphology in the upper layer of the CP, whereas cells with a

nonmigratory profile in deeper layer showed predominant basal body docking and in some cases budding procilia. These observations suggested that cessation of migration is a necessary step before docking of the mother centriole to the membrane and the subsequent ciliogenesis. Furthermore, because centrioles are an integral part of the centrosome during neuronal migration (Higginbotham and Gleeson, 2007; Tsai et al., 2007), this conclusion is not unexpected. It is also not surprising that the laminar positions of neocortical neurons are not dramatically altered in brains of mice that have mutations in genes that disrupt neuronal ciliogenesis, because the centrioles have already performed their role in migration prior to docking.

Detailed analysis of the centrioles of cortical cells at E16.5 showed the presence of procilia or short membranous protrusions (0.1–0.8 μm long) growing in the distal aspect of the mother centriole. Serial section analysis revealed that these procilia were present in cells with docked centrioles and in some cases also inside a vesicle attached to undocked centrioles, most likely immediately before docking to the membrane (Sorokin, 1962, 1968; for review see Pedersen et al., 2008). We cannot discard the possibility that some form of cilia could be present at earlier stages of development or in other pallial compartments, for example, in early-migrating immature neurons or in the population of immature neurons with multipolar morphology in the intermediate zone. However, if there is any previous form of cilia, it is very likely transient and probably reabsorbed before final migration of the neurons to their destination in the cortex, insofar as our data suggest that cilia are not present in migrating neurons in the CP. More extensive studies are needed to assess this possibility.

From our data we propose the following model (Fig. 14). When a migrating neuron reaches its appropriate lamina, the mother centriole migrates and docks with the nearby plasma membrane, either directly or attaching a vesicle to their distal tip prior to docking (Sorokin, 1968). Membrane docking generally occurs close to the proximal portion of the leading process that will become the apical dendrite (present results; Anastas et al., 2011). Once the mother centriole docks to the membrane, the procilium grows slightly (~0.2–0.5 μm) and reaches about 0.5–2 μm by P0 and P4. We differentiate procilia from cilia based on the lack of axonemal organization. We define the procilia as membranous protrusions characterized by the lack of axoneme that instead have only an axonemal rudiment extending about 100–300 nm into the procilia. The procilia cytoplasm is filled with diffuse material and frequently contains vesicles and rod-like structures and occasionally short and disorganized microtubules. The term *procilia* has been used by other investigators (Morris and Scholey, 1997; Sfakianos et al., 2007) to describe short, budding cilia in different contexts, sometimes including a well-developed axoneme.

Our description of procilia matches previous observations of the budding primary cilia in diverse avian and mammalian tissues (Sorokin, 1962, 1968) and in the chick developing neural tube (Sotelo and Trujillo-Cenoz, 1958). However, Sotelo and Trujillo-Cenoz reported various cycles of complete ciliogenesis in a period of 4.5 days, indicating a quick assembly of cilia (with fully elongated axoneme), in sharp contrast to the very slow development of procilia from E16.5 to P0 and P4 recorded in our study. We cannot entirely rule out the possibility that the developing axoneme in budding cilia of young neurons is susceptible to rapid microtubule breakdown before the specimen is fully fixed, a possibility that would explain the lack of axoneme at early ages. However, this alternative is in doubt given our observations of cilia with well-organized axonemes in P0 tissues. In fact, it should be emphasized that cilia development is not a synchronous and homogeneous process in the neocortex and that differences in length and axonemal content are present particularly at early postnatal times. For example, in the same brain in which we detected (rare) neuronal cilia in the deepest CP with well-developed axonemes, we also observed (rare) neurons in the upper CP with docked centrioles lacking a clear procilium. This difference in cilia development would seem to follow the inside-out pattern of corticogenesis and to correlate with the length differences observed with ACIII staining. Furthermore, at P0, ACIII staining revealed occasional neurons in the subplate exhibiting relatively longer procilia than other layers, suggesting that those cells could display more mature axonemes than the ones found at the EM level. Similarly, at P4, ACIII staining revealed some relatively long procilia located in the subplate and in a subpopulation of neurons in layer 5. EM analysis at the same age revealed lack of axonemes in all procilia analyzed, but procilia in neurons in the deep CP were frequently enriched with microtubular content, suggesting the beginning of axonemal development. Based on this, we propose that axoneme elongation begins ~P0 only in some cells in the subplate, but it is an ongoing process that develops further by P4 in the deep CP and extends subsequently to all layers and probably parallels the cilia elongation pattern reported from ACIII staining. In fact, the axoneme was first observed in all layers at P8, coincident with significant ACIII immunodetection by Western blot and growth in length of cilia. This coincidence suggests that axoneme development is probably responsible for the secondary elongation of the cilia.

Although we focused our study on neurons, at P0 and P4 the high packing density of cortical cells and the

incomplete expression of NeuN (Lyck et al., 2007) preclude the selective study of neurons. Therefore, it is possible that some ACIII^{+} particles would belong to non-neuronal cells. With animals older than P4, we could analyze neuronal cilia more reliably because of the lower neuronal density and mature NeuN expression. However, some cilia could be incomplete as a result of section trimming, and we are measuring the planar projection of cilia

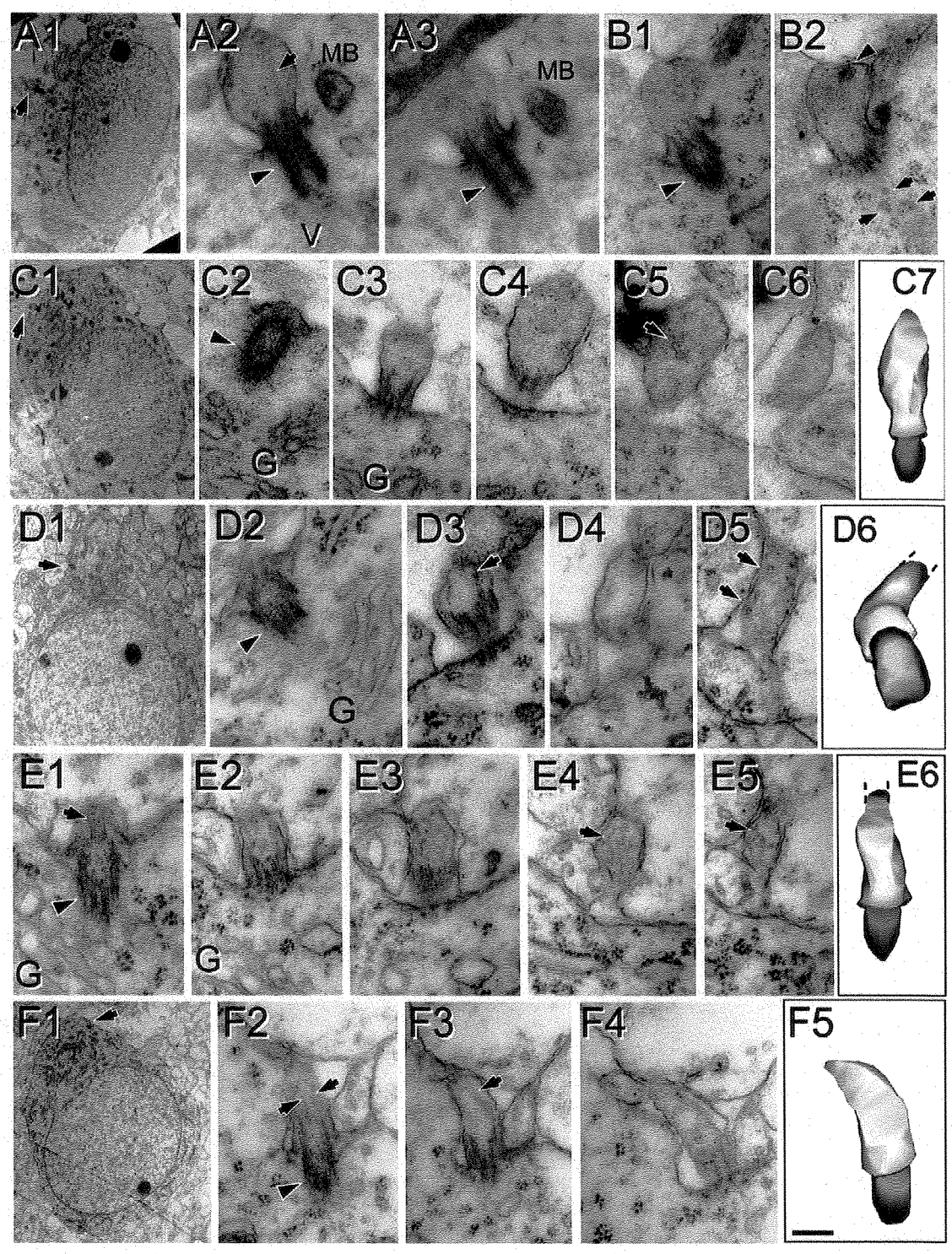

Figure 8

and therefore underestimating their length. Therefore, our quantification study is not intended to provide precise values for neuronal cilia length but seeks to give a general picture of cilia distribution and elongation in different cortical layers during development. Similarly, we focused on cells with neuronal features in our EM analysis, but we cannot discard the possibility that some nonneuronal cilia were included in the study.

From P7 onward, a more or less steady elongation of cilia is observed, first and faster in deep layers, which is followed later by upper layers. Length values stabilize between P60 and P90, with average lengths of about 5 μm in all layers, except for layer 5, which has longer cilia (~6 μm on average and up to ~11 μm), far from the maxima in other layers. Layer 1 is unlike layers 2–6 because of its scarce neuronal content, but, as expected, the few neurons detectable with NeuN typically exhibited a long cilium enriched with ACIII. Initially, layer 1 neurons displayed long cilia compared with upper laminae, but after P7 their values were similar to those of other layers. These laminar differences in length and rate of growth could be related to differences in neuron/soma size and maturation rate in different layers (Lund et al., 1977; Van Eden and Uylings, 1985), but we did not study those relationships in the present work. On the other hand, we did not find significant differences in estimated cilia length between sexes.

Surprisingly, we found that the lengths of cilia at P170 and P365 were decreased compared with P60–P90. The explanation for this decrease is currently unclear. It is possible that cilia slightly shorten with aging, but another possibility is a reduced or incomplete localization of ACIII in older animals. ACIII staining tapers toward the tip of the cilium (Poole et al., 1997; present results), so reduced levels of ACIII could lead to incomplete filling of the cilia length. Separate studies on aged rats (>3years) did not show significant cilia shortening (data not shown), suggesting that cilia, as visualized with ACIII, do not continue to shorten with advanced aging. Further studies are needed to clarify these questions.

Overall, our study shows that ciliogenesis is a protracted process in mouse neocortex: procilia seem to remain undifferentiated from late fetal to early postnatal stages, and the subsequent elongation of axonemes and cilia takes several weeks to complete, until P60–P90 (Fig. 14). This delayed time course of cilia maturation is very surprising given that cilia growth can be very rapid (on the order of hours) in many nonneural cells in culture (Tucker et al., 1979a,b) and on the order of days in the chick neural tube (Sotelo and Trujillo-Cenoz, 1958). Furthermore, cilia are observed within days on cultured neurons (derived from fetal/perinatal tissues) from a variety of brain regions, including hippocampus, striatum, amygdala, cerebellum, and spinal cord (Barzi et al., 2010; Belgacem and Borodinsky, 2011; Berbari et al., 2007; Domire et al., 2010; Miyoshi et al., 2009). It is difficult to compare the growth that we see in vivo with that of these newly maturing neurons until studies are performed that describe the in vivo development of these structures in each brain region. It is noteworthy that neurons from different brain regions grow cilia of different lengths (Fuchs and Schwark, 2004), but determining whether neurons from different brain regions exploit different mechanisms to control the onset and duration of ciliogenesis requires further analysis. With respect to neocortex (and possibly other regions), prolonged maturation of cilia overlaps with neocortical neuron maturation that comprises key

Figure 8. Procilia in P4 neocortex. Cells of interest and procilia are shaded to help with identification. Illustrated are examples of procilia lacking axonemes (A–C) and procilia located in the deep cortical plate with some microtubular structures but lacking a well-formed axoneme (D–F). **A–C:** Enlarged, apparently immature procilia, present both in the deep (A) and in the superficial (B,C) cortical plate. A1: Low-magnification view of a cell with neuronal morphology in the deep cortical plate; the arrow indicates the location of the procilium. A2,3: Serial longitudinal sections along the basal body (arrowhead) and procilium containing some microtubules (arrow). A multivesicular body (MB) and vesicles (V) could be found in the vicinity. B: Serial longitudinal sections along the basal body (arrowhead in B1) and stubby procilium containing a dark structure (arrowhead in B2). Vesicles (arrows in B2) were common close to the basal body. C1: Low-magnification view of a cell with neuronal morphology located in the deep cortical plate; the arrow indicates the location of the procilium. C2–6: Serial oblique sections through the basal body (arrowhead) and procilium (C3–6) containing vesicle-like structures (arrow in C5). C7: 3D reconstruction of the basal body (gray) and the cilium (white). **D–F:** Examples of procilia containing microtubule-like structures. D1: Low-magnification view of a cell with neuronal morphology located in the deep cortical plate; the arrow indicates the location of the procilium. D2–5: Serial sections (70 nm thick) through the procilium. D2: The basal body (arrowhead) and the adjacent Golgi apparatus (G). D3–5: Oblique sections through the procilium showing lack of axoneme with presence of scattered tubular structures (arrows). D6: 3D reconstruction of the basal body (gray) and the cilium (white). E1–6: Serial longitudinal sections along the basal body (arrowhead in E1) and the procilium containing disorganized microtubules (arrows). Golgi apparatus (G) vesicles were located close to the basal body. E6: 3D reconstruction of the basal body (gray) and the cilium (white). F1: Low-magnification view of the cell with neuronal morphology; the arrow indicates the location of the procilium. F2–5: Serial longitudinal sections along the basal body (arrowhead in F2) and the procilium that contains a few microtubules in a parallel arrangement (arrows), compatible with a developing axoneme. F5: 3D reconstruction of the basal body (gray) and the cilium (white). Scale bar = 0.2 μm in F5 (applies to F2–5); 2 μm for A1,C1,F1; 0.18 for A2,3,B1,2,C2–6,D6,E1–5; 0.25 for C7; 3 μm for D1; 0.16 μm for D2–5; 0.22 for E6. [Color figure can be viewed in the online issue, which is available at wileyonlinelibrary.com.]

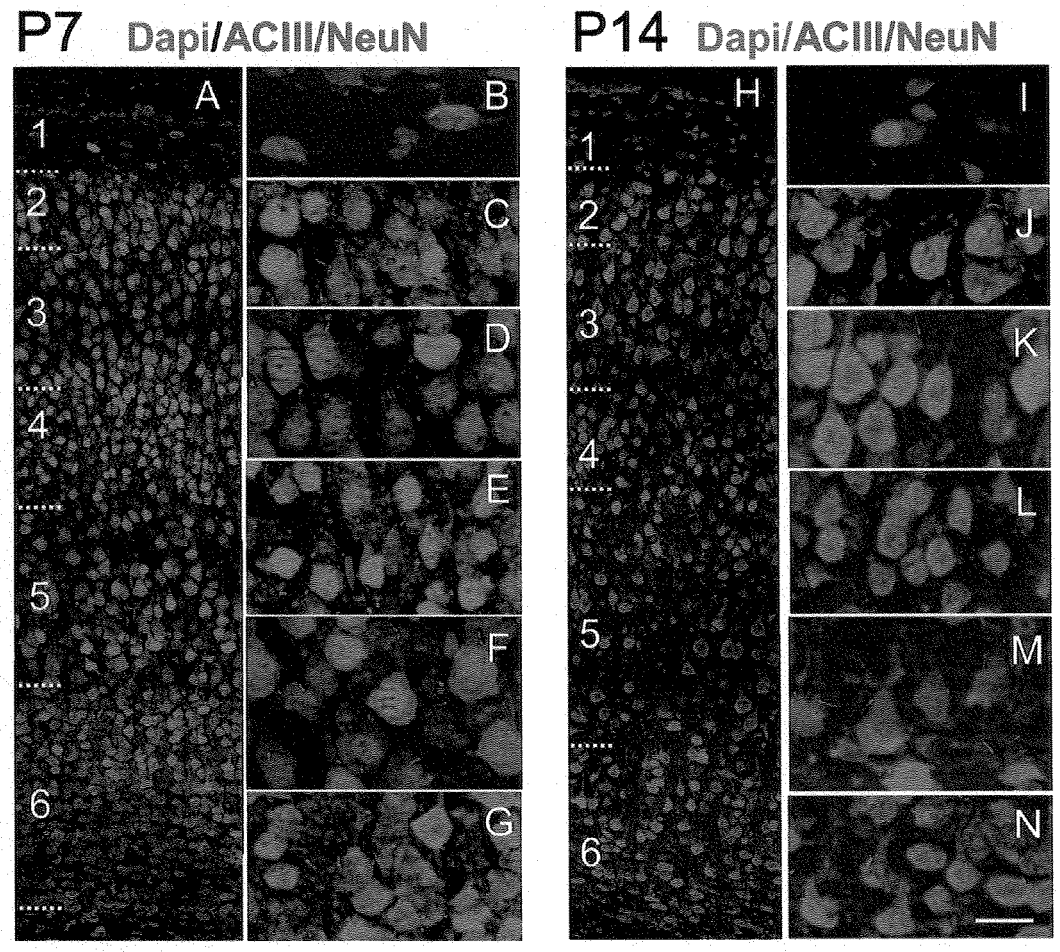

Figure 9. ACIII^{+} cilia extend from neurons in all lamina of neocortex at P7 and P14. **A:** Low-magnification view of P7 neocortex immunostained for ACIII (green) and NeuN (red) and counterstained with DAPI (blue). **B–G:** High-magnification views of layers 1 (B), 2 (C), 3 (D), 4 (E), 5 (F), and 6 (G). Compared with P4 (Fig. 5), layers are more developed, neuropil is expanding, and cilia are longer and growing at similar rates in all layers (see Table 2). **H–N:** Low-magnification view of P14 neocortex immunostained for ACIII and NeuN and counterstained with DAPI. High-magnification views of layers 1 (I), 2 (J), 3 (K), 4 (L), 5 (M), and 6 (N) are shown at right. Note the expansion of the neuropil and more elongated appearance of cilia in all layers. At this age, cilia lengths reach ~70–90% of maximal lengths (see Table 2). Scale bar = 20 μm in N (applies to I–N); 70 μm for A; 24 μm for B–G; 70 μm for H.

developmental processes such as dendrite growth and synaptogenesis, processes that are defined by actin and microtubule rearrangements and extensive vesicle trafficking, similar to ciliogenesis (Kim et al., 2010). Whether the coincidental developmental time frames of cilia and other neuronal processes are interrelated also requires further study.

Appearance of signalling machinery in neuronal cilia

ACIII can exist at different molecular weights (e.g., ~125 and ~200 kDa) based on glycosylation (Wei et al., 1996). We found that ACIII from cortex appeared to be in the less glycosylated ~125 kDa form as reported by others (Murthy and Makhlouf, 1997). We also found that this differed from the more glycosylated form that is observed in lysates of olfactory epithelium (Wong et al., 2000; present study). The significance of these different forms of ACIII between different brain regions is unclear.

Our analysis of ACIII protein in fetal cortical lysates showed early detection at very low levels at E13.5, E16, and E18.5. These results could correspond to the formation of procilia starting at E13.5, although we cannot rule out the possibility that our blots are detecting nonneuronal or potentially nonciliar ACIII expression. At E18.5, we observed short ACIII^{+} procilia coinciding with pericentrin^{+} basal bodies. Later, as development continues

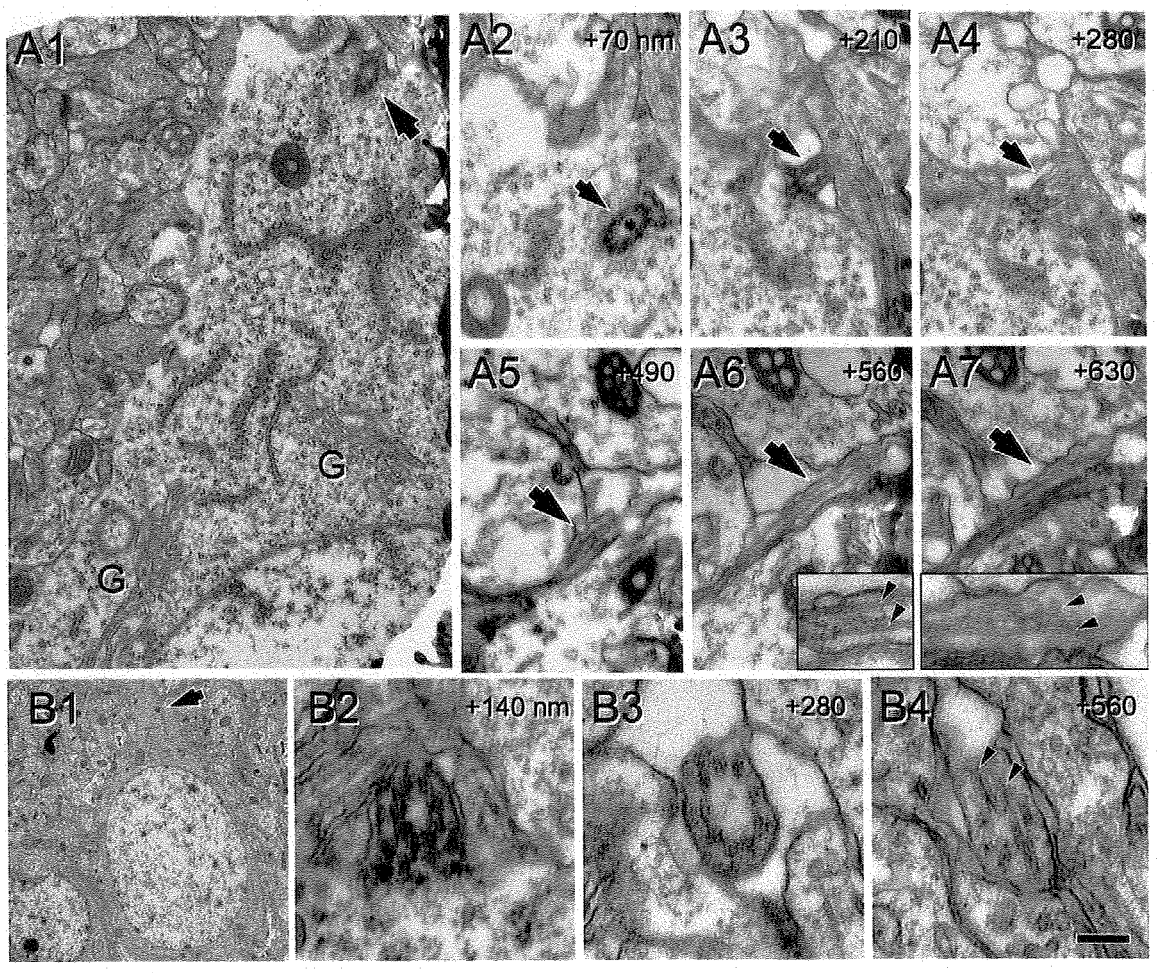

Figure 10. Ultrastructure of cilia at P8. Cells of interest and procilia are shaded to help with identification. **A:** Serial micrographs of a cilium at P8. A1: Panoramic view of the cytoplasm and initial apical dendrite of a pyramidal neuron with the basal body attached to the membrane (arrow). G, Golgi apparatus. A2–7: Serial sections of the cilium (arrow) protruding outside of the cell. Well-formed and structured microtubules in the proximal segment (**insets** in A6,7) appear disorganized distally (inset in A7). Numbers in upper right corner indicate the Z distance between sections in nanometers. **B:** Serial sections of a cilium from a pyramidal neuron at P8. B1: Panoramic view of the pyramidal cell. Cilium location is indicated (arrow). B2–4: Serial micrographs of the cilia from neuron in B1. B2 illustrates the transition between the basal body and the cilium, and B3,4 are transverse and oblique sections through the cilium showing a straight morphology and a well-developed axoneme along the available length of 0.56 μm. Vesicles were less frequent at this age. Scale bar = 0.12 μm in B4 (applies to B2–4); 0.5 μm for A1; 0.4 μm for A2–7; 5 μm for B1. [Color figure can be viewed in the online issue, which is available at wileyonlinelibrary.com.]

postnatally, ACIII expression levels increase dramatically, which directly correlated with the elongation of ACIII positive cilia throughout the neocortex. These levels may also correlate with the cellular production or available levels of cytosolic tubulin, which recently were reported to correspond to cilia length (Sharma et al., 2011). It is unclear why the levels of ACIII protein at P60 appear to be lower than earlier in development. Whether this reflects a role for ACIII earlier in development during cilia elongation (Ou et al., 2009), a change in ACIII concentration within cilia over time, or some other mechanism requires further study.

From E16.5 through P0 until ~P4, our EM analysis showed a slight growth of the prociliar length without apparent axonemal development (except for some subplate cells). The elongation of the cilia axoneme is coordinated by intraflagellar transport (IFT), a bidirectional trafficking mechanism to shuttle cilia components to and from the cilium tip (Pedersen and Rosenbaum, 2008). Mutations in IFT molecules are often associated with defective assembly of primary cilia. For example, Pazour and colleagues (2000) showed that impairment of IFT in mice resulted in short cilia resembling the procilia shown here. Thus, it is tempting to speculate that IFT might not

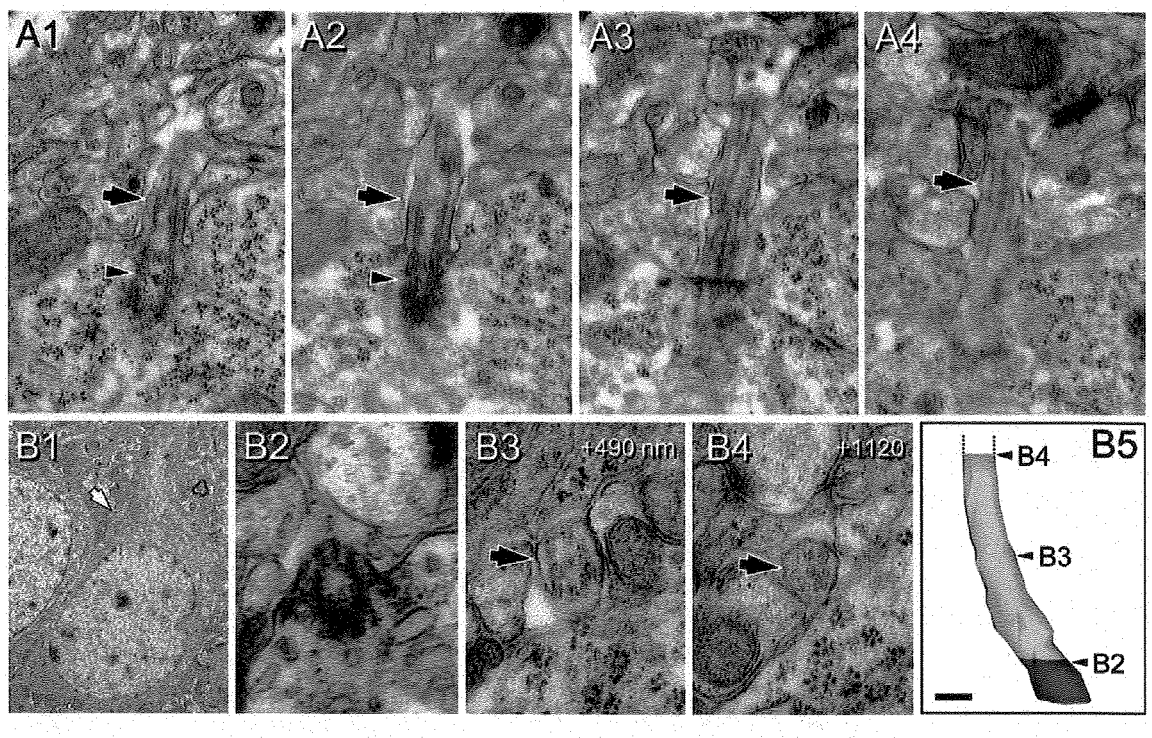

Figure 11. Ultrastructure of cilia at P60. Cells of interest and procilia are shaded to help with identification. **A:** Serial sections along the basal body (arrowhead) and proximal segment (arrow) of a neuronal cilium. Notice the well-developed microtubules. **B:** Serial transverse sections of a pyramidal cell cilium (incomplete). B1: Panoramic view of a pyramidal neuron. Location of the cilium is indicated (arrow). B2–4: Details of transverse sections through the cilium of the pyramidal neuron in B1. B2: Transition basal body-cilium. B3: Middistance of the series. B4: Final section at about 1.2 μm from the origin. Note the rounded shape of the ciliar membrane and the well-developed axoneme along the available length. B5: 3D reconstruction of the basal body (gray) and the (incomplete) cilium (white). Positions of images B2–4 are indicated. Numbers in upper right corner indicate the Z distance to the cilium origin in nanometers. Scale bar = 0.18 μm in B5; 0.17 μm for A; 1.5 μm for B1; 0.1 for B2–4. [Color figure can be viewed in the online issue, which is available at wileyonlinelibrary.com.]

be fully active at these early stages of ciliogenesis, and later development of this mechanism could be responsible for axoneme and cilia elongation. This is one potential hypothesis for future studies on neuronal cilia.

The EM micrographs typically revealed Golgi apparatus and different types of vesicles in close apposition to the basal body and centriole and also inside the procilia, suggesting that trafficking to the newly forming cilium might be significant at these ages. The presence of ACIII in procilia from E18.5 to P4, when the axoneme is poorly developed, suggests that ACIII localization to the procilium is, or at least can be, independent of the presence of a fully developed axoneme. This is notable in light of the fact that downregulation of BBS2 and BBS4 (Bardet-Biedl syndrome proteins, which regulate vesicular transport to the cilium) impedes SSTR3 but not ACIII localization in cilia and does not notably alter cilia elongation (Berbari et al., 2008). For cell lines, it has been suggested that ACIII can contribute to the elongation of cilia (Ou et al., 2009). However, ACIII-deficient mice extend cilia of comparable lengths and remain able to traffic neuronal cilia receptors such as SSTR3 (Wang et al., 2009). Taken together, these data suggest that independent routes of protein trafficking to the cilium may underlie the developmental time course of receptor expression and cilium maturation.

In hippocampus, SSTR3 appears in cilia between ~P0 and ~P3 (Stanic et al., 2009), and, for neocortex, we previously observed SSTR3 in neonatal rat neocortex (Anastas et al., 2011). However, no studies are available on the development of SSTR3 localization in cilia in the neocortex. We must await further characterization of content and developmental appearance of other neuronal cilia receptors.

Neuronal cilia do not seem essential for proper neuronal migration or for acquisition of neuronal polarity

We observed that, in pyramidal neurons (Anastas et al., 2011; present data), the docking of the basal body generally forms on the pial side of the cell. However, in the

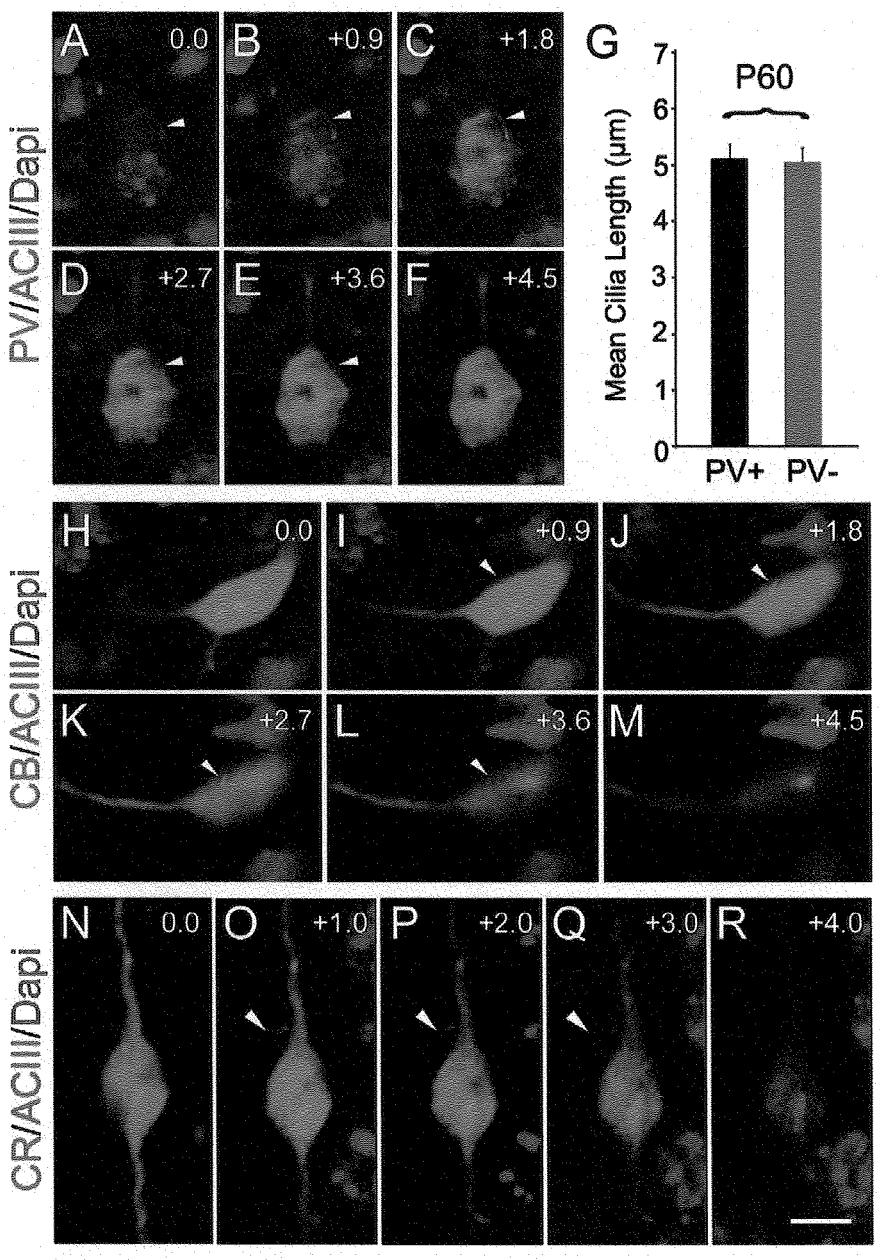

Figure 12. Different interneuron subtypes in neocortex extend cilia. Examples of ciliated interneurons in the neocortex of P60 mice. **A–F:** An ACIII$^+$ (arrow) cilium extending out of a parvalbumin (PV)-positive cell. **G:** Bar graph shows cilia length between PV$^+$ and neighboring PV$^-$ cells were comparable (~5 μm). **H–M:** Example of a calbindin (CB)-positive interneuron with an ACIII$^+$ cilium (arrow). **N–R:** A calretinin (CR)-positive interneuron extending an ACIII$^+$ cilium (arrow). Interestingly, some bipolar CR$^+$ cells extended their cilia from the proximal part of the ascending (pial-oriented) dendrite, as illustrated. Numbers in the right upper corner of images indicate z-step increments in micrometers. Scale bar = 7.5 μm in R (applies to N–R); 12 μm for A–F; 10 μm for H–M.

major interneuron subtypes, PV$^+$ and CB$^+$ cells, the cilia/basal body seemed to be more randomly located on the soma. CR$^+$ cells, however, often exhibit a highly polarized morphology, and we found that the cilia could be in the "apical" dendrite. Overall, these data suggest that the positioning of the cilium might be related to the polarity of the neural cell type in that there is correlation between the docking location of the basal body and the relative position of the mother centriole as migration ceases. However, it seems that cilia formation is not essential for

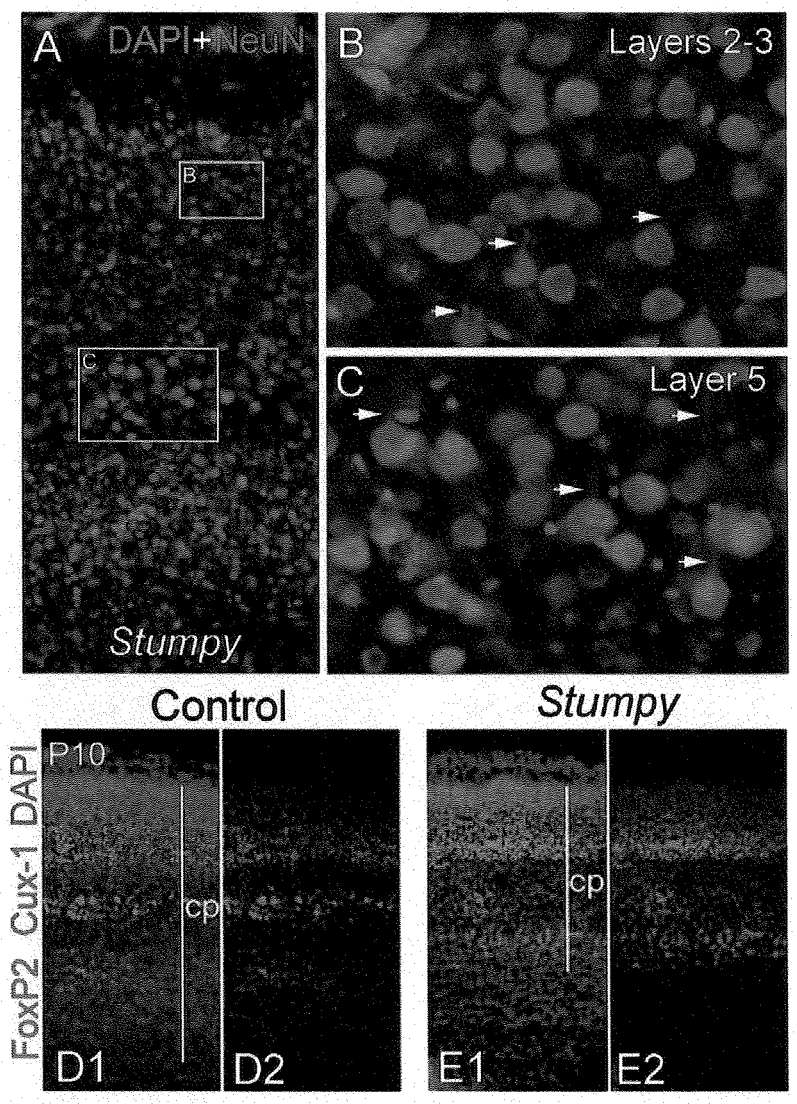

Figure 13. Mutants lacking cilia show normal gross cytoarchitecture. **A:** Panoramic view of the neocortex of Δ*Stumpy* mutant mice immunostained for NeuN (green) and counterstained with DAPI (blue). The boxed areas in A represent higher magnification views of layers 2–3 (**B**) and 5 (**C**). In spite of the cortical compression resulting from hydrocephalus, Δ*Stumpy* mice lacking cilia exhibit normal polarization in pyramidal neurons, with well-formed and oriented apical dendrites (arrows in B,C). **D,E:** Panoramic view of the cortical plate (cp) of P10 control (D1,2) and Δ*Stumpy* mice (E1,2) immunostained for Cux1 (upper layer neurons marker; green) and Foxp2 (deeper layer neurons marker; red). Stratification of cortical layers was also grossly preserved in mice lacking cilia. D2 and E2 have had the DAPI channel removed.

neuronal polarity or expression of layer-specific markers in neocortex. Despite a severe defect in ciliogenesis, analysis of mutant *Stumpy* mice revealed normal polarity of pyramidal neurons, with a well-developed apical dendrite. The preserved expression of laminar markers suggests that loss of cilia does not grossly disrupt timing of neuronal migration, which is consistent with our findings that cilia initiate growth postmigration. We cannot rule out that loss of cilia alters the fine positioning or morphology of cortical neurons. For example, we have observed subtle abnormalities in Purkinje cell position and morphology in the developing cerebellum of Δ*Stumpy* mice, but these changes could be secondary to granule cell dysgenesis or altered Sonic hedgehog signalling in the region (Breunig et al., 2008; Chizhikov et al., 2007; Spassky et al., 2008). Duplication of a neuron's cilium number also does not seem to alter the general orientation of pyramidal neurons (Anastas et al., 2011; Sarkisian et al.,

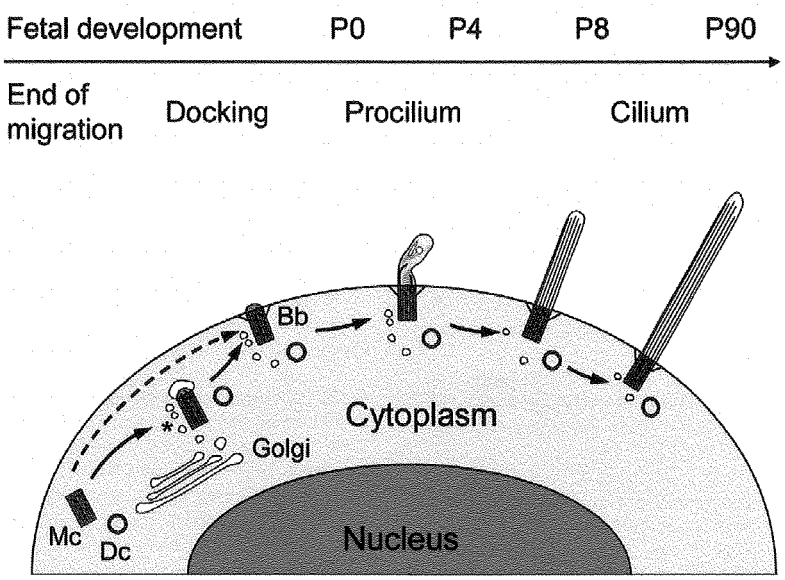

Figure 14. Model of ciliogenesis stages in mouse neocortical neurons. We propose the following model. Migrating neurons do not bear cilia; rather, their mother centriole (Mc) and daughter centriole (Dc) are free in the cytoplasm. Once cells terminate migration and reach their appropriate lamina, the mother centriole attaches a vesicle, likely from the Golgi apparatus, buds a very short procilium and docks to the plasma membrane. It is also possible that the mother centriole docks directly to the plasma membrane without vesicle attachment as indicated by the dashed arrow. Docking to the membrane involves developing specific structures such as transition filaments, and the mother centriole will become a basal body (Bb), frequently surrounded by vesicles (asterisk). This basal body will grow the procilium, a membranous expansion about 0.5–2 μm in length, whose main feature is the lack of proper axoneme and that typically contains vesicles, short and disorganized tubular structures, and electron-dense diffuse content. This procilium does not display typical axonemal characteristics until ~P8, although axonemal growth seems to start at ~P0 in some subplate cells and could start ~P4 in some populations of neurons that showed early elongation of cilia (e.g., some layer 5 neurons). Overall, cilia will take weeks to elongate fully toward a peak at ~P60–P90, with some differences between layers.

2001). Thus, dramatic changes to a neuron's cilium do not grossly affect its position or morphology. Determining how or whether such mutations ultimately influence intracellular signalling pathways or connections between neurons requires further investigation.

Despite the increased attention given to this organelle, more precise genetic manipulations will be needed to assess the role of primary cilia in neurons definitively. Moreover, a proper understanding of the dynamics of ciliogenesis will be needed to harness these technologies and to create informed hypotheses about these organelles. Our detailed description of the process of neuronal ciliogenesis will be useful for these endeavors and for future studies examining the significance and functional role of neuronal cilia.

ACKNOWLEDGMENTS

We thank Drs. Mladen-Roko Rasin and Nenad Sestan for providing us with EM-prepared tissue sections. We also thank Dr. Jill Verlander and George Kasnic of the University of Florida Core EM Facility, Doug Smith of the Cell and Tissue Analysis Core Facility, Dorit Siebzehnrubl, and Dr. Kirill Ukhanov for technical assistance.

LITERATURE CITED

Airaksinen MS, Eilers J, Garaschuk O, Thoenen H, Konnerth A, Meyer M. 1997. Ataxia and altered dendritic calcium signaling in mice carrying a targeted null mutation of the calbindin D28k gene. Proc Natl Acad Sci U S A 94: 1488–1493.

Amador-Arjona A, Elliott J, Miller A, Ginbey A, Pazour GJ, Enikolopov G, Roberts AJ, Terskikh AV. 2011. Primary cilia regulate proliferation of amplifying progenitors in adult hippocampus: implications for learning and memory. J Neurosci 31:9933–9944.

Anastas SB, Mueller D, Semple-Rowland SL, Breunig JJ, Sarkisian MR. 2011. Failed cytokinesis of neural progenitors in citron kinase-deficient rats leads to multiciliated neurons. Cereb Cortex 21:338–344. (Epub 2010, Jun 4).

Barzi M, Berenguer J, Menendez A, Alvarez-Rodriguez R, Pons S. 2010. Sonic-hedgehog-mediated proliferation requires the localization of PKA to the cilium base. J Cell Sci 123: 62–69.

Bearzatto B, Servais L, Roussel C, Gall D, Baba-Aissa F, Schurmans S, de Kerchove d'Exaerde A, Cheron G, Schiffmann SN. 2006. Targeted calretinin expression in granule cells

of calretinin-null mice restores normal cerebellar functions. FASEB J 20:380–382.

Belgacem YH, Borodinsky LN. 2011. Sonic hedgehog signaling is decoded by calcium spike activity in the developing spinal cord. Proc Natl Acad Sci U S A 108:4482–4487.

Bennouna-Greene V, Kremer S, Stoetzel C, Christmann D, Schuster C, Durand M, Verloes A, Sigaudy S, Holder-Espinasse M, Godet J, Brandt C, Marion V, Danion A, Dietemann JL, Dollfus H. 2011. Hippocampal dysgenesis and variable neuropsychiatric phenotypes in patients with Bardet-Biedl syndrome underline complex CNS impact of primary cilia. Clin Genet (E-pub 25 April 2011).

Berbari NF, Bishop GA, Askwith CC, Lewis JS, Mykytyn K. 2007. Hippocampal neurons possess primary cilia in culture. J Neurosci Res 85:1095–1100.

Berbari NF, Lewis JS, Bishop GA, Askwith CC, Mykytyn K. 2008. Bardet-Biedl syndrome proteins are required for the localization of G protein-coupled receptors to primary cilia. Proc Natl Acad Sci U S A 105:4242–4246.

Bishop GA, Berbari NF, Lewis J, Mykytyn K. 2007. Type III adenylyl cyclase localizes to primary cilia throughout the adult mouse brain. J Comp Neurol 505:562–571.

Brailov I, Bancila M, Brisorgueil MJ, Miquel MC, Hamon M, Verge D. 2000. Localization of 5-HT_6 receptors at the plasma membrane of neuronal cilia in the rat brain. Brain Res 872:271–275.

Breunig JJ, Sarkisian MR, Arellano JI, Morozov YM, Ayoub AE, Sojitra S, Wang B, Flavell RA, Rakic P, Town T. 2008. Primary cilia regulate hippocampal neurogenesis by mediating sonic hedgehog signaling. Proc Natl Acad Sci U S A 105: 13127–13132.

Celio MR, Heizmann CW. 1981. Calcium-binding protein parvalbumin as a neuronal marker. Nature 293:300–302.

Celio MR, Baier W, Scharer L, Gregersen HJ, de Viragh PA, Norman AW. 1990. Monoclonal antibodies directed against the calcium binding protein Calbindin D-28k. Cell Calcium 11:599–602.

Chizhikov VV, Davenport J, Zhang Q, Shih EK, Cabello OA, Fuchs JL, Yoder BK, Millen KJ. 2007. Cilia proteins control cerebellar morphogenesis by promoting expansion of the granule progenitor pool. J Neurosci 27:9780–9789.

Cho YJ, Lee JC, Kang BG, An J, Song HS, Son O, Nam DH, Cha CI, Joo KM. 2011. Immunohistochemical study on the expression of calcium binding proteins (calbindin-D28k, calretinin, and parvalbumin) in the cerebral cortex and in the hippocampal region of nNOS knock-out(−/−) mice. Anat Cell Biol 44:106–115.

Cohen E, Binet S, Meininger V. 1988. Ciliogenesis and centriole formation in the mouse embryonic nervous system. An ultrastructural analysis. Biol Cell 62:165–169.

Dahl HA. 1963. Fine structure of cilia in rat cerebral cortex. Z Zellforsch Mikrosk Anat 60:369–386.

Davenport JR, Watts AJ, Roper VC, Croyle MJ, van Groen T, Wyss JM, Nagy TR, Kesterson RA, Yoder BK. 2007. Disruption of intraflagellar transport in adult mice leads to obesity and slow-onset cystic kidney disease. Curr Biol 17: 1586–1594.

Defelipe J, Gonzalez-Albo MC, Del Rio MR, Elston GN. 1999. Distribution and patterns of connectivity of interneurons containing calbindin, calretinin, and parvalbumin in visual areas of the occipital and temporal lobes of the macaque monkey. J Comp Neurol 412:515–526.

Domire JS, Mykytyn K. 2009. Markers for neuronal cilia. Methods Cell Biol 91:111–121.

Domire JS, Green JA, Lee KG, Johnson AD, Askwith CC, Mykytyn K. 2010. Dopamine receptor 1 localizes to neuronal cilia in a dynamic process that requires the Bardet-Biedl syndrome proteins. Cell Mol Life Sci (E-pub 9 December 2010).

Doxsey SJ, Stein P, Evans L, Calarco PD, Kirschner M. 1994. Pericentrin, a highly conserved centrosome protein involved in microtubule organization. Cell 76:639–650.

Dredge BK, Jensen KB. 2011. NeuN/Rbfox3 Nuclear and cytoplasmic isoforms differentially regulate alternative splicing and nonsense-mediated decay of Rbfox2. PLoS ONE 6: e21585.

Dubreuil V, Marzesco AM, Corbeil D, Huttner WB, Wilsch-Brauninger M. 2007. Midbody and primary cilium of neural progenitors release extracellular membrane particles enriched in the stem cell marker prominin-1. J Cell Biol 176: 483–495.

Einstein EB, Patterson CA, Hon BJ, Regan KA, Reddi J, Melnikoff DE, Mateer MJ, Schulz S, Johnson BN, Tallent MK. 2010. Somatostatin signaling in neuronal cilia is critical for object recognition memory. J Neurosci 30:4306–4314.

Feng L, Cooper JA. 2009. Dual functions of Dab1 during brain development. Mol Cell Biol 29:324–332.

Ferland RJ, Cherry TJ, Preware PO, Morrisey EE, Walsh CA. 2003. Characterization of Foxp2 and Foxp1 mRNA and protein in the developing and mature brain. J Comp Neurol 460:266–279.

Fiala JC. 2005. Reconstruct: a free editor for serial section microscopy. J Microsc 218:52–61.

Fuchs JL, Schwark HD. 2004. Neuronal primary cilia: a review. Cell Biol Int 28:111–118.

Goetz SC, Anderson KV. 2010. The primary cilium: a signalling centre during vertebrate development. Nat Rev Genet 11: 331–344.

Green JA, Mykytyn K. 2010. Neuronal ciliary signaling in homeostasis and disease. Cell Mol Life Sci 67:3287–3297.

Han YG, Spassky N, Romaguera-Ros M, Garcia-Verdugo JM, Aguilar A, Schneider-Maunoury S, Alvarez-Buylla A. 2008. Hedgehog signaling and primary cilia are required for the formation of adult neural stem cells. Nat Neurosci 11: 277–284.

Handel M, Schulz S, Stanarius A, Schreff M, Erdtmann-Vourliotis M, Schmidt H, Wolf G, Hollt V. 1999. Selective targeting of somatostatin receptor 3 to neuronal cilia. Neuroscience 89:909–926.

Higginbotham HR, Gleeson JG. 2007. The centrosome in neuronal development. Trends Neurosci 30:276–283.

Jurczyk A, Pino SC, O'sullivan-Murphy B, Addorio M, Lidstone EA, Diiorio P, Lipson KL, Standley C, Fogarty K, Lifshitz L, Urano F, Mordes JP, Greiner DL, Rossini AA, Bortell R. 2010. A novel role for the centrosomal protein, pericentrin, in regulation of insulin secretory vesicle docking in mouse pancreatic beta-cells. PLoS ONE 5:e11812.

Kao HT, Li P, Chao HM, Janoschka S, Pham K, Feng J, McEwen BS, Greengard P, Pieribone VA, Porton B. 2008. Early involvement of synapsin III in neural progenitor cell development in the adult hippocampus. J Comp Neurol 507: 1860–1870.

Kim J, Lee JE, Heynen-Genel S, Suyama E, Ono K, Lee K, Ideker T, Aza-Blanc P, Gleeson JG. 2010. Functional genomic screen for modulators of ciliogenesis and cilium length. Nature 464:1048–1051.

Kim KK, Adelstein RS, Kawamoto S. 2009. Identification of neuronal nuclei (NeuN) as Fox-3, a new member of the Fox-1 gene family of splicing factors. J Biol Chem 284: 31052–31061.

Lee JH, Gleeson JG. 2010. The role of primary cilia in neuronal function. Neurobiol Dis 38:167–172.

LeVay S. 1973. Synaptic patterns in the visual cortex of the cat and monkey. Electron microscopy of Golgi preparations. J Comp Neurol 150:53–85.

Li A, Saito M, Chuang JZ, Tseng YY, Dedesma C, Tomizawa K, Kaitsuka T, Sung CH. 2011. Ciliary transition zone activation of phosphorylated Tctex-1 controls ciliary resorption, S-phase entry and fate of neural progenitors. Nat Cell Biol 13:402-411.

Lund JS, Boothe RG, Lund RD. 1977. Development of neurons in the visual cortex (area 17) of the monkey (*Macaca nemestrina*): a Golgi study from fetal day 127 to postnatal maturity. J Comp Neurol 176:149-188.

Lyck L, Kroigard T, Finsen B. 2007. Unbiased cell quantification reveals a continued increase in the number of neocortical neurones during early post-natal development in mice. Eur J Neurosci 26:1749-1764.

Miyoshi K, Kasahara K, Miyazaki I, Asanuma M. 2009. Lithium treatment elongates primary cilia in the mouse brain and in cultured cells. Biochem Biophys Res Commun 388: 757-762.

Morris RL, Scholey JM. 1997. Heterotrimeric kinesin-II is required for the assembly of motile 9 + 2 ciliary axonemes on sea urchin embryos. J Cell Biol 138:1009-1022.

Mullen RJ, Buck CR, Smith AM. 1992. NeuN, a neuronal specific nuclear protein in vertebrates. Development 116: 201-211.

Murthy KS, Makhlouf GM. 1997. Differential coupling of muscarinic m2 and m3 receptors to adenylyl cyclases V/VI in smooth muscle. Concurrent M2-mediated inhibition via Galphai3 and m3-mediated stimulation via Gbetagammaq. J Biol Chem 272:21317-21324.

Nigg EA, Raff JW. 2009. Centrioles, centrosomes, and cilia in health and disease. Cell 139:663-678.

Ou Y, Ruan Y, Cheng M, Moser JJ, Rattner JB, van der Hoorn FA. 2009. Adenylate cyclase regulates elongation of mammalian primary cilia. Exp Cell Res 315:2802-2817.

Paxinos G, Franklin KBJ. 2004. The mouse brain in stereotaxic coordinates. London: Academic Press.

Pazour GJ, Dickert BL, Vucica Y, Seeley ES, Rosenbaum JL, Witman GB, Cole DG. 2000. Chlamydomonas IFT88 and its mouse homologue, polycystic kidney disease gene tg737, are required for assembly of cilia and flagella. J Cell Biol 151:709-718.

Pedersen LB, Rosenbaum JL. 2008. Intraflagellar transport (IFT) role in ciliary assembly, resorption and signalling. Curr Top Dev Biol 85:23-61.

Pedersen LB, Veland IR, Schroder JM, Christensen ST. 2008. Assembly of primary cilia. Dev Dyn 237:1993-2006.

Poole CA, Jensen CG, Snyder JA, Gray CG, Hermanutz VL, Wheatley DN. 1997. Confocal analysis of primary cilia structure and colocalization with the Golgi apparatus in chondrocytes and aortic smooth muscle cells. Cell Biol Int 21:483-494.

Rasin MR, Gazula VR, Breunig JJ, Kwan KY, Johnson MB, Liu-Chen S, Li HS, Jan LY, Jan YN, Rakic P, Sestan N. 2007. Numb and Numbl are required for maintenance of cadherin-based adhesion and polarity of neural progenitors. Nat Neurosci 10:819-827.

Rooryck C, Pelras S, Chateil JF, Cances C, Arveiler B, Verloes A, Lacombe D, Goizet C. 2007. Bardet-Biedl syndrome and brain abnormalities. Neuropediatrics 38:5-9.

Saino-Saito S, Hozumi Y, Goto K. 2011. Excitotoxicity by kainate-induced seizure causes diacylglycerol kinase zeta to shuttle from the nucleus to the cytoplasm in hippocampal neurons. Neurosci Lett 494:185-189.

Sarkisian MR, Frenkel M, Li W, Oborski JA, LoTurco JJ. 2001. Altered interneuron development in the cerebral cortex of the flathead mutant. Cereb Cortex 11:734-743.

Sarkisian MR, Bartley CM, Chi H, Nakamura F, Hashimoto-Torii K, Torii M, Flavell RA, Rakic P. 2006. MEKK4 signaling regulates filamin expression and neuronal migration. Neuron 52:789-801.

Sfakianos J, Togawa A, Maday S, Hull M, Pypaert M, Cantley L, Toomre D, Mellman I. 2007. Par3 functions in the biogenesis of the primary cilium in polarized epithelial cells. J Cell Biol 179:1133-1140.

Sharma N, Berbari NF, Yoder BK. 2008. Ciliary dysfunction in developmental abnormalities and diseases. Curr Top Dev Biol 85:371-427.

Sharma N, Kosan ZA, Stallworth JE, Berbari NF, Yoder BK. 2011. Soluble levels of cytosolic tubulin regulate ciliary length control. Mol Biol Cell 22:808-816.

Sorokin S. 1962. Centrioles and the formation of rudimentary cilia by fibroblasts and smooth muscle cells. J Cell Biol 15: 363-377.

Sorokin SP. 1968. Centriole formation and ciliogenesis. Aspen Emphysema Conf 11:213-216.

Sotelo JR, Trujillo-Cenoz O. 1958. Electron microscope study on the development of ciliary components of the neural epithelium of the chick embryo. Z Zellforsch Mikrosk Anat 49:1-12.

Spassky N, Han YG, Aguilar A, Strehl L, Besse L, Laclef C, Ros MR, Garcia-Verdugo JM, Alvarez-Buylla A. 2008. Primary cilia are required for cerebellar development and Shh-dependent expansion of progenitor pool. Dev Biol 317: 246-259.

Stanic D, Malmgren H, He H, Scott L, Aperia A, Hokfelt T. 2009. Developmental changes in frequency of the ciliary somatostatin receptor 3 protein. Brain Res 1249:101-112.

Stillman AA, Krsnik Z, Sun J, Rasin MR, State MW, Sestan N, Louvi A. 2009. Developmentally regulated and evolutionarily conserved expression of SLITRK1 in brain circuits implicated in Tourette syndrome. J Comp Neurol 513:21-37.

Town T, Breunig JJ, Sarkisian MR, Spilianakis C, Ayoub AE, Liu X, Ferrandino AF, Gallagher AR, Li MO, Rakic P, Flavell RA. 2008. The stumpy gene is required for mammalian ciliogenesis. Proc Natl Acad Sci U S A 105:2853-2858.

Tsai JW, Bremner KH, Vallee RB. 2007. Dual subcellular roles for LIS1 and dynein in radial neuronal migration in live brain tissue. Nat Neurosci 10:970-979.

Tucker RW, Pardee AB, Fujiwara K. 1979a. Centriole ciliation is related to quiescence and DNA synthesis in 3T3 cells. Cell 17:527-535.

Tucker RW, Scher CD, Stiles CD. 1979b. Centriole deciliation associated with the early response of 3T3 cells to growth factors but not to SV40. Cell 18:1065-1072.

Tury A, Mairet-Coello G, Dicicco-Bloom E. 2011. The cyclin-dependent kinase inhibitor p57Kip2 regulates cell cycle exit, differentiation, and migration of embryonic cerebral cortical precursors. Cereb Cortex 21:1840-1856.

Van Eden CG, Uylings HB. 1985. Cytoarchitectonic development of the prefrontal cortex in the rat. J Comp Neurol 241:253-267.

Waclaw RR, Ehrman LA, Pierani A, Campbell K. 2010. Developmental origin of the neuronal subtypes that comprise the amygdalar fear circuit in the mouse. J Neurosci 30: 6944-6953.

Wang Y, Yin X, Rosen G, Gabel L, Guadiana SM, Sarkisian MR, Galaburda AM, Loturco JJ. 2011. Dcdc2 knockout mice display exacerbated developmental disruptions following knockdown of doublecortin. Neuroscience 190:398-408.

Wang Z, Li V, Chan GC, Phan T, Nudelman AS, Xia Z, Storm DR. 2009. Adult type 3 adenylyl cyclase-deficient mice are obese. PLoS ONE 4:e6979.

Wei J, Wayman G, Storm DR. 1996. Phosphorylation and inhibition of type III adenylyl cyclase by calmodulin-dependent protein kinase II in vivo. J Biol Chem 271:24231-24235.

Wei J, Zhao AZ, Chan GC, Baker LP, Impey S, Beavo JA, Storm DR. 1998. Phosphorylation and inhibition of olfactory adenylyl cyclase by CaM kinase II in neurons: a mechanism for attenuation of olfactory signals. Neuron 21: 495–504.

Westra JW, Peterson SE, Yung YC, Mutoh T, Barral S, Chun J. 2008. Aneuploid mosaicism in the developing and adult cerebellar cortex. J Comp Neurol 507:1944–1951.

White EL, Rock MP. 1980. Three-dimensional aspects and synaptic relationships of a Golgi-impregnated spiny stellate cell reconstructed from serial thin sections. J Neurocytol 9: 615–636.

Whitfield JF. 2004. The neuronal primary cilium—an extrasynaptic signaling device. Cell Signal 16:763–767.

Willaredt MA, Hasenpusch-Theil K, Gardner HA, Kitanovic I, Hirschfeld-Warneken VC, Gojak CP, Gorgas K, Bradford CL, Spatz J, Wolfl S, Theil T, Tucker KL. 2008. A crucial role for primary cilia in cortical morphogenesis. J Neurosci 28: 12887–12900.

Wonders CP, Anderson SA. 2006. The origin and specification of cortical interneurons. Nat Rev Neurosci 7:687–696.

Wong ST, Trinh K, Hacker B, Chan GC, Lowe G, Gaggar A, Xia Z, Gold GH, Storm DR. 2000. Disruption of the type III adenylyl cyclase gene leads to peripheral and behavioral anosmia in transgenic mice. Neuron 27:487–497.

Xu H, He JH, Xiao ZD, Zhang QQ, Chen YQ, Zhou H, Qu LH. 2010. Liver-enriched transcription factors regulate microRNA-122 that targets CUTL1 during liver development. Hepatology 52:1431–1442.

Zimmermann L, Schwaller B. 2002. Monoclonal antibodies recognizing epitopes of calretinins: dependence on Ca^{2+}-binding status and differences in antigen accessibility in colon cancer cells. Cell Calcium 31:13–25.